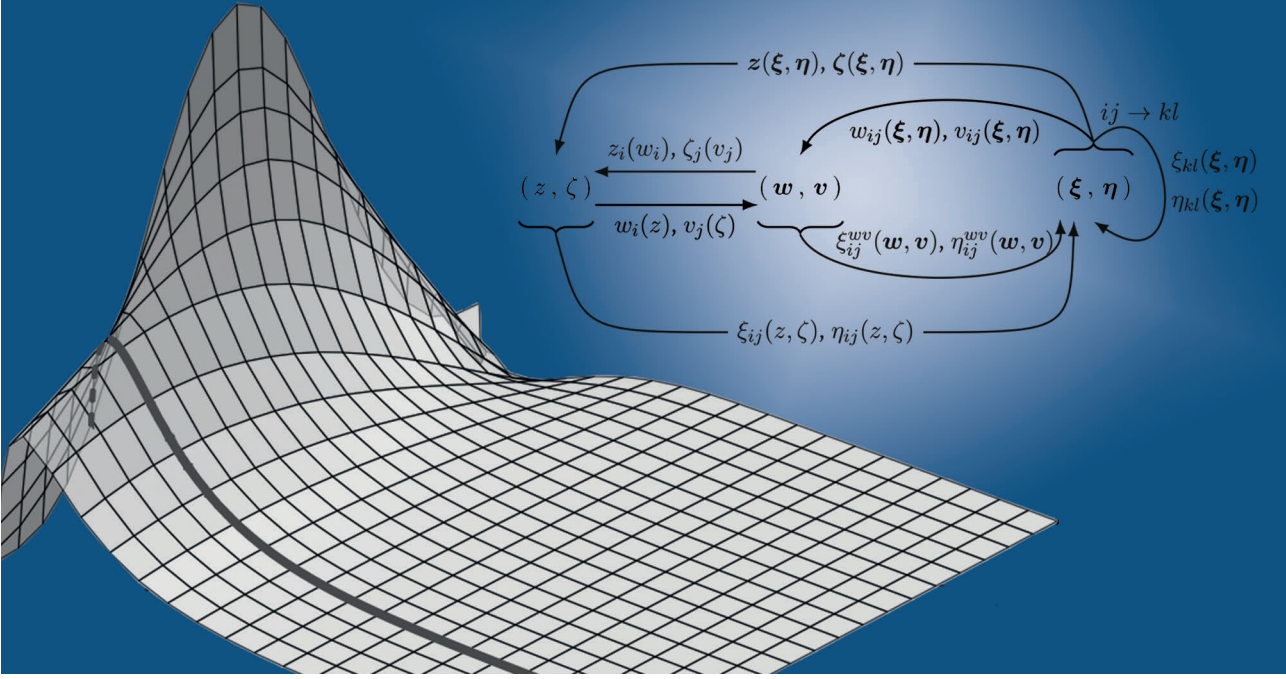

FAU Forschungen, Reihe B, Medizin, Naturwissenschaft, Technik 36

Simon Kerschbaum

Backstepping Control of Coupled Parabolic Systems with Varying Parameters

FAU UNIVERSITY PRESS

Simon Kerschbaum

Backstepping Control of Coupled Parabolic Systems with Varying Parameters

FAU Forschungen, Reihe B
Medizin, Naturwissenschaft, Technik
Band 36

Herausgeber der Reihe:
Wissenschaftlicher Beirat der FAU University Press

Simon Kerschbaum

Backstepping Control of Coupled Parabolic Systems with Varying Parameters

Erlangen
FAU University Press
2021

Bibliografische Information der Deutschen Nationalbibliothek:
Die Deutsche Nationalbibliothek verzeichnet diese Publikation in der Deutschen Nationalbibliografie; detaillierte bibliografische Daten sind im Internet über http://dnb.d-nb.de abrufbar.

Bitte zitieren als
Kerschbaum, Simon. 2021. Backstepping Control of Coupled Parabolic Systems with Varying Parameters. FAU Forschungen, Reihe B, Medizin, Naturwissenschaft, Technik Band 36. Erlangen: FAU University Press.
DOI: 10.25593/978-3-96147-391-5.

Autoren-Kontaktinformation: Simon Kerschbaum,
simon.kerschbaum@fau.de, ORCID 0000-0001-7352-054X

Der vollständige Inhalt des Buchs ist als PDF über den OPUS-Server der Friedrich-Alexander-Universität Erlangen-Nürnberg abrufbar:
https://opus4.kobv.de/opus4-fau/home

Als ergänzendes Material findet sich der MATLAB®-Code, mit welchem die in diesem Werk aufgeführten Beispiele erzeugt wurden, unter [119] zum Download.

Verlag und Auslieferung:
FAU University Press, Universitätsstraße 4, 91054 Erlangen
Druck: docupoint GmbH

ISBN: 978-3-96147-390-8 (Druckausgabe)
eISBN: 978-3-96147-391-5 (Online-Ausgabe)
ISSN: 2198-8102
DOI: 10.25593/978-3-96147-391-5

Backstepping Control of Coupled Parabolic Systems with Varying Parameters

Backstepping-Regelung verkoppelter parabolischer Systeme mit veränderlichen Parametern

Der Technischen Fakultät

der Friedrich-Alexander-Universität

Erlangen-Nürnberg

zur Erlangung des Doktorgrades

DOKTOR-INGENIEUR

vorgelegt von

Simon Kerschbaum, M.Sc.

aus Fürth

Als Dissertation genehmigt
von der Technischen Fakultät
der Friedrich-Alexander-Universität Erlangen-Nürnberg
Tag der mündlichen Prüfung: 13.07.2020

Vorsitzender des Promotionsorgans: Prof. Dr.-Ing. habil. Andreas Paul Fröba

Gutachter: Prof. Dr.-Ing. habil. Joachim Deutscher
Univ.-Prof. Dr.-Ing. Frank Woittennek

Danksagung

Die vorliegende Dissertation ist im Rahmen meiner Tätigkeit als wissenschaftlicher Mitarbeiter am Lehrstuhl für Regelungstechnik der Friedrich-Alexander-Universität Erlangen-Nürnberg entstanden.

Mein besonderer Dank gilt an dieser Stelle meinem Doktorvater Herrn Prof. Dr.-Ing. habil. Joachim Deutscher, der diese Arbeit als Leiter der Forschungsgruppe „unendlich-dimensionale Systeme“ mit außerordentlichem Interesse und Engagement begleitet hat. Seine wertvollen Anregungen und die bereichernden Diskussionen haben in höchstem Maße zum Gelingen dieser Arbeit beigetragen.

Den Lehrstuhlinhabern Prof. Dr.-Ing. habil. Günter Roppenecker und Prof. Dr.-Ing. Knut Graichen gilt mein Dank für die Gewährung des nötigen Freiraums zur Bearbeitung der Aufgaben sowie für das entgegengebrachte Vertrauen, welches Herr Graichen darüber hinaus durch die Übernahme des Prüfungsvorsitzes in der mündlichen Prüfung zum Ausdruck brachte. Herrn Univ.-Prof. Dr.-Ing. Frank Woittennek danke ich für die Anfertigung des Zweitgutachtens sowie die aufschlussreichen Gespräche und konstruktiven Anmerkungen. Ebenso bedanke ich mich bei Herrn Prof. Dr. Günter Leugering für seine aktive Beteiligung an der Prüfungskommission.

Mein uneingeschränkter Dank gilt zudem meinen Kollegen Jakob Gabriel und Ferdinand Fischer für die Durchsicht der Arbeit, die vielen spannenden Diskussionen und die sehr gute Zusammenarbeit. Nicht zuletzt gebührt mein Dank meiner Schwester Anja für das Gegenlesen des Manuskripts und ihre sprachliche Expertise.

Allen Kolleginnen und Kollegen des Lehrstuhls möchte ich besonders für die angenehme, professionelle und freundschaftliche Zusammenarbeit danken. An die Zeit am Lehrstuhl werde ich immer sehr gerne zurück denken.

Abstract

Technical processes such as in biological or chemical reactors, magnetohydrodynamic channel flows, or crystallization processes are described by *coupled parabolic partial differential equations*. Typically, these equations are nonlinear and require a proper linear reformulation to be able to apply common control design methods. Due to time dependent reaction kinetics, time-varying spatial domains or by the linearization of a system around a desired trajectory, the equations can be traced back to the class of coupled parabolic systems with space and time dependent coefficients. So far, no constructive controller design methods exist for this system class. Therefore, this thesis considers the backstepping design method for coupled parabolic systems with space and time dependent coefficients on one-dimensional spatial domains and actuation at one or both boundaries of the domain. The backstepping design of a state feedback controller and observer for one-sided actuation and sensing is presented for the general class of coupled parabolic *partial integro-differential-equations* with spatially varying diffusion coefficients, a space and time dependent reaction matrix and time-varying boundary matrices. By a boundedly invertible Volterra-integral transformation, called *backstepping* transformation, the system and observer error dynamics are mapped into a uniformly exponentially stable target system. Due to the invertibility of the transformation, this stability property also applies for the controlled system and the observer error dynamics.

To determine the required controller and observer gains, the so-called kernel equations determining the utilized transformation need to be solved. To this end, they are converted into integral equations, allowing to utilize the method of successive approximations, which provides a systematic, practical tool for the controller and observer determination. Combining observer and state feedback controller leads to an exponentially stable *output-feedback controller* for which the separation property holds.

A natural restriction for the controller performance in applications are input constraints. One way to further increase the decay rate of a controlled system without exceeding these limits is to add additional actuators to dis-

tribute the control effort. In the case of boundary controlled systems, this leads to the *bilateral* case with inputs at both ends of the spatial domain. The backstepping design method for time dependent coupled parabolic systems with bilateral actuation is presented based on a *folding*-transformation, which maps the system into a representation with unilateral, i. e. one-sided actuation. Hence, the usual backstepping transformation can be utilized. An additional Fredholm-type integral transformation is introduced to enable an assignable decay rate in the bilateral case. Applying the folding-transformation requires to introduce certain folding-boundary conditions to ensure the regularity of the solution. These are inherited by the derived kernel equations, resulting in a boundary coupling so that a new procedure for their solution is necessary. By introducing different directions of integrations for the coupled kernel elements, they can be converted into integral equations like in the unilateral case, leading to the same constructive solution procedure.

Kurzzusammenfassung

Viele technische Prozesse, wie in biologischen oder chemischen Reaktoren, magnetohydrodynamische Strömungen oder Kristallisationsprozesse werden durch *verkoppelte parabolische partielle Differentialgleichungen* beschrieben. Diese Gleichungen sind typischerweise nichtlinear und müssen in geeigneter Form linearisiert werden, um vorhandene Entwurfsmethoden anwenden zu können. Aufgrund zeitabhängiger Reaktionskinetiken, zeitabhängigen Ortsbereichen oder der Linearisierung entlang von Solltrajektorien können diese Systeme auf die Klasse der verkoppelten parabolischen Systeme mit orts- und zeitabhängigen Koeffizienten zurückgeführt werden. Hierfür existieren bislang jedoch keine konstruktiven Entwurfsmethoden. Deshalb behandelt diese Arbeit die Backstepping-Methode für verkoppelte parabolische Systeme mit orts- und zeitabhängigen Koeffizienten auf eindimensionalen Ortsbereichen und sowohl ein- als auch beidseitiger Aktuierung. Der Backstepping-Entwurf von Zustandsrückführung und Beobachter für einseitige Aktuierung und Messung wird für die allgemeine Klasse parabolischer *partieller Integro-Differentialgleichungen* mit ortsabhängigen Diffusionskoeffizienten, orts- und zeitabhängigem Reaktionsterm und zeitveränderlichen Randbedingungsmatrizen formuliert. Durch eine beschränkt invertierbare Integral-Transformation, genannt *Backstepping*-Transformation, werden System- und Beobachterfehlerdynamik auf ein gleichmäßig exponentiell stabiles Zielsystem transformiert. Durch die Invertierbarkeit der Transformation ist sichergestellt, dass diese Stabilitätseigenschaft auch für das geregelte System bzw. die Beobachterfehlerdynamik gilt.

Um die zur Stabilisierung benötigten Regler- und Beobachterverstärkungen zu berechnen, müssen die sogenannten Kerngleichungen gelöst werden, welche die beschriebene Transformation festlegen. Hierzu werden sie in Integralgleichungen umgewandelt, welche mit der Methode der *sukzessiven Approximation* gelöst werden können. Dies ergibt ein systematisches und praktikables Werkzeug zur Bestimmung von Zustandsregler und Beobachter. Der durch die Kombination von Zustandsregler und Beobachter entstehende

Ausgangsregler sorgt für die exponentielle Stabilisierung des Systems und erfüllt das Separationsprinzip.

Eine natürliche Grenze für das erzielbare dynamische Verhalten geregelter Systeme stellen Eingangsbeschränkungen dar. Eine Möglichkeit, das Abklingverhalten eines Systems bei vorhandener Stellbegrenzung weiter zu beschleunigen ist das Hinzunehmen zusätzlicher Stellglieder. Bei Systemen mit Randeingriff führt dies zum *bilateralen* Fall, bei dem sich Systemeingänge an beiden Enden des Ortsbereichs befinden. Der Entwurf des bilateralen Zustandsreglers für zeitabhängige verkoppelte parabolische Systeme mit beidseitiger Aktuierung basiert auf einer *Faltungstransformation*, welche das System in eine unilaterale Darstellung, d. h. mit einseitiger Aktuierung, überführt. Dies ermöglicht die Anwendung der bekannten Backstepping-Transformation. Diese wird um eine Fredholm-Integraltransformation ergänzt, um auch im bilateralen Fall eine einstellbare Abklingrate des Systems zu ermöglichen. Das Falten des Ortsbereichs erfordert die Einführung bestimmter Faltungs-Randbedingungen, welche die Regularität der Lösung sicherstellen. Diese finden sich auch in den resultierenden Kerngleichungen wieder und führen zu einer neuen Verkopplung des Kerns am Rand seines Definitionsbereichs, was eine Anpassung der Lösungsstrategie erfordert. Durch die Einführung unterschiedlicher Integrationsrichtungen für die verkoppelten Kernelemente können die Kerngleichungen wie im unilateralen Fall in Integralgleichungen überführt werden, wodurch die gleiche konstruktive Entwurfsmethode ermöglicht wird.

Contents

1 Introduction

Modern controller design approaches for technical systems are based on a mathematical model of the system, abstracting the relevant system behaviour into mathematical equations. Depending on the characteristics of the system under consideration, called *plant*, it may be sufficient to use *ordinary differential equations* (ODEs) to describe the dynamics. However, if the time-behaviour of the system variables is significantly distributed over one or several spatial coordinates, *partial differential equations* (PDEs) are required to represent the system's dynamics. This leads to *distributed-parameter systems* (DPS), describing the system class whose dynamics incorporate at least one PDE.

The main subclasses of DPS derived from the type of the PDE are *parabolic* systems describing balancing processes like heat transfer or matter diffusion, *hyperbolic* systems modelling transport phenomena like time delay, fluid flow or wave propagation and *biharmonic* systems which represent quantities with spatially distributed oscillations appearing for example in flexible mechanical structures. Each of these classes have strong unique characteristics, which cannot be found in one of the other classes. Consequently, the controller design for each of these classes leads to its own theoretical field.

As a common tool to handle DPS, the *abstract* formulation in terms of operators on Hilbert spaces [26] allows to describe such systems by a state-space representation. In contrast to ODEs, the state belongs to a suitable infinite-dimensional function space rather than to a finite-dimensional vector space and, in the linear case, the system operator is not a matrix but a differential operator. This provides the basis for various controller design methods for DPS, where especially optimal control by solving Riccati-equations [67] and modal approaches [16, 32, 102] turned out to be effective.

If the inputs and outputs of the DPS are distributed over the spatial domain, the abstract description leads to *bounded* operators in the state space representation. Then, the controller and observer design methods become similar to the finite-dimensional case, which has been studied intensely during the 80s (see e. g. [8] and the contained references). In practice, however, many

DPS can only interact with their environment through their boundary. This leads to *unbounded* operators in the abstract representation, rising new mathematical challenges. In particular, the application of the state space method in the framework of *regular linear systems* [105, 106] or *boundary control systems* [26, 89] requires a strong mathematical background on functional analysis and operator theory.

The second widespread class of methods can be described as *PDE-based*, meaning that they directly consider the PDE rather than its abstract representation. The most important approaches in this fields are either based on the extension of Lyapunov's theory for PDEs [71, 76] or the *backstepping* method [63].

Transformation-based design methods or *normal form approaches* are very common in control theory, especially in the field of nonlinear [52, 53, 61] or time-varying systems [90]. As an extension of the backstepping method for ODEs, PDE-backstepping [63] is such a normal form approach[1] as well, making its success not surprising at first glance. The astonishing fact, however, is its power despite its simplicity. The first important fact is that due to the structure of the utilized transformation in form of a *Volterra-integral transformation*, structural invertibility is always ensured. Moreover, while ODEs must mostly be of a certain structure to be able to apply a specific normal form transformation, it turned out that most PDEs with boundary actuation or sensing appearing in applications automatically have the required structure to be able to apply backstepping. This becomes apparent when having a short look on the history of PDE-backstepping.

1.1 The origin of infinite-dimensional backstepping

The terminology *backstepping*[2] was initially introduced by [58] and the related works as a method for the control design of a certain class of nonlinear ODEs which are at least *strict-feedback*[3] systems and is explained in detail in [64]. Described in a simplified manner, these systems contain a chain of integrators exciting an input-affine system. Now the idea is to use the output, say ξ_1, of the integrator chain as a *virtual input* for the affine system and to determine its value to stabilize the affine system as a nonlinear function $\varphi(x)$ of the states x. Then, „stepping back" one step in the integrator chain, the input of

[1] An interesting interpretation of the backstepping transformation was established in [35] by showing that it can be seen as an infinite-dimensional map into *controller canonical form*.

[2] In detail, this was called *integrator backstepping*.

[3] To be precise, the systems must at least be *block-strict-feedback* systems. The so-called *pure-feedback* and *strict-feedback* systems are subclasses thereof.

the last integrator, ξ_2 is considered as virtual input to control the output ξ_1 of the integrator chain to the desired calculated stabilizing function $\varphi(x)$. To this end, new coordinates $z_1 = \xi_1 - \varphi(x)$ describing the deviation of ξ_1 and its desired value are introduced, which need to be stabilized, i. e. controlled to zero. This *backstepping* is repeated consecutively until the actual input of the integrator chain is determined as a function of the original states x, which is the control law.

This method gained vast popularity, since it allowed to obtain explicit stabilizing feedback laws and provided the ability to include perturbations, disturbances and unmodelled dynamics [9] as the stabilization is proved by the help of Lyapunov-functions. In addition, it can be combined with adaptive control [64]. On the other hand, the restriction to strict-feedback systems is no obstacle for many applications. Therefore, great efforts to generalize this method to PDEs began at the beginning of this century in the research group of M. Krstic [9, 10, 12–15, 69].

The first ideas in this direction started by a finite-difference discretization of a parabolic PDE [9]. Realizing that the resulting ODEs have the required strict-feedback form, ODE-backstepping could be applied. However, since this leads to an eigenvalue placement for all eigenvalues, the controller gains tend to infinity with increasing approximation order. The authors understood that the ODE-backstepping changes the parabolic character of the equation and that a suitable transformation needed to preserve it. Therefore, the target system of the transformation is the key which needs to be chosen different to the ODE-backstepping case and is later called the „subtle difference between ODE backstepping and PDE backstepping“ [63]. Setting the finite-difference approximation of a stable heat equation as the target system of the transformation, they now determined a finite-dimensional invertible transformation between the approximations. It turns out that this transformation is calculated recursively with highly oscillating and non-converging elements. However, the resulting control law has an existing bounded limit when the approximation order goes to infinity. The transformation matrix has a lower triangular structure, as known from ODE-backstepping. Extended to infinite dimensions, the limit of this transformation is a *Volterra-integral transformation*. Showing that it is possible by principle to stabilize the system with a change of coordinates that is such a transformation paved the way for the actual infinite-dimensional backstepping.

Due to the structure of the Volterra-integral transformation, it can be regarded as an infinite-dimensional transformation matrix that has a lower-triangular structure with ones on the main diagonal. The entries below the

main diagonal correspond to the values of the *kernel* of the transformation. It is obvious that such a matrix is invertible by principle, which can be seen as the outstanding property of the PDE-backstepping transformation.

The subsequent works [69, 79, 81] were the first to consider this problem more generally and introduced the backstepping method in its form to which it is known nowadays. The backstepping transformation is formulated as a map of the original system into a suitably chosen target system with stable dynamics and the same differential operator as the original system. Comparing original and target system in combination with the utilized transformation, conditions on the kernel of the transformation are derived. They consist of a PDE with a hyperbolic differential operator[4] and rather uncommon BCs forming a *boundary value problem* (BVP) for the kernel, called *kernel equations*.

With this approach, the stabilization problem is turned into the solvability analysis of the kernel equations. These are converted into integral equations, which can be solved by fixed-point iteration. Having proved the uniform convergence of this iteration, a series truncation can be applied, allowing the *successive approximation* of the solution, which provides a practical tool for the explicit or numerical calculation of the kernel.

In fact, [22, 23, 78] had already considered these problems long before, but only for the purpose of analysing the well-posedness of initial boundary value problems (IBVPs) for parabolic PDEs with spatially and temporally varying coefficients. Thus, they were „rather poorly-known“ [93] to the control community so that [69] independently discovered the ideas for the backstepping design[5]. With these results, the modern PDE-backstepping was born as the starting point for generalizations into various different directions. Though it has not much in common with the original ODE-backstepping except that the structure of the transformation can be regarded as triangular in both cases and that it is a transformation into a stable target system, the inventors kept the name *backstepping* to emphasize the analogy [63, Ch. 4.10].

To put it in a nutshell, the backstepping method for PDEs can be seen as a transformation-based design procedure for boundary controlled DPS. It turned out especially successful due to its explicit calculations, requiring a comparably low amount of mathematical background.

[4] In physics, the appearing PDE is known as Klein-Gordon equation.

[5] The work of Smyshlyaev [79] which is based on [69] is the first who cites [23, 78]. His extension to time-varying systems [81] is the first to actually utilize the results of [23].

1.2 Contribution

The birth of PDE-backstepping not only gave rise to numerous considered applications including observer design [80], systems with Volterra-nonlinearities [94, 95], higher-order spatial domains [55, 72], output regulation [33], robust output regulation [28], control of the Schrödinger-equation [109] or finite-time stabilization [24, 83]. It was also generalized to time dependent coefficients [73, 81, 100], motivated by various applications such as time-varying spatial domains [54, 62], state-of-charge estimation in lithium-ion batteries [85] or chemical reactors with time dependent reaction kinetics [2]. Moreover, time dependent coefficients appear when linearizing a nonlinear system around a desired trajectory, e. g. when applying flatness-based tracking control [73]. A more detailed overview of different applications of backstepping can be found in [93].

The backstepping control of *coupled* parabolic systems has been in the research focus especially for the past five years. Though [1, 99] already examined systems of two coupled parabolic PDEs with constant and equal diffusion coefficients, it took some time until the considered system class was further extended. Inspired by the results achieved for hyperbolic systems [25, 36, 37], where coupled systems arise naturally in applications as well, [5, 6] generalized the controller and observer design to n coupled parabolic systems with constant parameters and equal diffusion coefficients. In this case, the matrix-valued kernel has a diagonal structure with equal entries, so that the kernel equations to be solved are the same as in the scalar case. Subsequently, [7, 68, 74] extended the setup to distinct diffusion coefficients, where the solvability of the appearing kernel equations can only be ensured if the structure of the target system is restricted. Choosing a target system with the same couplings as in the original system allows to trace the solution back to the scalar case again. This idea was applied in several applications like sliding mode control [46] or the backstepping observer design for coupled semi-linear parabolic systems with constant coefficients [43]. By including the time-dependent nonlinearity in the target system, solving the kernel equations with the results from the scalar case is directly possible in the latter reference. However, the method is not capable to handle spatially varying coefficients.

In the meantime, the case of coupled hyperbolic systems, which is still an active research topic, was studied intensely in numerous contributions (see [3, 4, 24, 29–31, 34, 39, 42, 65, 84]). The results of [50, 51] in this field provided new ideas for the generalization of the backstepping method in the parabolic case. Thus, the very general setup of coupled parabolic PDEs with

distinct diffusion coefficients, when all parameters are spatially varying was considered by [98]. Here, the authors achieved the required structure of the target system to obtain solvable kernel equations by a local coupling term with strictly lower-triangular structure. The resulting kernel equations can no more be traced back to the scalar case but are transformed into the form in which they appear during the backstepping design of hyperbolic systems, whose solvability has already been shown in [50, 51]. Based on these results, [17, 18] presented the corresponding observer design for two and n coupled systems, respectively. Therein, [18] further simplified the target system to eliminate all appearing couplings by a Fredholm-type integral transformation.

However, since the kernel equations in the scalar parabolic case [79] had been solved without a backtrace to the hyperbolic case, the generalization of this *direct* solution to the case of coupled systems was still of particular interest. The first idea to this solution was given in [111] for PDEs with constant diffusion coefficients. Then, [113] provided the direct solution of the kernel equations for general *partial integro-differential equations* (PIDEs), with spatially varying, distinct diffusion coefficients. This is the direct extension of the original result [79] to coupled systems and provides the basis for further considerations like observer-based output regulation [114] and robust output regulation [115]. Just like in [79], the kernel equations are converted into integral equations and solved by fixed-point iteration.

This thesis covers the extension of the backstepping method to the class of coupled parabolic systems with space and time dependent coefficients. While the control of time-varying systems is a rather difficult subject even for ODEs, where plenty of results are available, hardly anything can be found for DPS. Particularly, operator-theory becomes significantly more complicated and is less founded as in the time-invariant case. Moreover, there exists no modal decomposition of the time-varying system operator. On the other hand, a completely different approach in control theory for DPS is to create a finite-dimensional approximation of the system, which can be handled by standard control methods for ODEs rather then designing a controller for the DPS. This *early-lumping* approach is widespread in practical applications. In the time dependent case, it leads to a time-varying approximation model of probably high order. The theory of stabilizing time-varying ODEs, however, suffers under the fact that it may become computationally and numerically problematic for high system orders [90, 91]. Therefore, the controller design for the system class in question is a very challenging task and it is of great interest to determine realizable solutions to this problem.

With the direct solution of the kernel equations in [113], the basis for the extension to the time-varying case was built. This was finally presented in [118] for coupled PDEs with Robin BCs.

The second main contribution of this thesis is the *bilateral* backstepping control of coupled parabolic systems. The first work in this direction was presented in [97], where the backstepping method on balls of arbitrary dimension with actuation on their whole boundary was introduced. This inspired the work [96] on scalar parabolic systems actuated at both ends of their domain, called *bilateral* case, since this is nothing else than a one-dimensional ball. It was shown that there are two possibilities to include bilateral actuation in the backstepping design. The first one is to apply a symmetric backstepping transformation which results in different kernel equations as in the unilateral case and the second one is to apply a certain *folding* transformation to map the system into a form with unilateral actuation, to be able to apply the standard backstepping transformation. In the scalar case, the resulting system then consists of two coupled PDEs, where the results for coupled systems come into play. This was further studied in [19, 20], where it was shown that the *folding point* can be used as a design parameter to influence the distribution of the control effort between the inputs. These approaches are based on the transformation of the kernel equations into the form in which they appear in the hyperbolic case like in [98]. Due to the folding transformation, the kernel is coupled by special *folding BCs*, requiring significant changes in the solution procedure of the kernel equations.

Rather than using the hyperbolic results, [113] provided the basis to tackle the bilateral problem with a direct solution of the kernel equations. With this, the extension of the folding technique to coupled parabolic PDEs works in a straightforward fashion and is presented in [117].

Therefore, there are two main contributions of the present thesis. The first one is the extension of the unilateral backstepping control method to the controller and observer design of coupled parabolic PIDEs with space and time dependent coefficients. As already mentioned, some of the results to this problem have been published in [118] but are further extended in view of integral terms, general BCs, possibly equal diffusion coefficients and the time-varying observer design.

The second contribution is the bilateral backstepping design method for time-varying coupled parabolic PDEs, where the time-invariant case has mainly been published in [117].

In the unilateral case, the classical Volterra-type backstepping transformation is enough to map the original time-varying system into a set of time-

invariant systems with time dependent couplings and a *cascade* structure, allowing an explicit prescription of the uniform convergence of the closed-loop system, which is a very strong property for time-varying DPS. To achieve the same in the bilateral case, a second, combined *Volterra-Fredholm-type transformation* is applied, which is the generalization of the one presented in [20]. The kernel equations are converted into integral equations in both cases, allowing the solution by *fixed-point iteration*, which is shown to converge uniformly. This provides the piecewise classical solution of the kernel equations even for non-analytic system parameters of certain *Gevrey classes* and a practical tool for the kernel calculation.

Hence, this thesis provides a systematic approach for the controller and observer design for a broad class of coupled parabolic systems. The obtained methods can be the starting point for further applications such as output regulation, fault detection, the consideration of ODE-actuation and -sensing, adaptive control or flatness-based control.

1.3 Outline of the thesis

In *Chapter 2*, the backstepping method is extended to the design of state feedback controllers for coupled parabolic PIDEs with space and time dependent reaction, spatially varying diffusion and general boundary conditions (BCs). After the introduction of the considered system class, the target system is introduced with appropriate local coupling terms ensuring the solvability of the kernel equations. They are derived subsequently together with the control law. The closed-loop stability is proved on basis of the stability of the target system and the invertibility of the backstepping transformation. The main part of the chapter is devoted to the solvability analysis of the kernel equations. This is performed by a sequence of transformation, mapping them into integral equations. The convergence of their solving fixed-point iteration is shown, providing the method of *successive approximations* as a practical solution tool. For the computation of the controller gains, the spatial derivative of the kernel needs to be calculated. To avoid numerical deviations, a systematic procedure based on another fixed-point iteration is presented. Finally, simulation results confirm the applicability of the proposed design method.

Chapter 3 presents the observer design for the considered system class with boundary measurement, which can be regarded as dual to the state feedback controller design. After the construction of the observer, the observer gains and kernel equations are briefly derived. The solution of the kernel equations is established by a duality transformation, mapping them into the represen-

tation of the state feedback controller's kernel equations. After the stability of the observer error dynamics is proved, simulations demonstrate the functionality of the observer. Finally, the combination of the designed observer with a state feedback controller of Chapter 2 resulting in an *output-feedback controller* is proved to fulfil the *separation property*, which is again validated by simulations.

The backstepping design for systems with bilateral actuation is the subject of *Chapter 4*. This is handled by a *folding transformation* mapping the system into a representation with unilateral actuation. Its introduction is followed by the presentation of the applied two-step transformation approach and the resulting target system, the stabilizing control law and the proof of closed-loop stability. The subsequent solvability analysis of the appearing kernel equations is again based on a conversion into integral equations, which requires significant changes compared to Chapter 2 due to the appearing folding BCs and the new type of transformation. The spatial derivatives of the kernel, needed for the control law, can again be calculated without performing a numerical differentiation. Thereafter, the backstepping design of an observer for in-domain measurements is shortly discussed to introduce the folding method as the basis for the observer-design. Finally, simulation results for both bilateral state feedback controllers and the considered observers, as well as the combination of both, verify the applicability of the proposed methods.

A brief summary of the presented methods and an outlook on possible continuative research fields will conclude the thesis.

1.4 Remarks on notation

Derivatives

For the sake of readability, different notations for derivatives are used, inspired by the reader-friendly notation in [63]. Lagrange's notation for the derivative of one-variable functions $f'(x) = \frac{\mathrm{d}}{\mathrm{d}x} f(x)$ and Newton's notation $\dot{x}(t) = \frac{\mathrm{d}}{\mathrm{d}t} x(t)$ for the time derivative are complemented by the short forms $\partial_x = \frac{\partial}{\partial x}$, $\mathrm{d}_x = \frac{\mathrm{d}}{\mathrm{d}x}$, as well as index notation for partial and ordinary derivatives, i. e. $f_x(t,x) = \partial_x f(t,x)$ and $(f(z,t)x(t))_t = \mathrm{d}_t(f(z,t)x(t))$. If the differentiated variable is not obvious by context, it corresponds to the one in the definition of the function. For example, if $f : (x,y) \mapsto f(x,y)$, then $f_x(x,x) = f_x(x,y)|_{y=x} = \frac{\partial f(x,y)}{\partial x}|_{y=x}$.

Conditional expressions
To symbolize that an expression is only valid or existent under some conditions, brackets with subscripts are used. As example

$$[f]_{\substack{a > b \\ c < d}}$$

means that f is only valid for $a > b$ and $c < d$. If $a \not> b$ or $c \not< d$, the expression is treated as non-existent.

Well-posedness
For notational convenience, systems are called *well-posed* which means that the abstract initial value problem related to the system is well-posed in the sense of Hadamard (see e. g. [26, Ch. 2.1]).

Function spaces
The symbol $L_2(a, b)$ denotes the vector space of absolutely square Lebesgue integrable functions on a closed domain $[a, b]$. If L_2 is equipped with a suitable inner product it becomes a Hilbert space. A subset of L_2 with existing weak second order derivatives is denoted by the Sobolev space H^2, i. e. $h \in H^2(a, b) \leftrightarrow \{h \in L_2(a, b) | h, h' \text{ abs. continuous}, h'' \in L_2(a, b)\}$.

2 Backstepping state feedback control design for coupled parabolic PIDEs

In this chapter, the design of a stabilizing state feedback controller for systems of coupled parabolic *partial integro-differential equations* (PIDEs) with boundary inputs is presented. The considered system class is introduced in the next section, followed by the applied backstepping transformation and the selection of the target system. Subsequently, the control law and the kernel equations are derived. In Section 2.4, the stability of the closed-loop system is verified by showing uniform exponential stability of the target system, as well as the bounded invertibility of the backstepping transformation. The largest part of the chapter is dedicated to the solvability of the kernel equations, proved in Section 2.5, followed by the computation of the kernel derivatives in Section 2.6, which are needed to realize the control law. Finally, Section 2.7 provides simulation results confirming the effectiveness of the proposed control design method.

2.1 Problem formulation

The coupled parabolic systems with space and time dependent coefficients under consideration are described by the PIDEs

$$\begin{aligned} x_t(z,t) = (\Lambda(z)x_z(z,t))_z + \widetilde{\Phi}(z,t)x_z(z,t) + A(z,t)x(z,t) \\ + A_0(z,t)x(0,t) + \int_0^z F(z,\zeta,t)x(\zeta,t)\mathrm{d}\zeta \end{aligned} \tag{2.1}$$

on the domain $z \in (0,1)$, $t \in \mathbb{R}_{t_0}^+ = \{t \in \mathbb{R} : t > t_0\}$, $t_0 \in \mathbb{R}_0^+$, with the initial conditions (ICs) $x(z,t_0) = x_0(z)$. Here, $x(z,t) = \mathrm{col}(x_1(z,t),\dots,x_n(z,t)) \in \mathbb{R}^n$, $n \in \mathbb{N}$, is the state vector depending on the independent variables $z \in [0,1]$, interpreted as *space* and $t \geq t_0$, interpreted as *time*. The operator col describes a column vector of its arguments. Imagining a number line reaching from left to right, the boundaries $z = 0$ and $z = 1$ are called left and right, respectively. Basically, the spatial domain can have an arbitrary

length but it is well-known that it can always be mapped to $[0, 1]$ by a suitable norming transformation (see e. g. [82]).

In most scenarios, the elements of the state vector represent physical values such as certain mass concentrations or temperatures. The first term on the right-hand side of (2.1) describes a corresponding process like matter diffusion or heat conduction and may for example be obtained by using either Fick's law of diffusion or Fourier's law of heat conduction in combination with the continuity equation [47]. Consequently, $\Lambda(z) = \mathrm{diag}(\lambda_1(z), \ldots, \lambda_n(z))$, $\lambda_i(z) \in \mathbb{R}^+$, contains the diffusion or heat conduction coefficients for the single elements of the state vector and is called *diffusion matrix*[1]. From a mathematical point of view, it is reasonable to perform the outer differentiation so that the resulting PIDE reads

$$x_t(z,t) = \Lambda(z)x_{zz}(z,t) + \underbrace{(\Lambda'(z) + \widetilde{\Phi}(z,t))}_{\Phi(z,t)} x_z(z,t) + A(z,t)x(z,t) + A_0(z,t)x(0,t) + \int_0^z F(z,\zeta,t)x(\zeta,t)\mathrm{d}\zeta, \tag{2.2}$$

which is the most common form of describing parabolic PIDEs in the context of control. The second term on the right-hand side of (2.1) often describes an advection process, that is the change of a quantity by matter transport. Thus, the *advection matrix* $\widetilde{\Phi}(z,t) = \mathrm{diag}(\tilde{\phi}_1(z,t), \ldots, \tilde{\phi}_n(z,t))$, $\tilde{\phi}_i(z,t) \in \mathbb{R}$ contains the transport velocities for the different states. In (2.2), the coefficient matrix $\Phi(z,t) = \mathrm{diag}(\phi_1(z,t), \ldots, \phi_n(z,t))$ with $\phi_i(z,t) = \lambda_i'(z) + \tilde{\phi}_i(z,t)$ now depends on the diffusion and the advection coefficients, but for convenience will simply be called advection matrix.

The *reaction matrix* $A(z,t) \in \mathbb{R}^{n\times n}$ may be fully occupied and describes the main interaction between the different states. Its source depends on the physical background of the system, but for the example of a chemical reactor, it is obtained by a linearization of the reaction rate which depends on concentrations and temperature. Even for scalar diffusion-advection-reaction equations, i. e. with only a single state, this parameter may lead to instability and is the main motivation for applying a stabilizing controller.

Allowing the *local coupling term* $A_0(z,t)x(0,t)$ with $A_0(z,t) \in \mathbb{R}^{n\times n}$ and the *integral term* $\int_0^z F(z,\zeta,t)x(\zeta,t)\mathrm{d}\zeta$ with $F(z,\zeta) \in \mathbb{R}^{n\times n}$, further enlarges the class of considered systems. As an example, the modelling of crystalliza-

[1] It is also possible to apply the presented backstepping method to systems with time dependent diffusivity. However, as this coefficient remains time dependent in the target system, its stability analysis is strongly impeded.

tion processes [21] or the coupling of a hyperbolic fast subsystem [111] leads to such integral terms.

Depending on the physical origin of the modelled system, (2.2) may be equipped with different types of *boundary conditions* (BCs). Interpreting the state as a temperature, the most natural BC is a heat transfer or insulation, which is described by a Robin-type BC, short *Robin BC*, $x_{i,z}(z_b,t) = q_i^{z_b}(t)x_i(z_b,t)$, $z_b \in \{0,1\}$, where $q_i^{z_b}(t) \in \mathbb{R}$ is the heat transfer coefficient (which equals zero for insulation, leading to a *Neumann BC*). However, it may also be reasonable to include Dirichlet-type BCs, again short *Dirichlet BCs*, i. e. $x(z_b,t) = 0$, for example if the state is a mass concentration which can explicitly be set at the boundary. Indeed, even the combination of both types of BCs for different elements of the state vector may be required, which will be called *mixed BCs*[2]. Assuming that at the left boundary, the first m states of the system are subject to Dirichlet BCs and the remaining $p = n - m$ states suffice Robin BCs, they can be written as

$$E_1^\top x(0,t) = 0 \tag{2.3a}$$

$$E_2^\top x_z(0,t) = Q_0(t)E_2^\top x(0,t) \tag{2.3b}$$

with

$$E_1 = \begin{bmatrix} I_m \\ 0 \end{bmatrix} \quad \text{and} \quad E_2 = \begin{bmatrix} 0 \\ I_p \end{bmatrix}, \quad E_1E_1^\top + E_2E_2^\top = I. \tag{2.4}$$

The matrix

$$Q_0(t) = \operatorname{diag}(q_{m+1}^0(t), \dots, q_n^0(t)) \in \mathbb{R}^{p\times p} \tag{2.5}$$

of the heat transfer coefficients $q_i^0(t)$ needs to be a diagonal matrix. This means that no couplings at the left boundary are considered. Their indices $(m+1,\dots,n)$ are chosen such that they correspond to the respective state indices. Obviously, the states can always be ordered in a way such that the structure (2.3) is achieved.

Remark 2.1.1. It is also possible to handle arbitrary, i. e. non-diagonal matrices $Q_0(t)$ at the left boundary with the presented method, but the couplings cannot be eliminated by the backstepping transformation in the case of mutually different diffusion coefficients. Thus, they need to be included in the target system, requiring a different method for the stability proof (see e. g. [98]). The only exception are states with equal diffusion coefficients, which

[2] In some references, Robin BCs are referred to as mixed BCs [86], which is confusing in the case of systems with multiple states, i. e. multiple BCs.

can be coupled at the left boundary. Being a very specific case, it is excluded here. ◁

To provide a compact notation, (2.3) can be equivalently written as

$$(\theta_0(t)x(t))(0) = 0 \tag{2.6a}$$

with the formal matrix differential operator

$$\theta_0(t)h = E_2E_2^\top h_z + \underbrace{(E_1E_1^\top - E_2Q_0(t)E_2^\top)}_{B_0^d(t)}h. \tag{2.6b}$$

At the right boundary, it is assumed that the system can be actuated. Thus, the corresponding BC reads

$$(\theta_1(t)x(t))(1) = u(t) \tag{2.7a}$$

with

$$\theta_1(t)h = B_1^n h_z + B_1^d(t)h \tag{2.7b}$$

wherein the diagonal matrix $B_1^n \in \mathbb{R}^{n\times n}$ may only have ones or zeros as entries[3] and $B_1^d(t) \in \mathbb{R}^{n\times n}$ is an arbitrary matrix. Of course the diagonal elements $B_{1,ii}^n$ and $B_{1,ii}^d(t)$ cannot both be zero, since this would imply no BC for the state x_i. Moreover, it is assumed that if $B_{1,ii}^n = 0$ then $B_{1,ii}^d(t) = 1$, which is always possible via dividing the corresponding row in $B_1^d(t)$ by $B_{1,ii}^d(t)$.

Remark 2.1.2. Since the right boundary is subject to the actuation, the corresponding BC does not affect the backstepping transformation. Therefore, θ_1 may basically be any bounded functional. Specifying homogeneous Dirichlet-BCs in the target system allows the determination of the control law in the same way (see [72]). The choice (2.7b) is made because it is most likely to appear in technical applications. ◁

Depending on the matrices B_1^n and $B_1^d(t)$ in (2.7b), there are $m_1 \leq n$ Dirichlet BCs, and $p_1 = n - m_1$ Robin BCs on the right boundary. Consequently, there always exists a permuted vector $x^*(z,t) = Px(z,t)$ with $P^\top = P^{-1}$ such that with the permuted input $u^*(t) = Pu(t)$ the right BC reads

$$\bar{E}_1^\top x^*(1,t) = \bar{E}_1^\top u^*(t) \tag{2.8a}$$

$$\bar{E}_2^\top x_z^*(1,t) = Q_1(t)\bar{E}_2^\top x^*(1,t) + \bar{E}_2^\top u^*(t), \tag{2.8b}$$

[3] The BC can always be reformulated such that this condition is fulfilled.

where $\bar{E}_1^\top = \begin{bmatrix} I_{m_1} & 0 \end{bmatrix}$, $\bar{E}_2^\top = \begin{bmatrix} 0 & I_{p_1} \end{bmatrix}$ with $\bar{E}_1\bar{E}_1^\top + \bar{E}_2\bar{E}_2^\top = I$. Therein, $Q_1(t) \in \mathbb{R}^{p_1 \times p_1}$ is an arbitrary matrix. Inserting the permutation, (2.8) can be written as

$$\underbrace{\bar{E}_1^\top P}_{S_d^\top} x(1,t) = \underbrace{\bar{E}_1^\top P}_{S_d^\top} u(t) \tag{2.9a}$$

$$\underbrace{\bar{E}_2^\top P}_{S_r^\top} x_z(1,t) = Q_1(t) \underbrace{\bar{E}_2^\top P}_{S_r^\top} x(1,t) + \underbrace{\bar{E}_2^\top P}_{S_r^\top} u(t), \tag{2.9b}$$

where the matrices $S_d^\top \in \mathbb{R}^{m_1 \times n}$ and $S_r^\top \in \mathbb{R}^{p_1 \times n}$ select the states with Dirichlet, respectively Robin BCs at the right boundary out of the original state vector, so that $S_d S_d^\top + S_r S_r^\top = I$. Consequently, an even more compact, equivalent representation of the right BC (2.7) is

$$\underbrace{\left(S_d S_d^\top - S_r Q_1(t) S_r^\top\right) x(1,t) + S_r S_r^\top x_z(1,t)}_{(\theta_1(t)x(t))(1)} = u(t). \tag{2.10}$$

For a successful backstepping design, the parameters of the plant must fulfil some regularity assumptions. In view of the spatial coordinate z, the order of required differentiability follows from the upmost derivative that is needed at some point in the design or analysis. In respect of t, it will be shown that the coefficients need to be smooth functions, i. e. there exist infinitely many derivatives. Moreover, as the coefficients may originate from a linearization of a nonlinear system around a desired trajectory (see e. g. [73, 101]), it is eligible to allow non-analytic functions of time. This is done with the following definition (see [118]). However, note that designs based on a linearization need to be handled with care in the infinite-dimensional case. In particular, the stability of the linearization at an equilibrium does not automatically imply the stability of the original system in a neighbourhood of the equilibrium. This is further analysed in [56].

Definition 2.1.3 (Gevrey classes). A function $f \in C^\infty(\mathbb{R}_{t_0}^+)$ is said to be of *Gevrey class* $G_\alpha(\mathbb{R}_{t_0}^+)$ with *Gevrey order* α if for every closed interval $\mathcal{I} \subset \mathbb{R}_{t_0}^+$, there exists a constant $D > 0$ such that

$$\sup_{t \in \mathcal{I}} |\mathrm{d}_t^q f(t)| \leq D^{q+1}(q!)^\alpha, \quad \forall q \in \mathbb{N}_0 \tag{2.11}$$

holds (see [72, Def. B.1]). ◀

Note that f is real analytic for $\alpha = 1$ and non-analytic for $\alpha > 1$. As will be seen in Section 2.5.6, all system parameters must have a Gevrey order

$\alpha \in [1,2)$ w. r. t. t, in order to ensure the solvability of the kernel equations for the considered system class.

Remark 2.1.4. Using flatness-based trajectory planning [73] requires the planned trajectories to be of Gevrey order $\alpha \in (1,2]$. Consequently, there exist possible trajectories with $\alpha \in [1,2)$ leading to system parameters with the same regularity. ◁

Together with the spatial requirements, the regularity assumptions are summed up as follows.

Assumption 2.1.5 (Regularity of the system parameters). The parameters of the system are assumed to fulfil

$$\lambda_i \in C^2[0,1] \tag{2.12a}$$
$$\Phi(\cdot,t), A(\cdot,t), A_0(\cdot,t) \in (C[0,1])^{n\times n} \tag{2.12b}$$
$$\Phi(z,\cdot), A(z,\cdot), A_0(z,\cdot) \in (G_\alpha(\mathbb{R}^+_{t_0}))^{n\times n} \tag{2.12c}$$
$$F(\cdot,\cdot,t) \in (C([0,1]^2))^{n\times n} \tag{2.12d}$$
$$F(z,\zeta,\cdot) \in (G_\alpha(\mathbb{R}^+_{t_0}))^{n\times n} \tag{2.12e}$$
$$B_0^d \in (G_\alpha(\mathbb{R}^+_{t_0}))^{n\times n} \tag{2.12f}$$

with $\alpha \in [1,2)$. ◀

Note that according to (2.11), $G_{\alpha_1}(\mathbb{R}^+_{t_0}) \subset G_{\alpha_2}(\mathbb{R}^+_{t_0})$ if $\alpha_1 < \alpha_2$, so that in the case of system parameters with different Gevrey orders α_i, all parameters belong to the Grevrey class with the largest Gevrey order $\alpha = \max(\alpha_i)$.

For the backstepping design, it makes a big difference if the diffusion coefficients λ_i are equal or not. Both cases may be handled with the presented method. However, in the case of spatially varying coefficients, it may be possible that they intersect only at some points z_i. This leads to a completely new setup for which the ideas of [88] in the scalar case are of interest, but lies beyond the scope of this work. Therefore, the following assumption is made.

Assumption 2.1.6 (Diffusion coefficients). The diffusion coefficients are strictly positive and can only be equal or completely different. This means that only

$$\lambda_i(z) > 0 \quad \forall z \in [0,1] \tag{2.13a}$$

and

$$\lambda_i(z) \equiv \lambda_j(z) \quad \forall z \in [0,1], \text{ or} \tag{2.13b}$$
$$\lambda_i(z) \neq \lambda_j(z) \quad \forall z \in [0,1] \tag{2.13c}$$

may hold for $i, j = 1, \dots, n$. Consequently, the expression $\lambda_i < \lambda_j$ is introduced as a shorthand form for $\lambda_i(z) < \lambda_j(z)$, $\forall z \in [0,1]$. The same holds for other relations. ◀

Due to the diagonality of Λ and Φ, the advection term can always be eliminated by applying the boundedly invertible *Hopf-Cole-type state transformation*

$$\breve{x}(z,t) = \underbrace{\exp\left(\tfrac{1}{2}\int_0^z \Lambda^{-1}(\zeta)(\Lambda'(\zeta) + \Phi(\zeta,t))\mathrm{d}\zeta\right)}_{H(z,t)} x(z,t), \tag{2.14}$$

introduced in [49]. Differentiating (2.14) twice w. r. t. z and inserting the result in the time derivative $\breve{x}_t(z,t)$ yields the new dynamics

$$\begin{aligned}
\breve{x}_t(z,t) &= \Lambda(z)\breve{x}_{zz}(z,t) + \Big(\tfrac{1}{2}\Lambda^{-1}(z)\Lambda'(z)\Phi(z,t) - \tfrac{1}{2}\Phi'(z) + A(z,t) \\
&\quad - \tfrac{1}{4}\Lambda^{-1}(z)\Phi^2(z,t) + \tfrac{1}{2}\int_0^z \Lambda^{-1}(\zeta)\Phi_t(\zeta,t)\mathrm{d}\zeta\Big)\breve{x}(z,t) \\
&\quad + H(z,t)A_0(z,t)\breve{x}(0,t) + \int_0^z H(z,t)F(z,\zeta,t)H^{-1}(\zeta,t)\breve{x}(\zeta,t)\mathrm{d}\zeta \\
&= \Lambda(z)x_{zz}(z,t) + \breve{A}(z,t)x(z,t) \\
&\quad + \breve{A}_0(z,t)x(0,t) + \int_0^z \breve{F}(z,\zeta,t)x(\zeta,t)\mathrm{d}\zeta.
\end{aligned} \tag{2.15}$$

Applying (2.14) to the BCs leads to

$$\breve{\theta}_0(t)[\breve{x}(t)](0) = 0 \tag{2.16a}$$
$$\breve{\theta}_1(t)[\breve{x}(t)](1) = \breve{u}(t) \tag{2.16b}$$

with $\breve{u}(t) = H(1,t)u(t)$. The boundary operators read

$$\breve{\theta}_i(t)h = B_i^n h_z + \breve{B}_i^d(t)h, \quad i = 0, 1, \tag{2.17}$$

where

$$\breve{B}_0^d(t) = \begin{bmatrix} I_m & 0 \\ 0 & -\breve{Q}_0(t) \end{bmatrix} \tag{2.18}$$

and $\breve{Q}_0(t) = \mathrm{diag}(\breve{q}_{m+1}(t), \dots, \breve{q}_n(t))$ as well as

$$\breve{q}_i(t) = H_{ii}(1,t)(\tfrac{1}{2}\lambda_i^{-1}(1)\phi_i(1,t) + q_i^0(t)), \quad i = m+1, \dots, n. \tag{2.19}$$

Since the matrix $B_1^d(t)$ in (2.7b) can be fully occupied, the right boundary needs a distinction of cases. Denote by $b_i^\top$ and $\breve{b}_i^\top$ the row vectors of $B_1^d(t)$ and $\breve{B}_1^d(t)$, respectively, i. e. $B_1^d(t) = \operatorname{col}(b_1(t), \dots, b_n(t))$ and $\breve{B}_1^d(t) = \operatorname{col}(\breve{b}_1(t), \dots, \breve{b}_n(t))$. Then

$$\breve{b}_i^\top(t) = \begin{cases} H_{ii}(1,t)b_i^\top(t)H^{-1}(1,t) - \frac{1}{2}\lambda_i^{-1}(1)\phi_i(1,t), & B_{1,ii}^n = 1 \text{ (Robin)} \\ H_{ii}(1,t)b_i^\top(t)H^{-1}(1,t), & B_{1,ii}^n = 0 \text{ (Dirichlet).} \end{cases} \tag{2.20a}$$

As a consequence of this transformation, the resulting system has the same structure as (2.2) with (2.6) and (2.7), except that the advection term $\Phi(z,t)x(z,t)$ is eliminated. Therefore, it can be neglected without loss of generality.

In summary, the considered system class reads

$$\begin{aligned} x_t(z,t) &= \Lambda(z)x_{zz}(z,t) + A(z,t)x(z,t) \\ &\quad + A_0(z,t)x(0,t) + \int_0^z F(z,\zeta,t)x(\zeta,t)\mathrm{d}\zeta \end{aligned} \tag{2.21a}$$

$$(\theta_0(t)x(t))(0) = 0 \tag{2.21b}$$

$$(\theta_1(t)x(t))(1) = u(t) \tag{2.21c}$$

with (2.21a) defined on $z \in (0,1)$ and $t \in \mathbb{R}_{t_0}^+$ and θ_0, θ_1 defined in (2.6b) respectively (2.7b) or equivalently (2.10).

Remark 2.1.7. It is also possible to keep the advection term in the design procedure by including it into the target system. In that way it is also possible to include non-diagonal advection matrices leading to an advective coupling, like also considered in [98]. The kernel equations then contain first order derivatives but can be solved with the same method as presented here, with some technical modifications. However, this impedes the stability analysis of the target system. In [98], a Lyapunov-based approach is used, which does not allow the direct specification of the decay rate. If the advection matrix is diagonal, the Hopf-Cole-transformation can be applied to the target system for the stability analysis. However, at least in the case of existing Robin BCs, the transformation will lead to time dependent boundary matrices which cannot be eliminated and again hinder the stability analysis. ◁

Using the backstepping method, the Volterra-type integral transformation

$$\tilde{x}(z,t) = x(z,t) - \int_0^z K(z,\zeta,t)x(\zeta,t)\mathrm{d}\zeta = (\mathcal{T}_c(t)x(t))(z), \tag{2.22}$$

called *backstepping transformation*, is applied to map the given system into a target system in which the stability is given or can be set by the user via parameters. If (2.22) is boundedly invertible, the stability property of the target system automatically applies to the original system. Due to the transformation, all destabilizing components in the plant are in some sense shifted to the right boundary, where they can be eliminated by the degree of freedom, that is the input $u(t)$. The resulting expression for $u(t)$ is the state feedback control law.

For this reason, the target system is one of the key aspects in the backstepping design. At least, it needs to be stable under a correct choice of parameters and it must ensure that the transformation (2.22) exists, or in other words, that the kernel $K(z,\zeta,t) \in \mathbb{R}^{n\times n}$ of the transformation can be determined.

2.2 Selection of the target system

The causes for instability in the original system (2.21) are the matrices $A(z,t)$, $A_0(z,t)$, $F(z,\zeta,t)$ as well as the boundary matrices $B_i^d(t)$. Thus, it is desirable to eliminate them by the backstepping transformation. Moreover, as known from the single PDE case, it is possible to influence the stability of a parabolic system by the reaction parameter. For this reason, the *target system* is chosen as

$$\begin{aligned}\tilde{x}_t(z,t) &= \Lambda(z)\tilde{x}_{zz}(z,t) - \widetilde{A}(z,t)\tilde{x}(z,t)\\ &\quad - \widetilde{A}_0(z,t)\big(E_1E_1^\top \tilde{x}_z(0,t) + E_2E_2^\top \tilde{x}(0,t)\big) \qquad (2.23a)\\ (\tilde{\theta}_0 x(t))(0) &= 0 \qquad (2.23b)\\ (\tilde{\theta}_1 x(t))(1) &= 0 \qquad (2.23c)\end{aligned}$$

(see [118]). Here, $\widetilde{A}(z,t) \in \mathbb{R}^{n\times n}$ is a matrix set by the user to modify the stability. Later, its structure will be further restricted to allow a simple proof of stability and ensure solvability of the kernel equations. For a greater flexibility, the design procedure however is presented with the general $\widetilde{A}(z,t) \in \mathbb{R}^{n\times n}$ with $\widetilde{A}_{ij} \in (C^1[0,1]\times G_\alpha(\mathbb{R}^+_{t_0}))$.

The matrix $\widetilde{A}_0(z,t) = [\widetilde{A}_{0,ij}(z,t)]$, $i,j = 1,\dots,n$ has the elements

$$\widetilde{A}_{0,ij}(z,t) = \begin{cases} 0, & \lambda_i \geq \lambda_j \\ \widetilde{A}^0_{ij}(z,t), & \lambda_i < \lambda_j, \end{cases} \qquad (2.24)$$

where the conditions $\lambda_i \bullet \lambda_j$ are short forms for $\{\forall i,j = 1,\dots,n | \lambda_i \bullet \lambda_j\}$ with some relation $\bullet$. It needs to be included in the target system to obtain

solvable kernel equations and was first introduced in [98] for coupled parabolic systems. If it were not included, the possibly fully coupled system (2.21) could be mapped into a system of completely decoupled equations (2.23) (if $\widetilde{A}(z,t)$ is diagonal). This would lead to overdetermined kernel equations so that no kernel K exists for this mapping. By including $\widetilde{A}_0(z,t)$ with entries $\widetilde{A}_{ij}^0$ dependent on K, the kernel equations become solvable and due to its special structure with only a maximum of $n(n-1)/2$ non-zero elements, the target system is a cascade of exponentially stable systems (if $\widetilde{A}(z,t)$ is chosen appropriately) which significantly eases its stability analysis. In [113] it was shown that the type of the local term ($\tilde{x}_z(0)$ or $\tilde{x}(0)$) to be included by $\widetilde{A}_{0,ij}$ depends on the left BC. In particular, Robin BCs require the term $\tilde{x}(0)$, whereas Dirichlet BCs require $\tilde{x}_z(0)$ (obviously, $\tilde{x}(0)$ would be without influence in the Dirichlet case, as the BC implied $\tilde{x}(0)=0$). Using the definition of E_1, E_2 in (2.4) leads to the present coupling term in (2.23a).

Remark 2.2.1. In the case of equal diffusion coefficients, the local coupling term is not required which can be seen at (2.24). Moreover, it is also possible to further restrict the choice of $\widetilde{A}$ in (2.23a) to ensure the solvability of the kernel equations. This is shown in [44] for PDEs with spatially varying diffusion coefficients and a constant reaction matrix. However, this leads to a fully coupled target system including the integral and local coupling terms and allowing no precise determination of the stability margin. In the time dependent case, the resulting time dependent target system would make the stability analysis even more difficult. ◁

In the target system, Robin BCs are converted to Neumann-type. That way, possible couplings on the right side are eliminated and the BCs become time-invariant. In the general operator formulation, the operators in (2.23) then read

$$\tilde{\theta}_0 h = E_1 E_1^\top h + E_2 E_2^\top h_z \tag{2.25a}$$

$$\tilde{\theta}_1 h = \underbrace{S_d S_d^\top}_{\widetilde{B}_1^d} h + \underbrace{S_r S_r^\top}_{\widetilde{B}_1^n = B_1^n} h_z. \tag{2.25b}$$

2.3 The control law and the kernel equations

In order to render the calculation steps clear, the dependency of the variables on their independent variables is omitted from now on. Only if some of the variables are substituted or to emphasize the dependency, they are written down. That means, if no independent variables are written, the

reader needs to insert the independent variables on which the dependent variable is defined. In most cases, this is obvious by context. As example, the backstepping transformation (2.22) is compactly written in the form

$$\tilde{x} = x - \int_0^z Kx(\zeta, t)\mathrm{d}\zeta, \tag{2.26}$$

where $\tilde{x} = \tilde{x}(z,t)$, $x = x(z,t)$ except inside the integral and $K = K(z,\zeta,t)$.

To ensure the transformation (2.22) maps the original system (2.21) into the desired target system (2.23), the kernel K and the input u must be chosen appropriately. This is stated in the following proposition.

Proposition 2.3.1 (Control law and kernel equations)**.** *The* control law

$$\begin{aligned} u(t) = &\left(B_1^d(t) + B_1^n K(1,1,t) - \widetilde{B}_1^d\right)x(1,t) \\ &+ \int_0^1 \underbrace{\left(B_1^n K_z(1,\zeta,t) + \widetilde{B}_1^d K(1,\zeta,t)\right)}_{R(\zeta,t)} x(\zeta,t)\mathrm{d}\zeta =: \mathcal{K}(t)x(t) \end{aligned} \tag{2.27}$$

and the backstepping transformation (2.22) *with* $K(z,\zeta,t)$ *being the solution of the* kernel equations

$$\Lambda K_{zz} - (K\Lambda(\zeta))_{\zeta\zeta} = KA(\zeta,t) + \widetilde{A}K - F + \int_\zeta^z K(z,\bar{\zeta},t)F(\bar{\zeta},\zeta,t)\mathrm{d}\bar{\zeta} + K_t \tag{2.28a}$$

$$\Lambda K(z,z,t) - K(z,z,t)\Lambda = 0 \tag{2.28b}$$

$$K_\zeta(z,z,t)\Lambda + \Lambda \mathrm{d}_z K(z,z,t) + \Lambda K_z(z,z,t) = -(A + \widetilde{A}) - K(z,z,t)\Lambda' \tag{2.28c}$$

$$K(z,0,t)\Lambda(0)E_1 = -\widetilde{A}_0 E_1 \tag{2.28d}$$

$$\begin{aligned} K(z,0,t)\Lambda'(0)E_2 + K_\zeta(z,0,t)\Lambda(0)E_2 = &(\mathcal{T}_c A_0)E_2 + K(z,0,t)\Lambda(0)E_2 Q_0(t) \\ &- \widetilde{A}_0\left(E_1 E_1^\top K(0,0,t)E_2 - E_2\right) \end{aligned} \tag{2.28e}$$

$$E_2^\top K(0,0,t)E_2 = Q_0(t) \tag{2.28f}$$

with (2.28a) *defined on the open triangular spatial domain* $\mathcal{D} = \{z,\zeta \in \mathbb{R} \mid 0 < \zeta < z < 1\}$ *and* $t \in \mathbb{R}_{t_0}^+$ *map the original system* (2.21) *into the target system* (2.23).

Proof. To determine the conditions on u and K for the desired mapping, it is convenient to begin with the transformation of the BCs. The spatial derivative

$$\tilde{x}_z = x_z - K(z,z,t)x - \int_0^z K_z x(\zeta,t)\mathrm{d}\zeta \tag{2.29}$$

of (2.22) is used to determine

$$E_1^\top \tilde{x}(0,t) \overset{(2.22)}{=} E_1^\top x(0,t) \overset{(2.3a)}{=} 0 \tag{2.30a}$$

$$E_2^\top \tilde{x}_z(0,t) \overset{(2.29)}{=} \underbrace{E_2^\top x_z(0,t)}_{\overset{(2.3b)}{=} Q_0(t) E_2^\top x(0,t)} - E_2^\top K(0,0,t) \underbrace{x(0,t)}_{E_1 E_1^\top x(0,t) + E_2 E_2^\top x(0,t)}$$

$$= \left(Q_0(t) - E_2^\top K(0,0,t) E_2\right) E_2^\top \tilde{x}(0,t). \tag{2.30b}$$

Consequently, the condition

$$E_2^\top K(0,0,t) E_2 = Q_0(t) \tag{2.31}$$

needs to be fulfilled to obtain (2.23b). The right BC is transformed by applying the boundary operator (2.25b) on the target system state and inserting (2.22) and (2.29), which yields

$$\begin{aligned}
(\tilde{\theta}_1 \tilde{x}(t))(1) &\overset{(2.25)}{=} B_1^n \tilde{x}_z(1,t) + \widetilde{B}_1^d \tilde{x}(1,t) \\
&\overset{(2.29)}{=} B_1^n x_z(1,t) - B_1^n K(1,1,t) x(1,t) - \int_0^1 B_1^n K_z(1,\zeta,t) x(\zeta,t) \mathrm{d}\zeta \\
&\quad + \widetilde{B}_1^d x(1,t) - \widetilde{B}_1^d \int_0^1 K(1,\zeta,t) x(\zeta,t) \mathrm{d}\zeta \\
&\overset{(2.7)}{=} u(t) - \left(B_1^d(t) + B_1^n K(1,1,t) - \widetilde{B}_1^d\right) x(1,t) \\
&\quad - \int_0^z \left(B_1^n K_z(1,\zeta) + \widetilde{B}_1^d K(1,\zeta,t)\right) x(\zeta,t) \mathrm{d}\zeta.
\end{aligned} \tag{2.32}$$

Obviously, the BC (2.23c) is obtained if the input u fulfils (2.27).

The remaining conditions on K are set by the mapping of the original PIDE (2.21a) into the target system PDE (2.23a). Therefore, the transformation (2.22) needs to be inserted into both equations, leading to expressions for $\tilde{x}_t$, which can be set equal.

To this end, (2.21a) is inserted into the time derivative of the transformation (2.22) which is calculated to

$$\begin{aligned}
\tilde{x}_t &= x_t - \int_0^z \Big(K_t x(\zeta,t) + K x_t(\zeta,t) \Big) \mathrm{d}\zeta \\
&= \Lambda x_{zz} + A x + A_0 x(0,t) + \int_0^z F x(\zeta,t) \mathrm{d}\zeta
\end{aligned}$$

$$\underbrace{-\int_0^z K\Lambda(\zeta)x_{\zeta\zeta}(\zeta,t)\mathrm{d}\zeta}_{(\star_1)} - \int_0^z KA(\zeta,t)x(\zeta,t)\mathrm{d}\zeta - \int_0^z KA_0(\zeta,t)\mathrm{d}\zeta x(0,t)$$
$$\underbrace{-\int_0^z K\int_0^\zeta F(\zeta,\bar{\zeta},t)x(\bar{\zeta},t)\mathrm{d}\bar{\zeta}\mathrm{d}\zeta}_{(\star_2)} - \int_0^z K_t x(\zeta,t)\mathrm{d}\zeta \tag{2.33}$$

being an expression for $\tilde{x}_t$ in terms of the original state x. In order to factorize the terms appearing under an integral, the expressions $(\star_1)$ and $(\star_2)$ need to be reformulated such that they contain $x(\zeta,t)$. Integration by parts is performed on $(\star_1)$ to obtain

$$\begin{aligned}
&-\int_0^z K\Lambda(\zeta)x_{\zeta\zeta}(\zeta,t)\mathrm{d}\zeta\\
&\quad = -\left[K\Lambda(\zeta)x_\zeta(\zeta,t)\right]_0^z + \left[(K_\zeta\Lambda(\zeta)+K\Lambda'(\zeta))x(\zeta,t)\right]_0^z\\
&\qquad -\int_0^z (K\Lambda(\zeta))_{\zeta\zeta}x(\zeta,t)\mathrm{d}\zeta\\
&\quad = -K(z,z,t)\Lambda x_z + K(z,0,t)\Lambda(0)x_z(0,t) + K_\zeta(z,z,t)\Lambda x\\
&\qquad + K(z,z,t)\Lambda' x - K_\zeta(z,0,t)\Lambda(0)x(0,t)\\
&\qquad - K(z,0,t)\Lambda'(0)x(0,t) - \int_0^z (K\Lambda(\zeta))_{\zeta\zeta}x(\zeta,t)\mathrm{d}\zeta.
\end{aligned} \tag{2.34}$$

The term $(\star_2)$ is reformulated by changing the order of integration. This yields

$$\begin{aligned}
&\int_0^z\int_0^\zeta K(z,\zeta,t)F(\zeta,\bar{\zeta},t)x(\bar{\zeta},t)\mathrm{d}\bar{\zeta}\mathrm{d}\zeta = \int_0^z\int_{\bar{\zeta}}^z K(z,\zeta,t)F(\zeta,\bar{\zeta},t)x(\bar{\zeta},t)\mathrm{d}\zeta\mathrm{d}\bar{\zeta}\\
&= \int_0^z\int_\zeta^z K(z,\bar{\zeta},t)F(\bar{\zeta},\zeta,t)x(\zeta,t)\mathrm{d}\bar{\zeta}\mathrm{d}\zeta = \int_0^z\int_\zeta^z K(z,\bar{\zeta},t)F(\bar{\zeta},\zeta,t)\mathrm{d}\bar{\zeta}x(\zeta,t)\mathrm{d}\zeta.
\end{aligned} \tag{2.35}$$

Now the transformation (2.22) is inserted into the target system PDE (2.23a). To this end, (2.29) and the second spatial derivative

$$\tilde{x}_{zz} = x_{zz} - \mathrm{d}_z K(z,z,t)x - K(z,z,t)x_z - K_z(z,z,t)x - \int_0^z K_{zz}x(\zeta,t)\mathrm{d}\zeta, \tag{2.36}$$

of (2.22) are needed. With (2.29), (2.36) and (2.22), the target PDE (2.23a) can be expressed as

$$\begin{aligned}\tilde{x}_t = {}& \Lambda x_{zz} - \Lambda \mathrm{d}_z K(z,z,t)x - \Lambda K(z,z,t)x_z - \Lambda K_z(z,z,t)x \\ & - \Lambda \int_0^z K_{zz}x(\zeta,t)\mathrm{d}\zeta - \widetilde{A}x + \widetilde{A}\int_0^z Kx(\zeta,t)\mathrm{d}\zeta \\ & + \widetilde{A}_0(E_1E_1^\top K(0,0,t) - E_2E_2^\top)x(0,t) - \widetilde{A}_0E_1E_1^\top x_z(0,t)\end{aligned} \tag{2.37}$$

in terms of the original state x.

The obtained expressions (2.33) and (2.37) are compared by subtraction while inserting (2.34) and (2.35), leading to

$$\begin{aligned}\tilde{x}_t - \tilde{x}_t = {}& (\Lambda K(z,z,t) - K(z,z,t)\Lambda)x_z \\ & + \Big(A + K_\zeta(z,z,t)\Lambda + K(z,z,t)\Lambda' + \Lambda \mathrm{d}_z K(z,z,t) + \Lambda K_z(z,z,t) + \widetilde{A}\Big)x \\ & + \int_0^z \Big(F - (K\Lambda(\zeta))_{\zeta\zeta} - KA(\zeta,t) - \int_\zeta^z K(z,\bar{\zeta},t)F(\bar{\zeta},\zeta,t)\mathrm{d}\bar{\zeta} \\ & \qquad + \Lambda K_{zz} - \widetilde{A}K - K_t\Big)x(\zeta,t)\mathrm{d}\zeta \\ & + \Big(A_0 - K_\zeta(z,0,t)\Lambda(0) - K(z,0,t)\Lambda'(0) \\ & \qquad - \int_0^z KA_0(\zeta,t)\mathrm{d}\zeta - \widetilde{A}_0(E_1E_1^\top K(0,0,t) - E_2E_2^\top)\Big)x(0,t) \Big\} (\star_3) \\ & + \Big(K(z,0,t)\Lambda(0) + \widetilde{A}_0E_1E_1^\top\Big)x_z(0,t).\end{aligned} \tag{2.38}$$

In order to include the given information of the left BC (2.3), note that

$$x(0,t) = E_1 \underbrace{E_1^\top x(0,t)}_{\overset{(2.3a)}{=}0} + E_2E_2^\top x(0,t) \tag{2.39a}$$

$$x_z(0,t) = E_1E_1^\top x_z(0,t) + E_2 \underbrace{E_2^\top x_z(0,t)}_{\overset{(2.3b)}{=}Q_0(t)E_2^\top x(0)} \tag{2.39b}$$

and insert it into $(\star_3)$ to obtain

$$\begin{aligned}(\star_3) = \Big(&A_0E_2 - K_\zeta(z,0,t)\Lambda(0)E_2 - K(z,0,t)\Lambda'(0)E_2 - \int_0^z KA_0(\zeta,t)E_2\mathrm{d}\zeta\\ &- \widetilde{A}_0(E_1E_1^\top K(0,0,t)E_2 - E_2) + K(z,0,t)\Lambda(0)E_2Q_0(t)\Big)E_2^\top x(0,t)\\ &+ \Big(K(z,0,t)\Lambda(0)E_1 + \widetilde{A}_0E_1\Big)E_1^\top x_z(0,t). \end{aligned} \tag{2.40a}$$

Since the left side of (2.38) is zero, all terms on the right side need to vanish to achieve a valid equation independent of the value of x. Together with (2.31), this leads to the conditions (2.28) that need to be fulfilled by K and thus proves the proposition. ■

The appearance of the kernel K in the control law (2.27) reveals that it is not only required to investigate the *existence* of a suitable K, mapping (2.21) into (2.23), but it also needs to be determined. Together with its BCs (2.28b)–(2.28f), the PIDE (2.28a) is a rather atypical problem, consisting of a temporal-spatial differential operator and uncommon BCs on the closed spatial domain $\bar{\mathcal{D}} : \{z, \zeta \in \mathbb{R} \,|\, 0 \leq \zeta \leq z \leq 1\}$. Verifying the solvability of these equations is the main challenge in the backstepping design. It is shown in Section 2.5 that the kernel equations attain a piecewise continuous solution, which can be determined using the method of *successive approximations*.

2.4 Closed-loop stability

To be sure that the closed-loop system is exponentially stable, the target system (2.23) needs to be stable and the applied backstepping transformation needs to be boundedly invertible. Then, the states of the original system can be calculated from the states of the target system by a bounded map so that the stability property of the target system automatically applies to the original system.

Choosing the reaction matrix of the target system as

$$\widetilde{A}(z,t) = \mu_c I + \bar{A}(z,t), \tag{2.41a}$$

with

$$\bar{A}_{ij}(z,t) = \begin{cases} 0, & \lambda_i \geq \lambda_j \\ \breve{A}_{ij}(z,t), & \lambda_i < \lambda_j, \end{cases} \tag{2.41b}$$

where μ_c and the non-zero elements $\breve{A}_{ij} \in (C^1[0,1] \times G_\alpha(\mathbb{R}^+_{t_0}))$ can be set by the user, the following theorem can be stated.

Theorem 2.4.1 (Closed-loop stability)
Assume that $\widetilde{A}$ is chosen according to (2.41) and $\mu_c > \mu_{\max}$, where $\mu_{\max}$ is the largest eigenvalue of (2.23) for $\widetilde{A}(z,t) \equiv 0$ and $\widetilde{A}_0(z,t) \equiv 0$. Then, the closed-loop system (2.21) with (2.27) and K being the solution of (2.28) is well-posed and uniformly exponentially stable in the weighted L_2-norm $\|h\| = \left(\int_0^1 \|\Lambda^{-\frac{1}{2}}(z)h(z)\|_{\mathbb{C}^n}^2 \mathrm{d}z\right)^{1/2}$, i. e.

$$\|x(t)\| \leq M\mathrm{e}^{(\mu_{\max}-\mu_c+c)(t-t_0)}\|x(t_0)\|, \quad t \geq t_0 \tag{2.42}$$

for all $x(t_0) \in (L_2(0,1))^n$ satisfying the BCs (2.21b), (2.21c), an $M \geq 1$, any $t_0 \geq 0$ and any $c > 0$, i. e. the stability margin is $\mu_c - \mu_{\max}$.

This theorem is proved in the next two sections by showing the stability of the target system and the invertibility of the backstepping transformation.

2.4.1 Stability of the target system

The choice of $\widetilde{A}(z,t)$ according to (2.41a) and of $\widetilde{A}_0(z,t)$ in the target system are of fundamental importance for the stability proof. Note that $\bar{A}(z,t)$ in (2.41) has the same occupancy as $\widetilde{A}_0(z,t)$. Therefore, the target system has a cascade structure, allowing to use the Riesz-spectral property of the subsystems for a very precise determination of the stability margin. In fact, it can be set by the user per specification of μ_c whereas $\bar{A}(z,t)$ has no influence on the decay rate but allows a greater design flexibility. To be precise, the stability of the target system is formulated in the following lemma.

Lemma 2.4.2 (Stability of the target system)**.** *Assume that $\widetilde{A}$ is chosen according to (2.41) and $\mu_c > \mu_{\max}$, where $\mu_{\max}$ is the largest eigenvalue of (2.23) for $\mu_c = 0$, $\widetilde{A}_0(z,t) \equiv 0$ and $\bar{A}(z,t) \equiv 0$. Then, the target system (2.23) is well-posed and uniformly exponentially stable in the weighted L_2-norm $\|h\| = \left(\int_0^1 \|\Lambda^{-\frac{1}{2}}(z)h(z)\|_{\mathbb{C}^n}^2 \mathrm{d}z\right)^{1/2}$, i. e.*

$$\|\tilde{x}(t)\| \leq \widetilde{M}\mathrm{e}^{(\mu_{\max}-\mu_c+c)(t-t_0)}\|\tilde{x}(t_0)\|, \quad t \geq t_0 \tag{2.43}$$

for all $\tilde{x}(t_0) \in (L_2(0,1))^n$ satisfying the BCs (2.23b), (2.23c), an $\widetilde{M} \geq 1$, any $t_0 \geq 0$ and any $c > 0$, i. e. the stability margin is $\mu_c - \mu_{\max}$.

Proof. It is convenient to rearrange the state vector $\tilde{x}(z,t)$ such that the diffusion coefficients are ordered descending. To this end, introduce the new state

$$\tilde{x}^*(z,t) = P\tilde{x}(z,t) \tag{2.44}$$

with the permutation matrix P, fulfilling $P^{-1} = P^\top$, so that the elements of $\Lambda^*(z) = P\Lambda P^\top = \operatorname{diag}(\lambda_1^*(z), \dots, \lambda_n^*(z))$ suffice the relation $\lambda_1^* \geq \dots \geq \lambda_n^*$. With this, the target system (2.23) takes the form

$$\begin{aligned}\tilde{x}_t^*(z,t) = \Lambda^*(z)\tilde{x}_{zz}^*(z,t) - \mu_c\tilde{x}^*(z) - \bar{A}^*(z,t)\tilde{x}^*(z,t)\\ - \widetilde{A}_0^*(z,t)\big(\underbrace{PE_1E_1^\top P^\top}_{R_1}\tilde{x}_z^*(0,t) + \underbrace{PE_2E_2^\top P^\top}_{R_2}\tilde{x}^*(0,t)\big)\end{aligned} \tag{2.45a}$$

$$\tilde{\theta}_0[P^\top x^*(t)](0) = (\tilde{\theta}_0^* x^*(t))(0) = 0 \tag{2.45b}$$

$$\tilde{\theta}_1[P^\top x^*(t)](1) = (\tilde{\theta}_1^* x^*(t))(1) = 0. \tag{2.45c}$$

Due to the structure of $\widetilde{A}_0(z,t)$ and $\bar{A}(z,t)$ according to (2.24) and (2.41b), the matrices $\widetilde{A}_0^*(z,t)$ and $\bar{A}^*(z,t)$ become strictly lower triangular due to the permutation, i. e.

$$\widetilde{A}_0^*(z,t) = P\widetilde{A}_0(z,t)P^\top = \begin{bmatrix} 0 & \dots & \dots & 0 \\ \widetilde{A}_{0,21}^*(z,t) & \ddots & \ddots & \vdots \\ \vdots & \ddots & \ddots & \vdots \\ \widetilde{A}_{0,n1}^*(z,t) & \dots & \widetilde{A}_{0,n\,n-1}^*(z,t) & 0 \end{bmatrix} \tag{2.46a}$$

$$\bar{A}^*(z,t) = P\bar{A}(z,t)P^\top = \begin{bmatrix} 0 & \dots & \dots & 0 \\ \bar{A}_{21}^*(z,t) & \ddots & \ddots & \vdots \\ \vdots & \ddots & \ddots & \vdots \\ \bar{A}_{n1}^*(z,t) & \dots & \bar{A}_{n\,n-1}^*(z,t) & 0 \end{bmatrix}. \tag{2.46b}$$

Consequently, (2.45) has a cascade structure. In particular, (2.45a) describes a cascade of time-invariant systems with time dependent couplings, which is a huge easement for the stability analysis.

Now introduce the operators

$$\mathcal{A}_i h = \lambda_i^* h'', \quad i = 1, \dots, n, \tag{2.47a}$$

$$D(\mathcal{A}_i) = \{h \in H^2(0,1) \,|\, e_i^\top(\tilde{\theta}_0^* e_i h)(0) = e_i^\top(\tilde{\theta}_1^* e_i h)(1) = 0\} \tag{2.47b}$$

in the Hilbert space $L_2(0,1)$ with the weighted inner product

$$\langle h_1, h_2\rangle = \int_0^1 \lambda_i^*(z) h_1(z)\bar{h}_2(z)\mathrm{d}z \tag{2.48}$$

and the induced weighted L_2-norm $\|h\| = \left(\int_0^1 \lambda_i^*(z)|h(z)|^2\mathrm{d}z\right)^{1/2}$. The largest eigenvalue $\mu_{\max} \in \mathbb{R}$ of $\mathcal{A}_i$ exists, because $-\mathcal{A}_i$ are *Sturm-Liouville operators* [27]. In particular, $-\mathcal{A}_i$ has a discrete real point spectrum and $\mathcal{A}_i$ only

has a finite number of eigenvalues in the right half-plane. Considering the eigenvalue problem of the operator $\mathcal{A}_i - \mu_c I$ shows that the term $-\mu_c I$ simply shifts all eigenvalues by $-\mu_c$. Consequently, $-(\mathcal{A}_i - \mu_c I)$ are Sturm-Liouville (and thus Riesz-spectral) operators with a discrete, real point spectrum and $\mathcal{A}_i - \mu_c I$ have a finite number of eigenvalues in the right half-plane, implying that the *spectrum determined growth assumption* [26, Ch. 5.5] is fulfilled. Consequently, the decay rate of their generated C_0-*semigroups* $\mathcal{T}_i(t)$ depends on their largest eigenvalue [48]. Specifically, $\|\mathcal{T}_i(t)h\| \leq M_i \mathrm{e}^{(\mu_{\max}-\mu_c)t}\|h\|$, $t > 0$, $M_i \geq 1$ holds for $h \in D(\mathcal{A}_i)$.

This implies that the abstract IVP

$$\dot{\tilde{x}}_1^*(t) = (\mathcal{A}_1 - \mu_c I)\tilde{x}_1^*(t), \quad t \in \mathbb{R}_{t_0}^+ \tag{2.49a}$$

$$\tilde{x}_1^*(t_0) = \tilde{x}_{01}^* \in D(\mathcal{A}_1), \tag{2.49b}$$

belonging to the first state of the permuted target system (2.45) is well-posed and its solution is given by

$$\tilde{x}_1^*(t) = \mathcal{T}_1(t - t_0)\tilde{x}_1^*(t_0) \tag{2.50}$$

with the bound

$$\|\tilde{x}_1^*(t)\| \leq M_1 \mathrm{e}^{(\mu_{\max}-\mu_c)(t-t_0)}\|\tilde{x}_1^*(t_0)\|. \tag{2.51}$$

Note that the matrices R_1 and R_2 in (2.45a) simply select the states with Dirichlet, respectively Robin BCs out of the permuted state vector. Thus, it is

$$e_i^\top R_1 \tilde{x}^* = r_{1i}^\top \tilde{x}^* = \begin{cases} \tilde{x}_i^*, & i : \text{Dirichlet} \\ 0, & i : \text{Robin} \end{cases} \tag{2.52a}$$

$$e_i^\top R_2 \tilde{x}^* = r_{2i}^\top \tilde{x}^* = \begin{cases} 0, & i : \text{Dirichlet} \\ \tilde{x}_i^*, & i : \text{Robin}. \end{cases} \tag{2.52b}$$

Now introduce the operator $\mathcal{E}_1 h = e_1^\top R_1 e_1 h_z(0) + e_1^\top R_2 e_1 h(0)$, $h \in D(\mathcal{A}_1)$, to write the abstract IVP belonging to the second state as

$$\dot{\tilde{x}}_2^*(t) = (\mathcal{A}_2 - \mu_c I)\tilde{x}_2^*(t) + \bar{A}_{21}^*(\cdot, t)\tilde{x}_1^*(t) + \widetilde{A}_{0,21}^*(\cdot, t)\mathcal{E}_1\tilde{x}_1^*(t), \quad t \in \mathbb{R}_{t_0}^+ \tag{2.53a}$$

$$\tilde{x}_2^*(t_0) = \tilde{x}_{02}^* \in D(\mathcal{A}_2). \tag{2.53b}$$

The solution of (2.53) is given by

$$\tilde{x}_2^*(t) = \mathcal{T}_2(t - t_0)\tilde{x}_2^*(t_0) + \int_{t_0}^t \mathcal{T}_2(t - \tau)\Big(\bar{A}_{21}^*(\cdot, \tau)\tilde{x}_1^*(\tau) + \widetilde{A}_{0,21}^*(\cdot, \tau)\mathcal{E}_1\tilde{x}_1^*(\tau)\Big)\mathrm{d}\tau, \tag{2.54}$$

where (2.50) is inserted to obtain

$$\tilde{x}_2^*(t) = \mathcal{T}_2(t-t_0)\tilde{x}_2^*(t_0) + \int_{t_0}^{t} \mathcal{T}_2(t-\tau) \cdot \Big(\bar{A}_{21}^*(\cdot,\tau)\mathcal{T}_1(\tau-t_0)\tilde{x}_1^*(t_0) + \widetilde{A}_{0,21}^*(\cdot,\tau)\mathcal{E}_1\mathcal{T}_1(\tau-t_0)\tilde{x}_1^*(t_0)\Big)\mathrm{d}\tau. \tag{2.55}$$

While $\bar{A}_{21}^*(\cdot,\tau)$ is a bounded operator (simply a function of space), $\mathcal{E}_1$ is an unbounded operator. As shown in Appendix A.1, the boundary evaluations appearing in $\mathcal{E}_1$ are relatively bounded w. r. t. $\mathcal{A}_1 - \mu_c$. Thus, the same property is valid for $\mathcal{E}_1$. Moreover, $\mathcal{A}_1$ is a *sectorial Riesz-spectral operator* implying the analyticity of $\mathcal{T}_1$ [48]. Consequently, as shown in Lemma A.2.1, $\mathcal{E}_1(\tau)\mathcal{T}_1(\tau-t_0)$ is a bounded linear operator with $\|\mathcal{E}_1(\tau)\mathcal{T}_1(\tau-t_0)h\| \leq M_1 \mathrm{e}^{(\mu_{\max}-\mu_c)(\tau-t_0)}\|h\|$, $h \in D(\mathcal{A}_1)$. This and the fact that $|\bar{A}_{21}^*(z,t)| \leq \bar{M}$ and $|\widetilde{A}_{0,21}^*| \leq \bar{A}$ are bounded by some finite numbers $\bar{M}, \bar{A}$ can be used to determine the bound for the second state as

$$\begin{aligned}
\|\tilde{x}_2^*(t)\| &\leq \|\mathcal{T}_2(t-t_0)\|\|\tilde{x}_2^*(t_0)\| + \int_{t_0}^{t} \|\mathcal{T}_2(t-\tau)\| \\
&\quad \cdot \Big(\bar{M}\|\mathcal{T}_1(\tau-t_0)\tilde{x}_1^*(t_0)\| + \bar{A}\|\mathcal{E}_1\mathcal{T}_1(\tau-t_0)\tilde{x}_1^*(t_0)\|\Big)\mathrm{d}\tau && \text{(2.56a)} \\
&\leq \|\mathcal{T}_2(t-t_0)\|\|\tilde{x}_2^*(t_0)\| + \int_{t_0}^{t} \|\mathcal{T}_2(t-\tau)\| \\
&\quad \cdot \Big(\bar{M}M_1\mathrm{e}^{(\mu_{\max}-\mu_c)(\tau-t_0)}\|\tilde{x}_1^*(t_0)\| + \bar{A}M_1\mathrm{e}^{(\mu_{\max}-\mu_c)(\tau-t_0)}\|\tilde{x}_1^*(t_0)\|\Big)\mathrm{d}\tau && \text{(2.56b)} \\
&\leq M_2\mathrm{e}^{(\mu_{\max}-\mu_c)(t-t_0)}\|\tilde{x}_2^*(t_0)\| \\
&\quad + \int_0^t M_2\mathrm{e}^{(\mu_{\max}-\mu_c)(t-\tau)}(\bar{M}+\bar{A})M_1\mathrm{e}^{(\mu_{\max}-\mu_c)(\tau-t_0)}\|\tilde{x}_1^*(t_0)\|\mathrm{d}\tau && \text{(2.56c)} \\
&= M_2\mathrm{e}^{(\mu_{\max}-\mu_c)(t-t_0)}\|\tilde{x}_2^*(t_0)\| \\
&\quad + \int_{t_0}^t M_1M_2(\bar{M}+\bar{A})\mathrm{e}^{(\mu_{\max}-\mu_c)(t-t_0)}\|\tilde{x}_1^*(t_0)\|\mathrm{d}\tau && \text{(2.56d)} \\
&= M_2\mathrm{e}^{(\mu_{\max}-\mu_c)(t-t_0)}\|\tilde{x}_2^*(t_0)\| \\
&\quad + M_1M_2(\bar{M}+\bar{A})\mathrm{e}^{(\mu_{\max}-\mu_c)(t-t_0)}(t-t_0)\|\tilde{x}_1^*(t_0)\|. && \text{(2.56e)}
\end{aligned}$$

Utilizing the fact that every exponential function grows faster than a linear function, independently of the growth rate, meaning

$$t - t_0 \leq \breve{M}e^{c(t-t_0)}, \quad \forall c > 0 \tag{2.57a}$$

for some finite $\breve{M}$, leads to

$$\mathrm{e}^{(\mu_{\max}-\mu_c)(t-t_0)}(t-t_0) \leq \breve{M}\mathrm{e}^{(\mu_{\max}-\mu_c+c)(t-t_0)}. \tag{2.57b}$$

Moreover, per definition of the Euclidean norm, $\|\tilde{x}_i^*(t_0)\| \leq \|\tilde{x}^*(t_0)\|$. Inserting this in (2.56e) gives

$$\|\tilde{x}_2^*(t)\| \leq \widetilde{M}_2\mathrm{e}^{(\mu_{\max}-\mu_c+c)(t-t_0)}\|\tilde{x}^*(t_0)\| \tag{2.58}$$

for some constant $\widetilde{M}_2 \geq 1$. This procedure can be repeated for all states $\tilde{x}_i^*$, $i = 3, \ldots, n$, showing that in total

$$\|\tilde{x}^*(t)\| \leq M^*\mathrm{e}^{(\mu_{\max}-\mu_c+c)(t-t_0)}\|\tilde{x}^*(t_0)\|, \quad M^* \geq 1 \tag{2.59}$$

holds for some M^* and $\forall c > 0$. As the states $\tilde{x}^*$ are nothing else than the permuted target system states, the same stability property holds for $\tilde{x}(t)$ with the corresponding weighted L_2-norm $\|h\| = \left(\int_0^1 \|\Lambda^{-\frac{1}{2}}(z)h(z)\|^2\mathrm{d}z\right)^{1/2}$, i. e. (2.23) is uniformly exponentially stable with the desired stability margin $\mu_{\max} - \mu_c$.

Due to the fact that the generated C_0-semigroups $\mathcal{T}_i$, $i = 1, \ldots, n$ are analytic (see above), ICs in $L_2(0,1)$ lead to a unique mild solution of (2.23) (see [26, Lem. 3.1.5]) , which proves the lemma. ■

Remark 2.4.3. Due to the cascade structure of the target system, the decay rate of the target system is given by $\mu_{\max} - \mu_c + c$, $\forall c > 0$ (instead of $\mu_{\max} - \mu_c$ as for scalar systems, cf. [33]). Because c can be infinitely small, the achieved decay rate is in fact nearly as fast as in the scalar case. ◁

2.4.2 Invertibility of the backstepping transformation

The backstepping transformation (2.22) maps the dynamics of the original system into the exponentially stable target system. Though being intuitive, it will be shown at the end of this section that this stability property is transferred back to the original system if there exists a bounded mapping $\tilde{x} \to x$, which is stated in the following lemma.

Lemma 2.4.4 (Inverse backstepping transformation)**.** *The backstepping transformation* (2.22) *has a bounded inverse*

$$x(z,t) = \tilde{x}(z,t) + \int_0^z L(z,\zeta,t)\tilde{x}(\zeta,t)\mathrm{d}\zeta = (\mathcal{T}_c^{-1}(t)\tilde{x}(t))(z), \tag{2.60}$$

where $L(z,\zeta,t) \in \bar{\mathcal{D}} \times \mathbb{R}^+_{t_0}$ *is the solution of the* inverse kernel equations

$$\Lambda L_{zz} - (L\Lambda(\zeta))_{\zeta\zeta} = -AL - L\widetilde{A}(\zeta,t) - F - \int_\zeta^z F(\zeta,\bar{\zeta},t)L(\bar{\zeta},\zeta,t)\mathrm{d}\bar{\zeta} + L_t \tag{2.61a}$$

$$L(z,z,t)\Lambda - \Lambda L(z,z,t) = 0 \tag{2.61b}$$

$$L_\zeta(z,z,t)\Lambda + \Lambda \mathrm{d}_z L(z,z,t) + \Lambda L_z(z,z,t) = -(\widetilde{A} + A) - L(z,z,t)\Lambda' \tag{2.61c}$$

$$L(z,0,t)\Lambda(0)E_1 = -\mathcal{T}_c^{-1}[\widetilde{A}_0(t)E_1] \tag{2.61d}$$

$$L(z,0,t)\Lambda'(0)E_2 + L_\zeta(z,0,t)\Lambda(0)E_2 = A_0E_2 + \mathcal{T}_c^{-1}[\widetilde{A}_0(t)E_2] \tag{2.61e}$$

$$E_2^\top L(0,0,t)E_2 = Q_0(t), \tag{2.61f}$$

with (2.61a) *defined on* $\mathcal{D} \times \mathbb{R}^+_{t_0}$.

Proof. Since the backstepping transformation is a Volterra-integral transformation, it is known that the corresponding inverse transformation is again of this type. Thus it needs to be investigated if (2.60) exists. To this end, the steps for determining the kernel equations (see Section 2.3) need to be done again, with (2.22) replaced by (2.60) and interchanging the role of the original and the target system.

Prior to determining the conditions for L, it is useful to derive some basic relations between (2.22) and (2.60), originating solely from their definitions. Inserting (2.60) into (2.22) yields

$$\tilde{x} = \tilde{x} + \int_0^z L\tilde{x}(\zeta,t)\mathrm{d}\zeta - \int_0^z K\tilde{x}(\zeta,t)\mathrm{d}\zeta - \int_0^z \int_0^\zeta KL(\zeta,\bar{\zeta},t)\tilde{x}(\bar{\zeta},t)\mathrm{d}\bar{\zeta}\mathrm{d}\zeta, \tag{2.62}$$

where the order of integration in the double integral is changed to obtain

$$\int_0^z \Big(L - K - \int_\zeta^z K(z,\bar{\zeta},t)L(\bar{\zeta},\zeta,t)\mathrm{d}\bar{\zeta}\Big)x(\zeta,t)\mathrm{d}\zeta = 0, \tag{2.63}$$

which implies

$$L(z,\zeta,t) = K(z,\zeta,t) + \int_\zeta^z K(z,\bar{\zeta},t)L(\bar{\zeta},\zeta,t)\mathrm{d}\bar{\zeta}. \tag{2.64a}$$

The same calculation can be performed when inserting (2.22) into (2.60), i. e. doing the other way round. Then, the equation

$$L(z,\zeta,t) = K(z,\zeta,t) + \int_\zeta^z L(z,\bar{\zeta},t)K(\bar{\zeta},\zeta,t)\mathrm{d}\bar{\zeta} \tag{2.64b}$$

is obtained. Together, (2.64) are called *reciprocity relations* (cf. [63, Ch. 4.5]).

Like it was done for (2.22), it is convenient to consider the transformation of the BCs now. The Dirichlet BCs

$$E_1^\top x(0,t) \overset{(2.60)}{=} E_1^\top \tilde{x}(0,t) = 0 \tag{2.65}$$

are automatically fulfilled. For the Robin BCs,

$$\begin{aligned} E_2^\top x_z(0,t) &\overset{(2.60)}{=} \underbrace{E_2^\top \tilde{x}_z(0,t)}_{0} + E_2^\top L(0,0,t) \underbrace{\tilde{x}(0,t)}_{E_2 E_2^\top \tilde{x}(0,t)} \overset{(2.3b)}{=} Q_0(t) E_2^\top x(0,t) \\ E_2^\top L(0,0,t) E_2 E_2^\top x(0,t) &= Q_0(t) E_2^\top x(0,t) \end{aligned} \tag{2.66}$$

leads to the condition

$$E_2^\top L(0,0,t) E_2 = Q_0(t), \tag{2.67}$$

which is compatible to (2.28f) with the reciprocity relations.

The right BC (2.7) yields

$$\begin{aligned} (\theta_1(t)x(t))(1) &= B_1^n x_z(1,t) + B_1^d(t) x(1,t) \\ &\overset{(2.60)}{=} \underbrace{B_1^n \tilde{x}_z(1,t) + \overbrace{\widetilde{B}_1^d \tilde{x}(1,t)}^{0} - \widetilde{B}_1^d \tilde{x}(1,t)}_{(\tilde{\theta}_1 \tilde{x}(t))(1)=0} + B_1^n L(1,1,t)\tilde{x}(1,t) \\ &\quad + B_1^n \int_0^1 L_z(1,\zeta,t)\tilde{x}(\zeta,t)\mathrm{d}\zeta + B_1^d(t)\tilde{x}(1,t) \\ &\quad + B_1^d(t) \int_0^1 L(1,\zeta,t)\tilde{x}(\zeta,t)\mathrm{d}\zeta \overset{(2.21c)}{=} u(t) \end{aligned} \tag{2.68}$$

after the insertion of $0 = \widetilde{B}_1^d \tilde{x}(1,t) - \widetilde{B}_1^d \tilde{x}(1,t)$. However, $u(t)$ is already determined by the control law (2.27) in terms of K. Inserting (2.60) into (2.27), this reads

$$\begin{aligned} u(t) &= \Big(-\widetilde{B}_1^d + B_1^d(t) + B_1^n K(1,1,t)\Big)\tilde{x}(1,t) \\ &\quad + \int_0^1 \Big(-\widetilde{B}_1^d + B_1^d(t) + B_1^n K(1,1,t)\Big) L(1,\zeta,t)\tilde{x}(\zeta,t)\mathrm{d}\zeta \\ &\quad + \int_0^1 \Big(B_1^n K_z(1,\zeta,t) + \widetilde{B}_1^d K(1,\zeta,t)\Big)\tilde{x}(\zeta,t)\mathrm{d}\zeta \\ &\quad + \int_0^1 \Big(B_1^n K_z(1,\zeta,t) + \widetilde{B}_1^d K(1,\zeta,t)\Big) \int_0^\zeta L(\zeta,\bar{\zeta},t)\tilde{x}(\bar{\zeta},t)\mathrm{d}\bar{\zeta}\mathrm{d}\zeta. \end{aligned} \tag{2.69}$$

The last term is reformulated by changing the order of integration and $K(1,1,t) = L(1,1,t)$ according to (2.64) is inserted in the first line. The result

$$\begin{aligned} u(t) = &\Big(-\widetilde{B}_1^d + B_1^d(t) + B_1^n L(1,1,t)\Big)\tilde{x}(1,t) \\ &+ \int_0^1 \Big(-\widetilde{B}_1^d + B_1^d(t) + B_1^n K(1,1,t)\Big) L(1,\zeta,t)\tilde{x}(\zeta,t)\mathrm{d}\zeta \\ &+ \int_0^1 \Big(B_1^n K_z(1,\zeta,t) + \widetilde{B}_1^d K(1,\zeta,t)\Big)\tilde{x}(\zeta,t)\mathrm{d}\zeta \\ &+ \int_0^1 \int_\zeta^1 \Big(B_1^n K_z(1,\bar{\zeta},t) + \widetilde{B}_1^d K(1,\bar{\zeta},t)\Big) L(\bar{\zeta},\zeta,t)\mathrm{d}\bar{\zeta}\tilde{x}(\zeta,t)\mathrm{d}\zeta \end{aligned} \tag{2.70}$$

is now subtracted from (2.68), which yields

$$\begin{aligned} 0 = &\int_0^1 \Big(B_1^n L_z(1,\zeta,t) - B_1^n K_z(1,\zeta,t) - B_1^n K(1,1,t)L(1,\zeta,t) \\ &- B_1^n \int_\zeta^1 K_z(1,\bar{\zeta},t)L(\bar{\zeta},\zeta,t)\mathrm{d}\bar{\zeta} \\ &+ \widetilde{B}_1^d L(1,\zeta,t) - \widetilde{B}_1^d K(1,\zeta,t) + \widetilde{B}_1^d \int_\zeta^1 K(1,\bar{\zeta},t)L(\bar{\zeta},\zeta,t)\mathrm{d}\bar{\zeta}\Big)\tilde{x}(\zeta,t)\mathrm{d}\zeta. \end{aligned} \tag{2.71}$$

The first reciprocity relation (2.64a) induces that the last line in (2.71) is zero. For the previous lines, differentiate (2.64a) w. r. t. z to get

$$L_z(z,\zeta,t) = K_z(z,\zeta,t) + K(z,z,t)L(z,\zeta,t) + \int_\zeta^z K_z(z,\bar{\zeta},t)L(\bar{\zeta},\zeta,t)\mathrm{d}\bar{\zeta}, \tag{2.72}$$

respectively

$$L_z(1,\zeta,t) = K_z(1,\zeta,t) + K(1,1,t)L(1,\zeta,t) + \int_\zeta^1 K_z(1,\bar{\zeta},t)L(\bar{\zeta},\zeta,t)\mathrm{d}\bar{\zeta}. \tag{2.73}$$

Thus, (2.71) can be written as

$$0 = \int_0^1 B_1^n L_z(1,\zeta,t)\tilde{x}(\zeta,t)\mathrm{d}\zeta - \int_0^1 B_1^n L_z(1,\zeta,t)\tilde{x}(\zeta,t)\mathrm{d}\zeta = 0, \tag{2.74}$$

which reveals that the right boundary condition is automatically mapped correctly by the inverse transformation (2.60), without posing any conditions on L.

Now the transformation of the PDE (2.23a) into the original PIDE (2.21a) may be investigated. In analogy to Section 2.3, (2.23a) is inserted into the time derivative of (2.60) and the spatial derivatives of (2.60) are inserted into (2.21a). Comparing the results directly leads to (2.61).

To ensure that (2.60) is a bounded map, there must exist a bounded solution $L(z,\zeta,t)$ of (2.61). This BVP has a similar structure as (2.28) so that the solvability of the latter may be used for (2.61). However, it is shown in Section 2.5 that the matrix $\widetilde{A}_0$ is introduced in order to get well-posed kernel equations. By determining the values of $\widetilde{A}_0$ dependent on the kernel K, the number of conditions imposed on K by the BCs (2.28d) and (2.28e) is reduced to ensure they can be fulfilled. Consequently, $\widetilde{A}_0$ is already determined uniquely, providing no further degree of freedom to reduce the number of conditions on L. At first sight, this might lead to overdetermined equations (2.61), because the BCs (2.61e) and (2.61f) now pose a condition for each element L_{ij}. Using the reciprocity relations again indeed shows that expressing the non-zero elements of $\widetilde{A}_0$ by L through the BCs (2.61e) and (2.61f) is exactly the same as when expressing them by K through the BCs (2.28d) and (2.28e). Consequently, the number of conditions posed on L is the same as of those posed on K. This is proved in Appendix B.1.

The remaining difference between the inverse (2.61) and the original kernel equations (2.28) is the order of the appearing matrix multiplications. Where K is multiplied from left, L is multiplied from right and vice versa. Using the same method as in Section 2.5 to prove the solvability of (2.61) reveals that all steps remain the same, except that the interchanging $i \to j$ in the right-hand side of (2.190) is required for the proof of convergence. Consequently, (2.61) have a bounded solution implying the boundedness of the inverse transformation (2.60), which proves the lemma. ■

Remark 2.4.5. The invertibility of the backstepping-transformation is expected due to its Volterra-type. An operator-theoretic analysis would probably reveal the invertibility as well. However, the determination of the inverse kernel equations as a straightforward method to prove the invertibility became the common way to keep the required amount of mathematical knowledge as small as possible.

Rather than determining the governing equations for L and analysing their solvability, it is also possible to analyse the solvability of (2.64a) or (2.64b) and determining their solution via fixed-point iteration. This is especially interesting for practice, since the corresponding implementation is far less complex than another solution of the kernel equations. ◁

Now that the stability of the target system and the boundedness of (2.60) are known, the following proof is simple.

Proof of Theorem 2.4.1. Since (2.60) is a bounded operator, it is $\|x(t)\| \leq a\|\tilde{x}(t)\|$ for some finite number $a \geq 0$. Due to the boundedness of (2.22), the same applies the other way round so that $\|\tilde{x}(t_0)\| \leq \tilde{a}\|x(t_0)\|$ with another finite constant $\tilde{a} \geq 0$. According to Lemma 2.4.2, this leads to

$$\begin{aligned} \|x(t)\| &\leq a\widetilde{M}\mathrm{e}^{(\mu_{\max}-\mu_c+c)(t-t_0)}\tilde{a}\|x(t_0)\| \\ &\leq M\mathrm{e}^{(\mu_{\max}-\mu_c+c)(t-t_0)}\|x(t_0)\|, \end{aligned} \tag{2.75}$$

for an $M \geq 1$, any $t_0 > 0$ and any $c > 0$. Since c may be arbitrarily small, the resulting stability margin is $\mu_c - \mu_{\max}$. ■

2.5 Solution of the kernel equations

The previous sections have pointed out that it is of fundamental importance in the backstepping design that the kernel equations (2.28) are solvable, which is shown in this section. In the end, the following theorem will be proved.

Theorem 2.5.1 (Kernel equations)
The kernel equations (2.28) have a unique, piecewise continuous solution on the domain $\bar{\mathcal{D}} : \{z, \zeta \in \mathbb{R} \,|\, 0 \leq \zeta \leq z \leq 1\}$, $t \in \mathbb{R}_{t_0}^+$.

The method for solving the kernel equations is based on two changes of coordinates, which allow the transformation of (2.28a) into an integral equation. The integral equation is solved by applying fixed-point iteration, which is converging absolutely and uniformly. That allows a series truncation after a sufficient number of iterations leading to a realizable approach for determining their solution, called method of *successive approximations*. This procedure was first presented in [22, 23], called the method of *integral operators* to analyse the well-posedness of IBVPs for parabolic systems with time-varying coefficients. However, [69] was the first to apply the same in the framework of backstepping control and dealt with scalar heat equations with spatially varying reaction. Subsequently, it was applied for the solution of the kernel equations for a variety of different system classes in several publications. Especially [79] used the method to solve the kernel equations for parabolic PIDEs with spatially varying coefficients. Most recently, this procedure was generalized to be applied for coupled parabolic PIDEs with

spatially varying coefficients in [113]. Though [98] has shown that it is also possible to solve the kernel equations for this system class by tracing them back to the hyperbolic case, the direct solution of the kernel equations by the method of successive approximations paved the way to combine existing results for time-dependent coefficients [72, 81, 100] with the results for coupled parabolic systems in [113]. This finally led to the contribution [118] which considered parabolic PDEs with space and time dependent coefficients.

Hence, the main results of this chapter have been presented in [118] but are extended in view of the local coupling term, the integral term, mixed BCs and possibly equal diffusion coefficients. Moreover, the convergence proof is slightly modified to ensure convergence for diffusion coefficients with overlapping ranges.

2.5.1 Component form of the kernel equations

As it is in general hard to obtain the solution of a matrix-valued PIDE directly, the first step to solve (2.28) is to consider it in its *component form*. That is, a BVP for each element K_{ij}, is determined by multiplying (2.28) with $e_i^\top$ from left and e_j from right, where e_i denotes the i-th unit vector. Considering the resulting equations for all $i, j = 1, \dots, n$, they are mathematically identical to (2.28).

It is easy to see that (2.28a) is equivalent to

$$\begin{aligned}\lambda_i K_{ij,zz} - (K_{ij}\lambda_j(\zeta))_{\zeta\zeta} = &\sum_{k=1}^{n}\Big(K_{ik}A_{kj}(\zeta,t) + \widetilde{A}_{ik}K_{kj}\Big) + K_{ij,t} \\ &- F_{ij} + \int_\zeta^z \sum_{k=1}^{n} K_{ik}(z,\bar{\zeta},t)F_{kj}(\bar{\zeta},\zeta,t)\mathrm{d}\bar{\zeta}, \quad (2.76)\end{aligned}$$

$(z,\zeta) \in \mathcal{D}$, $t \in \mathbb{R}_{t_0}^+$, showing that the BVPs for the elements K_{ij} are coupled due to the appearing matrix multiplications. The first BC (2.28b) reads

$$\begin{aligned}\lambda_i K_{ij}(z,z,t) - K_{ij}(z,z,t)\lambda_j &= 0 \\ (\lambda_i - \lambda_j)K_{ij}(z,z,t) &= 0. \quad (2.77)\end{aligned}$$

Depending on the relation of the diffusion coefficients, there are two cases to consider. If $\lambda_i = \lambda_j$[4], (2.77) is automatically fulfilled and implies no condition on K. Otherwise

$$K_{ij}(z,z,t) = 0, \quad \text{for} \quad \lambda_i \neq \lambda_j \quad (2.78)$$

[4] This is at least the case for $i = j$, i. e. the diagonal elements.

must hold.

The second BC (2.28c) can be rewritten as

$$K_{ij,\zeta}(z,z,t)\lambda_j + \lambda_i \mathrm{d}_z K_{ij}(z,z,t) + \lambda_i K_{ij,z}(z,z,t) \\ = -(A_{ij} + \widetilde{A}_{ij}) - K_{ij}(z,z,t)\lambda_j'. \quad (2.79)$$

With the knowledge of (2.78), the same case distinction can be applied here. If $\lambda_i = \lambda_j$, using the fact that $K_{ij,z}(z,z,t) + K_{ij,\zeta}(z,z,t) = \mathrm{d}_z K_{ij}(z,z,t)$, (2.79) simplifies to

$$2\lambda_i \mathrm{d}_z K_{ij}(z,z,t) = -(A_{ij} + \widetilde{A}_{ij}) - K_{ij}(z,z,t)\lambda_i' \quad (2.80a)$$

$$\mathrm{d}_z K_{ij}(z,z,t) = -\frac{A_{ij} + \widetilde{A}_{ij}}{2\lambda_i} - \frac{\lambda_i'}{2\lambda_i} K_{ij}(z,z,t), \quad (2.80b)$$

which is an ODE on the diagonal $\zeta = z$ of the spatial domain. Its solution is given by

$$K_{ij}(z,z,t) = K_{ij}(0,0,t)\mathrm{e}^{-\int_0^z \frac{\lambda_i'(\zeta)}{2\lambda_i(\zeta)}\mathrm{d}\zeta} \\ - \int_0^z \frac{A_{ij}(\zeta,t) + \widetilde{A}_{ij}(\zeta,t)}{2\lambda_i(\zeta)} \mathrm{e}^{-\int_\zeta^z \frac{\lambda_i'(\bar{\zeta})}{2\lambda_i(\bar{\zeta})}\mathrm{d}\bar{\zeta}} \mathrm{d}\zeta, \quad (2.81)$$

where

$$\int_0^z \frac{\lambda_i'(\zeta)}{\lambda_i(\zeta)}\mathrm{d}\zeta = \ln \lambda_i(z) - \ln \lambda_i(0) = \ln \frac{\lambda_i(z)}{\lambda_i(0)}. \quad (2.82)$$

Consequently,

$$\begin{aligned} K_{ij}(z,z,t) &= K_{ij}(0,0,t)\mathrm{e}^{\frac{1}{2}\ln\frac{\lambda_i(0)}{\lambda_i(z)}} - \int_0^z \frac{A_{ij}(\zeta,t) + \widetilde{A}_{ij}(\zeta,t)}{2\lambda_i(\zeta)} \mathrm{e}^{\frac{1}{2}\ln\frac{\lambda_i(\zeta)}{\lambda_i(z)}}\mathrm{d}\zeta \\ &= K_{ij}(0,0,t)\sqrt{\frac{\lambda_i(0)}{\lambda_i(z)}} - \int_0^z \frac{A_{ij}(\zeta,t) + \widetilde{A}_{ij}(\zeta,t)}{2\lambda_i(\zeta)} \sqrt{\frac{\lambda_i(\zeta)}{\lambda_i(z)}}\mathrm{d}\zeta \\ &= K_{ij}(0,0,t)\sqrt{\frac{\lambda_i(0)}{\lambda_i(z)}} - \int_0^z \frac{A_{ij}(\zeta,t) + \widetilde{A}_{ij}(\zeta,t)}{2\sqrt{\lambda_i(\zeta)\lambda_i(z)}}\mathrm{d}\zeta. \end{aligned} \quad (2.83)$$

In the second case $\lambda_i \neq \lambda_j$, (2.78) implies $\mathrm{d}_z K_{ij}(z,z,t) = 0$. This in turn leads to

$$\begin{aligned} \mathrm{d}_z K_{ij}(z,z,t) &= K_{ij,z}(z,z,t) + K_{ij,\zeta}(z,z,t) = 0 \\ K_{ij,\zeta}(z,z,t) &= -K_{ij,z}(z,z,t), \end{aligned} \quad (2.84)$$

which can be inserted into (2.79) to obtain

$$K_{ij,z}(z,z,t) = -\frac{A_{ij}+\widetilde{A}_{ij}}{\lambda_i-\lambda_j}. \tag{2.85a}$$

The third and fourth BC (2.28d) and (2.28e) require special attention, as they contain the matrix $\widetilde{A}_0$. Their component form reads

$$K_{ij}(z,0,t)\lambda_j(0) = \widetilde{A}_{0,ij}, \quad \text{for} \quad j \le m \tag{2.86a}$$

$$\begin{aligned} &K_{ij}(z,0,t)(\lambda_j'(0) - \lambda_j(0)q_j^0(t)) + K_{ij,\zeta}(z,0,t)\lambda_j(0) \\ &\quad = e_i^\top(\mathcal{T}_c A_0)e_j - e_i^\top \widetilde{A}_0(E_1E_1^\top K(0,0,t)E_2 + E_2)e_j \quad \text{for} \quad j > m. \end{aligned} \tag{2.86b}$$

In view of (2.24) and (2.86a), the condition

$$K_{ij}(z,0,t) = 0, \quad \text{for} \quad j \le m,\ \lambda_i \ge \lambda_j \tag{2.87}$$

is obtained. For the investigation of (2.86b), first note that $E_2 e_j = e_j$ for $j > m$. Thus, it is

$$e_i^\top \widetilde{A}_0(E_1E_1^\top K(0,0,t)E_2 + E_2)e_j = e_i^\top \widetilde{A}_0 E_1 E_1^\top K(0,0,t)e_j + e_i^\top \widetilde{A}_0 e_j, \tag{2.88}$$

where the second summand vanishes if $\lambda_i \ge \lambda_j$ in view of (2.24). The first summand can be rewritten with the definition of the matrix multiplication

$$e_i^\top \widetilde{A}_0 E_1 E_1^\top K(0,0,t)e_j = \sum_{k=1}^{m} \widetilde{A}_{0,ik}K_{kj}(0,0,t). \tag{2.89}$$

Here the matrices $E_1E_1^\top$ require the sum to be performed only until $k = m$. To achieve a non-vanishing result, both factors, $\widetilde{A}_{0,ik}$ and $K_{kj}(0,0,t)$ must not be zero. While (2.24) implies the requirement $\lambda_i < \lambda_k$, (2.78) leads to the condition $\lambda_k = \lambda_j$. Thus, for (2.89) to be non-vanishing, $\lambda_i < \lambda_j$ must hold. Consequently, in the case $\lambda_i \ge \lambda_j$, (2.86b) can be rewritten as

$$K_{ij}(z,0,t)(\lambda_j'(0) - \lambda_j(0)q_j^0(t)) + K_{ij,\zeta}(z,0,t)\lambda_j(0) = e_i^\top(\mathcal{T}_c A_0)e_j, \text{ for } j > m. \tag{2.90}$$

In the case $\lambda_i < \lambda_j$, (2.86) can be fulfilled by choosing the elements of $\widetilde{A}_{0,ij}$ as

$$\widetilde{A}_{0,ij} = K_{ij}(z,0,t)\lambda_j(0), \quad \text{for} \quad j \leq m \tag{2.91a}$$

$$\begin{aligned}\widetilde{A}_{0,ij} = &- K_{ij}(z,0,t)(\lambda_j'(0) - \lambda_j(0)q_j^0(t)) - K_{ij,\zeta}(z,0,t)\lambda_j(0) \\ &+ e_i^\top(\mathcal{T}_c A_0)e_j - \sum_{k=1}^{m}\Big(\widetilde{A}_{0,ik}K_{kj}(0,0,t)\Big), \quad \text{for} \quad j > m \\ = &- K_{ij}(z,0,t)(\lambda_j'(0) - \lambda_j(0)q_j^0(t)) - K_{ij,\zeta}(z,0,t)\lambda_j(0) \\ &+ e_i^\top(\mathcal{T}_c A_0)e_j - \sum_{k=1}^{m}\Big[K_{ik}(z,0,t)\lambda_k(0)K_{kj}(0,0,t)\Big]_{\lambda_k = \lambda_j}, \text{ for } j > m.\end{aligned} \tag{2.91b}$$

Combining (2.28f), (2.78) and (2.87) shows that the value $K_{ij}(0,0,t)$ is defined except for the special case $i \leq m$, $j > m$, $\lambda_i = \lambda_j$. Here $K_{ij}(0,0,t)$ is a degree of freedom $K_{ij}^0(t)$. In summary,

$$K_{ij}(0,0,t) =: K_{0,ij}(t) = \begin{cases} q_j^0(t), & i = j,\ i,j > m \\ K_{ij}^0(t), & \lambda_i = \lambda_j, i \leq m, j > m \\ 0, & \text{else.} \end{cases} \tag{2.92}$$

With this, the *component form* reads

$$\begin{aligned}\lambda_i K_{ij,zz} - (K_{ij}\lambda_j(\zeta))_{\zeta\zeta} = &\sum_{k=1}^{n}\Big(K_{ik}A_{kj}(\zeta,t) + \widetilde{A}_{ik}K_{kj}\Big) + K_{ij,t} \\ &- F_{ij} + \int_\zeta^z \sum_{k=1}^{n} K_{ik}(z,\bar{\zeta},t)F_{kj}(\bar{\zeta},\zeta,t)\mathrm{d}\bar{\zeta}\end{aligned} \tag{2.93a}$$

$$[K_{ij}(z,z,t) = 0]_{\lambda_i \neq \lambda_j} \tag{2.93b}$$

$$\left[K_{ij,z}(z,z,t) = -\frac{A_{ij} + \widetilde{A}_{ij}}{\lambda_i - \lambda_j}\right]_{\lambda_i \neq \lambda_j} \tag{2.93c}$$

$$\left[K_{ij}(z,z,t) = K_{0,ij}(t)\sqrt{\frac{\lambda_i(0)}{\lambda_i(z)}} - \int_0^z \frac{A_{ij}(\zeta,t) + \widetilde{A}_{ij}(\zeta,t)}{2\sqrt{\lambda_i(\zeta)\lambda_i(z)}}\mathrm{d}\zeta\right]_{\lambda_i = \lambda_j} \tag{2.93d}$$

$$[K_{ij}(z,0,t) = 0]_{\substack{j \leq m \\ \lambda_i \geq \lambda_j}} \tag{2.93e}$$

$$\left[K_{ij}(z,0,t)(\lambda_j'(0)-\lambda_j(0)q_j^0(t))+K_{ij,\zeta}(z,0,t)\lambda_j(0)=\ e_i^\top(\mathcal{T}_c A_0)e_j\right]_{\substack{j>m\\ \lambda_i\geq\lambda_j}}. \tag{2.93f}$$

Note that for $\lambda_i = \lambda_j$, the types of BCs appearing are similar as in the scalar case (see [79]), i. e. one BC on the boundary $(z,0)$ and one BC on the boundary (z,z). However, for $\lambda_i \neq \lambda_j$, there are two BCs on (z,z) and the BC at $(z,0)$ is removed in the case of $\lambda_i < \lambda_j$ due to the inclusion of $\widetilde{A}_0$ in the target system. If (2.93e) and (2.93f) needed to be fulfilled for each K_{ij}, then the kernel equations were overdetermined, which will be seen later.

Remark 2.5.2. The following contents are all concerned about the component form (2.93). Thus, it greatly increases the readability to omit the indices $_{ij}$. To mark a variable dependent on indices, boldface notation will be used from now on, i. e.

$$\boldsymbol{X} \coloneqq X_I, \tag{2.94}$$

for arbitrary variables X and index tuples I. This is used for various types of variables, containing matrices and functions. The substituted indices are unambiguous by context. ◁

2.5.2 Standard form of the kernel equations

In order to transform (2.93) into integral equations, it first has to be mapped into canonical coordinates. It can be seen in [22] that using the normal form coordinates of the wave equation, namely $\xi = \frac{1}{2}(z+\zeta)$ and $\eta = \frac{1}{2}(z-\zeta)$ is sufficient for this step in the case of scalar systems, i. e. $n = 1$. In the multi-variable case ($n > 1$) with different diffusion coefficients, this approach cannot be directly applied to (2.93), because the derivatives $\boldsymbol{K}_{zz}$ and $\boldsymbol{K}_{\zeta\zeta}$ have different factors. Thus, the first step is the *elimination of the leading coefficients*, which follows the idea in [81] and leads to the *standard form* of the kernel equations. This is stated in the following lemma.

Lemma 2.5.3 (Standard form of kernel equations)**.** *The change of coordinates*[5]

$$\boldsymbol{w} = w_i(z) \coloneqq \phi_i(z), \qquad \boldsymbol{v} = v_j(\zeta) \coloneqq \phi_j(\zeta) \tag{2.95a}$$

$$z = z_i(\boldsymbol{w}) \coloneqq \phi_i^{-1}(\boldsymbol{w}), \qquad \zeta = \zeta_j(\boldsymbol{v}) \coloneqq \phi_j^{-1}(\boldsymbol{v}) \tag{2.95b}$$

[5] The symbols z, ζ as well as $\boldsymbol{w} = w_i$ and $\boldsymbol{v} = v_j$ are used for both the points in the respective coordinate systems, as well as the corresponding coordinate maps.

with

$$\phi_i(z) = \int_0^z \frac{1}{\sqrt{\lambda_i(\zeta)}} \mathrm{d}\zeta, \quad i = 1, \dots, n, \ z \in [0, 1], \tag{2.96}$$

for the new kernel variable

$$\bar{\boldsymbol{K}}(\boldsymbol{w}, \boldsymbol{v}, t) = \bar{K}_{ij}(\phi_i(z), \phi_j(\zeta), t) \coloneqq \lambda_j(\zeta) K_{ij}(z, \zeta, t), \tag{2.97}$$

leads to the standard form of the kernel equations

$$\begin{aligned}
&\bar{\boldsymbol{K}}_{\boldsymbol{ww}} - \bar{\boldsymbol{K}}_{\boldsymbol{vv}} - \frac{\lambda_i'}{2\sqrt{\lambda_i}} \bar{\boldsymbol{K}}_{\boldsymbol{w}} + \frac{\lambda_j'(\zeta)}{\sqrt{\lambda_j(\zeta)}} \bar{\boldsymbol{K}}_{\boldsymbol{v}} \\
&\quad = \sum_{k=1}^{n} \left(\frac{\lambda_j(\zeta)}{\lambda_k(\zeta)} \bar{K}_{ik} A_{kj}(\zeta, t) + \widetilde{A}_{ik} \bar{K}_{kj} \right) + \bar{\boldsymbol{K}}_t \\
&\qquad - \lambda_j(\zeta) \boldsymbol{F} + \int_\zeta^z \sum_{k=1}^{n} \frac{\lambda_j(\zeta)}{\lambda_k(\bar{\zeta})} \bar{K}_{ik}(\boldsymbol{w}, v_j(\bar{\zeta}), t) F_{kj}(\bar{\zeta}, \zeta, t) \mathrm{d}\bar{\zeta}
\end{aligned} \tag{2.98a}$$

$$\left[\bar{\boldsymbol{K}}(\boldsymbol{w}, v_j(z(\boldsymbol{w})), t) = 0 \right]_{\lambda_i \neq \lambda_j} \tag{2.98b}$$

$$\left[\bar{\boldsymbol{K}}_{\boldsymbol{w}}(\boldsymbol{w}, v_j(z(\boldsymbol{w})), t) = \frac{(\boldsymbol{A} + \widetilde{\boldsymbol{A}}) \lambda_j \sqrt{\lambda_i}}{\lambda_j - \lambda_i} \right]_{\lambda_i \neq \lambda_j} \tag{2.98c}$$

$$\left[\bar{\boldsymbol{K}}(\boldsymbol{w}, \boldsymbol{w}, t) = \boldsymbol{K}_0(t) \sqrt{\lambda_i(0) \lambda_i(z)} - \int_0^z \frac{(\boldsymbol{A}(\bar{z}, t) + \widetilde{\boldsymbol{A}}(\bar{z}, t))}{2} \sqrt{\frac{\lambda_i(z)}{\lambda_i(\bar{z})}} \mathrm{d}\bar{z} \right]_{\lambda_i = \lambda_j} \tag{2.98d}$$

$$\left[\bar{\boldsymbol{K}}(\boldsymbol{w}, 0, t) = 0 \right]_{\substack{j \leq m \\ \lambda_i \geq \lambda_j}} \tag{2.98e}$$

$$\begin{aligned}
&\Bigg[\bar{\boldsymbol{K}}_{\boldsymbol{v}}(\boldsymbol{w}, 0, t) - q_j^0(t) \sqrt{\lambda_j(0)} \bar{\boldsymbol{K}}(\boldsymbol{w}, 0, t) \\
&\quad = \sqrt{\lambda_j(0)} \boldsymbol{A}_0 - \sqrt{\lambda_j(0)} \int_0^z \sum_{k=1}^{n} \frac{1}{\lambda_k(\bar{z})} \bar{K}_{ik}(\boldsymbol{w}, v_j(\bar{z})) A_{0,kj}(\bar{z}, t) \mathrm{d}\zeta \Bigg]_{\substack{j > m \\ \lambda_i \geq \lambda_j}},
\end{aligned} \tag{2.98f}$$

with (2.98a) *defined on* $(\boldsymbol{w}, \boldsymbol{v}) \in \mathcal{D}_{s,ij} = \boldsymbol{\mathcal{D}}_s = \{\boldsymbol{w}, \boldsymbol{v} \in \mathbb{R} \,|\, \boldsymbol{w} \in (0, \phi_i(1)), \boldsymbol{v} \in (0, v_j(z(\boldsymbol{w})))\}$, $t \in \mathbb{R}_{t_0}^+$. *In* (2.98), *the appearances of* (z, ζ) *are interpreted to be given by* (2.95b).

Proof. To be able to insert (2.97) into (2.93), the spatial derivatives of (2.97) are calculated as

$$\bar{\boldsymbol{K}}_z = \bar{\boldsymbol{K}}_{\boldsymbol{w}} \boldsymbol{w}_z \tag{2.99a}$$
$$\bar{\boldsymbol{K}}_{zz} = \bar{\boldsymbol{K}}_{\boldsymbol{ww}} \boldsymbol{w}_z^2 + \bar{\boldsymbol{K}}_{\boldsymbol{w}} \boldsymbol{w}_{zz} \tag{2.99b}$$
$$\bar{\boldsymbol{K}}_\zeta = \bar{\boldsymbol{K}}_{\boldsymbol{v}} \boldsymbol{v}_\zeta \tag{2.99c}$$
$$\bar{\boldsymbol{K}}_{\zeta\zeta} = \bar{\boldsymbol{K}}_{\boldsymbol{vv}} \boldsymbol{v}_\zeta^2 + \bar{\boldsymbol{K}}_{\boldsymbol{v}} \boldsymbol{v}_{\zeta\zeta}. \tag{2.99d}$$

With this,

$$\boldsymbol{K}_z = \frac{1}{\lambda_j(\zeta)} \bar{\boldsymbol{K}}_z \overset{(2.99a)}{=} \frac{1}{\lambda_j(\zeta)} \bar{\boldsymbol{K}}_{\boldsymbol{w}} \boldsymbol{w}_z \tag{2.100a}$$
$$\boldsymbol{K}_{zz} = \frac{1}{\lambda_j(\zeta)} \bar{\boldsymbol{K}}_{zz} \overset{(2.99b)}{=} \frac{1}{\lambda_j(\zeta)} \bar{\boldsymbol{K}}_{\boldsymbol{ww}} \boldsymbol{w}_z^2 + \frac{1}{\lambda_j(\zeta)} \bar{\boldsymbol{K}}_{\boldsymbol{w}} \boldsymbol{w}_{zz}, \tag{2.100b}$$

as well as (2.97) and (2.99d) can be inserted into (2.93a) to get

$$\begin{aligned} &\frac{\lambda_i}{\lambda_j(\zeta)} \bar{\boldsymbol{K}}_{\boldsymbol{ww}} \boldsymbol{w}_z^2 + \frac{\lambda_i}{\lambda_j(\zeta)} \bar{\boldsymbol{K}}_{\boldsymbol{w}} \boldsymbol{w}_{zz} - \bar{\boldsymbol{K}}_{\boldsymbol{vv}} \boldsymbol{v}_\zeta^2 - \bar{\boldsymbol{K}}_{\boldsymbol{v}} \boldsymbol{v}_{\zeta\zeta} \\ &\quad = \sum_{k=1}^{n} \left(\frac{1}{\lambda_k(\zeta)} \bar{K}_{ik} A_{kj}(\zeta, t) + \widetilde{A}_{ik} \frac{1}{\lambda_j(\zeta)} \bar{K}_{kj} \right) + \frac{1}{\lambda_j(\zeta)} \bar{\boldsymbol{K}}_t \\ &\qquad - \boldsymbol{F} + \int_\zeta^z \sum_{k=1}^{n} \frac{1}{\lambda_k(\bar{\zeta})} \bar{K}_{ik}(\boldsymbol{w}, v_k(\bar{\zeta}), t) F_{kj}(\bar{\zeta}, \zeta, t) \mathrm{d}\bar{\zeta}, \end{aligned} \tag{2.101}$$

where $\boldsymbol{w}$ and $\boldsymbol{v}$ must be interpreted as $\boldsymbol{w}(z)$ and $\boldsymbol{v}(\zeta)$ (see (2.95a)), so that $\bar{\boldsymbol{K}} = \bar{\boldsymbol{K}}(w_i(z), v_j(\zeta), t)$. After multiplying by $\lambda_j(\zeta)$, the new PIDE

$$\begin{aligned} &\lambda_i \boldsymbol{w}_z^2 \bar{\boldsymbol{K}}_{\boldsymbol{ww}} - \lambda_j(\zeta) \boldsymbol{v}_\zeta^2 \bar{\boldsymbol{K}}_{\boldsymbol{vv}} + \lambda_i \boldsymbol{w}_{zz} \bar{\boldsymbol{K}}_{\boldsymbol{w}} - \lambda_j(\zeta) \boldsymbol{v}_{\zeta\zeta} \bar{\boldsymbol{K}}_{\boldsymbol{v}} \\ &\quad = \sum_{k=1}^{n} \left(\frac{\lambda_j(\zeta)}{\lambda_k(\zeta)} \bar{K}_{ik} A_{kj}(\zeta, t) + \widetilde{A}_{ik} \bar{K}_{kj} \right) + \bar{\boldsymbol{K}}_t \\ &\qquad - \lambda_j(\zeta) \boldsymbol{F} + \int_\zeta^z \sum_{k=1}^{n} \frac{\lambda_j(\zeta)}{\lambda_k(\bar{\zeta})} \bar{K}_{ik}(\boldsymbol{w}, \boldsymbol{v}(\bar{\zeta}), t) F_{kj}(\bar{\zeta}, \zeta, t) \mathrm{d}\bar{\zeta} \end{aligned} \tag{2.102}$$

is obtained. In order to get the same spatial differential operator as in the scalar case, the respective factors of the second order derivatives must be 1, which leads to the conditions

$$\lambda_i(z) \boldsymbol{w}_z^2 = \lambda_i(z) \phi_i'(z)^2 \overset{!}{=} 1 \tag{2.103a}$$
$$\lambda_j(\zeta) \boldsymbol{v}_\zeta^2 = \lambda_j(\zeta) \phi_j'(\zeta)^2 \overset{!}{=} 1. \tag{2.103b}$$

Of course these both need to be valid for $i = 1, \dots, n$ and in (2.103a) $z \in [0, 1]$ as well as in (2.103b) $\zeta \in [0, 1]$ are independent variables so that both equations require the same, namely

$$\phi_i'(z) = \frac{1}{\sqrt{\lambda_i(z)}}, \quad i = 1, \dots, n, \tag{2.104}$$

with the simplest[6] solution (2.96). Note that each element $\bar{K}_{ij}$ of the kernel gets different coordinates. Moreover, it is remarkable that only n functions $\phi_1, \dots, \phi_n$ are needed for the coordinate transformation.

Luckily, the determined mapping (2.96) is strictly monotonically increasing, because $\lambda_i > 0$. Thus, there exist the unique inverses (2.95b) for $\boldsymbol{w} \in [0, \phi_i(1)]$, $\boldsymbol{v} \in [0, \phi_j(1)]$, allowing the formulation of

$$K(z(\boldsymbol{w}), \zeta(\boldsymbol{v}), t) = \frac{1}{\lambda_j(\zeta(\boldsymbol{v}))} \bar{\boldsymbol{K}}(\boldsymbol{w}, \boldsymbol{v}, t) \tag{2.105}$$

in terms of the new coordinates $(\boldsymbol{w}, \boldsymbol{v})$.

Now, (2.96) is inserted into (2.102) to obtain

$$\begin{aligned} &\bar{\boldsymbol{K}}_{\boldsymbol{ww}} - \bar{\boldsymbol{K}}_{\boldsymbol{vv}} - \frac{\lambda_i'}{2\sqrt{\lambda_i}} \bar{\boldsymbol{K}}_{\boldsymbol{w}} + \frac{\lambda_j'(\zeta)}{2\sqrt{\lambda_j(\zeta)}} \bar{\boldsymbol{K}}_{\boldsymbol{v}} \\ &\quad = \sum_{k=1}^{n} \left(\frac{\lambda_j(\zeta)}{\lambda_k(\zeta)} \bar{K}_{ik} A_{kj}(\zeta, t) + \widetilde{A}_{ik} \bar{K}_{kj} \right) + \bar{\boldsymbol{K}}_t \\ &\qquad - \lambda_j(\zeta) \boldsymbol{F} + \int_{\zeta}^{z} \sum_{k=1}^{n} \frac{\lambda_j(\zeta)}{\lambda_k(\bar{\zeta})} \bar{K}_{ik}(\boldsymbol{w}, \boldsymbol{v}(\bar{\zeta}), t) F_{kj}(\bar{\zeta}, \zeta, t) \mathrm{d}\bar{\zeta}. \end{aligned} \tag{2.106}$$

Equation (2.106) is now interpreted to be formulated in the new coordinates $(\boldsymbol{w}, \boldsymbol{v})$, that is $\bar{\boldsymbol{K}} = \bar{\boldsymbol{K}}(\boldsymbol{w}, \boldsymbol{v}, t)$ and $z = z(\boldsymbol{w})$, $\zeta = \zeta(\boldsymbol{v})$ according to (2.95b) holds from now on, unless explicitly stated otherwise.

In the next step, the BCs need to be mapped into the new coordinates. To this end, it is convenient to start with the transformation of the spatial boundaries. The kernel equations (2.93) have BCs on the boundaries $\Gamma_1 : (z, z)$ and $\Gamma_2 : (z, 0)$, which according to (2.96) are mapped as

$$(z, z) \to (\phi_i(z), \phi_j(z)) = (\phi_i(\phi_i^{-1}(\boldsymbol{w})), \phi_j(\phi_i^{-1}(\boldsymbol{w}))) = (\boldsymbol{w}, v_j(z(\boldsymbol{w}))) =: \bar{\Gamma}_1 \tag{2.107a}$$

$$(z, 0) \to (\phi_i(z), \phi_j(0)) = (\boldsymbol{w}(z), 0) = (\boldsymbol{w}, 0) =: \bar{\Gamma}_2, \tag{2.107b}$$

[6] The integration constant is set to zero in order to render the change of coordinates as simple as possible.

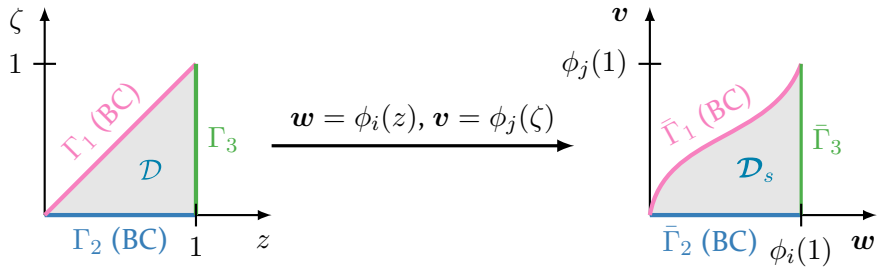

Figure 2.1: The spatial domains $\mathcal{D}$ respectively $\mathcal{D}_s$ in the original coordinates (z, ζ) and in the standard-form coordinates $(\boldsymbol{w}, \boldsymbol{v})$. The blue and pink lines represent the boundaries with BCs. In the case $\lambda_i = \lambda_j$, the boundary $\bar{\Gamma}_1$ is a straight line.

leading to the domain $\mathcal{D}_s$. Figure 2.1 shows a picture of the spatial domains in the original and new coordinates. The grey area is the respective spatial domain and the pink and blue lines are the boundaries with BCs. Due to the nonlinearity of (2.96), the straight line Γ_1 is in general mapped into a strictly monotonically increasing curve $\bar{\Gamma}_1$. Only in the special case $\lambda_i = \lambda_j$ it will still be a straight line described by $(\boldsymbol{w}, \boldsymbol{w})$. For that reason, (2.93d) in the new coordinates simply reads

$$\left[\bar{\boldsymbol{K}}(\boldsymbol{w},\boldsymbol{w},t) = \boldsymbol{K}_0(t)\sqrt{\lambda_i(0)\lambda_i(z)} - \int_0^z \frac{(\boldsymbol{A}(\bar{z},t)+\widetilde{\boldsymbol{A}}(\bar{z},t))}{2}\sqrt{\frac{\lambda_i(z)}{\lambda_i(\bar{z})}}\mathrm{d}\bar{z}\right]_{\lambda_i = \lambda_j} \tag{2.108}$$

after inserting (2.105). Accordingly, (2.93b) is mapped into

$$\left[\bar{\boldsymbol{K}}(\boldsymbol{w}, v_j(z(\boldsymbol{w})), t) = 0\right]_{\lambda_i \neq \lambda_j}. \tag{2.109}$$

To transform (2.93c), insert (2.100a) with (2.104). After a short rearranging,

$$\left[\bar{\boldsymbol{K}}_{\boldsymbol{w}}(\boldsymbol{w}, v_j(z(\boldsymbol{w})), t) = \frac{(\boldsymbol{A}+\widetilde{\boldsymbol{A}})\lambda_j\sqrt{\lambda_i}}{\lambda_j - \lambda_i}\right]_{\lambda_i \neq \lambda_j} \tag{2.110}$$

is deduced. It is trivial to see that (2.93e) implies

$$\left[\bar{\boldsymbol{K}}(\boldsymbol{w}, 0, t) = 0\right]_{\substack{j \leq m \\ \lambda_i \geq \lambda_j}} \tag{2.111}$$

and the remaining BC (2.93f) is transformed with the help of

$$\boldsymbol{K}_\zeta = \frac{-\lambda_j'(\zeta)}{\lambda_j^2(\zeta)}\bar{\boldsymbol{K}} + \frac{1}{\lambda_j(\zeta)\sqrt{\lambda_j(\zeta)}}\bar{\boldsymbol{K}}_{\boldsymbol{v}}, \tag{2.112}$$

which is obtained by solving (2.97) for $\boldsymbol{K} = K_{ij}$, differentiating w. r. t. ζ and inserting (2.99c). With (2.112) and (2.22), (2.93f) reads

$$\begin{aligned}\Big[&\bar{\boldsymbol{K}}_{\boldsymbol{v}}(\boldsymbol{w},0,t) - q_j^0(t)\sqrt{\lambda_j(0)}\bar{\boldsymbol{K}}(\boldsymbol{w},0,t)\\ &= \sqrt{\lambda_j(0)}\boldsymbol{A}_0 - \sqrt{\lambda_j(0)}\int_0^z \sum_{k=1}^{n} \frac{1}{\lambda_k(\bar{z})}\bar{K}_{ik}(\boldsymbol{w}, v_j(\bar{z}))A_{0,kj}(\bar{z},t)\mathrm{d}\bar{z}\Big]_{\substack{j>m\\ \lambda_i \geq \lambda_j}}.\end{aligned} \tag{2.113}$$

The expressions in the new coordinates $(\boldsymbol{w}, \boldsymbol{v})$ can be summarized to obtain (2.98). ■

Now the kernel equations are in a form that is known from the scalar case, e. g. [79]. The only difference are the appearing first order derivatives $\bar{\boldsymbol{K}}_{\boldsymbol{w}}$ and $\bar{\boldsymbol{K}}_{\boldsymbol{v}}$, which are thus eliminated in [113] by a Hopf-Cole-type transformation. However, it is shown in [118] that this elimination is not needed. Consequently, the canonical coordinates are now introduced.

2.5.3 Canonical coordinates and the spatial domains

Introduce the change of coordinates

$$\tilde{\boldsymbol{\xi}} = \tilde{\boldsymbol{\xi}}(\boldsymbol{w},\boldsymbol{v}) = \tilde{\xi}_{ij}(\boldsymbol{w},\boldsymbol{v}) = \boldsymbol{w} + \boldsymbol{v} \tag{2.114a}$$

$$\tilde{\boldsymbol{\eta}} = \tilde{\boldsymbol{\eta}}(\boldsymbol{w},\boldsymbol{v}) = \tilde{\eta}_{ij}(\boldsymbol{w},\boldsymbol{v}) = \boldsymbol{w} - \boldsymbol{v} \tag{2.114b}$$

for which the inverse is

$$\boldsymbol{w} = \frac{\tilde{\boldsymbol{\xi}} + \tilde{\boldsymbol{\eta}}}{2}, \qquad \boldsymbol{v} = \frac{\tilde{\boldsymbol{\xi}} - \tilde{\boldsymbol{\eta}}}{2}, \tag{2.115}$$

along with the new kernel element variables

$$\tilde{\boldsymbol{G}}(\tilde{\boldsymbol{\xi}},\tilde{\boldsymbol{\eta}},t) = \tilde{G}_{ij}(\tilde{\xi}_{ij}(\boldsymbol{w},\boldsymbol{v}),\tilde{\eta}_{ij}(\boldsymbol{w},\boldsymbol{v}),t) = \bar{\boldsymbol{K}}(\boldsymbol{w},\boldsymbol{v},t). \tag{2.116}$$

The coordinates (2.114) are the normal form coordinates of the wave equation and they are able to map the spatial differential operator $\bar{\boldsymbol{K}}_{\boldsymbol{ww}} - \bar{\boldsymbol{K}}_{\boldsymbol{vv}}$ into the significantly simpler one $\tilde{\boldsymbol{G}}_{\tilde{\boldsymbol{\xi}}\tilde{\boldsymbol{\eta}}}$. The resulting equation can easily be converted into an integral equation by formally integrating w. r. t. $\tilde{\boldsymbol{\xi}}$ and $\tilde{\boldsymbol{\eta}}$. Prior to deriving the BVP in the new coordinates, it is reasonable to have a look at how the spatial domain is affected by the map (2.114). In the scalar case, it is shown in [63] among many other publications, that the triangular

spatial domain in the original coordinates (seen in the left picture of Figure 2.1) is mapped into another triangular spatial domain with straight borders. However, as the diffusion coefficients are different in the present case, the mapping is started from the domain seen in the right picture of Figure 2.1. Here, the boundary $\bar{\Gamma}_1$ is no straight line in general. Thus, it is to be expected that resulting spatial domain after the transformation (2.114) will be the known triangle only in the special case of $\lambda_i = \lambda_j$.

Starting with the boundary $\bar{\Gamma}_2 : (\boldsymbol{w}, 0), \boldsymbol{w} \in [0, \phi_i(1)]$, it is easy to see that

$$\bar{\Gamma}_2 : \quad \left.\begin{aligned} \tilde{\boldsymbol{\xi}} &= \boldsymbol{w} + 0 \\ \tilde{\boldsymbol{\eta}} &= \boldsymbol{w} - 0 \end{aligned}\right\} \; \tilde{\boldsymbol{\xi}} = \tilde{\boldsymbol{\eta}} \tag{2.117}$$

showing that this boundary in the new coordinates reads

$$\widetilde{\Gamma}_2 : \quad (\tilde{\boldsymbol{\eta}}, \tilde{\boldsymbol{\eta}}), \quad \tilde{\boldsymbol{\eta}} \in [0, \phi_i(1)]. \tag{2.118}$$

For the boundary $\bar{\Gamma}_3 : (\phi_i(1), \boldsymbol{v}), \boldsymbol{v} \in [0, \phi_j(1)]$, it is

$$\bar{\Gamma}_3 : \quad \tilde{\boldsymbol{\xi}} = \phi_i(1) + \boldsymbol{v}, \quad \tilde{\boldsymbol{\xi}} \in [\phi_i(1), \phi_i(1) + \phi_j(1)] \tag{2.119a}$$

$$\tilde{\boldsymbol{\eta}} = \phi_i(1) - \boldsymbol{v}, \quad \tilde{\boldsymbol{\eta}} \in [\phi_i(1) - \phi_j(1), \phi_i(1)]. \tag{2.119b}$$

By solving (2.119a) for $\boldsymbol{v}$ and inserting the result into (2.119b), the boundary reads

$$\widetilde{\Gamma}_3 : \quad \tilde{\boldsymbol{\eta}} = 2\phi_i(1) - \tilde{\boldsymbol{\xi}}, \quad \tilde{\boldsymbol{\xi}} \in [\phi_i(1), \phi_i(1) + \phi_j(1)]. \tag{2.120}$$

To transform $\bar{\Gamma}_1$ that corresponds to $(z, z), z \in [0, 1]$ into the original coordinates, note that

$$\tilde{\boldsymbol{\xi}} = \boldsymbol{w}(z) + \boldsymbol{v}(z) = \phi_i(z) + \phi_j(z) \tag{2.121a}$$

$$\tilde{\boldsymbol{\eta}} = \boldsymbol{w}(z) - \boldsymbol{v}(z) = \phi_i(z) - \phi_j(z). \tag{2.121b}$$

Now define $\sigma_{ij}(z) := \phi_i(z) + \phi_j(z) \in [0, \phi_i(1) + \phi_j(1)]$ which is a strictly monotonically increasing function, because ϕ_i, $i = 1, \ldots, n$, have this property. Thus, there exists the inverse

$$z = \sigma_{ij}^{-1}(\tilde{\boldsymbol{\xi}}), \quad \tilde{\boldsymbol{\xi}} \in [0, \phi_i(1) + \phi_j(1)], \tag{2.122}$$

which can be inserted into (2.121b) to obtain the lower boundary

$$\widetilde{\Gamma}_1 : \quad \tilde{\boldsymbol{\eta}} = \phi_i(\sigma_{ij}^{-1}(\tilde{\boldsymbol{\xi}})) - \phi_j(\sigma_{ij}^{-1}(\tilde{\boldsymbol{\xi}})) =: \tilde{\boldsymbol{\eta}}_l(\tilde{\boldsymbol{\xi}}), \quad \tilde{\boldsymbol{\xi}} \in [0, \phi_i(1) + \phi_j(1)]. \tag{2.123}$$

To analyse the shape of this function, it is differentiated w. r. t. $\tilde{\boldsymbol{\xi}}$, yielding

$$\tilde{\boldsymbol{\eta}}_l'(\tilde{\boldsymbol{\xi}}) = \phi_i'(\sigma_{ij}^{-1}(\tilde{\boldsymbol{\xi}}))(\sigma_{ij}^{-1})'(\tilde{\boldsymbol{\xi}}) - \phi_j'(\sigma_{ij}^{-1}(\tilde{\boldsymbol{\xi}}))(\sigma_{ij}^{-1})'(\tilde{\boldsymbol{\xi}}). \tag{2.124}$$

Remembering that the derivative of an inverse function can be expressed in terms of the derivative of the original function by $(f^{-1})'(x) = \frac{1}{f'(f^{-1}(x))}$ and calculating $\sigma_{ij}'(z) = \phi_i'(z) + \phi_j'(z) \overset{(2.104)}{=} \frac{1}{\sqrt{\lambda_i(z)}} + \frac{1}{\sqrt{\lambda_j(z)}}$ as well as introducing the abbreviation $z_l = z_l(\tilde{\boldsymbol{\xi}}) = \sigma_{ij}^{-1}(\tilde{\boldsymbol{\xi}})$, (2.124) can be simplified to

$$\begin{aligned}\tilde{\boldsymbol{\eta}}_l'(\tilde{\boldsymbol{\xi}}) &= \frac{1}{\sqrt{\lambda_i(z_l)}} \frac{1}{\frac{1}{\sqrt{\lambda_i(z_l)}} + \frac{1}{\sqrt{\lambda_j(z_l)}}} - \frac{1}{\sqrt{\lambda_j(z_l)}} \frac{1}{\frac{1}{\sqrt{\lambda_i(z_l)}} + \frac{1}{\sqrt{\lambda_j(z_l)}}} \\ &= \left(\frac{1}{\sqrt{\lambda_i(z_l)}} - \frac{1}{\sqrt{\lambda_j(z_l)}} \right) \underbrace{\frac{1}{\frac{1}{\sqrt{\lambda_i(z_l)}} + \frac{1}{\sqrt{\lambda_j(z_l)}}}}_{>0}. \end{aligned} \tag{2.125}$$

Equation (2.125) shows that $\tilde{\boldsymbol{\eta}}_l'(\tilde{\boldsymbol{\xi}})$ has three different cases

$$\tilde{\boldsymbol{\eta}}_l'(\tilde{\boldsymbol{\xi}}) \begin{cases} > 0, & \lambda_i < \lambda_j \\ = 0, & \lambda_i = \lambda_j \\ < 0, & \lambda_i > \lambda_j, \end{cases} \tag{2.126}$$

where the different properties hold $\forall \tilde{\boldsymbol{\xi}} \in [0, \phi_i(1) + \phi_j(1)]$ so that $\tilde{\boldsymbol{\eta}}_l(\tilde{\boldsymbol{\xi}})$ can either be a strictly monotonically increasing, a constant or a strictly monotonically decreasing function of $\tilde{\boldsymbol{\xi}}$.

The resulting spatial domains for the three different cases are depicted in Figure 2.2. In the case $\lambda_i = \lambda_j$, the transformed domain is the classical one, known from the scalar case. The two BCs at $\widetilde{\Gamma}_1$ and $\widetilde{\Gamma}_2$ are needed to determine the solution when formally integrating w. r. t. $\tilde{\boldsymbol{\xi}}$ and $\tilde{\boldsymbol{\eta}}$ (symbolized by the coloured arrows), because every integration starts at a BC. In the case $\lambda_i \neq \lambda_j$, there are two BCs at $\widetilde{\Gamma}_1$, (2.98b) and (2.98c). Looking at $\lambda_i > \lambda_j$, it can be seen that both BCs are needed to determine the solution in the area $\tilde{\boldsymbol{\eta}} < 0$ of the domain, because $\tilde{\boldsymbol{\eta}} = \tilde{\boldsymbol{\eta}}_l(\tilde{\boldsymbol{\xi}})$ is not only the lower boundary, but also the left boundary of this part of the domain. For $\lambda_i < \lambda_j$, however, the last picture of Figure 2.2 reveals that if there were a BC at $\widetilde{\Gamma}_2$, the solution in the part of the domain where $\tilde{\boldsymbol{\eta}} < \phi_i(1) - \phi_j(1)$ would be overdetermined. Thus, the BC at $\widetilde{\Gamma}_2$ was removed by introducing the local coupling matrix $\widetilde{A}_0$ in the target system according to (2.24). Moreover, the integration w. r. t. $\boldsymbol{\xi}$ in this case needs to be performed in the other direction, which is no problem

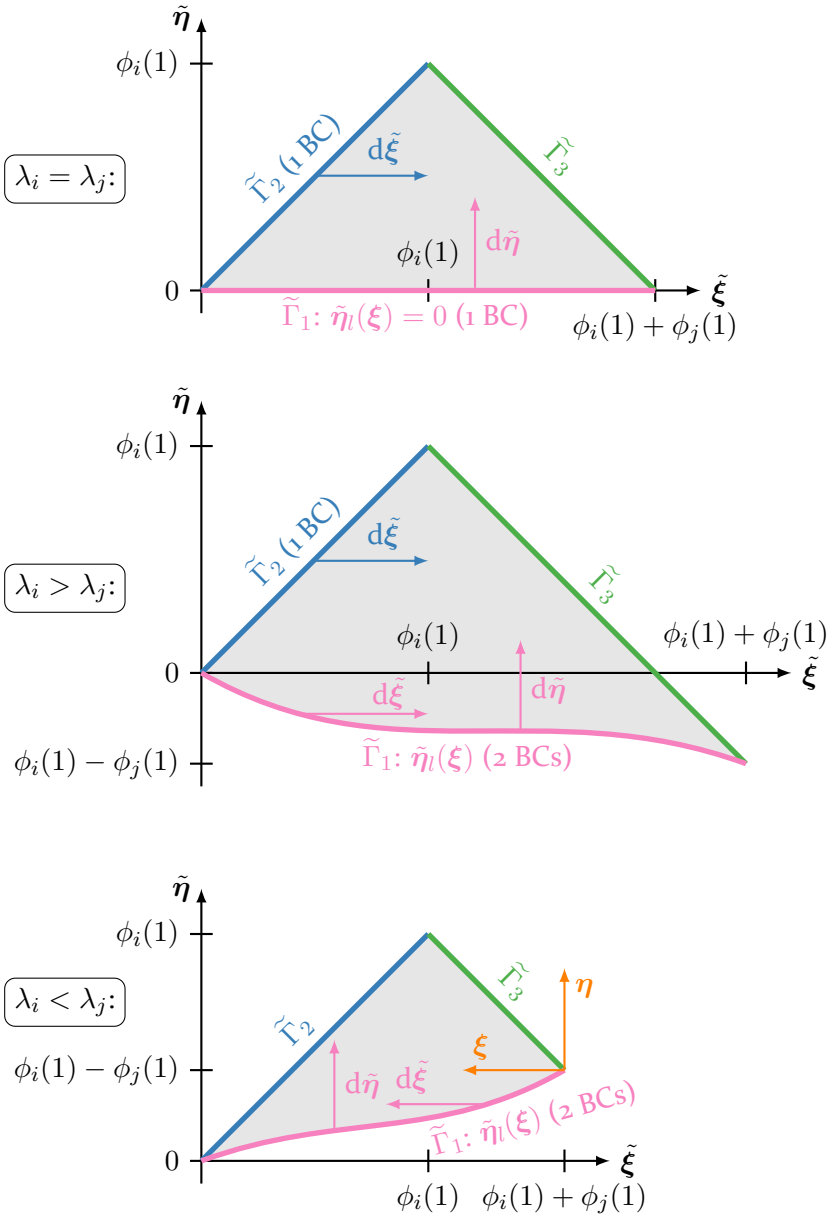

Figure 2.2: Spatial domains of the canoncial coordinates in the three different cases $\lambda_i = \lambda_j$, $\lambda_i > \lambda_j$ and $\lambda_i < \lambda_j$. For the case $\lambda_i = \lambda_j$, the spatial domain known from the scalar case is obtained. For $\lambda_i > \lambda_j$, the lower boundary $\tilde{\boldsymbol{\eta}}_l(\tilde{\boldsymbol{\xi}})$ is strictly monotonically decreasing, whereas it is strictly monotonically increasing for $\lambda_i < \lambda_j$. The arrows symbolize the directions of the formal integrations for converting into an integral equation as well as the new coordinate system $(\boldsymbol{\xi}, \boldsymbol{\eta})$ for $\lambda_i < \lambda_j$.

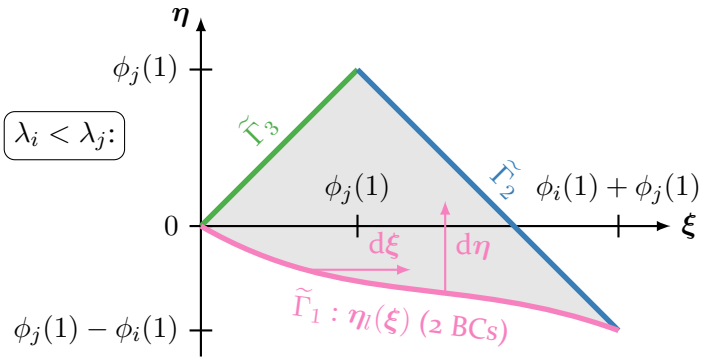

Figure 2.3: Spatial domain of the canonical kernel elements with $\lambda_i < \lambda_j$ after the introduction of $\boldsymbol{\xi}, \boldsymbol{\eta}$. It now has the same form as the case $\lambda_i > \lambda_j$ except that there is no BC at $\widetilde{\Gamma}_3$.

from a mathematical point of view but may be confusing at some point. In order to create a spatial domain with a similar shape in each case, new coordinates $\boldsymbol{\xi}, \boldsymbol{\eta}$ are introduced for $\lambda_i < \lambda_j$ as depicted with orange colour in Figure 2.2. This additional change of coordinates

$$\left.\begin{aligned} \boldsymbol{\xi} &= \phi_i(1) + \phi_j(1) - \tilde{\boldsymbol{\xi}} && \text{(2.127a)} \\ \boldsymbol{\eta} &= -(\phi_i(1) - \phi_j(1)) + \tilde{\boldsymbol{\eta}} && \text{(2.127b)} \end{aligned}\right\} \text{ for } \lambda_i < \lambda_j$$

$$\left.\begin{aligned} \boldsymbol{\xi} &= \tilde{\boldsymbol{\xi}} && \text{(2.127c)} \\ \boldsymbol{\eta} &= \tilde{\boldsymbol{\eta}} && \text{(2.127d)} \end{aligned}\right\} \text{ for } \lambda_i \geq \lambda_j$$

leads to the spatial domain for $\lambda_i < \lambda_j$ shown in Figure 2.3, which has the same form as in the case $\lambda_i > \lambda_j$ now. Once again, this new spatial domain visualizes the necessity for eliminating the BC at $\widetilde{\Gamma}_2$, because this now is the right boundary, reaching into the domain $\boldsymbol{\eta} < 0$. However, by eliminating this BC with the introduction of $\widetilde{A}_0$, the part $\boldsymbol{\eta} \geq 0$ of the domain now is underdetermined due to the missing BC at $\widetilde{\Gamma}_3$. This problem will be overcome by introducing an *artificial BC*, being a degree of freedom in the design. This means that the requirement to map (2.21) into (2.23) does not completely determine the backstepping transformation.

It is apparent in Figure 2.3 that even for $\lambda_i < \lambda_j$, the lower boundary of the spatial domain, now $\boldsymbol{\eta}_l(\boldsymbol{\xi})$, is strictly monotonically decreasing. To check this, insert (2.124) into (2.127b) and use (2.127a) to obtain

$$\boldsymbol{\eta}_l(\boldsymbol{\xi}) = \boldsymbol{\eta}\big|_{\tilde{\boldsymbol{\eta}}=\tilde{\boldsymbol{\eta}}_l} = \phi_j(1) - \phi_i(1) + \tilde{\boldsymbol{\eta}}_l(\phi_i(1) + \phi_j(1) - \boldsymbol{\xi}) \qquad \text{(2.128)}$$

and thus

$$\eta_l'(\xi) = -\underbrace{\tilde{\eta}_l'(\tilde{\xi}(\xi))}_{>0} < 0. \tag{2.129}$$

In summary, the obtained spatial domain in canonical coordinates can be formulated as

$$\bar{\mathcal{D}}_{c,ij} = \bar{\boldsymbol{\mathcal{D}}}_c = \Big\{\xi, \eta \in \mathbb{R} \,\Big|\, 0 \le \xi \le \phi_i(1) + \phi_j(1), \\ \eta_l(\xi) \le \eta \le \min\big(\xi, 2\min(\phi_i(1), \phi_j(1)) - \xi\big)\Big\}. \tag{2.130}$$

To avoid the necessity of case distinctions in every step from now on, (2.127) is rewritten with the help of a *sign parameter*

$$s = s_{ij} = \begin{cases} 1, & \lambda_i \ge \lambda_j \\ -1, & \lambda_i < \lambda_j \end{cases} \tag{2.131}$$

leading to

$$\xi = \frac{1-s}{2}(\phi_i(1) + \phi_j(1)) + s\tilde{\xi} \tag{2.132a}$$

$$\eta = -\frac{1-s}{2}(\phi_i(1) - \phi_j(1)) + \tilde{\eta}. \tag{2.132b}$$

Inserting the definition (2.114) of $(\tilde{\xi}, \tilde{\eta})$, the resulting transformation to the *canonical coordinates* is

$$\xi = \xi^{wv}(w, v) = \xi_{ij}^{wv}(w, v) = s(w + v) + \frac{1-s}{2}(\phi_i(1) + \phi_j(1)) \tag{2.133a}$$

$$\eta = \eta^{wv}(w, v) = \eta_{ij}^{wv}(w, v) = w - v - \frac{1-s}{2}(\phi_i(1) - \phi_j(1)), \tag{2.133b}$$

which can also be found in [113, 118]. Inserting (2.133) into $\xi + s\eta$ and $\xi - s\eta$ yields

$$\xi + s\eta = 2sw + (1-s)\phi_i(1) \tag{2.134a}$$

$$\xi - s\eta = 2sv + (1-s)\phi_j(1), \tag{2.134b}$$

leading to its bounded inverse transformation

$$w = w_{ij}(\xi, \eta) = \frac{s\xi + \eta}{2} + \frac{s-1}{2}\phi_i(1) \tag{2.135a}$$

$$v = v_{ij}(\xi, \eta) = \frac{s\xi - \eta}{2} + \frac{s-1}{2}\phi_j(1). \tag{2.135b}$$

To be unambiguous, the transformations $\boldsymbol{\xi}^{wv}$ and $\boldsymbol{\eta}^{wv}$ mapping from the standard form coordinates into the canonical coordinates are marked with the superscript ^{wv}. This is necessary because the definition of $\boldsymbol{w}, \boldsymbol{v}$ according to (2.95a) can be inserted in (2.133) to obtain the nonlinear *one-step coordinate transformation*

$$\boldsymbol{\xi} = \boldsymbol{\xi}(z,\zeta) = \xi_{ij}(z,\zeta) = s(\phi_i(z) + \phi_j(\zeta)) + \frac{1-s}{2}(\phi_i(1) + \phi_j(1)) \tag{2.136a}$$

$$\boldsymbol{\eta} = \boldsymbol{\eta}(z,\zeta) = \eta_{ij}(z,\zeta) = \phi_i(z) - \phi_j(\zeta) - \frac{1-s}{2}(\phi_i(1) - \phi_j(1)) \tag{2.136b}$$

with its bounded inverse

$$z = z_{ij}(\boldsymbol{\xi},\boldsymbol{\eta}) = \boldsymbol{z}(\boldsymbol{\xi},\boldsymbol{\eta}) = \phi_i^{-1}\left(w_{ij}(\boldsymbol{\xi},\boldsymbol{\eta})\right) = \phi_i^{-1}\left(\frac{s\boldsymbol{\xi}+\boldsymbol{\eta}}{2} + \frac{1-s}{2}\phi_i(1)\right) \tag{2.137a}$$

$$\zeta = \zeta_{ij}(\boldsymbol{\xi},\boldsymbol{\eta}) = \boldsymbol{\zeta}(\boldsymbol{\xi},\boldsymbol{\eta}) = \phi_j^{-1}\left(v_{ij}(\boldsymbol{\xi},\boldsymbol{\eta})\right) = \phi_j^{-1}\left(\frac{s\boldsymbol{\xi}-\boldsymbol{\eta}}{2} + \frac{1-s}{2}\phi_j(1)\right), \tag{2.137b}$$

following from (2.95b) with (2.135). The corresponding partial derivatives in both directions are calculated by applying the chain rule in combination with $(f^{-1})'(x) = \frac{1}{f'(f^{-1}(x))}$ and (2.104). The results

$$\boldsymbol{\xi}_z(z,\zeta) = \frac{s}{\sqrt{\lambda_i(z)}}, \qquad \boldsymbol{\xi}_\zeta(z,\zeta) = \frac{s}{\sqrt{\lambda_j(\zeta)}} \tag{2.138a}$$

$$\boldsymbol{\eta}_z(z,\zeta) = \frac{1}{\sqrt{\lambda_i(z)}}, \qquad \boldsymbol{\eta}_\zeta(z,\zeta) = -\frac{1}{\sqrt{\lambda_j(\zeta)}} \tag{2.138b}$$

as well as

$$\boldsymbol{z}_{\boldsymbol{\xi}}(\boldsymbol{\xi},\boldsymbol{\eta}) = \frac{s}{2}\sqrt{\lambda_i(z)}, \qquad \boldsymbol{z}_{\boldsymbol{\eta}}(\boldsymbol{\xi},\boldsymbol{\eta}) = \frac{1}{2}\sqrt{\lambda_i(z)} \tag{2.139a}$$

$$\boldsymbol{\zeta}_{\boldsymbol{\xi}}(\boldsymbol{\xi},\boldsymbol{\eta}) = \frac{s}{2}\sqrt{\lambda_j(\zeta)}, \qquad \boldsymbol{\zeta}_{\boldsymbol{\eta}}(\boldsymbol{\xi},\boldsymbol{\eta}) = -\frac{1}{2}\sqrt{\lambda_j(\zeta)}, \tag{2.139b}$$

where (z,ζ) is interpreted to be given by (2.137), will be used several times.

Now that the final coordinate transformation is determined, the *canonical kernel elements* are introduced as

$$\boldsymbol{G}(\boldsymbol{\xi},\boldsymbol{\eta},t) = G_{ij}(\xi_{ij}(\boldsymbol{w},\boldsymbol{v}),\eta_{ij}(\boldsymbol{w},\boldsymbol{v}),t) = \bar{\boldsymbol{K}}(\boldsymbol{w},\boldsymbol{v},t), \tag{2.140}$$

forming a new kernel matrix $G = [G_{ij}]$. Obviously, each element of G is defined over its own coordinate system $\boldsymbol{\xi}$, $\boldsymbol{\eta}$ depending on the indices i, j,

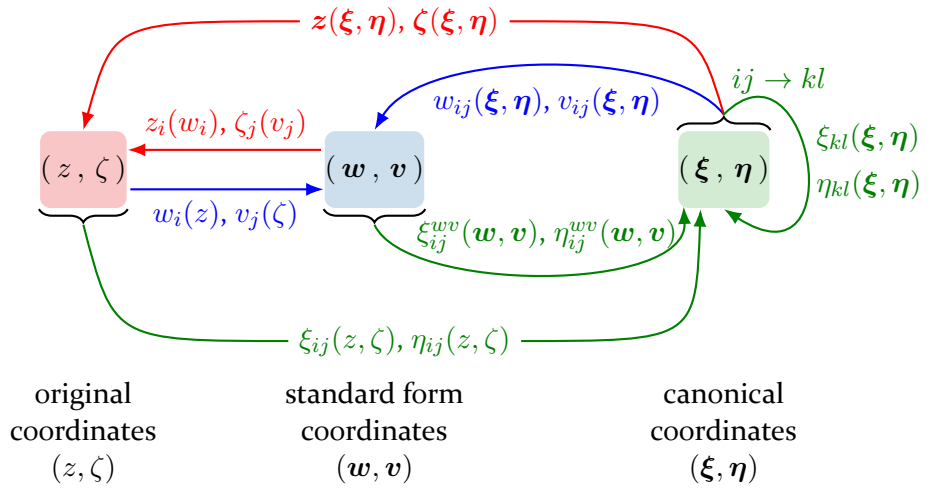

Figure 2.4: Overview of the applied coordinate transformations to map the kernel equations into their canonical form.

or, more precise, the diffusion coefficients λ_i, λ_j. Due to the inverse map (2.137) they can always be converted into each other. This means that the coordinates of each element G_{ij} can be inserted into any other element G_{kl}, $k,l = 1,\dots,n$ with the corresponding coordinate transformations

$$\begin{aligned} G_{kl}(\boldsymbol{\xi},\boldsymbol{\eta},t) &= G_{kl}(\xi_{ij},\eta_{ij},t) \\ &\coloneqq G_{kl}\Big(\xi_{kl}\big(\boldsymbol{z}(\boldsymbol{\xi},\boldsymbol{\eta}),\boldsymbol{\zeta}(\boldsymbol{\xi},\boldsymbol{\eta})\big),\eta_{kl}\big(\boldsymbol{z}(\boldsymbol{\xi},\boldsymbol{\eta}),\boldsymbol{\zeta}(\boldsymbol{\xi},\boldsymbol{\eta})\big),t\Big), \end{aligned} \tag{2.141}$$

which is important to handle the coupling of the different kernel elements.

To keep an overview of the applied coordinate transformations, Figure 2.4 shows them in a summarized fashion like in [113]. Important to keep in mind is that there is only „one“ original domain $\mathcal{D}$ and every point (z,ζ) of it is mapped into a unique point in each of the other domains.

2.5.4 Canonical kernel equations

With the required coordinate transformations, the kernel equations belonging to (2.140) can be derived.

Lemma 2.5.4 (Canonical kernel equations)**.** *The change of coordinates* (2.133) *with the new kernel element variables* (2.140) *and*

$$\boldsymbol{H}(\boldsymbol{\xi},\boldsymbol{\eta},t) = H_{ij}(\xi_{ij},\eta_{ij},t) \coloneqq \boldsymbol{G}_{\boldsymbol{\xi}}(\boldsymbol{\xi},\boldsymbol{\eta},t), \tag{2.142}$$

maps (2.98) *into its* canonical first-order representation

$$\boldsymbol{H}_{\boldsymbol{\eta}} = -\frac{\bar{\boldsymbol{a}}_{\Delta}}{4}\boldsymbol{H} + \frac{\boldsymbol{s}\bar{\boldsymbol{a}}_{\Sigma}}{4}\boldsymbol{G}_{\boldsymbol{\eta}} + \frac{\boldsymbol{s}}{4}\sum_{k=1}^{n}\Big(\frac{\lambda_j(\zeta)}{\lambda_k(\zeta)}G_{ik}A_{kj}(\zeta,t) + \widetilde{A}_{ik}G_{kj}\Big) + \frac{\boldsymbol{s}}{4}\boldsymbol{G}_t$$
$$- \frac{\boldsymbol{s}}{4}\lambda_j(\zeta)\boldsymbol{F} + \frac{\boldsymbol{s}}{4}\int_{\zeta}^{z}\sum_{k=1}^{n}\frac{\lambda_j(\zeta)}{\lambda_k(\bar{\zeta})}G_{ik}(z,\bar{\zeta},t)F_{kj}(\bar{\zeta},\zeta,t)\mathrm{d}\bar{\zeta} \tag{2.143a}$$

$$\boldsymbol{G}_{\boldsymbol{\xi}} = \boldsymbol{H} \tag{2.143b}$$

with the BCs

$$[\boldsymbol{G}(\boldsymbol{\xi}_l(\boldsymbol{\eta}),\boldsymbol{\eta},t) = 0]_{\substack{\lambda_i \neq \lambda_j \\ \boldsymbol{\eta} < 0}} \tag{2.143c}$$

$$\Big[\boldsymbol{H}(\boldsymbol{\xi},\boldsymbol{\eta}_l(\boldsymbol{\xi}),t) = \underbrace{\frac{(\boldsymbol{A}+\widetilde{\boldsymbol{A}})\lambda_j(z)\sqrt{\lambda_i(z)}\boldsymbol{\eta}_l'}{(\lambda_j(z)-\lambda_i(z))(\boldsymbol{s}\boldsymbol{\eta}_l'-1)}}_{\boldsymbol{c}^1(z,t)}\Big]_{\substack{\lambda_i \neq \lambda_j \\ z\,=\,\boldsymbol{z}(\boldsymbol{\xi},\boldsymbol{\eta}_l(\boldsymbol{\xi}))}} \tag{2.143d}$$

$$\Big[\boldsymbol{H}(\boldsymbol{\xi},\boldsymbol{\eta}_l(\boldsymbol{\xi}),t) = \boldsymbol{K}_0(t)\sqrt{\lambda_i(0)}\frac{\lambda_i'}{4} - \frac{(\boldsymbol{A}+\widetilde{\boldsymbol{A}})\sqrt{\lambda_i}}{4}$$
$$- \int_0^z \frac{(\boldsymbol{A}(\zeta,t)+\widetilde{\boldsymbol{A}}(\zeta,t))\lambda_i'}{8\sqrt{\lambda_i(\zeta)}}\mathrm{d}\zeta =: \boldsymbol{c}^2(z,t)\Big]_{\substack{\lambda_i\,=\,\lambda_j \\ z\,=\,\boldsymbol{z}(\boldsymbol{\xi},\boldsymbol{\eta}_l(\boldsymbol{\xi}))}} \tag{2.143e}$$

$$[\boldsymbol{G}(\boldsymbol{\xi}_l(\boldsymbol{\eta}),\boldsymbol{\eta},t) = 0]_{\substack{j\,\leq\,m \\ \lambda_i\,\geq\,\lambda_j \\ \boldsymbol{\eta}\,\geq\,0}} \tag{2.143f}$$

$$\Big[\boldsymbol{G}(\boldsymbol{\xi}_l(\boldsymbol{\eta}),\boldsymbol{\eta},t) = \int_0^{\boldsymbol{\eta}}\Big(2\boldsymbol{H}(\bar{\eta},\bar{\eta},t) - q_j^0(t)\sqrt{\lambda_j(0)}\boldsymbol{G}(\bar{\eta},\bar{\eta},t)$$
$$+ \sqrt{\lambda_j(0)}\int_0^{\boldsymbol{z}(\boldsymbol{\xi}_l(\bar{\eta}),\bar{\eta})}\sum_{k=1}^{n}\frac{1}{\lambda_k(\zeta)}G_{ik}(\boldsymbol{z}(\boldsymbol{\xi}_l(\bar{\eta}),\bar{\eta}),\zeta,t)A_{0,kj}(\zeta,t)\mathrm{d}\zeta\Big)\mathrm{d}\bar{\eta}$$
$$\underbrace{-\sqrt{\lambda_j(0)}\int_0^{\boldsymbol{\eta}}\boldsymbol{A}_0(\boldsymbol{z}(\boldsymbol{\xi}_l(\bar{\eta}),\bar{\eta}),t)\mathrm{d}\bar{\eta} + \lambda_j(0)\boldsymbol{K}_0(t)}_{\bar{\boldsymbol{c}}^3(\boldsymbol{\eta},t)}\Big]_{\substack{j\,>\,m \\ \lambda_i\,\geq\,\lambda_j \\ \boldsymbol{\eta}\,\geq\,0}} \tag{2.143g}$$

$$[\boldsymbol{G}(\boldsymbol{\xi}_l(\boldsymbol{\eta}),\boldsymbol{\eta},t) = \boldsymbol{g}(\boldsymbol{\eta},t)]_{\substack{\lambda_i\,<\,\lambda_j \\ \boldsymbol{\eta}\,\geq\,0}}\,, \tag{2.143h}$$

and $\bar{a}_\Delta(\xi,\eta) = a_\Delta(z(\xi,\eta),\zeta(\xi,\eta))$, $\bar{a}_\Sigma(\xi,\eta) = a_\Sigma(z(\xi,\eta),\zeta(\xi,\eta))$, *where*

$$a_\Delta(z,\zeta) = \frac{\lambda_j'(\zeta)}{2\sqrt{\lambda_j(\zeta)}} - \frac{\lambda_i'}{2\sqrt{\lambda_i}}, \quad a_\Sigma(z,\zeta) = \frac{\lambda_j'(\zeta)}{2\sqrt{\lambda_j(\zeta)}} + \frac{\lambda_i'}{2\sqrt{\lambda_i}} \tag{2.144}$$

and $\xi_l(\eta)$, $\eta_l(\xi)$ *are the left respectively lower boundaries of* $\bar{\mathcal{D}}_c$. *The PIDEs* (2.143b) *and* (2.143a) *are defined on the open domain* $(\xi,\eta) \in \mathcal{D}_c$,

$$\mathcal{D}_c = \Big\{\xi,\eta \in \mathbb{R} \,\Big|\, 0 < \xi < \phi_i(1) + \phi_j(1), \\ \eta_l(\xi) < \eta < \min\big(\xi, 2\min(\phi_i(1),\phi_j(1)) - \xi\big)\Big\}, \tag{2.145}$$

$t \in \mathbb{R}_{t_0}^+$ *and the functions* $g(\cdot,t) = g_{ij}(\cdot,t) \in C[0,\phi_j(1)]$, $g(z,\cdot) \in G_\alpha(\mathbb{R}_{t_0}^+)$, $\alpha \in [1,2)$ *are a degree of freedom.*

Proof. As already mentioned earlier, the aim of the canonical coordinates is to simplify the spatial operator of the PIDE (2.98a). Thus, the second order spatial derivatives of $\bar{K}$ need to be calculated in terms of G. Note that (2.133) implies

$$\xi_w = s, \quad \xi_v = s \tag{2.146a}$$
$$\eta_w = 1, \quad \eta_v = -1, \tag{2.146b}$$

which is used with the chain rule in

$$\bar{K}_w = G_w = G_\xi \xi_w + G_\eta \eta_w = sG_\xi + G_\eta \tag{2.147a}$$
$$\bar{K}_v = G_v = G_\xi \xi_v + G_\eta \eta_v = sG_\xi - G_\eta \tag{2.147b}$$
$$\begin{aligned}\bar{K}_{ww} &= s(G_\xi)_w + (G_\eta)_w = sG_{\xi\xi}\xi_w + sG_{\xi\eta}\eta_w + G_{\eta\xi}\xi_w + G_{\eta\eta}\eta_w \\ &= G_{\xi\xi} + 2sG_{\xi\eta} + G_{\eta\eta}\end{aligned} \tag{2.147c}$$
$$\begin{aligned}\bar{K}_{vv} &= s(G_\xi)_v - (G_\eta)_v = sG_{\xi\xi}\xi_v + sG_{\xi\eta}\eta_v - G_{\eta\xi}\xi_v - G_{\eta\eta}\eta_v \\ &= G_{\xi\xi} - 2sG_{\xi\eta} + G_{\eta\eta}.\end{aligned} \tag{2.147d}$$

Together with (2.140), (2.147) is now inserted into (2.98a), yielding the *canonical kernel PIDE*

$$\begin{aligned}
&4s\boldsymbol{G}_{\boldsymbol{\xi}\boldsymbol{\eta}} + \underbrace{\left(\frac{\lambda_j'(\zeta)}{2\sqrt{\lambda_j(\zeta)}} - \frac{\lambda_i'}{2\sqrt{\lambda_i}}\right)}_{\boldsymbol{a}_\Delta(z,\zeta)} s\boldsymbol{G}_{\boldsymbol{\xi}} - \underbrace{\left(\frac{\lambda_j'(\zeta)}{2\sqrt{\lambda_j(\zeta)}} + \frac{\lambda_i'}{2\sqrt{\lambda_i}}\right)}_{\boldsymbol{a}_\Sigma(z,\zeta)} \boldsymbol{G}_{\boldsymbol{\eta}} \\
&= \sum_{k=1}^{n}\left(\frac{\lambda_j(\zeta)}{\lambda_k(\zeta)} G_{ik} A_{kj}(\zeta,t) + \widetilde{A}_{ik} G_{kj}\right) + \boldsymbol{G}_t - \lambda_j(\zeta)\boldsymbol{F} \\
&\quad + \int_\zeta^z \sum_{k=1}^{n} \frac{\lambda_j(\zeta)}{\lambda_k(\bar{\zeta})} \underbrace{G_{ik}\left(\xi_{ik}\left(\boldsymbol{z}(\boldsymbol{\xi},\boldsymbol{\eta}),\bar{\zeta}\right), \eta_{ik}\left(\boldsymbol{z}(\boldsymbol{\xi},\boldsymbol{\eta}),\bar{\zeta}\right), t\right)}_{:= G_{ik}(z,\bar{\zeta},t)} F_{kj}(\bar{\zeta},\zeta,t)\mathrm{d}\bar{\zeta}.
\end{aligned} \tag{2.148}$$

Since (2.148) is interpreted in terms of the independent variables $\boldsymbol{\xi}, \boldsymbol{\eta}, t$, all appearances of ζ are assumed to mean $\boldsymbol{\zeta}(\boldsymbol{\xi},\boldsymbol{\eta})$ and all (implicit) appearances of z mean $\boldsymbol{z}(\boldsymbol{\xi},\boldsymbol{\eta})$. This assumption is made for all following equations. In turn, this allows to write

$$\boldsymbol{a}_\Delta(z,\zeta) = \boldsymbol{a}_\Delta(\boldsymbol{z}(\boldsymbol{\xi},\boldsymbol{\eta}),\boldsymbol{\zeta}(\boldsymbol{\xi},\boldsymbol{\eta})) =: \bar{\boldsymbol{a}}_\Delta(\boldsymbol{\xi},\boldsymbol{\eta}) \tag{2.149a}$$

$$\boldsymbol{a}_\Sigma(z,\zeta) = \boldsymbol{a}_\Sigma(\boldsymbol{z}(\boldsymbol{\xi},\boldsymbol{\eta}),\boldsymbol{\zeta}(\boldsymbol{\xi},\boldsymbol{\eta})) =: \bar{\boldsymbol{a}}_\Sigma(\boldsymbol{\xi},\boldsymbol{\eta}). \tag{2.149b}$$

Inserting (2.147a) and (2.147b) into (2.98c) and (2.98f) yields the *canonical BCs*

$$[\boldsymbol{G}(\boldsymbol{\xi},\boldsymbol{\eta}_l(\boldsymbol{\xi}),t) = 0]_{\lambda_i \neq \lambda_j} \tag{2.150a}$$

$$\left[s\boldsymbol{G}_{\boldsymbol{\xi}}(\boldsymbol{\xi},\boldsymbol{\eta}_l(\boldsymbol{\xi}),t) + \boldsymbol{G}_{\boldsymbol{\eta}}(\boldsymbol{\xi},\boldsymbol{\eta}_l(\boldsymbol{\xi}),t) = \frac{(\boldsymbol{A}+\widetilde{\boldsymbol{A}})\lambda_j\sqrt{\lambda_i}}{\lambda_j-\lambda_i}\right]_{\lambda_i \neq \lambda_j} \tag{2.150b}$$

$$\left[\boldsymbol{G}(\boldsymbol{\xi},0,t) = \underbrace{\boldsymbol{K}_0(t)\sqrt{\lambda_i(0)\lambda_i} - \int_0^z \frac{(\boldsymbol{A}(\zeta,t)+\widetilde{\boldsymbol{A}}(\zeta,t))}{2}\sqrt{\frac{\lambda_i}{\lambda_i(\zeta)}}\mathrm{d}\zeta}_{\boldsymbol{c}^4(z,t)}\right]_{\lambda_i = \lambda_j} \tag{2.150c}$$

$$[\boldsymbol{G}(\boldsymbol{\eta},\boldsymbol{\eta},t) = 0]_{\substack{j \leq m \\ \lambda_i \geq \lambda_j}} \tag{2.150d}$$

$$\Bigg[\boldsymbol{G}_{\boldsymbol{\xi}}(\boldsymbol{\eta},\boldsymbol{\eta},t)-\boldsymbol{G}_{\boldsymbol{\eta}}(\boldsymbol{\eta},\boldsymbol{\eta},t)=q_j^0(t)\sqrt{\lambda_j(0)}\boldsymbol{G}(\boldsymbol{\eta},\boldsymbol{\eta},t)$$
$$+\sqrt{\lambda_j(0)}\boldsymbol{A}_0-\sqrt{\lambda_j(0)}\int_0^{z(\boldsymbol{\eta},\boldsymbol{\eta})}\sum_{k=1}^{n}\frac{1}{\lambda_k(\zeta)}G_{ik}(z(\boldsymbol{\eta},\boldsymbol{\eta}),\zeta,t)A_{0,kj}(\zeta,t)\mathrm{d}\zeta\Bigg]_{\substack{j>m\\ \lambda_i\geq\lambda_j}}. \tag{2.150e}$$

These equations are complemented by the *artificial BC* needed for well-posed kernel equations. To make it as simple as possible, the value of the kernel on the boundary $\widetilde{\Gamma}_3$ for $\lambda_i<\lambda_j$ is simply set as

$$[\boldsymbol{G}(\boldsymbol{\eta},\boldsymbol{\eta},t)=\boldsymbol{g}(\boldsymbol{\eta},t)=g_{ij}(\boldsymbol{\eta},t)]_{\lambda_i<\lambda_j} \tag{2.150f}$$

with $g_{ij}(\cdot,t)\in C[0,\phi_j(1)]$, $g_{ij}(z,\cdot)\in G_\alpha(\mathbb{R}^+_{t_0})$, $\alpha\in[1,2)$.

The canonical kernel equations are now changed into a system of first-order equations. To this end, introduce (2.142). Obviously, inserting it into (2.148) leads to the *first-order canonical kernel PIDEs* (2.143a) and (2.143b). To convert them into integral equations, (2.143a) needs to be formally integrated w. r. t. $\boldsymbol{\eta}$ and (2.143b) w. r. t. $\boldsymbol{\xi}$. In general, the fundamental theorem of calculus says that given a continuous differentiable function $F(x)$,

$$\int_{x_0}^{x}F'(\bar{x})\mathrm{d}\bar{x}=F(x)-F(x_0). \tag{2.151}$$

Thus, eliminating the derivative $\boldsymbol{H}_{\boldsymbol{\eta}}$ in (2.143a) by integrating w. r. t. $\boldsymbol{\eta}$ will insert values of $\boldsymbol{H}$ at the starting point of the integration, i. e. the lower boundary $\eta_l(\boldsymbol{\xi})$ of the domain. This induces that a further reformulation of the BCs (2.150) in terms of the new variable $\boldsymbol{H}$ is required. Starting with (2.150a), $\boldsymbol{G}(\boldsymbol{\xi},\eta_l(\boldsymbol{\xi}),t)=0$ implies that its derivative w. r. t. ξ is also zero, i. e.

$$\begin{aligned}\mathrm{d}_{\boldsymbol{\xi}}\boldsymbol{G}(\boldsymbol{\xi},\eta_l(\boldsymbol{\xi}),t)&=0\\ \boldsymbol{G}_{\boldsymbol{\xi}}(\boldsymbol{\xi},\eta_l(\boldsymbol{\xi}),t)+\boldsymbol{G}_{\boldsymbol{\eta}}(\boldsymbol{\xi},\eta_l(\boldsymbol{\xi}),t)\eta_l'(\boldsymbol{\xi})&=0\\ \boldsymbol{G}_{\boldsymbol{\eta}}(\boldsymbol{\xi},\eta_l(\boldsymbol{\xi}),t)&=-\frac{\boldsymbol{G}_{\boldsymbol{\xi}}(\boldsymbol{\xi},\eta_l(\boldsymbol{\xi}),t)}{\eta_l'(\boldsymbol{\xi})},\end{aligned} \tag{2.152}$$

for $\lambda_i\neq\lambda_j$, which can be inserted with (2.142) into (2.150b) to obtain

$$\begin{aligned}\left(s-\frac{1}{\eta_l'}\right)\boldsymbol{H}(\boldsymbol{\xi},\eta_l(\boldsymbol{\xi}),t)&=\frac{(\boldsymbol{A}+\widetilde{\boldsymbol{A}})\lambda_j\sqrt{\lambda_i}}{\lambda_j-\lambda_i}\\ \left[\boldsymbol{H}(\boldsymbol{\xi},\eta_l(\boldsymbol{\xi}),t)=\frac{(\boldsymbol{A}+\widetilde{\boldsymbol{A}})\lambda_j\sqrt{\lambda_i}\eta_l'}{(\lambda_j-\lambda_i)(s\eta_l'-1)}\right]_{\lambda_i\neq\lambda_j}&.\end{aligned} \tag{2.153}$$

The denominator of the resulting expression contains the term $s\eta_l' - 1$, which must not be zero. Together with the definition of s and knowing that $\eta_l'(\xi) < 0,\ \forall \xi \in [0, \phi_i(1) + \phi_j(1)]$ (see (2.129)), it remains to show that $\eta_l'(\xi) \neq -1$ for $s = -1$[7]. To this end, insert (2.125) into (2.129) to get

$$\eta_l'(\xi) = -\left(\frac{1}{\sqrt{\lambda_i(z_l)}} - \frac{1}{\sqrt{\lambda_j(z_l)}}\right) \frac{1}{\frac{1}{\sqrt{\lambda_i(z_l)}} + \frac{1}{\sqrt{\lambda_j(z_l)}}}, \tag{2.154}$$

which can only be -1 if $\frac{1}{\sqrt{\lambda_i(z_l)}} - \frac{1}{\sqrt{\lambda_j(z_l)}} = \frac{1}{\sqrt{\lambda_i(z_l)}} + \frac{1}{\sqrt{\lambda_j(z_l)}}$, which is not possible for finite λ_i. Consequently the denominator in (2.153) cannot be zero.

The third BC (2.150c) is differentiated w. r. t. ξ, yielding

$$\begin{aligned} \boldsymbol{H}(\xi, 0, t) = \boldsymbol{K}_0(t)\sqrt{\frac{\lambda_i(0)}{\lambda_i(z)}}\frac{\lambda_i'(z)}{2}\boldsymbol{z}_\xi - \frac{\boldsymbol{A} + \widetilde{\boldsymbol{A}}}{2}\boldsymbol{z}_\xi \\ - \int_0^z \frac{(\boldsymbol{A}(\zeta, t) + \widetilde{\boldsymbol{A}}(\zeta, t))\lambda_i'(z)}{4\sqrt{\lambda_i(\zeta)\lambda_i(z)}}\mathrm{d}\zeta \boldsymbol{z}_\xi \end{aligned} \tag{2.155}$$

for $\lambda_i = \lambda_j$. To substitute $\boldsymbol{z}_\xi(\xi, 0)$, insert (2.139a) with $s = 1$ for $\lambda_i = \lambda_j$. With this, (2.155) is simplified to

$$\begin{aligned} \Bigg[\boldsymbol{H}(\xi, 0, t) = \boldsymbol{K}_0(t)\sqrt{\lambda_i(0)}\frac{\lambda_i'}{4} - \frac{(\boldsymbol{A} + \widetilde{\boldsymbol{A}})\sqrt{\lambda_i}}{4} \\ - \int_0^z \frac{(\boldsymbol{A}(\zeta, t) + \widetilde{\boldsymbol{A}}(\zeta, t))\lambda_i'}{8\sqrt{\lambda_i(\zeta)}}\mathrm{d}\zeta\Bigg]_{\lambda_i = \lambda_j}. \end{aligned} \tag{2.156}$$

To reformulate (2.150e), solve it for $\boldsymbol{G}_\eta(\eta, \eta, t)$ and insert the result into

$$\mathrm{d}_\eta \boldsymbol{G}(\eta, \eta, t) = \boldsymbol{G}_\xi(\eta, \eta, t) + \boldsymbol{G}_\eta(\eta, \eta, t), \tag{2.157}$$

to get for $\lambda_i \geq \lambda_j$ and $j > m$,

$$\begin{aligned} \mathrm{d}_\eta \boldsymbol{G}(\eta, \eta, t) = 2\boldsymbol{H}(\eta, \eta, t) - q_j^0(t)\sqrt{\lambda_j(0)}\boldsymbol{G}(\eta, \eta, t) \\ - \sqrt{\lambda_j(0)}\boldsymbol{A}_0 + \sqrt{\lambda_j(0)}\int_0^{z(\eta,\eta)} \sum_{k=1}^{n} \frac{1}{\lambda_k(\zeta)} G_{ik}(z, \zeta, t) A_{0,kj}(\zeta, t)\mathrm{d}\zeta, \end{aligned} \tag{2.158}$$

[7] Which implies $\lambda_i < \lambda_j$ according to (2.131).

which is an ODE determining the solution $\boldsymbol{G}(\boldsymbol{\eta}, \boldsymbol{\eta}, t)$ dependent on $\boldsymbol{H}(\boldsymbol{\eta}, \boldsymbol{\eta}, t)$ and the other kernel elements G_{ik} of this row i, which are integrated along ζ, corresponding to a not yet further specified curve in its coordinates (ξ_{ik}, η_{ik}). Instead of determining the solution of this ODE (which could be difficult, either) it is simply converted into an integral equation by formally integrating w. r. t. $\boldsymbol{\eta}$. This is sufficient for including the BC when converting the canonical PIDE (2.148) into an integral equation, because the result will be an integral equation anyway. Consequently,

$$\begin{aligned}
&\boldsymbol{G}(\boldsymbol{\eta}, \boldsymbol{\eta}, t) \\
&= \int_0^{\boldsymbol{\eta}} \Big(2\boldsymbol{H}(\bar{\eta}, \bar{\eta}, t) - q_j^0(t)\sqrt{\lambda_j(0)}\boldsymbol{G}(\bar{\eta}, \bar{\eta}, t) - \sqrt{\lambda_j(0)}\boldsymbol{A}_0(\boldsymbol{z}(\bar{\eta}, \bar{\eta}), t) \\
&+ \sqrt{\lambda_j(0)} \int_0^{\boldsymbol{z}(\bar{\eta}, \bar{\eta})} \sum_{k=1}^{n} \frac{1}{\lambda_k(\zeta)} G_{ik}(\boldsymbol{z}(\bar{\eta}, \bar{\eta}), \zeta, t) A_{0,kj}(\zeta, t) \mathrm{d}\zeta \Big) \mathrm{d}\bar{\eta} + \boldsymbol{G}(0, 0, t)
\end{aligned} \tag{2.159}$$

is the BC on $(\boldsymbol{\eta}, \boldsymbol{\eta})$ in this case. The value $\boldsymbol{G}(0, 0, t)$ can be calculated by

$$\boldsymbol{G}(0, 0, t) = \bar{\boldsymbol{K}}(0, 0, t) = \lambda_j(0)\boldsymbol{K}(0, 0, t) \overset{(2.92)}{=} \lambda_j(0)\boldsymbol{K}_0(t). \tag{2.160}$$

The canonical spatial domain $\mathcal{D}_c$ has the form shown in Figure 2.3 for all i, j, except that the lower boundary is $\boldsymbol{\eta} = 0$ for $\lambda_i = \lambda_j$. In order to get the representation (2.143), the common notation for the lower respectively left boundary of the spatial domain needs to be verified. For the first case, the function $\boldsymbol{\eta}_l(\boldsymbol{\xi})$ was already introduced to describe the lower boundary for $\lambda_i \neq \lambda_j$. However, inserting $\lambda_i = \lambda_j$ in its definition (2.128) with (2.123) reveals that $\boldsymbol{\eta}_l(\boldsymbol{\xi}) = 0$. Thus, $\boldsymbol{\eta}_l(\boldsymbol{\xi})$ indeed describes the lower boundary of the spatial domain for each i, j.

Figure 2.3 also shows that for the case $\lambda_i \neq \lambda_j$, the left boundary is split into two parts. In the upper part, it is obviously $(\boldsymbol{\eta}, \boldsymbol{\eta})$, while the lower part is described by $\boldsymbol{\eta}_l^{-1}(\boldsymbol{\eta})$. It is already known that $\boldsymbol{\eta}_l$ is a strictly monotonically decreasing function, so that its inverse exists. Combining these both cases allows the definition of the left boundary

$$\boldsymbol{\xi}_l(\boldsymbol{\eta}) := \begin{cases} \boldsymbol{\eta}, & \boldsymbol{\eta} \geq 0 \\ \boldsymbol{\eta}_l^{-1}(\boldsymbol{\eta}), & \boldsymbol{\eta} < 0. \end{cases} \tag{2.161}$$

As the area $\boldsymbol{\eta} < 0$ only exists for $\lambda_i \neq \lambda_j$, no further restriction needs to be made in it. Thus, (2.143) is obtained, proving the lemma. ■

Remark 2.5.5. Comparing the presented approach for converting the kernel equations into its canonical form with existing literature for the scalar case, especially [81] shows that the first step shown in Section 2.5.2, i. e. the elimination of the coefficients which lead the second order derivatives is just the same. However, in [81] and also in [113] there is another step after it, eliminating the first-order spatial derivatives. In [113] the resulting canonical kernel equations with the second-order spatial operator are transformed into a system of two first-order differential equations before converting them into integral equations. This is mainly done for the sake of readability and to bound comprehensiveness, but it was shown in [118] that the step to eliminate the first-order spatial derivatives is no longer needed if this conversion into the system of first-order differential equations is performed. ◁

2.5.5 Transformation into integral equations

Now (2.143b) can be formally integrated w. r. t. $\boldsymbol{\xi}$, starting at the left boundary of the spatial domain (see Figure 2.3). This yields

$$\boldsymbol{G}(\boldsymbol{\xi},\boldsymbol{\eta},t) = \boldsymbol{G}(\boldsymbol{\xi}_l(\boldsymbol{\eta}),\boldsymbol{\eta},t) + \int_{\boldsymbol{\xi}_l(\boldsymbol{\eta})}^{\boldsymbol{\xi}} \boldsymbol{H}(\bar{\xi},\boldsymbol{\eta},t)\mathrm{d}\bar{\xi}, \tag{2.162}$$

where $\boldsymbol{G}(\boldsymbol{\xi}_l(\boldsymbol{\eta}),\boldsymbol{\eta},t)$ can directly be substituted by the corresponding BCs (2.143c), (2.143f) and (2.143g).

Equation (2.143a) is integrated w. r. t. $\boldsymbol{\eta}$, yielding

$$\begin{aligned}
&\boldsymbol{H}(\boldsymbol{\xi},\boldsymbol{\eta},t) = \boldsymbol{H}(\boldsymbol{\xi},\boldsymbol{\eta}_l(\boldsymbol{\xi}),t)\\
&+\frac{1}{4}\int_{\boldsymbol{\eta}_l(\boldsymbol{\xi})}^{\boldsymbol{\eta}} \Bigg(-\bar{a}_{\Delta}(\boldsymbol{\xi},\bar{\eta})\boldsymbol{H}(\boldsymbol{\xi},\bar{\eta},t) + s\underbrace{\bar{a}_{\Sigma}(\boldsymbol{\xi},\bar{\eta})\boldsymbol{G}_{\bar{\eta}}(\boldsymbol{\xi},\bar{\eta},t)}_{(\star_4)}\\
&+ s\sum_{k=1}^{n}\Big(\frac{\lambda_j(\boldsymbol{\zeta}(\boldsymbol{\xi},\bar{\eta}))}{\lambda_k(\boldsymbol{\zeta}(\boldsymbol{\xi},\bar{\eta}))}G_{ik}(\boldsymbol{\xi},\bar{\eta},t)A_{kj}(\boldsymbol{\zeta}(\boldsymbol{\xi},\bar{\eta}),t) + \widetilde{A}_{ik}(\boldsymbol{z}(\boldsymbol{\xi},\bar{\eta}),t)G_{kj}(\boldsymbol{\xi},\bar{\eta},t)\Big)\\
&+ s\boldsymbol{G}_t(\boldsymbol{\xi},\bar{\eta},t) - s\lambda_j(\boldsymbol{\zeta}(\boldsymbol{\xi},\bar{\eta}))\boldsymbol{F}(\boldsymbol{z}(\boldsymbol{\xi},\bar{\eta}),\boldsymbol{\zeta}(\boldsymbol{\xi},\bar{\eta}),t)\\
&+ s\int_{\zeta(\boldsymbol{\xi},\bar{\eta})}^{\boldsymbol{z}(\boldsymbol{\xi},\bar{\eta})}\sum_{k=1}^{n}\frac{\lambda_j(\boldsymbol{\zeta}(\boldsymbol{\xi},\bar{\eta}))}{\lambda_k(\bar{\zeta})}G_{ik}(\boldsymbol{z}(\boldsymbol{\xi},\bar{\eta}),\bar{\zeta},t)F_{kj}(\bar{\zeta},\boldsymbol{\zeta}(\boldsymbol{\xi},\bar{\eta}),t)\mathrm{d}\bar{\zeta}\Bigg)\mathrm{d}\bar{\eta}.
\end{aligned} \tag{2.163}$$

Apparently, this is not yet a proper integral equation as it still contains the derivative $\boldsymbol{G}_{\boldsymbol{\eta}}$. Therefore, integration by parts is applied to $(\star_4)$, yielding

$$\begin{aligned}&\int_{\boldsymbol{\eta}_l(\boldsymbol{\xi})}^{\boldsymbol{\eta}} \bar{\boldsymbol{a}}_\Sigma(\boldsymbol{\xi},\bar{\eta})\boldsymbol{G}_{\bar{\eta}}(\boldsymbol{\xi},\bar{\eta},t)\mathrm{d}\bar{\eta}\\ &= \bar{\boldsymbol{a}}_\Sigma\boldsymbol{G} - \bar{\boldsymbol{a}}_\Sigma(\boldsymbol{\xi},\boldsymbol{\eta}_l(\boldsymbol{\xi}))\boldsymbol{G}(\boldsymbol{\xi},\boldsymbol{\eta}_l(\boldsymbol{\xi}),t) + \int_{\boldsymbol{\eta}_l(\boldsymbol{\xi})}^{\boldsymbol{\eta}} \bar{\boldsymbol{a}}_{\Sigma,\bar{\eta}}(\boldsymbol{\xi},\bar{\eta})\boldsymbol{G}(\boldsymbol{\xi},\bar{\eta},t)\mathrm{d}\bar{\eta},\end{aligned} \tag{2.164}$$

where an expression for $\bar{\boldsymbol{a}}_{\Sigma,\boldsymbol{\eta}}(\boldsymbol{\xi},\bar{\eta})$ can be found by differentiating its definition (2.149b) with $\boldsymbol{a}_\Sigma$ defined in (2.148). This leads to

$$\begin{aligned}\bar{\boldsymbol{a}}_{\Sigma,\boldsymbol{\eta}} &= \boldsymbol{a}_{\Sigma,\boldsymbol{z}}\boldsymbol{z}_{\boldsymbol{\eta}} + \boldsymbol{a}_{\Sigma,\zeta}\boldsymbol{\zeta}_{\boldsymbol{\eta}}\\ &= \frac{2\lambda_i\lambda_i'' - (\lambda_i')^2}{4\sqrt{\lambda_i}\lambda_i}\boldsymbol{z}_{\boldsymbol{\eta}} + \frac{2\lambda_j(\zeta)\lambda_j''(\zeta) - (\lambda_j'(\zeta))^2}{4\sqrt{\lambda_j(\zeta)}\lambda_j(\zeta)}\boldsymbol{\zeta}_{\boldsymbol{\eta}}\end{aligned} \tag{2.165}$$

and after inserting (2.139a), (2.139b),

$$\bar{\boldsymbol{a}}_{\Sigma,\boldsymbol{\eta}} = \frac{2\lambda_i\lambda_i'' - (\lambda_i')^2}{8\lambda_i} - \frac{2\lambda_j(\zeta)\lambda_j''(\zeta) - (\lambda_j'(\zeta))^2}{8\lambda_j(\zeta)} =: \tilde{\boldsymbol{a}}(z,\zeta). \tag{2.166}$$

Due to the integration by parts, the first integral equation (2.162) needs to be inserted for $\boldsymbol{G}$ in (2.164). Moreover, the BCs (2.150a) and (2.150c) replace $\boldsymbol{G}(\boldsymbol{\xi},\boldsymbol{\eta}_l(\boldsymbol{\xi}),t)$.

With these replacements and the insertion of the corresponding BCs, the integral equations are in the form that they are used in [113]. However, it was shown in [118], that the applied proof of convergence of the corresponding fixed-point iteration requires the term $\boldsymbol{G}_t$ to appear under a double integral. In the existing literature for scalar systems with time dependent coefficients, e. g. [72], the conversion into the first-order system is not performed. Thus, the time-derivatives of the kernel automatically appear under a double integral in the resulting integral equation. In the present case, one last step as presented in [118] is needed to ensure this.

Introduce the abbreviation $\boldsymbol{R}$ containing all terms appearing in the right-hand side of (2.163), except $\frac{\boldsymbol{s}}{4}\int_{\boldsymbol{\eta}_l(\boldsymbol{\xi})}^{\boldsymbol{\eta}} \boldsymbol{G}_t(\boldsymbol{\xi},\bar{\eta},t)\mathrm{d}\bar{\eta}$. Then, this integral equation can be rewritten as

$$\boldsymbol{H} = \boldsymbol{R} + \frac{\boldsymbol{s}}{4}\int_{\boldsymbol{\eta}_l(\boldsymbol{\xi})}^{\boldsymbol{\eta}} \boldsymbol{G}_t(\boldsymbol{\xi},\bar{\eta},t)\mathrm{d}\bar{\eta}. \tag{2.167}$$

Now separate the variable

$$\boldsymbol{H} = \boldsymbol{H}_1 + \boldsymbol{H}_2 \tag{2.168a}$$

into two parts, where

$$\boldsymbol{H}_2 := \frac{\boldsymbol{s}}{4} \int_{\boldsymbol{\eta}_l(\boldsymbol{\xi})}^{\boldsymbol{\eta}} \boldsymbol{G}_t(\boldsymbol{\xi}, \bar{\eta}, t) \mathrm{d}\bar{\eta}, \tag{2.168b}$$

i. e. H_2 is that part of the integral equation, which shall be put under another integral. Then, (2.167) can be written as

$$\begin{aligned} \boldsymbol{H}_1 + \boldsymbol{H}_2 &= \boldsymbol{R} + \boldsymbol{H}_2 \\ \boldsymbol{H}_1 &= \boldsymbol{R} \end{aligned} \tag{2.169}$$

being a new integral equation for $\boldsymbol{H}_1$. All that remains to be done is to insert (2.168) into $\boldsymbol{R}$ and into the integral equation (2.162) for $\boldsymbol{G}$.

The resulting integral equation for $\boldsymbol{G}$ reads

$$\boldsymbol{G}(\boldsymbol{\xi}, \boldsymbol{\eta}, t) = \boldsymbol{G}_0(\boldsymbol{\eta}, t) + \boldsymbol{F}_G[G, \boldsymbol{H}_1](\boldsymbol{\xi}, \boldsymbol{\eta}, t) \tag{2.170a}$$

with

$$\boldsymbol{G}_0(\boldsymbol{\eta}, t) = \lambda_j(0) \boldsymbol{K}_0(t) + [\bar{c}^3(\boldsymbol{\eta}, t)]_{\substack{j > m \\ \lambda_i \geq \lambda_j \\ \boldsymbol{\eta} \geq 0}} + [\boldsymbol{g}(\boldsymbol{\eta}, t)]_{\substack{\lambda_i < \lambda_j \\ \boldsymbol{\eta} \geq 0}} \tag{2.170b}$$

and

$$\begin{aligned} \boldsymbol{F}_G[G, \boldsymbol{H}_1](\boldsymbol{\xi}, \boldsymbol{\eta}, t) = \Bigg[& \int_0^{\boldsymbol{\eta}} \Big(2\boldsymbol{H}_1(\bar{\eta}, \bar{\eta}, t) - q_j^0(t) \sqrt{\lambda_j(0)} \boldsymbol{G}(\bar{\eta}, \bar{\eta}, t) \\ & + \sqrt{\lambda_j(0)} \int_0^{\boldsymbol{z}(\boldsymbol{\xi}_l(\bar{\eta}), \bar{\eta})} \sum_{k=1}^{n} \frac{1}{\lambda_k(\zeta)} G_{ik}(\boldsymbol{z}(\boldsymbol{\xi}_l(\bar{\eta}), \bar{\eta}), \zeta, t) A_{0,kj}(\zeta, t) \mathrm{d}\zeta \Big) \mathrm{d}\bar{\eta} \Bigg]_{\substack{j > m \\ \lambda_i \geq \lambda_j \\ \boldsymbol{\eta} \geq 0}} \\ & + \int_{\boldsymbol{\xi}_l(\boldsymbol{\eta})}^{\boldsymbol{\xi}} \boldsymbol{H}_1(\bar{\xi}, \boldsymbol{\eta}, t) \mathrm{d}\bar{\xi} + \left[\frac{1}{2} \int_0^{\boldsymbol{\eta}} \int_{\boldsymbol{\eta}_l(\bar{\eta})}^{\bar{\eta}} \boldsymbol{G}_t(\bar{\eta}, \bar{\bar{\eta}}, t) \mathrm{d}\bar{\bar{\eta}} \mathrm{d}\bar{\eta} \right]_{\substack{j > m \\ \lambda_i \geq \lambda_j \\ \boldsymbol{\eta} \geq 0}} \\ & + \frac{\boldsymbol{s}}{4} \int_{\boldsymbol{\xi}_l(\boldsymbol{\eta})}^{\boldsymbol{\xi}} \int_{\boldsymbol{\eta}_l(\bar{\xi})}^{\boldsymbol{\eta}} \boldsymbol{G}_t(\bar{\xi}, \bar{\eta}, t) \mathrm{d}\bar{\eta} \mathrm{d}\bar{\xi} \end{aligned} \tag{2.170c}$$

considering (2.131).

For $\boldsymbol{H}_1$, insert (2.170a) with (2.170b) and (2.170c) as well as (2.166) into (2.164). The result is substituted into (2.163) together with (2.168) and the

BCs (2.143c)–(2.143h) for $\boldsymbol{G}(\boldsymbol{\xi}_l(\boldsymbol{\eta}),\boldsymbol{\eta},t)$ and $\boldsymbol{H}(\boldsymbol{\xi},\boldsymbol{\eta}_l(\boldsymbol{\xi}),t)$ as well as (2.150a) and (2.150c) for $\boldsymbol{G}(\boldsymbol{\xi},\boldsymbol{\eta}_l(\boldsymbol{\xi}),t)$. Then, the resulting integral equation for $\boldsymbol{H}_1$ reads

$$\boldsymbol{H}_1(\boldsymbol{\xi},\boldsymbol{\eta},t)=\boldsymbol{H}_0(\boldsymbol{\xi},\boldsymbol{\eta},t)+\boldsymbol{F}_{H_1}[G,\boldsymbol{H}_1](\boldsymbol{\xi},\boldsymbol{\eta},t) \tag{2.171a}$$

with

$$\begin{aligned}\boldsymbol{H}_0(\boldsymbol{\xi},\boldsymbol{\eta},t)&=[\boldsymbol{c}^1(\boldsymbol{z}(\boldsymbol{\xi},\boldsymbol{\eta}_l(\boldsymbol{\xi})),t)]_{\lambda_i\neq\lambda_j}+[\boldsymbol{c}^2(\boldsymbol{z}(\boldsymbol{\xi},0),t)]_{\lambda_i=\lambda_j}\\&+\frac{\boldsymbol{s}}{4}\bar{\boldsymbol{a}}_\Sigma\boldsymbol{G}_0(\boldsymbol{\eta},t)+\Big[\frac{1}{4}\bar{\boldsymbol{a}}_\Sigma(\boldsymbol{\xi},0)\boldsymbol{c}^4(\boldsymbol{z}(\boldsymbol{\xi},0),t)\Big]_{\lambda_i=\lambda_j}\\&-\frac{\boldsymbol{s}}{4}\int_{\boldsymbol{\eta}_l(\boldsymbol{\xi})}^{\boldsymbol{\eta}}\lambda_j(\boldsymbol{\zeta}(\boldsymbol{\xi},\bar\eta))\boldsymbol{F}(\boldsymbol{z}(\boldsymbol{\xi},\bar\eta),\boldsymbol{\zeta}(\boldsymbol{\xi},\bar\eta),t)\mathrm{d}\bar\eta.\end{aligned} \tag{2.171b}$$

in view of (2.131) and

$$\begin{aligned}\boldsymbol{F}_{H_1}[G,\boldsymbol{H}_1](\boldsymbol{\xi},\boldsymbol{\eta},t)&=\frac{1}{4}\int_{\boldsymbol{\eta}_l(\boldsymbol{\xi})}^{\boldsymbol{\eta}}\Bigg(-\bar{\boldsymbol{a}}_\triangle(\boldsymbol{\xi},\bar\eta)\boldsymbol{H}_1(\boldsymbol{\xi},\bar\eta,t)\\&+\boldsymbol{s}\tilde{\boldsymbol{a}}\big(\boldsymbol{z}(\boldsymbol{\xi},\bar\eta),\boldsymbol{\zeta}(\boldsymbol{\xi},\bar\eta)\big)\boldsymbol{G}(\boldsymbol{\xi},\bar\eta,t)\\&+\boldsymbol{s}\sum_{k=1}^{n}\Big(\frac{\lambda_j(\boldsymbol{\zeta}(\boldsymbol{\xi},\bar\eta))}{\lambda_k(\boldsymbol{\zeta}(\boldsymbol{\xi},\bar\eta))}G_{ik}(\boldsymbol{\xi},\bar\eta,t)A_{kj}(\boldsymbol{\zeta}(\boldsymbol{\xi},\bar\eta),t)+\widetilde{A}_{ik}(\boldsymbol{z}(\boldsymbol{\xi},\bar\eta),t)G_{kj}(\boldsymbol{\xi},\bar\eta,t)\Big)\\&+\boldsymbol{s}\int_{\boldsymbol{\zeta}(\boldsymbol{\xi},\bar\eta)}^{\boldsymbol{z}(\boldsymbol{\xi},\bar\eta)}\sum_{k=1}^{n}\frac{\lambda_j(\boldsymbol{\zeta}(\boldsymbol{\xi},\bar\eta))}{\lambda_k(\bar\zeta)}G_{ik}(\boldsymbol{z}(\boldsymbol{\xi},\bar\eta),\bar\zeta,t)F_{kj}(\bar\zeta,\boldsymbol{\zeta}(\boldsymbol{\xi},\bar\eta),t)\mathrm{d}\bar\zeta\Bigg)\mathrm{d}\bar\eta\\&-\frac{s}{16}\int_{\boldsymbol{\eta}_l(\boldsymbol{\xi})}^{\boldsymbol{\eta}}\bar{\boldsymbol{a}}_\triangle(\boldsymbol{\xi},\bar\eta)\int_{\boldsymbol{\eta}_l(\boldsymbol{\xi})}^{\bar\eta}\boldsymbol{G}_t(\boldsymbol{\xi},\bar{\bar\eta},t)\mathrm{d}\bar{\bar\eta}\mathrm{d}\bar\eta+\frac{\boldsymbol{s}}{4}\bar{\boldsymbol{a}}_\Sigma\boldsymbol{F}_{\boldsymbol{G}}[G,\boldsymbol{H}_1].\end{aligned} \tag{2.171c}$$

Since the definition of ξ_l in (2.161) is piecewise, the corresponding BCs (2.143c) and (2.143f)–(2.143h) utilized for the integration w. r. t. $\boldsymbol{\xi}$ imply that for $\lambda_i\neq\lambda_j$ the line $\boldsymbol{\eta}=0$ in $\boldsymbol{\mathcal{D}}_c$ constitutes a *line of separation*, leading to a piecewise defined solution. Thus, only a piecewise classical solution of (2.28) can be obtained. Considering the line of separation in the original coordinates shows that it is no longer a straight line, but a strictly monotonically increasing line, defined by

$$\zeta=\phi_j^{-1}(\phi_i(z)),z\in[0,1],\qquad\lambda_i>\lambda_j \tag{2.172a}$$

$$z=\phi_i^{-1}(\phi_j(\zeta)),\zeta\in[0,1],\qquad\lambda_i<\lambda_j. \tag{2.172b}$$

2.5.6 Solution by fixed-point iteration

The integral equations (2.170) and (2.171) are now solved by fixed-point iteration. This section shows that this iteration converges absolutely and

uniformly. Hence, an accurate approximate solution is attainable by a series truncation, allowing a *successive approximation* of the solution.

The obtained integral equations for $\boldsymbol{G}$ and $\boldsymbol{H}_1$ can be written in the form

$$\boldsymbol{G} = \widetilde{\boldsymbol{F}}_G[G, \boldsymbol{H}_1] \tag{2.173a}$$

$$\boldsymbol{H}_1 = \widetilde{\boldsymbol{F}}_{H_1}[G, \boldsymbol{H}_1], \tag{2.173b}$$

with

$$\widetilde{\boldsymbol{F}}_G[G, \boldsymbol{H}_1] = \boldsymbol{G}_0 + \boldsymbol{F}_G[G, \boldsymbol{H}_1] \tag{2.174a}$$

$$\widetilde{\boldsymbol{F}}_{H_1}[G, \boldsymbol{H}_1] = \boldsymbol{H}_0 + \boldsymbol{F}_{H_1}[G, \boldsymbol{H}_1] \tag{2.174b}$$

and $\boldsymbol{G} = G_{ij}$, $\boldsymbol{H}_1 = H_{1,ij}$, $i, j = 1, \ldots, n$, implying that there are $2n^2$ equations which are coupled. Obviously, the solution that is looked for must be a *fixed point* for the operators $\widetilde{\boldsymbol{F}}_G$ and $\widetilde{\boldsymbol{F}}_{H_1}$ appearing in (2.173), which means that the values of the solution components $\boldsymbol{G}, \boldsymbol{H}_1$ do not change when applying $\widetilde{\boldsymbol{F}}_G$ respectively $\widetilde{\boldsymbol{F}}_{H_1}$ on them. This can be seen easily in (2.173). Consequently, it is a natural approach to look for a solution of (2.173) by applying fixed-point iteration.

In this method, the right-hand side of (2.173) is applied on an initial guess[8] $\boldsymbol{G}^0$, $\boldsymbol{H}_1^0$ for the solution. Then, the right-hand side of (2.173) is applied to the results again. This is repeated consecutively. If the procedure converges, the result obviously is a fixed point of the right-hand side of the equation and thus also a solution of (2.173).

Therefore, the challenge is to prove that the application of this fixed-point iteration indeed converges for at least one initial guess.

The mathematical formulation of the described iteration is

$$\boldsymbol{G}^0, \boldsymbol{H}_1^0\text{: initial guess}$$

$$\boldsymbol{G}^{l+1} = \widetilde{\boldsymbol{F}}_G[G^l, \boldsymbol{H}_1^l] \tag{2.175a}$$

$$\boldsymbol{H}_1^{l+1} = \widetilde{\boldsymbol{F}}_{H_1}[G^l, \boldsymbol{H}_1^l], \quad l \geq 0 \tag{2.175b}$$

and

$$\boldsymbol{G} = \lim_{l\to\infty} \boldsymbol{G}^l = \lim_{l\to\infty} \widetilde{\boldsymbol{F}}_G^l[G^0, \boldsymbol{H}_1^0] \tag{2.176a}$$

$$\boldsymbol{H}_1 = \lim_{l\to\infty} \boldsymbol{H}_1^l = \lim_{l\to\infty} \widetilde{\boldsymbol{F}}_{H_1}^l[G^0, \boldsymbol{H}_1^0]. \tag{2.176b}$$

[8] Typically the initial guess is 0.

For the convergence analysis, it is more convenient to consider it in the equivalent increment representation. To derive this, define the increments as

$$\Delta \boldsymbol{G}^l \coloneqq \boldsymbol{G}^{l+1} - \boldsymbol{G}^l \tag{2.177a}$$
$$\Delta \boldsymbol{H}_1^l \coloneqq \boldsymbol{H}_1^{l+1} - \boldsymbol{H}^l \tag{2.177b}$$

with the increment matrices $\Delta G = [\Delta G_{ij}]$ and $\Delta H_1 = [\Delta H_{1,ij}]$ so that

$$\boldsymbol{G} = \lim_{l\to\infty} \boldsymbol{G}^l = \sum_{l=0}^{\infty} \Delta \boldsymbol{G}^l \tag{2.178a}$$
$$\boldsymbol{H}_1 = \lim_{l\to\infty} \boldsymbol{H}_1^l = \sum_{l=0}^{\infty} \Delta \boldsymbol{H}_1^l. \tag{2.178b}$$

Now insert (2.175) into (2.178) to get

$$\Delta \boldsymbol{G}^l = \boldsymbol{G}^{l+1} - \boldsymbol{G}^l = \widetilde{\boldsymbol{F}}_G[G^l, \boldsymbol{H}_1^l] - \widetilde{\boldsymbol{F}}_G[G^{l-1}, \boldsymbol{H}_1^{l-1}] \tag{2.179a}$$
$$\Delta \boldsymbol{H}_1^l = \boldsymbol{H}_1^{l+1} - \boldsymbol{H}_1^l = \widetilde{\boldsymbol{F}}_{H_1}[G^l, \boldsymbol{H}_1^l] - \widetilde{\boldsymbol{F}}_{H_1}[G^{l-1}, \boldsymbol{H}_1^{l-1}]. \tag{2.179b}$$

Using the definitions of $\widetilde{F}_{\boldsymbol{G}}$ and $\widetilde{F}_{\boldsymbol{H}_1}$ in (2.174) yields

$$\Delta \boldsymbol{G}^l = \boldsymbol{G}_0 + \boldsymbol{F}_G[G^l, \boldsymbol{H}_1^l] - \boldsymbol{G}_0 - \boldsymbol{F}_G[G^{l-1}, \boldsymbol{H}_1^{l-1}] \tag{2.180a}$$
$$\Delta \boldsymbol{H}_1^l = \boldsymbol{H}_0 + \boldsymbol{F}_{H_1}[G^l, \boldsymbol{H}_1^l] - \boldsymbol{H}_0 - \boldsymbol{F}_{H_1}[G^{l-1}, \boldsymbol{H}_1^{l-1}]. \tag{2.180b}$$

Having a look at $\boldsymbol{F}_G$ and $\boldsymbol{F}_{H_1}$ reveals that they are linear in G and $\boldsymbol{H}_1$, so that

$$\Delta \boldsymbol{G}^l = \boldsymbol{F}_G[\underbrace{G^l - G^{l-1}}_{\Delta G^{l-1}}, \underbrace{\boldsymbol{H}_1^l - \boldsymbol{H}_1^{l-1}}_{\Delta \boldsymbol{H}_1^{l-1}}] \tag{2.181a}$$
$$\Delta \boldsymbol{H}_1^l = \boldsymbol{F}_{H_1}[\underbrace{G^l - G^{l-1}}_{\Delta G^{l-1}}, \underbrace{\boldsymbol{H}_1^l - \boldsymbol{H}_1^{l-1}}_{\Delta \boldsymbol{H}_1^{l-1}}], \quad l \geq 1, \tag{2.181b}$$

or

$$\Delta \boldsymbol{G}^{l+1} = \boldsymbol{F}_G[\Delta G^l, \Delta \boldsymbol{H}_1^l] \tag{2.182a}$$
$$\Delta \boldsymbol{H}_1^{l+1} = \boldsymbol{F}_{H_1}[\Delta G^l, \Delta \boldsymbol{H}_1^l], \quad l \geq 0, \tag{2.182b}$$

respectively, which is the *update law* of the fixed-point iteration. The advantage of this formulation lies in the representation of the solution in form of an infinite sum in (2.178) rather than a limes as in (2.176).

Using the simplest initial guess $\boldsymbol{G}^0 = \boldsymbol{H}_1^0 = 0$ implies

$$\Delta\boldsymbol{G}^0 = \boldsymbol{G}^1 - \boldsymbol{G}^0 = \widetilde{\boldsymbol{F}}_G[0,0] = \boldsymbol{G}_0 \tag{2.183a}$$

$$\Delta\boldsymbol{H}_1^0 = \boldsymbol{H}_1^1 - \boldsymbol{H}_1^0 = \widetilde{\boldsymbol{F}}_{H_1}[0,0] = \boldsymbol{H}_0 \tag{2.183b}$$

with which the following proposition holds.

Proposition 2.5.6 (Convergence of the fixed-point iteration)**.** *The fixed-point iteration* (2.182) *with* $\boldsymbol{F}_G$, $\boldsymbol{F}_{H_1}$ *according to* (2.170c), (2.171c) *and the starting values* (2.183) *converges absolutely and uniformly to the solution of* (2.170) *and* (2.171) *for* $\alpha \in [1,2)$*, where* α *is the Gevrey order of the system parameters.*

The proof of this proposition consists of the following steps:

1. Finding an appropriate, converging growth bound for the absolute values of the increments, which implies convergence of the fixed-point iteration by Weierstrass' test.

2. Proving the validity of the growth bound by mathematical induction.

To demonstrate the idea how to find a suitable growth bound, the mechanism of the fixed-point iteration is demonstrated at the simple example of the integral equation

$$x = c + \int_0^z x(\zeta)\mathrm{d}\zeta. \tag{2.184}$$

Starting with the initial guess $x^0 = 0$ yields $x^1 = c$ with the corresponding increment $\Delta x^0 = c$. Applying the integral in (2.184) repeatedly on Δx^0 yields $\Delta x^1 = cz$, $\Delta x^2 = c\frac{z^2}{2}$ and so on, leading to the formula for integrations

$$\Delta x^l = c\frac{z^l}{l!}. \tag{2.185}$$

Summing up all those elements, the well-known limit

$$x = \sum_{l=0}^{\infty} \Delta x^l = \sum_{l=0}^{\infty} c\frac{z^l}{l!} = c\mathrm{e}^z, \tag{2.186}$$

is obtained, which is the solution of (2.184). For this simple example, the value of the summands is explicitly found in terms of (2.185) by performing the integration. In the case of more general or complicated integral equations, it is no more possible to find the solution in such a closed-form. However, it is to be expected that due to the principle of the integrations, their basic form should be similar.

Rather than determining the summands explicitly, it is crucially easier to determine bounds for their absolute values. Luckily it is sufficient to find a converging upper bound of a series' elements in order to prove that the series converges absolutely and uniformly (see Appendix C.2 for the corresponding definitions). This is stated in *Weierstrass' test*, (see, e. g. [77]) and is formulated as follows.

Lemma 2.5.7 (Weierstrass' test)**.** *Let $\{f_n\}$ be a sequence of functions defined on the set X. If there exists a sequence $\{M_n\}$ such that $\forall x \in X$ and $\forall n \in \mathbb{N}^0$,*

$$|f_n(x)| \leq M_n, \tag{2.187}$$

then the series $\sum_{n=0}^{\infty} f_n$ converges absolutely[9] and uniformly on X if $\sum_{n=0}^{\infty} M_n$ converges.

This means that it is sufficient to know an upper bound for the growth of the absolute values $|\Delta x^l|$ and to prove that the series of this upper bound converges. The uniformity of the convergence then ensures that the continuity of the summands is inherited by the sum so that the result is the solution of the integral equation.

Considering scalar parabolic systems, the integral equation contains integrations w. r. t. ξ and η. Knowing (2.185), the intuitive idea in e. g. [79] was to assume

$$|\Delta G^l| \leq M^{l+1} \frac{(\xi+\eta)^l}{l!}. \tag{2.188}$$

Then, (2.188) was inserted into the integral equation and its validity was proved via induction. The limit of the corresponding series is an exponential function, just like in (2.186), so that the fixed-point iteration converged.

In the present case of coupled parabolic systems, this simple approach can no more be used, because every element G_{ij} respectively $H_{1,ij}$ has its own coordinate system (ξ_{ij}, η_{ij}) and the elements are coupled. Assuming a growth bound depending on (ξ_{ij}, η_{ij}) would imply a different growth bound for each element, which destroyed the proof of the induction step.

For this reason, [113] considered a growth bound formulated in terms of the *original coordinates* (z, ζ), which was completely independent of the kernel elements.[10] It was stated in [113] that the diffusion coefficients need to be different in the sense that $\lambda_1(z) > \ldots, \lambda_n(z), \forall z \in [0,1]$, which means

[9] In [77], only the uniform convergence is stated, but the absolute convergence directly follows from (2.187) and the convergence of $\{M_n\}$.

[10] Note that the growth bound $\frac{(\xi+\eta)^l}{l!}$ used in the scalar case could also be expressed as $\frac{(2z)^l}{l!}$ in the original coordinates.

that at each point z, $\lambda_i(z) > \lambda_j(z)$ for $i < j$. However, looking at the convergence proof in [113] reveals that in fact the proof only works if $\lambda_i(z) > \lambda_j(\zeta)$, $i < j$, $z \in [0,1]$, $\forall \zeta \in [0,z]$, which restricts the diffusion coefficients in the way that their ranges are disjoint. This can be relaxed by modifying the growth assumption used in [113] with the idea in [51], which considers a similar problem for hyperbolic systems, but leaves its statement without proof. Essentially, the growth assumption there is akin[11] to

$$|\Delta G_{ij}^l| \leq M^{l+1} \frac{\phi_i(z) - \gamma\phi_i(\zeta)}{l!}. \tag{2.189}$$

At first glance, this might lead to a problem, because it is no longer independent of the indices. The integral operators (2.170c) and (2.171c) however mostly contain sums of the form $\sum_{k=1}^n G_{ik}$, which originate from a premultiplication by G. Since (2.189) only depends on the row index i, which is equal for each element in the sum, it is suitable to be used here.

The only critical case is the multiplication $\sum_{k=1}^n \widetilde{A}_{ik} G_{kj}$ appearing in (2.171c), which does not exist for the hyperbolic case in [51]. It will be shown during the proof that the special structure of $\widetilde{A}$ according to (2.41) still ensures the applicability of this idea.

For systems with time dependent coefficients, [118] combined the ideas in [113] with the ideas to prove the convergence for scalar parabolic systems with time dependent coefficients in [72] and [100]. The time dependency of the kernel, specifically the appearance of its time derivative in the integral equations requires to include a growth assumption for the time derivatives of the kernel. As for both kernel element variables $\boldsymbol{G}$ and $\boldsymbol{H}_1$ the same growth bound is assumed, it is convenient to introduce a placeholder variable $\boldsymbol{X}$ that can be replaced by either $\boldsymbol{G}$ or $\boldsymbol{H}_1$. With this, the following proposition is stated as the combination of the ideas in [51, 118].

Lemma 2.5.8 (Growth assumption)**.** *Assume that $(\boldsymbol{\xi}, \boldsymbol{\eta})$ and (z, ζ) are related by (2.136) respectively (2.137). There exist constants $D > 0$, $M \geq 1$ such that for every closed interval $\mathcal{I} \subset \mathbb{R}_{t_0}^+$,*

$$\begin{aligned} \sup_{t\in\mathcal{I}} |\partial_t^p \Delta \boldsymbol{X}^l(\boldsymbol{\xi}, \boldsymbol{\eta}, t)| &\leq \underbrace{D^{p+l}\Big(\frac{(p+l)!}{l!}\Big)^\alpha \frac{1}{(l!)^{2-\alpha}}}_{P_\alpha(p,l)} M^{l+1} \underbrace{(\phi_i(z) - \gamma\phi_i(\zeta))}_{f_i(z,\zeta)=\boldsymbol{f}(z,\zeta)}{}^l \\ &= P_\alpha(p,l) M^{l+1} \boldsymbol{f}^l(z,\zeta) = P_\alpha(p,l) M^{l+1} \bar{\boldsymbol{f}}^l(\boldsymbol{\xi}, \boldsymbol{\eta}) \end{aligned} \tag{2.190}$$

[11] In [51], ϕ_i is defined as $\int_0^z \frac{1}{|\lambda_i(\zeta)|} \mathrm{d}\zeta$, where λ_i are the transport speeds.

holds for the pth time derivative of the increments $\Delta \boldsymbol{G}^l$, $\Delta \boldsymbol{H}_1^l$, where $\alpha \in [1,2)$ is the Gevrey order of the system parameters and

$$\gamma \in (\overline{\lambda}, 1), \tag{2.191a}$$

$$\overline{\lambda} = \max_{\lambda_i < \lambda_j} \max_{z} \sqrt{\frac{\lambda_i(z)}{\lambda_j(z)}}. \tag{2.191b}$$

Prior to proving its validity, it needs to be checked that the series of the assumed growth bound has a limit, i. e. converges. Since the fixed-point iteration is used to determine the solutions $\boldsymbol{G} = \partial_t^0 \boldsymbol{G}$ and $\boldsymbol{H} = \partial_t^0 \boldsymbol{H}$ in the end, it suffices to show the convergence for $p = 0$ in (2.190) (see [72]). This is stated in the following corollary.

Corollary 2.5.9 (Convergence of absolute bound)**.** *The infinite sum of the growth bound* (2.190) *with $p = 0$ converges for $\alpha \in [1,2)$.*

Proof. Inserting $p = 0$ in (2.190), the result

$$\sup_{t \in \mathcal{I}} |\Delta \boldsymbol{X}^l| \leq D^l \frac{M^{l+1} \bar{\boldsymbol{f}}^l}{(l!)^{2-\alpha}} \tag{2.192}$$

is summed up to obtain

$$\sum_{l=0}^{\infty} \sup_{t \in \mathcal{I}} |\Delta \boldsymbol{X}^l| \leq M \sum_{l=0}^{\infty} \left(MD\bar{\boldsymbol{f}}\right)^l \underbrace{\frac{1}{(l!)^{2-\alpha}}}_{a_l}, \tag{2.193}$$

which is a power series. Its radius of convergence can be calculated by applying the ratio test (see e. g. [77]), yielding

$$\begin{aligned} r &= \lim_{l \to \infty} \frac{a_{l+1}}{a_{l+2}} = \lim_{l \to \infty} \frac{((l+2)!)^{2-\alpha}}{((l+1)!)^{2-\alpha}} \\ &= \lim_{l \to \infty} (l+2)^{2-\alpha} = \infty, \quad \forall \alpha < 2. \end{aligned} \tag{2.194}$$

Consequently, the series (2.193) converges for $\alpha \in [1,2)$. ∎

According to Lemma 2.5.7, this implies the absolute and uniform convergence of (2.178), proving Proposition 2.5.6. The remaining and main task of this section is to prove Lemma 2.5.8 by mathematical induction.

Remark 2.5.10. In the simpler scalar case considered in [72], it is possible to show that convergence can also be established for $\alpha = 2$ if the constant D is small enough. This is because the integrations of the growth assumption in the integral equation can be performed explicitly. In the present case, however, the integrations can only be estimated by some bounds, so the condition on D cannot be determined. Therefore, the special case $\alpha = 2$ must be excluded here. ◁

Proof of Lemma 2.5.8. Looking at $\boldsymbol{G}_0$ and $\boldsymbol{H}_0$ according to (2.170b), (2.171b) it is easy to check that

$$\sup_{t\in\mathcal{I}} |\partial_t^p \Delta \boldsymbol{X}^0| = D D^p (p!)^\alpha \leq P_\alpha(p,0) M \bar{\boldsymbol{f}}^0 \tag{2.195a}$$

for some finite $M \geq D$, because all appearing functions in (2.170b), (2.171b) are of Gevrey class $G_\alpha(\mathbb{R}^+_{t_0})$ so that they can be estimated by (2.11). This is the right-hand side of (2.190) for $l = 0$, proving its validity for the initial values $\Delta \boldsymbol{G}^0$, $\Delta \boldsymbol{H}_1^0$, which is the base case for the induction proof.

In the following, the validity of (2.190) for all $l > 0$ is proved by assuming it for l (induction hypothesis) and proving the resulting validity for $l + 1$ (induction step). By mathematical induction, the validity for all l follows. This amounts to proving that

$$\sup_{t\in\mathcal{I}} |\partial_t^p \Delta \boldsymbol{G}^{l+1}| = \sup_{t\in\mathcal{I}} |\mathrm{d}_t^p \boldsymbol{F}_G[\Delta G^l, \Delta \boldsymbol{H}^l]| \overset{!}{\leq} P_\alpha(p, l+1) M^{l+2} \bar{\boldsymbol{f}}^{l+1}(\boldsymbol{\xi}, \boldsymbol{\eta}) \tag{2.196a}$$

$$\sup_{t\in\mathcal{I}} |\partial_t^p \Delta \boldsymbol{H}_1^{l+1}| = \sup_{t\in\mathcal{I}} |\mathrm{d}_t^p \boldsymbol{F}_{H_1}[\Delta G^l, \Delta \boldsymbol{H}^l]| \overset{!}{\leq} P_\alpha(p, l+1) M^{l+2} \bar{\boldsymbol{f}}^{l+1}(\boldsymbol{\xi}, \boldsymbol{\eta}), \tag{2.196b}$$

where the update law (2.182) of the fixed-point iteration was used for the equalities. To evaluate the right-hand sides of the equal signs in (2.196) with (2.170c) and (2.171c), the time derivatives and the absolute supremum are moved under the integrals, allowing to insert the growth assumption. The results are spatial integrals over the growth assumption. Therefore, it is advantageous to have a closer look at those integrals before actually writing this down. Performing these integrations is not possible in closed-form, because the growth assumption contains the nonlinear coordinate transformations $\phi_i(\boldsymbol{z}(\boldsymbol{\xi}, \boldsymbol{\eta}))$ and $\phi_i(\boldsymbol{\zeta}(\boldsymbol{\xi}, \boldsymbol{\eta}))$. However, it is possible to derive bounds for the integrals, which are summed up in Appendix B.2. In fact, tighter estimates can be found but (B.12) allows to prove convergence of the

fixed-point iteration. In addition to the results of Appendix B.2, the auxiliary results of Appendix C.3 are used in the following.

Now, (2.196a) is evaluated with (2.170c) to prove the induction step. To simplify writing, the notations $|\cdot|_{\mathcal{I}} = \sup_{t\in\mathcal{I}}|\cdot|$ and

$$[\cdot]_c \coloneqq [\cdot]_{\substack{j>m \\ \lambda_i \geq \lambda_j \\ \boldsymbol{\eta}\geq 0}} \tag{2.197}$$

are used in the following. This yields

$$\begin{aligned}
\sup_{t\in\mathcal{I}}|\partial_t^p \Delta \boldsymbol{G}^{l+1}| = \Bigg| \mathrm{d}_t^p \Bigg[\int_0^{\boldsymbol{\eta}} \Big(& 2\Delta \boldsymbol{H}_1^l(\bar\eta,\bar\eta,t) + q_j^0(t)\sqrt{\lambda_j(0)}\Delta \boldsymbol{G}^l(\bar\eta,\bar\eta,t) \\
& - \sqrt{\lambda_j(0)} \int_0^{\boldsymbol{z}(\boldsymbol{\xi}_l(\bar\eta),\bar\eta)} \sum_{k=1}^{n} \frac{1}{\lambda_k(\zeta)} \Delta G_{ik}^l(\boldsymbol{z}(\boldsymbol{\xi}_l(\bar\eta),\bar\eta),\zeta,t) A_{0,kj}(\zeta,t)\mathrm{d}\zeta \Big)\mathrm{d}\bar\eta \Bigg]_c \\
& + \int_{\boldsymbol{\xi}_l(\boldsymbol{\eta})}^{\boldsymbol{\xi}} \mathrm{d}_t^p \Delta \boldsymbol{H}_1^l(\bar\xi,\boldsymbol{\eta},t)\mathrm{d}\bar\xi + \Bigg[\frac{1}{2}\int_0^{\boldsymbol{\eta}} \int_{\boldsymbol{\eta}_l(\bar\eta)}^{\bar\eta} \mathrm{d}_t^p \Delta \boldsymbol{G}_t^l(\bar\eta,\bar{\bar\eta},t)\mathrm{d}\bar{\bar\eta}\mathrm{d}\bar\eta \Bigg]_c \\
& + \frac{s}{4}\int_{\boldsymbol{\xi}_l(\boldsymbol{\eta})}^{\boldsymbol{\xi}} \int_{\boldsymbol{\eta}_l(\bar\xi)}^{\boldsymbol{\eta}} \mathrm{d}_t^p \Delta \boldsymbol{G}_t^l(\bar\xi,\bar\eta,t)\mathrm{d}\bar\eta\mathrm{d}\bar\xi \Bigg|_{\mathcal{I}} \\
\leq \Bigg[\int_0^{\boldsymbol{\eta}} \Big(& 2|\partial_t^p \Delta \boldsymbol{H}_1^l(\bar\eta,\bar\eta,t)|_{\mathcal{I}} + \sqrt{\lambda_j(0)}|\mathrm{d}_t^p\big(q_j^0(t)\Delta \boldsymbol{G}^l(\bar\eta,\bar\eta,t)\big)|_{\mathcal{I}} \\
& + \sqrt{\lambda_j(0)} \int_0^{\boldsymbol{z}(\boldsymbol{\xi}_l(\bar\eta),\bar\eta)} \sum_{k=1}^{n} \frac{1}{\lambda_k(\zeta)} |\mathrm{d}_t^p\big(\Delta G_{ik}^l(\boldsymbol{z}(\boldsymbol{\xi}_l(\bar\eta),\bar\eta),\zeta,t)A_{0,kj}(\zeta,t)\big)|_{\mathcal{I}}\mathrm{d}\zeta \Big)\mathrm{d}\bar\eta \Bigg]_c \\
& + \int_{\boldsymbol{\xi}_l(\boldsymbol{\eta})}^{\boldsymbol{\xi}} |\partial_t^p \Delta \boldsymbol{H}_1^l(\bar\xi,\boldsymbol{\eta},t)|_{\mathcal{I}}\mathrm{d}\bar\xi + \Bigg[\frac{1}{2}\int_0^{\boldsymbol{\eta}} \int_{\boldsymbol{\eta}_l(\bar\eta)}^{\bar\eta} |\partial_t^{p+1} \Delta \boldsymbol{G}^l(\bar\eta,\bar{\bar\eta},t)|_{\mathcal{I}}\mathrm{d}\bar{\bar\eta}\mathrm{d}\bar\eta \Bigg]_c \\
& + \frac{1}{4}\int_{\boldsymbol{\xi}_l(\boldsymbol{\eta})}^{\boldsymbol{\xi}} \int_{\boldsymbol{\eta}_l(\bar\xi)}^{\boldsymbol{\eta}} |\partial_t^{p+1} \Delta \boldsymbol{G}^l(\bar\xi,\bar\eta,t)|_{\mathcal{I}}\mathrm{d}\bar\eta\mathrm{d}\bar\xi.
\end{aligned} \tag{2.198}$$

To be able to insert (2.190), the general Leibniz rule (see Lemma C.3.1) needs to be applied for every multiplication of an element with a time dependent coefficient. Doing so,

$$\begin{aligned}
|\mathrm{d}_t^p\big(q_j^0(t)\Delta \boldsymbol{G}^l(\bar\eta,\bar\eta,t)\big)|_{\mathcal{I}} &= \Bigg| \sum_{q=0}^{p} \binom{p}{q} \mathrm{d}_t^q q_j^0(t) \partial_t^{p-q} \Delta \boldsymbol{G}^l(\bar\eta,\bar\eta,t) \Bigg|_{\mathcal{I}} \\
&\leq \sum_{q=0}^{p} \binom{p}{q} \big|\mathrm{d}_t^q q_j^0(t)\big|_{\mathcal{I}} \big|\partial_t^{p-q} \Delta \boldsymbol{G}^l(\bar\eta,\bar\eta,t)\big|_{\mathcal{I}}
\end{aligned} \tag{2.199}$$

allows to insert (2.11) and (2.190), which leads to

$$|\mathrm{d}_t^p\big(q_j^0(t)\Delta \boldsymbol{G}^l(\bar{\eta},\bar{\eta},t)\big)|_{\mathcal{I}} \leq \sum_{q=0}^{p}\binom{p}{q} D^{q+1}(q!)^{\alpha} P_\alpha(p-q,l) M^{l+1}\bar{\boldsymbol{f}}^l(\bar{\eta},\bar{\eta}). \tag{2.200}$$

The very same is applied for $|\mathrm{d}_t^p\big(\Delta G_{ik}^l(\boldsymbol{z}(\boldsymbol{\xi}_l(\bar{\eta}),\bar{\eta}),\zeta,t)A_{0,kj}(\zeta,t)\big)|_{\mathcal{I}}$ showing

$$\begin{aligned}&|\mathrm{d}_t^p\big(\Delta G_{ik}^l(\boldsymbol{z}(\boldsymbol{\xi}_l(\bar{\eta}),\bar{\eta}),\zeta,t)A_{0,kj}(\zeta,t)\big)|_{\mathcal{I}}\\ &\quad\leq \sum_{q=0}^{p}\binom{p}{q} D^{q+1}(q!)^{\alpha} P_\alpha(p-q,l) M^{l+1}\boldsymbol{f}^l(\boldsymbol{z}(\boldsymbol{\xi}_l(\bar{\eta}),\bar{\eta}),\zeta).\end{aligned} \tag{2.201}$$

Now (2.190) is inserted for the remaining elements and all appearing factors are considered by multiplying with their finite common bound c_1. This yields

$$\begin{aligned}&|\partial_t^p \Delta \boldsymbol{G}^{l+1}|_{\mathcal{I}} \leq c_1\Bigg(\left[\int_0^{\boldsymbol{\eta}} P_\alpha(p,l)M^{l+1}\bar{\boldsymbol{f}}^l(\bar{\eta},\bar{\eta})\mathrm{d}\bar{\eta}\right]_c\\
&+\left[\int_0^{\boldsymbol{\eta}}\sum_{q=0}^{p}\binom{p}{q} D^{q+1}(q!)^{\alpha} P_\alpha(p-q,l) M^{l+1}\bar{\boldsymbol{f}}^l(\bar{\eta},\bar{\eta})\mathrm{d}\bar{\eta}\right]_c\\
&+\left[\int_0^{\boldsymbol{\eta}}\int_0^{\boldsymbol{z}(\boldsymbol{\xi}_l(\bar{\eta}),\bar{\eta})}\sum_{q=0}^{p}\binom{p}{q} D^{q+1}(q!)^{\alpha} P_\alpha(p-q,l) M^{l+1}\boldsymbol{f}^l(\boldsymbol{z}(\boldsymbol{\xi}_l(\bar{\eta}),\bar{\eta}),\zeta)\mathrm{d}\zeta\mathrm{d}\bar{\eta}\right]_c\\
&+\int_{\boldsymbol{\xi}_l(\boldsymbol{\eta})}^{\boldsymbol{\xi}} P_\alpha(p,l)M^{l+1}\bar{\boldsymbol{f}}^l(\bar{\xi},\boldsymbol{\eta})\mathrm{d}\bar{\xi}+\left[\int_0^{\boldsymbol{\eta}}\int_{\boldsymbol{\eta}_l(\bar{\eta})}^{\bar{\eta}} P_\alpha(p+1,l)M^{l+1}\bar{\boldsymbol{f}}^l(\bar{\eta},\bar{\eta})\mathrm{d}\bar{\eta}\mathrm{d}\bar{\eta}\right]_c\\
&+\int_{\boldsymbol{\xi}_l(\boldsymbol{\eta})}^{\boldsymbol{\xi}}\int_{\boldsymbol{\eta}_l(\bar{\xi})}^{\boldsymbol{\eta}} P_\alpha(p+1,l)M^{l+1}\bar{\boldsymbol{f}}^l(\bar{\xi},\bar{\eta})\mathrm{d}\bar{\eta}\mathrm{d}\bar{\xi}\Bigg),\end{aligned} \tag{2.202}$$

where the integrals are evaluated using (B.12). Note that $\boldsymbol{\xi}_l(\boldsymbol{\eta})=\boldsymbol{\eta}$ holds for the terms in brackets due to the condition $\boldsymbol{\eta}\geq 0$, so that (B.12b)–(B.12d) can be used. This yields

$$\begin{aligned}&|\partial_t^p \Delta \boldsymbol{G}^{l+1}|_{\mathcal{I}} \leq c_1\Bigg(\frac{2}{l+1}P_\alpha(p,l)M^{l+1}\bar{\boldsymbol{f}}^{l+1}(\boldsymbol{\xi},\boldsymbol{\eta})\mathrm{d}\bar{\eta}\\
&+\sum_{q=0}^{p}\binom{p}{q} D^{q+1}(q!)^{\alpha} P_\alpha(p-q,l) M^{l+1}\frac{c_3}{l+1}\bar{\boldsymbol{f}}^{l+1}(\boldsymbol{\xi},\boldsymbol{\eta})\end{aligned}$$

$$+\left[\int_0^{\boldsymbol{\eta}}\sum_{q=0}^{p}\binom{p}{q}D^{q+1}(q!)^{\alpha}P_\alpha(p-q,l)M^{l+1}\frac{c_4}{(l+1)}\bar{\boldsymbol{f}}^{l+1}(\bar{\eta},\bar{\eta})\mathrm{d}\bar{\eta}\right]_c$$
$$+P_\alpha(p,l)M^{l+1}\frac{c_2}{l+1}\bar{\boldsymbol{f}}^{l+1}(\boldsymbol{\xi},\boldsymbol{\eta})+\left[\int_0^{\boldsymbol{\eta}}P_\alpha(p+1,l)M^{l+1}\frac{c_4}{l+1}\bar{\boldsymbol{f}}^{l+1}(\bar{\eta},\bar{\eta})\mathrm{d}\bar{\eta}\right]_c$$
$$+\int_{\boldsymbol{\xi}_l(\boldsymbol{\eta})}^{\boldsymbol{\xi}}P_\alpha(p+1,l)M^{l+1}\frac{2}{l+1}\bar{\boldsymbol{f}}^{l+1}(\bar{\xi},\boldsymbol{\eta})\mathrm{d}\bar{\xi}\Bigg) \tag{2.203}$$

after performing the outer integrations. Using (B.12a) and (B.12c) once more,

$$|\partial_t^p\Delta\boldsymbol{G}^{l+1}|_{\mathcal{I}}\le c_1\Bigg(\frac{2}{l+1}P_\alpha(p,l)M^{l+1}\bar{\boldsymbol{f}}^{l+1}(\boldsymbol{\xi},\boldsymbol{\eta})$$
$$+\sum_{q=0}^{p}\binom{p}{q}D^{q+1}(q!)^{\alpha}P_\alpha(p-q,l)M^{l+1}\frac{c_3}{l+1}\bar{\boldsymbol{f}}^{l+1}(\boldsymbol{\xi},\boldsymbol{\eta})$$
$$+\sum_{q=0}^{p}\binom{p}{q}D^{q+1}(q!)^{\alpha}P_\alpha(p-q,l)M^{l+1}\frac{c_4c_3}{(l+1)\underbrace{(l+2)}_{>1}}\underbrace{\bar{\boldsymbol{f}}^{l+2}(\boldsymbol{\xi},\boldsymbol{\eta})}_{\le\bar{\boldsymbol{f}}^{l+1}(\boldsymbol{\xi},\boldsymbol{\eta})}$$
$$+P_\alpha(p,l)M^{l+1}\frac{c_2}{l+1}\bar{\boldsymbol{f}}^{l+1}(\boldsymbol{\xi},\boldsymbol{\eta})+P_\alpha(p+1,l)M^{l+1}\frac{c_4c_3}{(l+1)(l+2)}\bar{\boldsymbol{f}}^{l+2}(\boldsymbol{\xi},\boldsymbol{\eta})$$
$$+P_\alpha(p+1,l)M^{l+1}\frac{2c_2}{(l+1)(l+2)}\bar{\boldsymbol{f}}^{l+2}(\boldsymbol{\xi},\boldsymbol{\eta})\Bigg) \tag{2.204}$$

results, where equal terms can be factored out to get

$$|\partial_t^p\Delta\boldsymbol{G}^{l+1}|_{\mathcal{I}}\le\Bigg(\frac{c_1(2+c_2)}{l+1}P_\alpha(p,l)M^{l+1}\bar{\boldsymbol{f}}^{l+1}(\boldsymbol{\xi},\boldsymbol{\eta})$$
$$+\sum_{q=0}^{p}\binom{p}{q}D^{q+1}(q!)^{\alpha}P_\alpha(p-q,l)M^{l+1}\frac{c_1c_3(1+c_4)}{l+1}\bar{\boldsymbol{f}}^{l+1}(\boldsymbol{\xi},\boldsymbol{\eta})$$
$$+P_\alpha(p+1,l)M^{l+1}\frac{c_1(c_4c_3+2c_2)}{(l+1)(l+2)}\bar{\boldsymbol{f}}^{l+2}(\boldsymbol{\xi},\boldsymbol{\eta})\Bigg). \tag{2.205}$$

To simplify this expression, insert the definition of $P_\alpha(p,l)$ according to (2.190) and use (C.7b) to first note that for $\alpha\ge 1$,

$$\frac{P_\alpha(p,l)}{l+1}=D^{p+l}\Big(\frac{(p+l)!}{l!}\Big)^{\alpha}\frac{1}{(l!)^{2-\alpha}}\underbrace{\frac{1}{l+1}}_{\le\frac{1}{(l+1)^{2-\alpha}}}$$

$$\leq \frac{1}{D} D^{p+l+1} \Big(\frac{(p+l+1)!}{(l+1)!} \Big)^{\alpha} \frac{1}{((l+1)!)^{2-\alpha}}$$
$$= \frac{1}{D} P_{\alpha}(p, l+1) \tag{2.206}$$

can be substituted in the first line of (2.205). For the second line,

$$\sum_{q=0}^{p} \binom{p}{q} D^{q+1} (q!)^{\alpha} P_{\alpha}(p-q, l) \frac{1}{l+1}$$
$$= \sum_{q=0}^{p} \binom{p}{q} D^{q+1} (q!)^{\alpha} D^{p-q+l} \left(\frac{(p-q+l)!}{l!} \right)^{\alpha} \frac{1}{(l!)^{2-\alpha}} \frac{1}{l+1}$$
$$= D^{p+l+1} \sum_{q=0}^{p} \binom{p}{q} (p-q+l)!^{\alpha} (q!)^{\alpha} \frac{1}{(l!)^{\alpha} (l!)^{2-\alpha} (l+1)} \tag{2.207}$$

needs to be further simplified. To this end, note that

$$ab^{\alpha} \leq (ab)^{\alpha}, \quad a \geq 1, b > 0, \alpha \geq 1 \tag{2.208a}$$
$$\sum_i a_i^{\alpha} \leq (\sum_i a_i)^{\alpha}, \quad a_i > 0, \alpha \geq 1, \tag{2.208b}$$

so that the sum can be written as

$$\sum_{q=0}^{p} \binom{p}{q} (p-q+l)!^{\alpha} (q!)^{\alpha} \leq \left(\sum_{q=0}^{p} \binom{p}{q} (p-q+l)!(q!) \right)^{\alpha}$$
$$\overset{(C.7a)}{\leq} \left(\frac{(p+l+1)!}{l+1} \right)^{\alpha}. \tag{2.209}$$

Inserting this into (2.207) yields

$$\sum_{q=0}^{p} \binom{p}{q} D^{q+1} (q!)^{\alpha} P_{\alpha}(p-q, l) \frac{1}{l+1}$$
$$\leq D^{p+l+1} \left(\frac{(p+l+1)!}{(l+1)l!} \right)^{\alpha} \frac{1}{(l!)^{2-\alpha}(l+1)}$$
$$\leq D^{p+l+1} \left(\frac{(p+l+1)!}{(l+1)!} \right)^{\alpha} \frac{1}{(l+1)!^{2-\alpha}} = P_{\alpha}(p, l+1). \tag{2.210}$$

To simplify the third line in (2.205), use (2.190) for $P_\alpha(p+1,l)$ to get

$$\begin{aligned}\frac{P_\alpha(p+1,l)}{(l+1)(l+2)} &= D^{p+1+l}\left(\frac{(p+1+l)!}{l!}\right)^\alpha \frac{1}{(l!)^{2-\alpha}}\frac{1}{(l+1)(l+2)}\\ &= D^{p+1+l}\left(\frac{(p+1+l)!}{(l+1)!}\right)^\alpha \frac{(l+1)^\alpha}{(l+1)(l+2)}\frac{1}{(l!)^{2-\alpha}}.\end{aligned} \tag{2.211}$$

The fact that $(l+1)(l+2) > (l+1)^2$ leads to $\frac{1}{(l+1)(l+2)} < \frac{1}{(l+1)^2}$ implying $\frac{(l+1)^\alpha}{(l+1)(l+2)} \leq \frac{1}{(l+1)^{2-\alpha}}$. Consequently,

$$\frac{P_\alpha(p+1,l)}{(l+1)(l+2)} \leq D^{p+l+1}\left(\frac{(p+1+l)!}{(l+1)!}\right)^\alpha \frac{1}{(l+1)!^{2-\alpha}} = P_\alpha(p,l+1) \tag{2.212}$$

is obtained. Now, (2.206), (2.210) and (2.212) are inserted into (2.205) and $\bar{\boldsymbol{f}}^{l+2}(\boldsymbol{\xi},\boldsymbol{\eta}) \leq \bar{\boldsymbol{f}}^{l+1}(\boldsymbol{\xi},\boldsymbol{\eta})$ because $\bar{\boldsymbol{f}}(\boldsymbol{\xi},\boldsymbol{\eta}) \leq 1$ is used, yielding

$$\begin{aligned}|\partial_t^p \Delta \boldsymbol{G}^{l+1}|_{\mathcal{I}} &\leq M M^{l+1} P_\alpha(p,l+1)\bar{\boldsymbol{f}}^{l+1}(\boldsymbol{\xi},\boldsymbol{\eta})\\ &= M^{l+2} P_\alpha(p,l+1)\bar{\boldsymbol{f}}^{l+1}(\boldsymbol{\xi},\boldsymbol{\eta})\end{aligned} \tag{2.213}$$

if $M \geq \frac{c_1(2+c_2)}{D} + c_3 + c_4c_3 + c_1(c_4c_3+2c_2)$. As M can be arbitrarily large and all appearing constants are finite, (2.213) proves the induction step (2.196a) for the kernel element $\Delta \boldsymbol{G}^l$.

The same procedure has to be repeated for (2.196b), using (2.171c). However, rather than explicitly writing it down, it suffices to compare the types of appearing terms in (2.171c) to them in (2.170c). The spatial integrals in (2.171c) are the same as in (2.170c), except $\int_{\zeta(\boldsymbol{\xi},\bar{\eta})}^{\boldsymbol{z}(\boldsymbol{\xi},\bar{\eta})}(\ldots)\mathrm{d}\bar{\zeta}$, which is evaluated using (B.12e). Moreover (2.171c) contains the sum over $\widetilde{A}_{ik}G_{kj}$, which, after shifting the absolute value under the integral yields

$$\begin{aligned}&\int_{\boldsymbol{\eta}_l(\boldsymbol{\xi})}^{\boldsymbol{\eta}} \sum_{k=1}^{n} |\mathrm{d}_t^p\big(\widetilde{A}_{ik}(\boldsymbol{z}(\boldsymbol{\xi},\bar{\eta}),t)\Delta G_{kj}^l(\boldsymbol{\xi},\bar{\eta},t)\big)|_{\mathcal{I}}\mathrm{d}\bar{\eta}\\ &= \int_{\boldsymbol{\eta}_l(\boldsymbol{\xi})}^{\boldsymbol{\eta}} \sum_{k=1}^{n}\sum_{q=0}^{p}\binom{p}{q}|\partial_t^q \widetilde{A}_{ik}(\boldsymbol{z}(\boldsymbol{\xi},\bar{\eta}),t)\big|_{\mathcal{I}}|\partial_t^{p-q}\Delta G_{kj}^l(\boldsymbol{\xi},\bar{\eta},t)\big|_{\mathcal{I}}\mathrm{d}\bar{\eta}\\ &\leq \int_{\boldsymbol{\eta}_l(\boldsymbol{\xi})}^{\boldsymbol{\eta}} \sum_{k=1}^{n}\sum_{q=0}^{p}\binom{p}{q} D^{q+1}(q!)^\alpha P_\alpha(p-q,l)M^{l+1} f_k^l(\boldsymbol{z}(\boldsymbol{\xi},\bar{\eta}),\boldsymbol{\zeta}(\boldsymbol{\xi},\bar{\eta}))\mathrm{d}\bar{\eta},\end{aligned} \tag{2.214}$$

where the insertion of f_k is required because the kernel element has the row index k. The special structure of $\widetilde{A}$ according to (2.41) ensures that this expression is zero for $\lambda_i > \lambda_k$ or in other words, only needs to be considered for $\lambda_k \geq \lambda_i$. Hence, the integral in (2.214) can be evaluated using (B.12f). Then, the very same procedure as for $\Delta \boldsymbol{G}^l$ proves the validity of (2.196b), which is the proof of the induction step. Consequently, Lemma 2.5.8 is proven. ■

Remark 2.5.11. If the appearing parameters are independent of time, the Gevrey growth (2.11) is still valid. Specifically, for $q > 0$, the derivative is zero and for $q = 0$, the right-hand side of (2.11) becomes a constant. Thus, every bounded $\boldsymbol{G}_0$, $\boldsymbol{H}_0$ induce that $\Delta \boldsymbol{G}^0$ and $\Delta \boldsymbol{H}_1^0$ fulfil (2.190). ◁

2.5.7 Uniqueness and regularity of the kernel

As result of the previous section, the kernel integral equations (2.170) and (2.171) have a solution that is piecewise continuous w. r. t. $(\boldsymbol{\xi}, \boldsymbol{\eta})$, smooth w. r. t. t and can be determined by the method of successive approximations.

Due to the smoothness of the solution w. r. t. t, the proof of uniqueness shown in [79] is directly applicable in the present case, knowing that the difference of two possible solutions fulfils the homogeneous integral equation. Hence, its time derivative must fulfil the growth assumption (2.190). With the same argumentation as for the convergence proof, the solution of the homogeneous integral equation is the limit of the fixed-point iteration, which converges to zero, showing that there can only be one possible solution.

Remark 2.5.12 (Initial value of the kernel). Though the time-derivative K_t appears in (2.28), the initial value $K(z, \zeta, t_0)$ is no degree of freedom but it is uniquely determined by the boundary conditions. As long as the coupling matrix $\widetilde{A}_0(z, t)$ in (2.23a) is not specified, there are infinitely many different backstepping transformations into the target system, which becomes apparent at the well-posed BC (2.150f). Once this degree of freedom is specified, there is only one unique transformation mapping into the target system with the resulting coupling matrix. ◁

For the stability proofs, the piecewise continuity of the kernel is sufficient, because it maps L_2-ICs of the original system into L_2-ICs of the target system. However, it is worth noting that the obtained kernel is twice differentiable inside the areas above and below the line of separation if the regularity conditions

$$\Phi(\cdot, t), A(\cdot, t), A_0(\cdot, t) \in (C^1[0, 1])^{n \times n} \tag{2.215a}$$

$$F(\cdot,\cdot,t) \in (C^1([0,1]^2))^{n\times n} \tag{2.215b}$$
$$g_{ij}(\cdot,t) \in C^2[0,1], \quad i,j=1,\dots,n, \tag{2.215c}$$

hold in addition to Assumption 2.1.5. To show this, the derivatives are expressed in terms of the canonical kernel elements $\boldsymbol{G}$, $\boldsymbol{H}$. In the first step, use (2.100b) and note that (2.105) implies $(\lambda_j(\zeta)\boldsymbol{K})_{\zeta\zeta} = \bar{\boldsymbol{K}}_{\zeta\zeta}$. Then insert (2.99b) and (2.99d) revealing that the upmost appearing derivatives are $\bar{\boldsymbol{K}}_{ww}$ and $\bar{\boldsymbol{K}}_{vv}$. These are substituted by (2.147c), (2.147d), which yields

$$\bar{\boldsymbol{K}}_{ww} = \boldsymbol{H}_{\boldsymbol{\xi}} + 2s\boldsymbol{H}_{\boldsymbol{\eta}} + \boldsymbol{G}_{\boldsymbol{\eta}\boldsymbol{\eta}} \tag{2.216a}$$
$$\bar{\boldsymbol{K}}_{vv} = \boldsymbol{H}_{\boldsymbol{\xi}} - 2s\boldsymbol{H}_{\boldsymbol{\eta}} + \boldsymbol{G}_{\boldsymbol{\eta}\boldsymbol{\eta}} \tag{2.216b}$$

with the definition of (2.142). Consequently, it must be shown that $\boldsymbol{H}_{\boldsymbol{\xi}}$, $\boldsymbol{H}_{\boldsymbol{\eta}}$ and $\boldsymbol{G}_{\boldsymbol{\eta}\boldsymbol{\eta}}$ are bounded. To this end, note that $\boldsymbol{H}_1$ being the solution of (2.171) induces that $\boldsymbol{H}$ according to (2.168) is the piecewise continuous solution of (2.163), because $\boldsymbol{H}_1$ and $\boldsymbol{H}_2$ have this property. Thus, to obtain the required derivatives of $\boldsymbol{G}$ and $\boldsymbol{H}$, (2.162) needs to be differentiated twice w. r. t. $\boldsymbol{\xi}$ and (2.163) needs to be differentiated w. r. t. $\boldsymbol{\xi}$ and w. r. t. $\boldsymbol{\eta}$. Calculating the second derivative of (2.163) w. r. t. $\boldsymbol{\eta}$ and inserting this into $\boldsymbol{G}_{\boldsymbol{\eta}\boldsymbol{\eta}}$ reveals that the results are piecewise continuous functions because of the piecewise continuity of $\boldsymbol{G}$, $\boldsymbol{H}_1$ and $\boldsymbol{G}_t$ as well as (2.215) and Assumption 2.1.5. Consequently, the obtained solution $K = [\boldsymbol{K}]$, $\boldsymbol{K}(z,\zeta,t) = \frac{1}{\lambda_j(\zeta)}\boldsymbol{G}(\boldsymbol{\xi}(z,\zeta),\boldsymbol{\eta}(z,\zeta),t)$ is the piecewise classical solution of (2.28).

Example 2.5.13 *(Kernel visualization).*
To illustrate the solution of the kernel equations, they are solved for an academic example of the system (2.21) with $n=2$ and the spatially varying and time-invariant coefficients

$$\Lambda(z) = \begin{bmatrix} z^2+2 & 0 \\ 0 & \mathrm{e}^{-z}+\frac{1}{2} \end{bmatrix}, \quad A(z) = \begin{bmatrix} \mathrm{e}^{z/2} & -z \\ \frac{3z}{2}-2 & z^2 \end{bmatrix}, \quad A_0 = F = 0 \tag{2.217a}$$
$$B_0^n = I, \quad B_0^d = 0 \tag{2.217b}$$
$$B_1^n = I, \quad B_1^d = I \tag{2.217c}$$

for which $\lambda_1 > \lambda_2$. The controller is parameterized by $\mu_c = 1$ and $\bar{A}(z) = 0$, resulting in $\widetilde{A}(z) = I$ in (2.23). Figure 2.5 and Figure 2.6 show the solution of the kernel equations in the canonical and original coordinates in form of a surface plot with contour lines. The colour is proportional to the value of the solution, and ranges from blue to red. The degree of freedom is set to $g_{21}(\boldsymbol{\eta}) \equiv 0$, symbolized by the dashed green line. The remaining

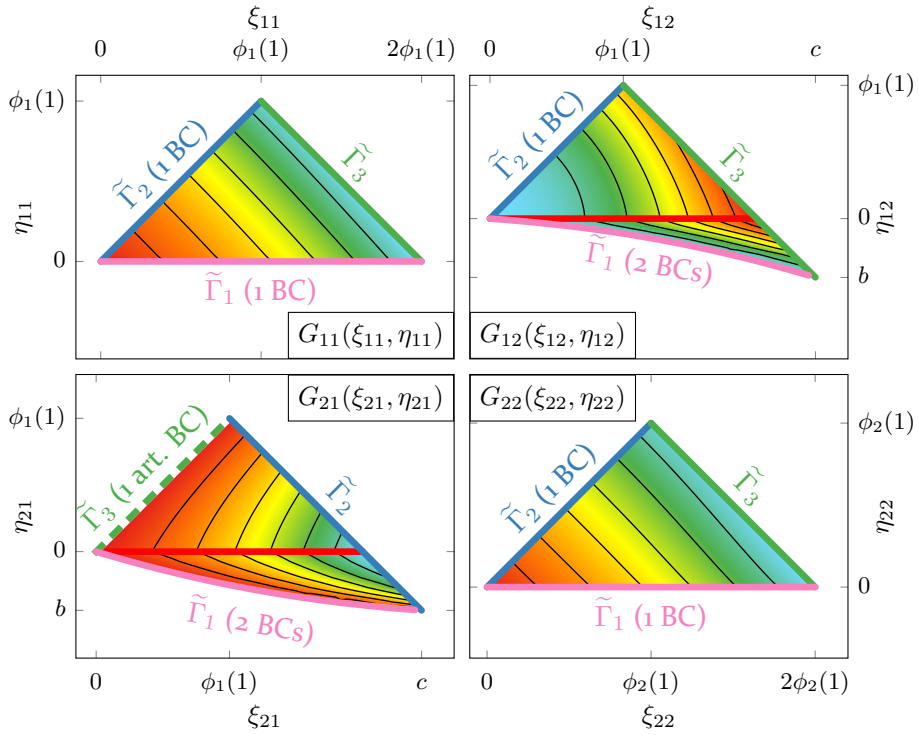

Figure 2.5: Surface plots of the kernel element solutions $\boldsymbol{G}(\boldsymbol{\xi}, \boldsymbol{\eta})$ in the canonical coordinates for $g_{21}(\boldsymbol{\eta}) = 0$. For $i \neq j$ the lower right corner of the domain is at $c = \phi_1(1) + \phi_2(1)$ and $b = \phi_1(1) - \phi_2(1)$ The coloured lines indicate the boundaries. For $i \neq j$, the red lines highlight the line of separation $\boldsymbol{\eta} = 0$, where the kernel is not differentiable. This is visualized by the black contour lines.

coloured lines represent the boundaries like in Figures 2.2 and 2.3 and the red line visualizes the line of separation located at $\boldsymbol{\eta} = 0$ in the canonical coordinates. In Figure 2.6, it can be seen that it is no longer a straight line, but a strictly monotonically increasing curve in the original coordinates according to (2.172). The black contour lines demonstrate the piecewise character of the solution for $i \neq j$, having a differentiability defect at the line of separation. To illustrate the influence of the artificial BC, Figure 2.7 shows the resulting solutions G_{21} and K_{21} for the arbitrary choice of $g_{21}(\eta_{21}) = -2\eta_{21}$. It can be seen that the form of the solution is affected by the artificial BC. Since the feedback gains depend on the kernel, they may therefore be influenced by the artificial BC. This is illustrated in the left picture of Figure 2.8, where the elements $R_{21}(z)$ and $R_{22}(z)$ of the distributed feedback gain in (2.27)

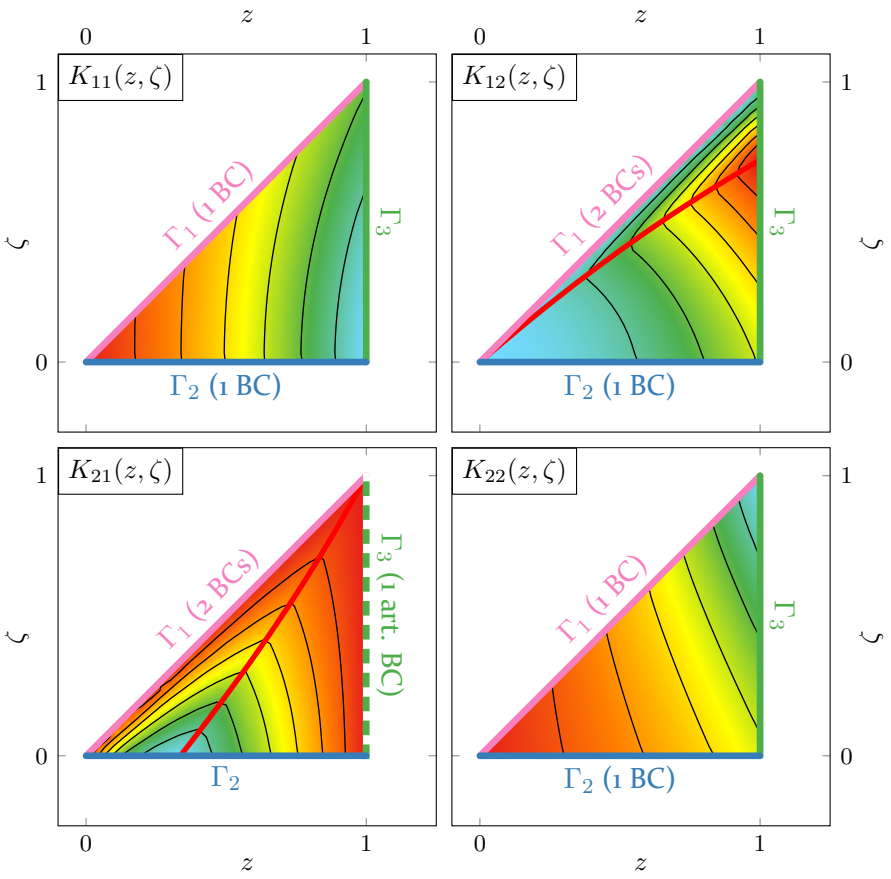

Figure 2.6: Surface plots of the kernel element solutions $\boldsymbol{K}(z,\zeta)$ in the original coordinates for Example 2.5.13 with the choice $g_{21}(\boldsymbol{\eta}) = 0$. The coloured lines indicate the boundaries. For $i \neq j$, the red line of separation is a strictly monotonically increasing non-straight line given by (2.172).

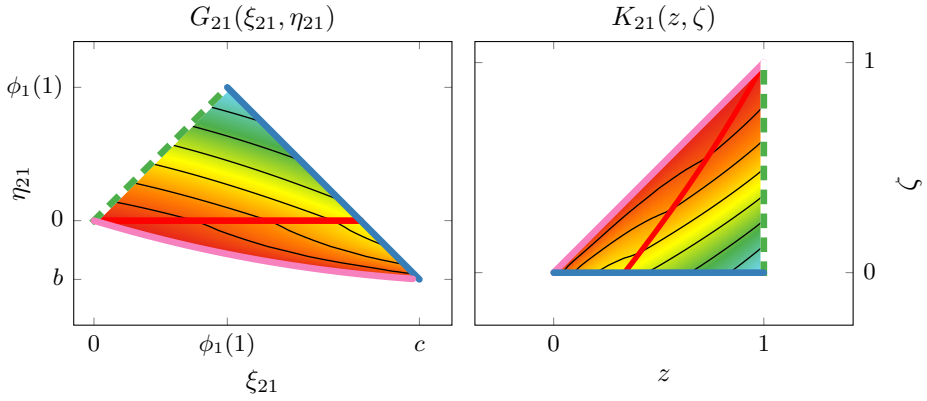

Figure 2.7: Solutions $G_{21}(\xi_{21}, \eta_{21})$ and $K_{21}(z, \zeta)$ for Example 2.5.13 with $g_{21}(\eta_{21}) = -2\eta_{21}$.

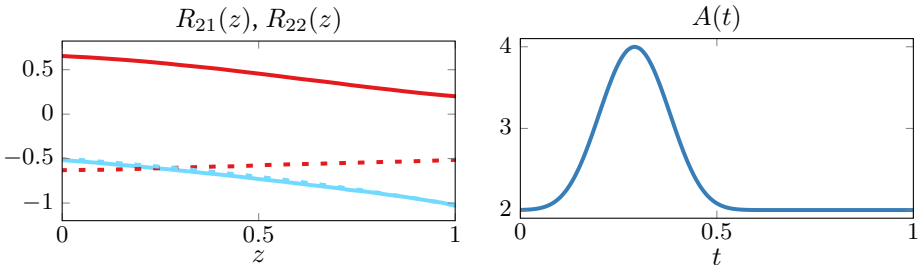

Figure 2.8: Left: Comparison of the distributed feedback gains $R_{21}(z)$ (——) and $R_{22}(z)$ (——) for the two choices of $g_{21}(\eta_{21}) = 0$ (solid) and $g_{21}(\eta_{21}) = -2\eta_{21}$ (dashed) in Example 2.5.13. Right: Reaction parameter $A(t)$ of the system considered in Example 2.5.14. It contains the non-analytic bump function $\Theta_2(t)$ with Gevrey order $\alpha = 1.5$.

are plotted. The gain $R_{21}(z)$ is strongly influenced by the choice of $g_{21}(\eta_{21})$. Due to the coupling of the kernel elements, the solution $K_{22}(z, \zeta)$ and thus $R_{22}(z)$ is also slightly affected. Though this is only a basic demonstration of the influence of $g_{21}(\eta_{21})$, it is imaginable to choose the value of the artificial BC with the aim to optimize some criterion like the control effort. ◁

Example 2.5.14 *(Time-varying kernel).*
To highlight the importance of considering the time dependency in the controller calculation, a system (2.21) with $n = 1$ and the parameters

$$\Lambda(z) = z^2 \cos(2\pi z) + \frac{3}{2}, \quad A(t) = 2 + 2\theta_2\left(\tfrac{7}{10}t + \tfrac{3}{10}\right) \tag{2.218a}$$

$$A_0 = F = 0 \tag{2.218b}$$

$$x_z(0,t) = q(t)x(0,t) = 2\sin(\pi t)x(0,t) \tag{2.218c}$$

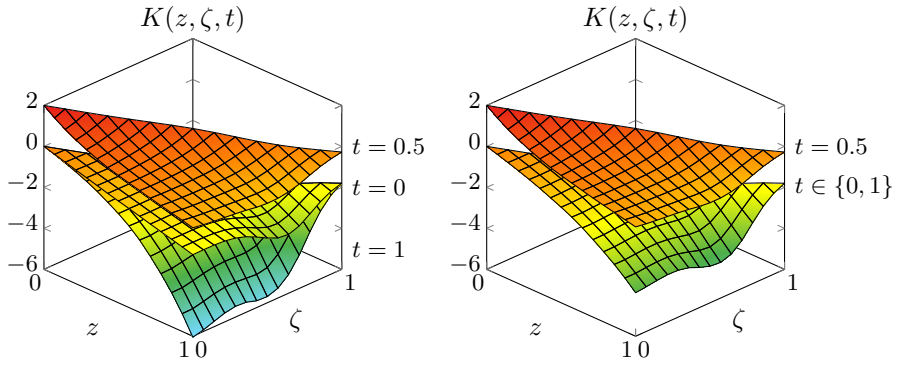

Figure 2.9: Solution of (2.28) for Example 2.5.14 (left) and comparison with the quasi-static solution (right) neglecting the time derivative of the kernel.

$$x_z(1,t) = -3tx(1,t) \tag{2.218d}$$

$$t_0 = 0 \tag{2.218e}$$

where

$$\theta_\omega(t) = \frac{\mathrm{e}^{-((1-t)t)^{-\omega}}}{\mathrm{e}^{-(\frac{1}{4})^{-\omega}}} \tag{2.219}$$

is the *normalized bump function* with Gevrey order $\alpha = 1 + \frac{1}{\omega}$ (see [66]), is considered in the time interval $t \in [0,1]$. With $\omega = 2$, $\alpha = 1.5$ is a Gevrey order realizable by the presented backstepping design method. The right picture in Figure 2.8 shows the form of the reaction parameter $A(t)$. The controller is parameterized by $\mu_c = 5$.

An intuitive approach for considering the time dependency of the system parameters is to discretize the time axis and calculate the controller gain at each time step as if the system was time-invariant, which is called *quasi-static* approach in the following. The solved kernel equations only differ by the term K_t in (2.28a), leading to an error in form of an additional term in the target system's PDE, whose stability is no more ensured. Figure 2.9 shows the solution of the kernel equations (2.28) in comparison to the the solution obtained with the quasi-static approach. Since for the time dependent parameters in (2.218), $A(0) \approx A(1)$ and $q(0) = q(1)$ holds, the quasi-static approach will lead to $K(z,\zeta,0) \approx K(z,\zeta,1)$ which can be verified in the right picture of Figure 2.9. However, when taking the time derivative into account, this is no longer valid, as can bee seen in the left picture of Figure 2.9. Naturally this has a great influence on the resulting controller gain. To make this visible, Figure 2.10 shows the distributed controller gain $R(z,t)$ in the two cases. It is

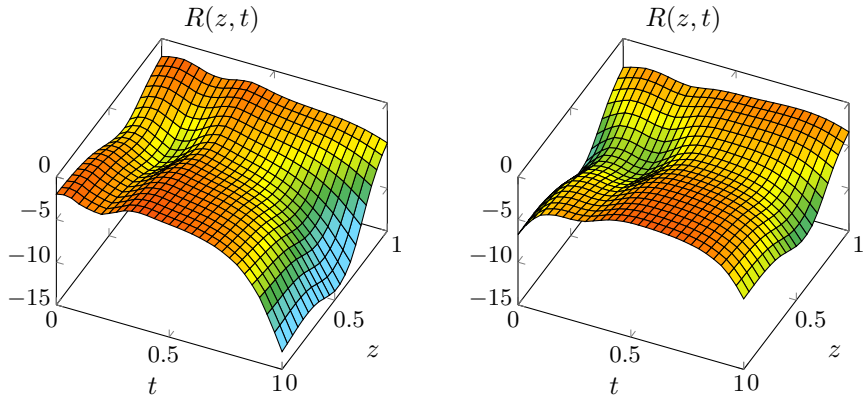

Figure 2.10: Distributed controller gain $R(z,t)$ with (left) and without (right) consideration of the kernel's time dependency.

obvious that the calculated controller gain in the quasi-static case will lead to a different and probably undesired behaviour, emphasizing the necessity to consider the general, time-varying problem. ◁

2.6 Computation of the kernel derivatives

To be able to realize the control law (2.27), the derivative $K_z(z,\zeta,t)$ needs to be determined and evaluated at the boundary $(1,\zeta,t)$. Computing the derivative with a numerical method, like finite differences, leads to a comparably large error due to the boundary evaluation. The same problem occurs for the determination of $K_\zeta(z,\zeta,t)$ needed at the boundary $(z,0,t)$ for the determination of (2.24) by (2.91). This is not required for the controller, however, it is helpful to be able to perform a simulation of the target system, in order to validate simulation results.

Rather than differentiating numerically, it is possible to directly calculate the derivatives via the kernel integral equations. To this end, first note that

$$\boldsymbol{K}_z(z,\zeta,t) = \frac{s}{\sqrt{\lambda_i(z)\lambda_j(\zeta)}}\boldsymbol{H}(\boldsymbol{\xi},\boldsymbol{\eta},t) + \frac{1}{\sqrt{\lambda_i(z)\lambda_j(\zeta)}}\boldsymbol{G}_{\boldsymbol{\eta}}(\boldsymbol{\xi},\boldsymbol{\eta},t) \tag{2.220a}$$

$$\boldsymbol{K}_\zeta(z,\zeta,t) = -\frac{\lambda_j'(\zeta)}{\lambda_j(\zeta)}\boldsymbol{K}(z,\zeta,t) + \frac{s}{\lambda_j^{3/2}(\zeta)}\boldsymbol{H}(\boldsymbol{\xi},\boldsymbol{\eta},t) - \frac{1}{\lambda_j^{3/2}(\zeta)}\boldsymbol{G}_{\boldsymbol{\eta}}(\boldsymbol{\xi},\boldsymbol{\eta},t), \tag{2.220b}$$

with $(\boldsymbol{\xi},\boldsymbol{\eta})$ according to (2.136) follows when applying the chain rule with (2.97), (2.140). While $\boldsymbol{H}(\boldsymbol{\xi},\boldsymbol{\eta},t)$ and $\boldsymbol{K}(z,\zeta,t)$ are directly available as the

solution of the integral equations (2.173) with (2.168), the derivative $\boldsymbol{G}_{\boldsymbol{\eta}}(\boldsymbol{\xi},\boldsymbol{\eta},t)$ still needs to be determined.

To this end, the PDE (2.148) is formally integrated w. r. t. $\boldsymbol{\xi}$ to obtain

$$\begin{aligned} 4s\big(\boldsymbol{G}_{\boldsymbol{\eta}}-\boldsymbol{G}_{\boldsymbol{\eta}}(\boldsymbol{\xi}_l(\boldsymbol{\eta}),\boldsymbol{\eta},t)\big)+\int_{\boldsymbol{\xi}_l(\boldsymbol{\eta})}^{\boldsymbol{\xi}}\bar{a}_{\Sigma}(\bar{\xi},\boldsymbol{\eta})\boldsymbol{G}_{\boldsymbol{\eta}}(\bar{\xi},\boldsymbol{\eta})\mathrm{d}\bar{\xi}\\ =\int_{\boldsymbol{\xi}_l(\boldsymbol{\eta})}^{\boldsymbol{\xi}}\Big(\boldsymbol{R}(\bar{\xi},\boldsymbol{\eta},t)-sa_{\Delta}(\bar{\xi},\boldsymbol{\eta})\boldsymbol{H}(\bar{\xi},\boldsymbol{\eta},t)\Big)\mathrm{d}\bar{\xi}, \end{aligned} \tag{2.221}$$

where $\boldsymbol{R}(\boldsymbol{\xi},\boldsymbol{\eta},t)$ is the right-hand side of (2.148). Note that all terms appearing in $\boldsymbol{R}$ as well as $\boldsymbol{H}$ are available as the solution of the integral equations (2.173). To express $\boldsymbol{G}_{\boldsymbol{\eta}}(\boldsymbol{\xi}_l(\boldsymbol{\eta}),\boldsymbol{\eta},t)$ by the BCs, (2.150b) and (2.150e) are solved for $\boldsymbol{G}_{\boldsymbol{\eta}}(\boldsymbol{\xi}_l(\boldsymbol{\eta}),\boldsymbol{\eta})=\boldsymbol{G}_{\boldsymbol{\eta}}(\boldsymbol{\xi}_l(\boldsymbol{\eta}),\boldsymbol{\eta}_l(\boldsymbol{\xi}_l(\boldsymbol{\eta})))$ and $\boldsymbol{G}_{\boldsymbol{\eta}}(\boldsymbol{\eta},\boldsymbol{\eta})$, respectively. Moreover, (2.150d) and (2.150f) are differentiated w. r. t. $\boldsymbol{\eta}$. Then, solving (2.221) for $\boldsymbol{G}_{\boldsymbol{\eta}}$ leads to the integral equation

$$\boldsymbol{G}_{\boldsymbol{\eta}}=\boldsymbol{G}_{\boldsymbol{\eta}}^{0}+\boldsymbol{F}_{\boldsymbol{G}_{\boldsymbol{\eta}}}[\boldsymbol{G}_{\boldsymbol{\eta}}] \tag{2.222a}$$

with

$$\begin{aligned} \boldsymbol{G}_{\boldsymbol{\eta}}^{0}=\frac{s}{4}\int_{\boldsymbol{\xi}_l(\boldsymbol{\eta})}^{\boldsymbol{\xi}}\Bigg(&-\bar{a}_{\Delta}(z,\zeta)s\boldsymbol{H}(\bar{\xi},\boldsymbol{\eta},t)+\sum_{k=1}^{n}\Big(\widetilde{A}_{ik}(\boldsymbol{z}(\bar{\xi},\boldsymbol{\eta}),t)G_{kj}(\bar{\xi},\boldsymbol{\eta},t)\\ &+\frac{\lambda_j(\boldsymbol{\zeta}(\bar{\xi},\boldsymbol{\eta}))}{\lambda_k(\boldsymbol{\zeta}(\bar{\xi},\boldsymbol{\eta}))}G_{ik}(\bar{\xi},\boldsymbol{\eta},t)A_{kj}(\boldsymbol{\zeta}(\bar{\xi},\boldsymbol{\eta}),t)\Big)\\ &+\boldsymbol{G}_t(\bar{\xi},\boldsymbol{\eta},t)-\lambda_j(\boldsymbol{\zeta}(\bar{\xi},\boldsymbol{\eta}))\boldsymbol{F}(\boldsymbol{z}(\bar{\xi},\boldsymbol{\eta}),\boldsymbol{\zeta}(\bar{\xi},\boldsymbol{\eta}),t)\\ &+\int_{\boldsymbol{\zeta}(\bar{\xi},\boldsymbol{\eta})}^{\boldsymbol{z}(\bar{\xi},\boldsymbol{\eta})}\sum_{k=1}^{n}\Big(\frac{\lambda_j(\boldsymbol{\zeta}(\bar{\xi},\boldsymbol{\eta}))}{\lambda_k(\bar{\zeta})}G_{ik}\big(\xi_{ik}\big(\boldsymbol{z}(\bar{\xi},\boldsymbol{\eta}),\bar{\zeta}\big),\eta_{ik}\big(\boldsymbol{z}(\bar{\xi},\boldsymbol{\eta}),\bar{\zeta}\big),t\big)\\ &\qquad\cdot F_{kj}(\bar{\zeta},\boldsymbol{\zeta}(\bar{\xi},\boldsymbol{\eta}),t)\Big)\mathrm{d}\bar{\zeta}\Bigg)\mathrm{d}\bar{\xi}\\ &+\Big[\boldsymbol{H}(\boldsymbol{\eta},\boldsymbol{\eta},t)-q_j(t)\sqrt{\lambda_j(0)}\boldsymbol{G}(\boldsymbol{\eta},\boldsymbol{\eta},t)-\sqrt{\lambda_j(0)}\boldsymbol{A}_0(\boldsymbol{z}(\boldsymbol{\eta},\boldsymbol{\eta}),t)\\ &+\sqrt{\lambda_j(0)}\int_0^{\boldsymbol{z}(\boldsymbol{\eta},\boldsymbol{\eta})}\sum_{k=1}^{n}\frac{1}{\lambda_k(\zeta)}G_{ik}(\boldsymbol{z}(\boldsymbol{\eta},\boldsymbol{\eta}),\zeta,t)A_{0,kj}(\zeta,t)\mathrm{d}\zeta\Big]_{\substack{j>m\\ \lambda_i\geq\lambda_j\\ \boldsymbol{\eta}\geq 0}}\\ &+\big[\boldsymbol{g}_{\boldsymbol{\eta}}(\boldsymbol{\eta},t)-\boldsymbol{H}(\boldsymbol{\eta},\boldsymbol{\eta},t)\big]_{\substack{\lambda_i<\lambda_j\\ \boldsymbol{\eta}\geq 0}}-\big[\boldsymbol{H}(\boldsymbol{\eta},\boldsymbol{\eta},t)\big]_{\substack{\lambda_i\geq\lambda_j\\ j\leq m\\ \boldsymbol{\eta}\geq 0}} \end{aligned}$$

$$+\left[c^1(\boldsymbol{z}(\boldsymbol{\xi}_l(\boldsymbol{\eta}),\boldsymbol{\eta}),t)\frac{(s\boldsymbol{\eta}_l'(\boldsymbol{\xi}_l(\boldsymbol{\eta}))-1)}{\boldsymbol{\eta}_l'(\boldsymbol{\xi}_l(\boldsymbol{\eta}))}-s\boldsymbol{H}(\boldsymbol{\xi}_l(\boldsymbol{\eta}),\boldsymbol{\eta},t)\right]_{\substack{\lambda_i\neq\lambda_j\\ \boldsymbol{\eta}<0}} \tag{2.222b}$$

and

$$\boldsymbol{F}_{\boldsymbol{G}_\eta}[\boldsymbol{G}_\eta]=-\frac{s}{4}\int_{\boldsymbol{\xi}_l(\boldsymbol{\eta})}^{\boldsymbol{\xi}} a_\Sigma(\bar{\xi},\boldsymbol{\eta})\boldsymbol{G}_{\boldsymbol{\eta}}(\bar{\xi},\boldsymbol{\eta},t)\mathrm{d}\bar{\xi}. \tag{2.222c}$$

In (2.222b), all elements are available as system parameters or from the solution of the integral equations (2.173) and known to be bounded. The resulting integral equation (2.221) may now be solved by fixed-point iteration, just like the integral equations (2.173) for the kernel. Its convergence follows with the same reasoning, but turns out very simple, since the integral operator (2.222c) is very simple. Note that for the numerical computation of (2.222b), it is helpful to use (2.140) and (2.97) to insert

$$\frac{1}{\lambda_k(\bar{\zeta})}G_{ik}\big(\xi_{ik}\big(\boldsymbol{z}(\bar{\xi},\boldsymbol{\eta}),\bar{\zeta}\big),\eta_{ik}\big(\boldsymbol{z}(\bar{\xi},\boldsymbol{\eta}),\bar{\zeta}\big),t\big)=K_{ik}(\boldsymbol{z}(\bar{\xi},\boldsymbol{\eta}),\bar{\zeta},t) \tag{2.223a}$$

and

$$\frac{1}{\lambda_k(\zeta)}G_{ik}(\boldsymbol{z}(\boldsymbol{\eta},\boldsymbol{\eta}),\zeta,t)=K_{ik}(\boldsymbol{z}(\boldsymbol{\eta},\boldsymbol{\eta}),\zeta,t), \tag{2.223b}$$

since both $G(\boldsymbol{\xi},\boldsymbol{\eta},t)$ and $K(z,\zeta,t)$ are known. The solution of (2.222) can then be used to calculate the kernel derivatives by (2.220), which will be referred to as *analytical* derivative in the following. Figure 2.11 shows the comparison of a numerically computed derivative $K_z(1,\zeta)$ for Example 2.5.13, which is needed for the control law (2.27), with the one calculated by (2.220a) with the solution of (2.222). In the numerical case, the differentiation matrix resulting from a finite element method with linear basis functions and 31 grid points is utilized to compute the derivative. However, with increasing values of ζ, the remaining discretized spatial vector to compute the derivative gets smaller until for $\zeta=1$, only one point $(1,1)$ is left (see Figure 2.1). As this makes the computation of a numerical derivative impossible by principle, $K_z(1,1)=K_z(1,1-\Delta z)$ is assumed for the numerical computation, where Δz is the step size of the discretization.

For the analytical derivative, the solution of (2.221) is calculated with 9 fixed-point iteration steps on the discretized $(\boldsymbol{\xi},\boldsymbol{\eta})$-grid on which the solution of (2.170) and (2.171) was determined. Though the numerical derivative results in a similar magnitude, especially $K_{12}(z,\zeta)$ has a very big deviation due to

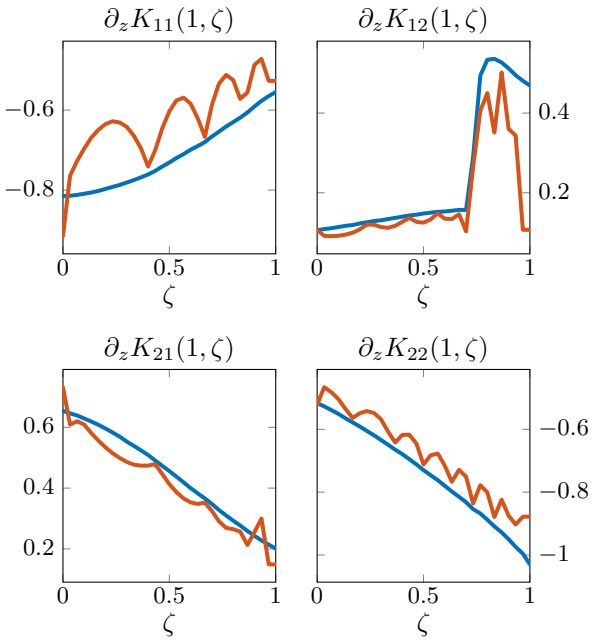

Figure 2.11: Comparison of the numerical and analytical derivative $K_z(1,\zeta)$ for the 2×2 kernel of Example 2.5.13. The numerical derivative (——) is calculated by the differentiation matrix resulting from a finite element method with linear basis functions and 31 grid points and the analytical derivative (——) is calculated by (2.220a) with (2.222), whose solution is determined by a fixed-point iteration with 9 steps.

the appearing discontinuity of the derivative originating from the line of separation (2.172) (see Figure 2.6). Therefore, it is advantageous to use the analytical derivatives (2.220) to avoid deviations in the controller gain.

2.7 Academic examples

To demonstrate the effectiveness of the backstepping controller, simulations are performed on a standard desktop computer with an Intel® Core™ i7-4790 CPU with 3.6 GHz, 32GB RAM, Microsoft Windows 10 Enterprise and MATLAB R2018a. In all simulations, the built-in variable-step solver `ODE15s` is used with an absolute and relative tolerance of 10^{-6} and a maximum step size of 0.02. Interpolants are created for the time dependent parameters stored in discretized form, and evaluated during run-time. The simulation models are created using the finite-elements method with linear basis functions like described in [92]. Therein, Robin BCs are included via integration by parts and Dirichlet BCs are approximated by Robin BCs of the form $x_z(z_b,t) +$

$10^5 x(z_b, t) = 10^5 f(t)$, $z_b \in \{0, 1\}$, where $f(t)$ is a general system input. The resulting approximation uses the differentiation matrices created by the function `matfem`, which is provided by [92].

Example 2.7.1 *(State feedback controlled system).*
Consider the plant (2.21) with $n = 3$ and the parameters

$$\Lambda(z) = \begin{bmatrix} z^2\cos(2\pi z) + \frac{3}{2} & 0 & 0 \\ 0 & z^2\cos(2\pi z) + \frac{3}{2} & 0 \\ 0 & 0 & \frac{9}{5}\left(\frac{1}{2} - \frac{1}{4}\sin\left(2\pi z - \frac{\pi}{6}\right)\right) \end{bmatrix}$$

$$A(z,t) = \begin{bmatrix} \frac{9}{2} - 6\theta_{1.25}(t) & 3\cos(2\pi(z+t)) & \Theta_{1.25}(t) \\ 2 + 2\sin(2\pi(z+t)) & 3 - 4\theta_{1.25}(t) & 1 \\ 3\cos(2\pi(z+t)) & -\Theta_{1.25}(t) & \frac{9}{2} - 6\theta_{1.25}(t) \end{bmatrix}$$

$$F(z,\zeta,t) = \begin{bmatrix} \mathrm{e}^{z+\zeta+1-t} & \mathrm{e}^{z-\zeta-t} & \sin(2\pi(z-t)) \\ \cos(\pi(z+\zeta-t)) & \mathrm{e}^{\zeta-z-t} & 1 - \mathrm{e}^{-(z+\zeta+t)} \\ \cos(2\pi(z+\zeta-t)) & \mathrm{e}^{-(z+\zeta+t)} & \sin(\pi(z+\zeta-t)) \end{bmatrix}$$

$$A_0(z,t) = \begin{bmatrix} 0 & \sin(2\pi(z+t)) & \cos(2\pi(z+t)) \\ 0 & -\sin(2\pi(-z+t)) & \cos(2\pi(-z+t)) \\ 0 & \sin(\pi(t+z)) & \cos(\pi(t+z)) \end{bmatrix}$$

$$t_0 = 0,$$

which is subject to $m = 1$ Dirichlet BCs and $p = 2$ Robin BCs with

$$Q_0(t) = I\Theta_{1.25}(t) \tag{2.224a}$$

at the left side (see (2.6b)) and $p_1 = 3$ Robin BCs with

$$Q_1(t) = t(1-t)\begin{bmatrix} -6 & & \\ & -4 & \\ & & -2 \end{bmatrix} \tag{2.224b}$$

on the right side (see (2.10)). In (2.224), the *normalized bump function*

$$\theta_\omega = \frac{\mathrm{e}^{-((1-t)t)^{-\omega}}}{\mathrm{e}^{-(\frac{1}{4})^{-\omega}}} \tag{2.225}$$

(see Example 2.5.14) and the *smooth step function*

$$\Theta_\omega(t) = \begin{cases} 0 & t < 0 \\ \frac{\int_0^t \theta_\omega(\tau)\mathrm{d}\tau}{\int_0^1 \theta_\omega(\tau)\mathrm{d}\tau} & 0 \le t \le 1 \\ 1 & t > 1 \end{cases} \tag{2.226}$$

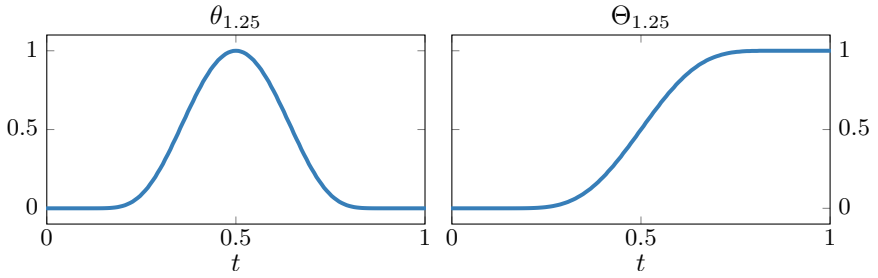

Figure 2.12: Non-analytic bump $\theta_{1.25}$ (left) and step $\Theta_{1.25}$ (right) functions with Gevrey order $\alpha = 1.8$.

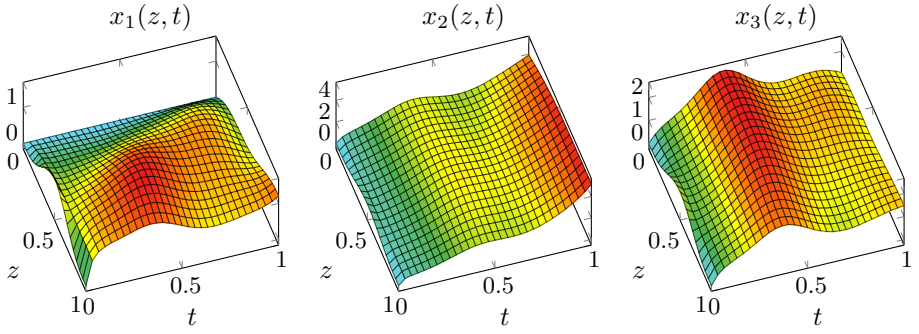

Figure 2.13: Open-loop state profiles $x_i(z,t)$, $i = 1,2,3$ for the plant (2.21) with parameters (2.224) and ICs $x_i(z,0) = \frac{3}{4}\sin(\pi z + 2\pi) + \frac{1}{4}\cos(3\pi z + \frac{\pi}{2})$.

are non-analytic functions with Gevrey order $\alpha = 1 + \frac{1}{\omega}$ [66] and are depicted in Figure 2.12. Consequently, the system parameters are of Gevrey order $\alpha = 1.8 \in [1,2)$, which allows the usage of the proposed backstepping design method. Note that the diffusion coefficients fulfil $\lambda_1 = \lambda_2 > \lambda_3$. The considered plant is unstable in that sense that the states will not converge to zero, which can be seen in the open-loop state profiles in Figure 2.13 resulting from a simulation with the ICs $x_i(z,0) = \frac{3}{4}\sin(\pi z + 2\pi) + \frac{1}{4}\cos(3\pi z + \frac{\pi}{2})$, $i = 1,2,3$, which are compatible to the BCs. Due to the time dependency of the system parameters, the states of the system initially increase, then decrease and finally increase again.

The state feedback controller (2.27) is parameterized by $\widetilde{A}(z,t) = \mu_c I = 8I$ and the degrees of freedom $\boldsymbol{g}(\boldsymbol{\eta},t)$, $\lambda_i < \lambda_j$ in (2.150f) as well as $K_{12}^0(t)$ in (2.92) are set to zero for simplicity. The simulations are performed in the time span $t \in [0,1]$. Note that in any case, it is only possible to compute the controller for a finite time range where the system parameters must be known.

This completely determines the kernel as the solution of (2.28), allowing its computation for the determination of the gains in (2.27).

The numerical implementation uses a discretization of the kernel $K(z, \zeta, t)$ with 31 points in each direction z, ζ and t. The canonical $(\boldsymbol{\xi}, \boldsymbol{\eta})$-grids resulting from the transformation (2.136) are resampled to ensure a minimum point distance of 0.02 in both directions $\boldsymbol{\xi}$ and $\boldsymbol{\eta}$. After each iteration step, the time derivatives $\boldsymbol{G}_t(\boldsymbol{\xi}, \boldsymbol{\eta}, t)$ of the kernel elements are calculated numerically. The fixed-point iteration (2.182) is performed until the increment drops below the limit of 10^{-5}, i. e. $\max_{ij,\boldsymbol{\xi},\boldsymbol{\eta},t} |\Delta \boldsymbol{X}(\boldsymbol{\xi}, \boldsymbol{\eta}, t)| < 10^{-5}$, $\Delta \boldsymbol{X} \in \{\Delta \boldsymbol{G}, \Delta \boldsymbol{H}_1\}$. This occurs after 20 iteration steps, where each step takes approximately 1.5 seconds of computing time. The controller is finally computed after a total time of about 51 seconds including auxiliary computations as well as the calculation of the inverse kernel by solving (2.64a) via fixed-point iteration.

The resulting space and time dependent controller gain $R(z, t)$ in (2.27) is depicted in Figure 2.14.

The controller is able to stabilize the system, which can be seen at the closed-loop state profiles in Figure 2.15.

To check that the controller forces the system to have the desired target system dynamics, the resulting state evolution $x(z, t)$ is transformed into the backstepping coordinates using (2.22) and the result is compared with a simulation of the target system (2.23). Figure 2.16 shows the resulting profiles for the transformed states $(\mathcal{T}_c(t)x(t))(z)$ (left) and the target system states $\tilde{x}(z, t)$ (right). It can be seen that possible numerical deviations resulting from the discretizations and the series truncation of (2.178) are too small to be visible.

Finally, the achieved decay rate set by the parameter μ_c can be verified in Figure 2.17. The norms of both the original system states $\|x(t)\|$ and the transformed states $\|\mathcal{T}_c(t)x(t)\|$ converge to zero with at least the desired decay rate. According to Theorem 2.4.1, this is $\|x(t)\| \leq M \mathrm{e}^{(-8+c)t} \|x(0)\|$, $\forall c > 0$, since $t_0 = 0$ and $\mu_{\max} = 0$ is the largest eigenvalue of the target system (2.23) with the given parameters due to the Neumann BCs. Moreover, the comparison of the norm $\|\tilde{x}(t)\|$ of the simulated the target system (2.23) with the norm $\|\mathcal{T}_c(t)x(t)\|$ of the transformed states in the left picture confirms that the backstepping controller forces the plant to have the desired closed-loop behaviour. The norm of the open-loop system virtualizes its changing stability properties. The right picture of Figure 2.17 show the related norms $\|\mathcal{T}_c(t)x(t)\| / \|\mathcal{T}_c(0)x(0)\|$ for different choices of the decay parameter $\mu_c \in \{4, 8, 16\}$. ◁

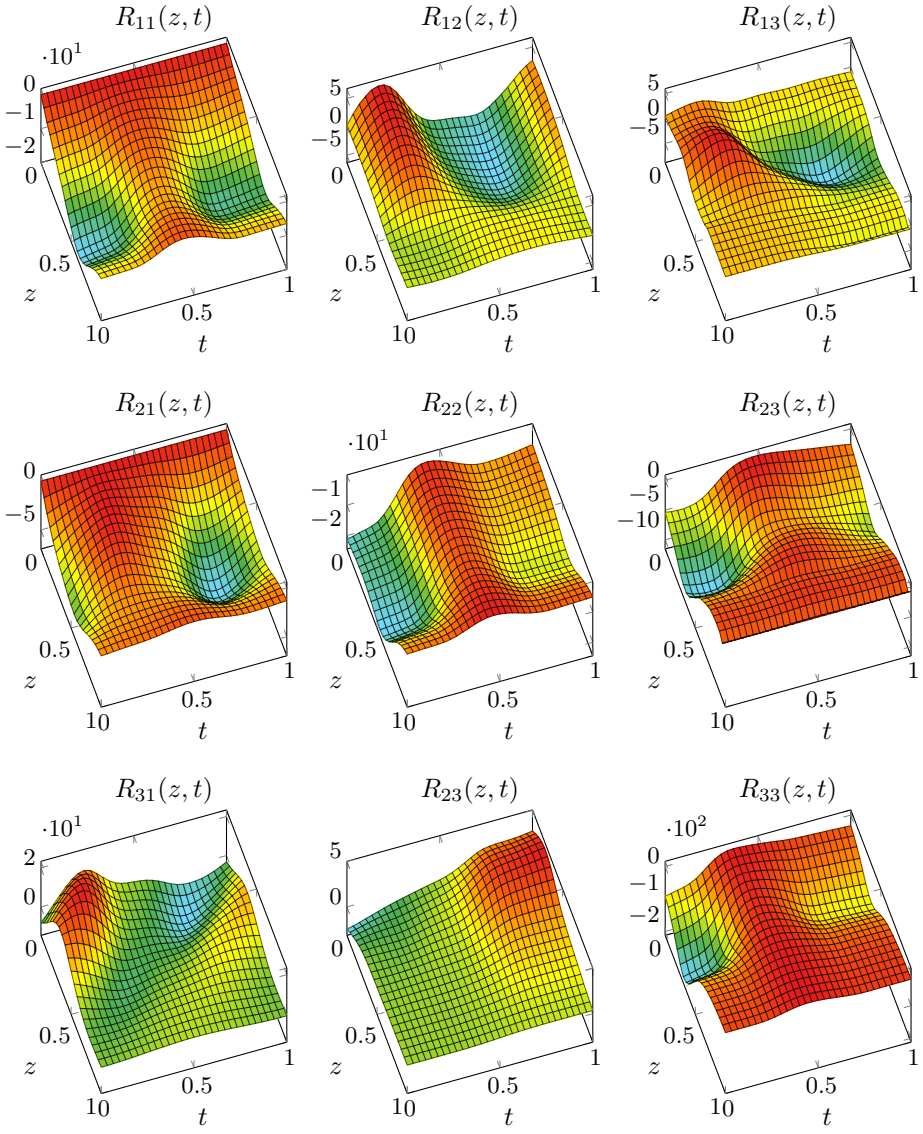

Figure 2.14: Distributed controller gain $R(z,t)$ for Example 2.7.1.

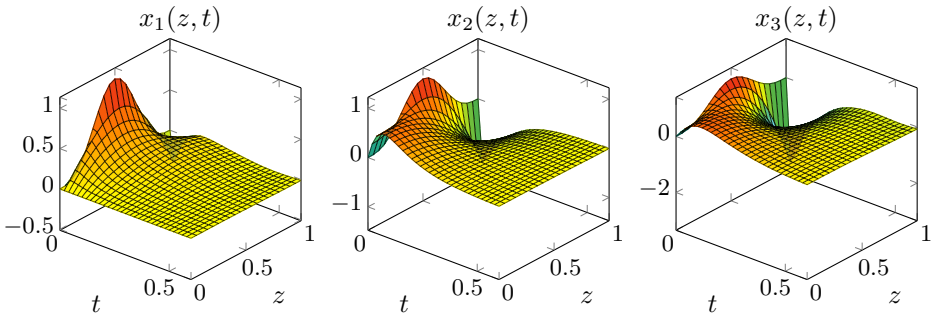

Figure 2.15: Closed-loop state profiles $x_i(z,t)$, $i = 1,\dots,3$ for the plant (2.21) with parameters (2.224), $\widetilde{A}(z,t) = 8I$ and ICs $x_i(z,0) = \frac{3}{4}\sin(\pi z + 2\pi) + \frac{1}{4}\cos(3\pi z + \frac{\pi}{2})$.

The solution of the kernel equations is the numeric bottleneck for the determination of the controller gains in the backstepping method. For the system of two coupled PDEs in Example 2.7.1, the solution could be determined in a very short time with a sufficient resolution.

However, due to the various numeric operations needed to perform the fixed-point iteration (2.182), especially the interpolation of values of one coordinate system (ξ_{ij}, η_{ij}) to the coordinate system (ξ_{ik}, η_{ik}) of a coupled element, a general statement on how the computation time will grow with the system order, is hardly possible. To receive an impression, this is investigated in the following example.

Example 2.7.2 *(Computation times).*
Consider a system (2.21) with the generic parameters

$$\Lambda(z) = \operatorname{diag}(n, n-1, \dots, 1) + zI \tag{2.227a}$$
$$A(z,t) = \underline{1}^n + (z-t)\underline{1}^n \tag{2.227b}$$
$$A_0(z,t) = \underline{1}^n - (z-t)\underline{1}^n \tag{2.227c}$$
$$F(z,\zeta,t) = \underline{1}^n + (z-\zeta+t)\underline{1}^n, \tag{2.227d}$$

where $\underline{1}^n$ is an $n \times n$ matrix full of ones and Neumann BCs, i. e.

$$x_z(0,t) = 0 \tag{2.227e}$$
$$x_z(1,t) = u(t). \tag{2.227f}$$

The kernel equations for the system (2.227) are now solved for different system orders $n = 1,\dots,16$. The spatial coordinates z, ζ, t are discretized by 31 points each and the canoncial coordinates (ξ_{ij}, η_{ij}) of each element are discretized such that there are 80 nodes in ξ_{ij} direction and the same node

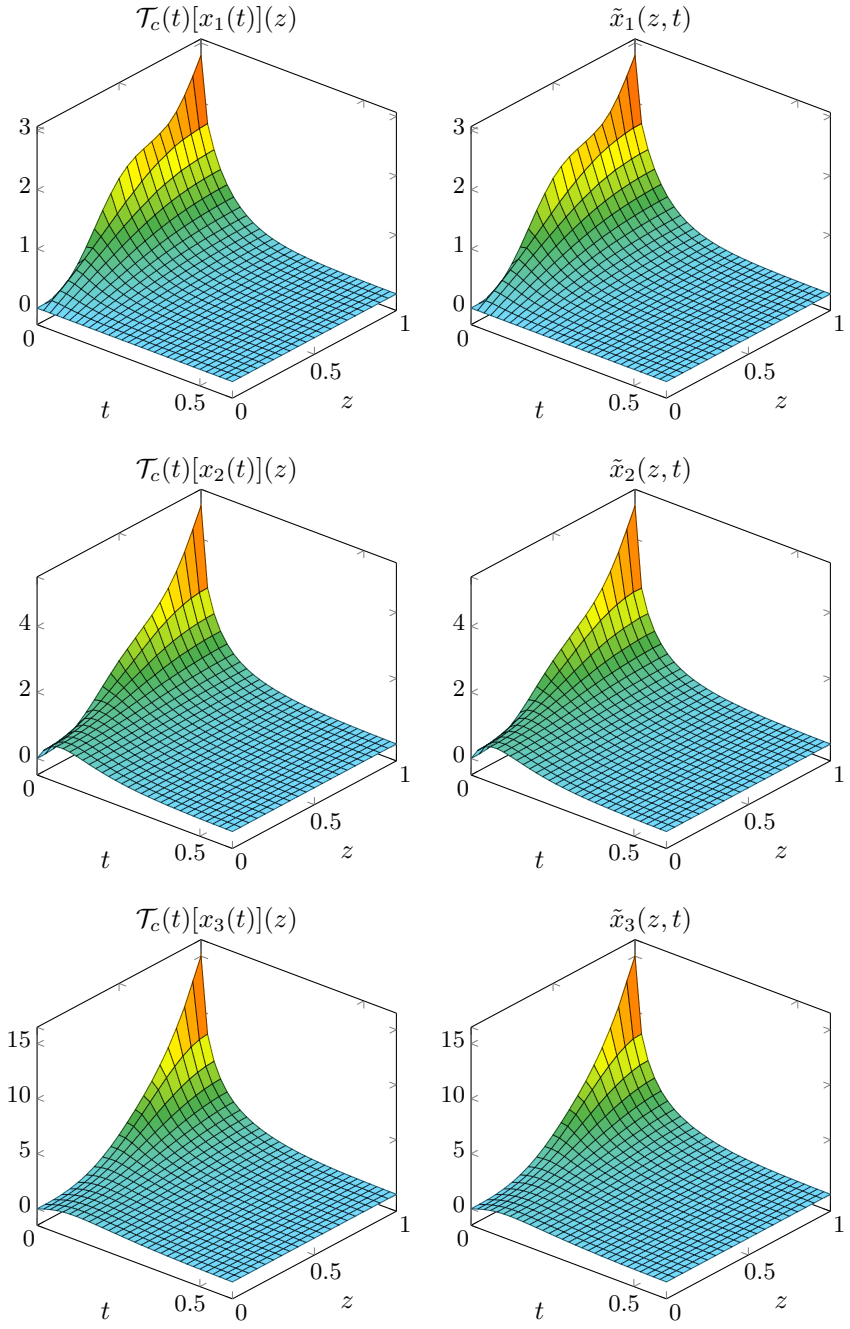

Figure 2.16: Transformed state profiles $(\mathcal{T}_c(t)x(t))(z)$ (left) and state evolutions $\tilde{x}(z,t)$ (right) resulting from a simulation of the target system (2.23).

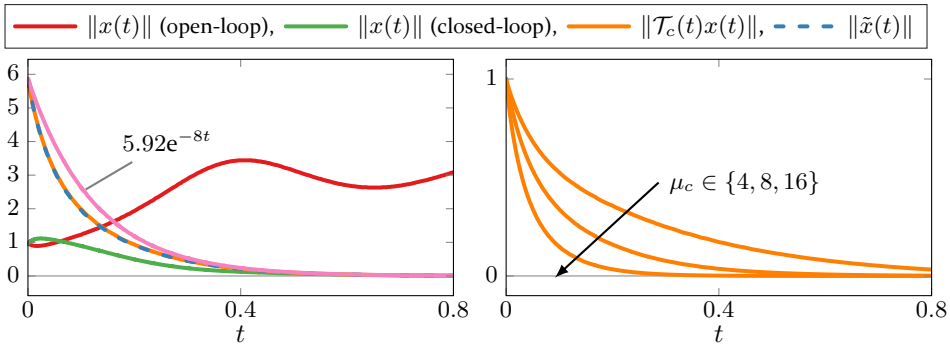

Figure 2.17: Left: Weighted L_2-norms $\|x(t)\|$ of the closed-loop and open-loop system states as well as the transformed states $\|\mathcal{T}_c(t)x(t)\|$ and the target system states $\|\tilde{x}(t)\|$. The pink curve is the desired decay rate $Me^{(\mu_{\max}-\mu_c)t}$, which is achieved. Right: Related norms $\|\mathcal{T}_c(t)x(t)\|/\|\mathcal{T}_c(0)x(0)\|$ of the transformed states for the different choices of $\mu_c \in \{4, 8, 16\}$.

distance in η_{ij}. Note that due to the asymmetric shape of the spatial domain (see Figure 2.2 and Figure 2.3) a different number of nodes in ξ_{ij} and η_{ij} direction results. For the case that the diffusion coefficients differ strongly in their magnitude, setting a fixed number of nodes in the canonical coordinates may be numerically better than a minimum node distance as in Example 2.7.1. The fixed-point iteration is stopped as soon as the maximum absolute increment $\max_{ij,\boldsymbol{\xi},\boldsymbol{\eta},t} |\Delta \boldsymbol{X}(\boldsymbol{\xi}, \boldsymbol{\eta}, t)|$, $\Delta \boldsymbol{X} \in \{\Delta \boldsymbol{G}, \Delta \boldsymbol{H}\}$ drops below 10^{-3}, which turned out to be a sufficient accuracy in simulations. It is noteworthy that this is reached after exactly 10 iterations for every considered system order. Figure 2.18 shows the computation times required to compute the kernel for the different system orders. The total computation time in the left picture includes all auxiliary procedures like initializing required objects and the computation of the inverse kernel by solving (2.64a). To confirm that the main contribution in the increase of computation time indeed originates from the fixed-point iteration, the right picture shows the average computation times for one iteration step. The computational effort seems to increase exponentially with approximately 50% increased time per order. Therefore, numerical problems may occur for high system orders. However, note that for $n = 16$ there are already $2n^2 = 512$ coupled integral equations of the form (2.170) and (2.171) with 256 different canonical coordinate systems $(\boldsymbol{\xi}, \boldsymbol{\eta})$. To handle the couplings between the elements, the solution of one element in the coordinates (ξ_{ij}, η_{ij}) needs to be evaluated at the coordinates (ξ_{ik}, η_{ik}) of each coupled element, requiring not only the calculation of the coordinate map, but also the interpolation of the solutions since the grid points of

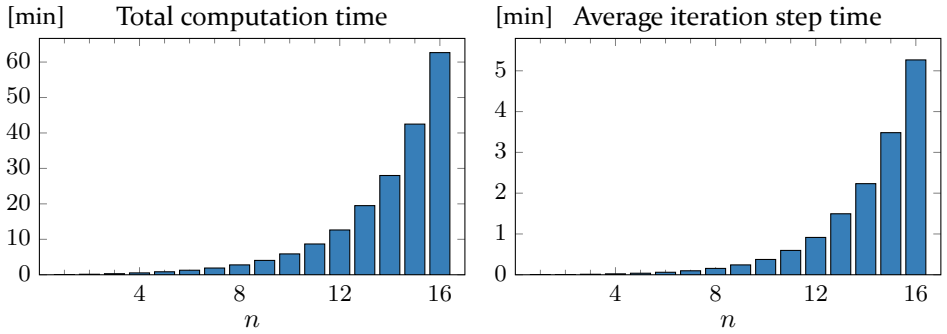

Figure 2.18: Computation time in minutes required for the solution of the kernel equations (left) and for one step of the fixed-point iteration (right) for different system orders $n = 1, \ldots, 16$.

one discretized coordinate system are not mapped into grid points of the coordinate system of the coupled element. ◁

Remark 2.7.3. Though a comparably large effort was devoted to an efficient numerical implementation of the solution of the kernel equations, there may still be vast potential to reduce the computation time. Moreover, by reducing the spatial resolutions to achieve a minimum but sufficient accuracy may allow the controller computation for a system with far larger order as in Example 2.7.2 but this depends on the particular problem. ◁

2.8 Concluding remarks

This section presented the backstepping design of stabilizing state feedback controllers for coupled parabolic PIDEs with space and time dependent coefficients. Existing results for scalar time dependent systems and coupled time constant systems can be extended to obtain a systematic controller design method for the system class in question. The stability of the time dependent target system can be shown systematically since the time dependency only appears in the coupling between the subsystems. Thus, a uniform exponential convergence, which can explicitly be set by the user, is achieved. The calculation of the controller gains requires the solution of the time dependent kernel equations which can be computed by the method of successive approximations providing a practical tool for the controller design. Simulation results verify the applicability of the proposed design method to a broad class of systems.

3 Backstepping observer design for coupled parabolic PIDEs

To be able to realize the control law (2.27), the full state $x(z,t)$ must be known. This is a problem even in the finite dimensional case, as in general, only a linear combination of the states is available as a measurement output. For this reason, observers are the classical method to reconstruct a system's state from the measurement. For PDEs, it is impossible by concept to have the full state as a measurement, because it contains an infinite number of points z. This problem is not overcome by designing an observer because the observer needs to be implemented, thus can only be finite-dimensional and lead to a finite-dimensional approximation of the system state. To determine such an approximation, two concepts have established in control theory, namely *early lumping* and *late lumping*. Both have in common that by increasing the order of the observer, the accuracy of the approximation increases as well. However, as the names already imply, the early lumping method uses an approximation of the plant (lumped plant) to design a finite-dimensional observer whereas in the late lumping method, an infinite dimensional observer is designed for the original system and subsequently it is approximated (lumped controller). Of course this requires a design method for the infinite dimensional system, which can be seen as an effort, but by exploiting the properties of this system, it aims on a greater design flexibility or a better performance as in the early lumping case. Moreover, the approximation is separated from the design process. Changing the order of the approximation requires no redesign of the observer, in contrast to the early lumping method.

Though having a few exceptions [87, 108], the backstepping controller design method is basically suitable for systems with boundary inputs. Analogously, it may be used for the observer design for systems with boundary measurement. It turned out as a powerful tool for the late lumping design of state observers for a variety of different system classes (see [55, 80] for the scalar parabolic case).

For coupled parabolic systems, first results considered equal and constant diffusion coefficients and constant reaction [6] or different diffusion and constant reaction [68]. Recently, [114] used the backstepping method to design a disturbance observer for coupled parabolic PIDEs with spatially varying parameters and distinct diffusion coefficients. Based on these results, a state observer for the considered system class with time dependent coefficients is designed in this chapter.

To this end, the observer is presented in the next section and its error dynamics to be stabilized are derived. Then, the target system for the backstepping transformation is introduced and the observer gains are determined using the backstepping method, which leads to the observer kernel equations. Their solvability is analysed subsequently by utilizing the duality between controller and observer design. The adjacent target system's stability analysis exploits its cascade structure similar to the target system in the state feedback controller design. The combination of the designed boundary observer with the state feedback controller of Chapter 2 to a dynamic output feedback controller is presented in Section 3.8, where the separation property is proved to hold. Finally, the obtained results are verified in simulations.

3.1 Problem formulation

To be able to reconstruct the system state by an observer, it is assumed that an anti-collocated boundary measurement is available at the left boundary, given by

$$y_m(t) = (\mathcal{C}_m x(t))(0) \tag{3.1}$$

with

$$\mathcal{C}_m h = \begin{bmatrix} I_m & 0 \\ 0 & 0_p \end{bmatrix} h_z + \begin{bmatrix} 0_m & 0 \\ 0 & I_p \end{bmatrix} h \tag{3.2}$$

so that it is independent of the BC.

Remark 3.1.1. For a *collocated* measurement, i. e. at $z = 1$, the applied backstepping transformation during the observer design is spatially anti-causal, so that the spatially causal terms $A_0(z,t)x(0,t)$ and $\int_0^z F(z,\zeta,t)x(\zeta,t)\mathrm{d}\zeta$ cannot be eliminated. Consequently, to cover the described class of PIDEs, the measurement must be *anti-collocated*, meaning on the opposite side of the actuation. ◁

For the design of the state feedback controller, an arbitrary boundary matrix was allowed in the right BC (2.7b) of the system due to the position of the actuation, whereas the left boundary matrix in (2.3b) needed to be a diagonal

matrix. For the observer design with an anti-collocated measurement, this behaves the other way round. Of course this implies that for an output feedback controller being the combination of the state feedback controller and the state observer, both boundary matrices need to be diagonal.[1] Nevertheless, the observer design is an interesting stand-alone problem which cannot only be used for realizing a state feedback controller but also for the system diagnosis and supervision. Therefore, it is presented for arbitrary matrices at the left boundary, leading to the BC

$$(\vartheta_0(t)x(t))(0) = 0 \tag{3.3a}$$

with

$$\vartheta_0(t)h = \underbrace{(E_1E_1^\top - E_2\bar{Q}_0(t)E_2^\top)}_{\bar{B}_0^d(t)}h + \underbrace{E_2E_2^\top}_{\bar{B}_0^n}h', \tag{3.3b}$$

where $\bar{Q}_0(t) \in \mathbb{R}^{p\times p}$, is an arbitrary matrix.

The right BC reads

$$(\vartheta_1(t)x(t))(1) = u(t) \tag{3.4a}$$

with

$$\vartheta_1(t)h = \left(S_dS_d^\top - S_r\bar{Q}_1(t)S_r^\top\right)h + S_rS_r^\top h'. \tag{3.4b}$$

Here, $\bar{Q}_1(t) \in \mathbb{R}^{p_1\times p_1}$ needs to be a diagonal matrix with $\bar{Q}_1 \in G_\alpha(\mathbb{R}^+_{t_0})$.

In summary, the considered system class for the observer design reads

$$\begin{aligned} x_t(z,t) &= \Lambda(z)x_{zz}(z,t) + A(z,t)x(z,t) \\ &\quad + A_0(z,t)x(0,t) + \int_0^z F(z,\zeta,t)x(\zeta,t)\mathrm{d}\zeta && \text{(3.5a)}\\ (\vartheta_0(t)x(t))(0) &= 0 && \text{(3.5b)}\\ (\vartheta_1(t)x(t))(1) &= u(t) && \text{(3.5c)}\\ y_m(t) &= (\mathcal{C}_m x(t))(0) && \text{(3.5d)}\\ x(z,t_0) &= x_0(z) && \text{(3.5e)} \end{aligned}$$

with (3.5a) defined on $z \in (0,1)$ and $t \in \mathbb{R}^+_{t_0}$.

In this chapter, a state observer is designed for the system (3.5) that uses the measurement (3.5d) and reconstructs the system's state exponentially with a uniform stability margin specified by the user.

[1] Or included in the target system, see Remark 2.1.1.

3.2 Observer composition

As it is the principle of an observer (see e. g. [70]), it is constructed to have a simulator term, which is a model of the system, complemented by correction terms that feed back the deviation of the measured output and the reconstructed output. This output injection is not only possible in the PIDE but also in the BCs. Consequently, the observer reads

$$\begin{aligned}\hat{x}_t(z,t) &= \Lambda(z)\hat{x}_{zz}(z,t) + A(z,t)\hat{x}(z,t) + A_0(z,t)\hat{x}(0,t)\\ &\quad + \int_0^z F(z,\zeta,t)\hat{x}(\zeta,t)\mathrm{d}\zeta + L(z,t)\Big(y_m(t) - (\mathcal{C}_m\hat{x}(t))(0)\Big)\end{aligned} \tag{3.6a}$$

$$\vartheta_0(t)(\hat{x}(t))(0) = L_0(t)\Big(y_m(t) - (\mathcal{C}_m\hat{x}(t))(0)\Big) \tag{3.6b}$$

$$\vartheta_1(t)(\hat{x}(t))(1) = u(t) + L_1(t)\Big(y_m(t) - (\mathcal{C}_m\hat{x}(t))(0)\Big) \tag{3.6c}$$

$$\hat{x}(z,t_0) = \hat{x}_0(z), \tag{3.6d}$$

with $\hat{x}(z,t) \in \mathbb{R}^n$ being the reconstructed state, $\hat{x}_o(z)$ the observer initial value and $L(z,t), L_0(t), L_1(t) \in \mathbb{R}^{n\times n}$ the observer gains to be determined. The aim is to choose them in such a way that $\lim_{t\to\infty}\hat{x}(z,t) = x(z,t)$, i. e. that the observer reconstructs the actual state of the plant. In other words, the observer error

$$e(z,t) = x(z,t) - \hat{x}(z,t) \tag{3.7}$$

shall converge to zero for $t \to \infty$. By differentiating (3.7) w. r. t. t and inserting (2.21), (3.6) and (3.7), the *observer error dynamics* reads

$$\begin{aligned}e_t(z,t) &= \Lambda(z)e_{zz}(z,t) + A(z,t)e(z,t) + A_0(z,t)e(0,t)\\ &\quad + \int_0^z F(z,\zeta,t)e(\zeta,t)\mathrm{d}\zeta - L(z,t)(\mathcal{C}_m e(t))(0)\end{aligned} \tag{3.8a}$$

$$\vartheta_0(t)(e(t))(0) = -L_0(t)(\mathcal{C}_m e(t))(0) \tag{3.8b}$$

$$\vartheta_1(t)(e(t))(1) = -L_1(t)(\mathcal{C}_m e(t))(0). \tag{3.8c}$$

In view of (3.7), the observer gains $L(z,t)$, $L_0(t)$, $L_1(t)$ need to be determined such that (3.8) becomes exponentially stable.

3.3 Selection of the target system

Following the backstepping approach and [114], the observer backstepping transformation

$$e(z,t) = \tilde{e}(z,t) - \int_0^z P(z,\zeta,t)\tilde{e}(\zeta,t)\mathrm{d}\zeta =: (\mathcal{T}_o^{-1}(t)\tilde{e}(t))(z) \tag{3.9}$$

is applied to map (3.8) into the *observer target system*

$$\tilde{e}_t(z,t) = \Lambda(z)\tilde{e}_{zz}(z,t) - \widetilde{A}_o(z,t)\tilde{e}(z,t) \tag{3.10a}$$

$$(\tilde{\theta}_0\tilde{e}(t))(0) = 0 \tag{3.10b}$$

$$(\tilde{\theta}_1\tilde{e}(t))(1) = -\int_0^1 \widetilde{A}_1(\zeta,t)\tilde{e}(\zeta,t)\mathrm{d}\zeta \tag{3.10c}$$

where $\tilde{\theta}_0$ and $\tilde{\theta}_1$ are defined in (2.25).

In contrast to the controller target system (2.23), a coupling of the states is included via the matrix $\widetilde{A}_1(z,t) = [\widetilde{A}_{1,ij}(z,t)]$, $i,j = 1,\dots,n$ in an integral term at the right boundary rather than inside the PDE. Its elements are

$$\widetilde{A}_{1,ij}(z,t) = \begin{cases} 0, & \lambda_i \leq \lambda_j \\ \widetilde{A}^1_{ij}(z,t), & \lambda_i > \lambda_j, \end{cases}^{2} \tag{3.11}$$

where $\widetilde{A}^1_{ij}(z,t)$ are determined by the kernel $P(z,\zeta,t)$. By this choice, the observer target system is formally dual to the controller target system. In the time-invariant case, it is possible to exploit this for the stability analysis (see Remark 3.6.2 and appendix D).

In analogy to (2.41), the matrix

$$\widetilde{A}_o(z,t) = \mu_o I + \bar{A}_o(z,t) \tag{3.12a}$$

with

$$\bar{A}_{o,ij}(z,t) = \begin{cases} 0, & \lambda_i \leq \lambda_j \\ \breve{A}_{o,ij}(z,t), & \lambda_i > \lambda_j \end{cases} \tag{3.12b}$$

is set by the user to specify the stability margin and the dynamics of the system and its structure ensures that the target system attains a cascade structure.

[2] Note that $\widetilde{A}_0$ in (2.23a) has non-zero entries for $\lambda_i < \lambda_j$, whereas $\widetilde{A}_1$ for $\lambda_i > \lambda_j$.

3.4 Observer gains and the kernel equations

The observer design is based on the *inverse* transformation $\mathcal{T}_o^{-1}$ (3.9) mapping $\tilde{e} \to e$. Basically, starting with its inverse

$$\tilde{e}(z,t) = e(z,t) + \int_0^z P_I(z,\zeta,t)e(\zeta,t)\mathrm{d}\zeta =: (\mathcal{T}_o(t)e(t))(z) \tag{3.13}$$

is also possible, but it turns out that the observer gains depend on the kernel $P(z,\zeta,t)$ of the inverse transformation (3.9). Thus, it is handy to start with (3.9), leading to the following proposition.

Proposition 3.4.1 (Observer gains and kernel equations)**.** *Let $P(z,\zeta,t)$ be the solution of*

$$\Lambda P_{zz} - (P\Lambda(\zeta))_{\zeta\zeta} = -P\widetilde{A}_o(\zeta,t) - AP + F - \int_\zeta^z F(z,\bar{\zeta},t)P(\bar{\zeta},\zeta,t)\mathrm{d}\bar{\zeta} + P_t \tag{3.14a}$$

$$P(z,z,t)\Lambda - \Lambda P(z,z,t) = 0 \tag{3.14b}$$

$$P_\zeta(z,z,t)\Lambda + \Lambda \mathrm{d}_z P(z,z,t) + \Lambda P_z(z,z,t) = A + \widetilde{A}_o - P(z,z,t)\Lambda' \tag{3.14c}$$

$$\vartheta_1(t)[P(\cdot,\zeta,t)](1) = -\widetilde{A}_1(\zeta,t) + S_r S_r^\top P(1,1,t)S_d S_d^\top \widetilde{A}_1(\zeta,t) \tag{3.14d}$$

$$S_r^\top P(1,1,t)S_r = -\bar{Q}_1(t), \tag{3.14e}$$

where (3.14a) is defined on $\mathcal{D} : \{z,\zeta \in \mathbb{R} \,|\, 0 < \zeta < z < 1\}$ and $t \in \mathbb{R}_{t_0}^+$. Then, the transformation (3.9) and the observer gains

$$L(z,t)E_1 = -P(z,0,t)\Lambda(0)E_1 \tag{3.15a}$$

$$\begin{aligned} L(z,t)E_2 = {} & A_0(z,t)E_2 - P(z,0,t)\Lambda(0)E_1E_1^\top P(0,0,t)E_2 \\ & + P(z,0,t)\Lambda'(0)E_2 + P_\zeta(z,0,t)\Lambda(0)E_2 \end{aligned} \tag{3.15b}$$

$$L_0(t)E_1 = 0 \tag{3.15c}$$

$$L_0(t)E_2 = E_2E_2^\top P(0,0,t)E_2 + E_2\bar{Q}_0(t) \tag{3.15d}$$

$$L_1(t) = 0 \tag{3.15e}$$

map the observer target system (3.10) into the observer error dynamics (3.8).

Proof. Starting with the BCs, inserting (3.9) into (3.8b) with (2.6b) yields

$$\begin{aligned}\vartheta_0(t)(e(t))(0) &\overset{(2.6b)}{=} \big(E_1E_1^\top - E_2\bar{Q}_0(t)E_2^\top\big)e(0,t) + E_2E_2^\top e_z(0,t)\\ &\overset{(3.9)}{=} \big(E_1E_1^\top - E_2\bar{Q}_0(t)E_2^\top\big)\tilde{e}(0,t)\\ &\quad + E_2E_2^\top\tilde{e}_z(0,t) - E_2E_2^\top P(0,0,t)\tilde{e}(0,t)\\ &\overset{(3.8b)}{=} -L_0(t)(\mathcal{C}_m e(t))(0),\end{aligned} \tag{3.16}$$

where (3.9) needs to be inserted again to express the measurement in the new coordinates. This yields

$$\begin{aligned}(\mathcal{C}_m e(t))(0) &\overset{(3.2)}{=} E_1E_1^\top e_z(0,t) + E_2E_2^\top e(0,t)\\ &\overset{(3.9)}{=} E_1E_1^\top\tilde{e}_z(0,t) - E_1E_1^\top P(0,0,t)\tilde{e}(0,t) + E_2E_2^\top\tilde{e}(0,t),\end{aligned} \tag{3.17}$$

which is inserted into (3.16) to obtain

$$\begin{aligned}&\underbrace{E_1E_1^\top\tilde{e}(0,t) + E_2E_2^\top\tilde{e}_z(0,t)}_{\tilde{\theta}_0(\tilde{e}(t))(0)\overset{(3.10b)}{=}0} - E_2\bar{Q}_0(t)E_2^\top\tilde{e}(0,t) - E_2E_2^\top P(0,0,t)\tilde{e}(0,t)\\ &= -L_0(t)E_1E_1^\top\tilde{e}_z(0,t) - L_0(t)\big(-E_1E_1^\top P(0,0,t) + E_2E_2^\top\big)\tilde{e}(0,t).\end{aligned} \tag{3.18}$$

Now insert

$$\tilde{e}(0,t) = E_1\underbrace{E_1^\top\tilde{e}(0,t)}_{\overset{(3.10b)}{=}0} + E_2E_2^\top\tilde{e}(0,t) \tag{3.19a}$$

$$\tilde{e}_z(0,t) = E_1E_1^\top\tilde{e}_z(0,t) + E_2\underbrace{E_2^\top\tilde{e}_z(0,t)}_{\overset{(3.10b)}{=}0} \tag{3.19b}$$

and (3.15c) leading to

$$\Big(E_2\bar{Q}_0(t) + E_2E_2^\top P(0,0,t)E_2 - L_0(t)E_2\Big)E_2^\top\tilde{e}(0,t) = 0 \tag{3.20}$$

which is fulfilled due to (3.15d).

For the right BC, insert (3.9) into (3.8c) with (3.4b) and (3.15e) to get

$$\begin{aligned}
0 &= \Big(S_d S_d^\top - S_r \bar{Q}_1(t) S_r^\top\Big) e(1,t) + S_r S_r^\top e_z(1,t) \\
&= \Big(S_d S_d^\top - S_r \bar{Q}_1(t) S_r^\top\Big) \tilde{e}(1,t) \\
&\quad - \Big(S_d S_d^\top - S_r \bar{Q}_1(t) S_r^\top\Big) \int_0^1 P(1,\zeta,t)\tilde{e}(\zeta,t)\mathrm{d}\zeta \\
&\quad + S_r S_r^\top \tilde{e}_z(1,t) - S_r S_r^\top P(1,1,t)\tilde{e}(1,t) - S_r S_r^\top \int_0^1 P_z(1,\zeta,t)\tilde{e}(\zeta,t)\mathrm{d}\zeta \\
&= -\int_0^1 \underbrace{\Big(\big(S_d S_d^\top - S_r \bar{Q}_1(t) S_r^\top\big) P(1,\zeta,t) + S_r S_r^\top P_z(1,\zeta,t)\Big)}_{\vartheta_1[P(\cdot,\zeta,t)](1)} \tilde{e}(\zeta,t)\mathrm{d}\zeta \\
&\quad + \underbrace{S_d S_d^\top \tilde{e}(1,t) + S_r S_r^\top \tilde{e}_z(1,t)}_{(\tilde{\theta}_1 \tilde{e}(\cdot,t))(1)} - \big(S_r \bar{Q}_1(t) S_r^\top + S_r S_r^\top P(1,1,t)\big)\tilde{e}(1,t).
\end{aligned} \tag{3.21}$$

Solving for $(\tilde{\theta}_1(t)\tilde{e}(\cdot,t))(1)$ and inserting (3.14d) yields

$$\begin{aligned}
(\tilde{\theta}_1 \tilde{e}(\cdot,t))(1) = &- \int_0^1 \Big(\widetilde{A}_1(\zeta,t) - S_r S_r^\top P(1,1,t) S_d S_d^\top \widetilde{A}_1(\zeta,t)\Big)\tilde{e}(\zeta,t)\mathrm{d}\zeta \\
&+ \big(S_r \bar{Q}_1(t) S_r^\top + S_r S_r^\top P(1,1,t)\big)\tilde{e}(1,t).
\end{aligned} \tag{3.22}$$

After inserting $\tilde{e}(1,t) = S_d S_d^\top \tilde{e}(1,t) + S_r S_r^\top \tilde{e}(1,t)$,

$$\begin{aligned}
(\tilde{\theta}_1 \tilde{e}(\cdot,t))(1) = &- \int_0^1 \Big(\widetilde{A}_1(\zeta,t) - S_r S_r^\top P(1,1,t) S_d S_d^\top \widetilde{A}_1(\zeta,t)\Big)\tilde{e}(\zeta,t)\mathrm{d}\zeta \\
&+ S_r S_r^\top P(1,1,t) S_d S_d^\top \tilde{e}(1,t) \\
&+ \big(S_r \bar{Q}_1(t) + S_r S_r^\top P(1,1,t) S_r\big) S_r^\top \tilde{e}(1,t)
\end{aligned} \tag{3.23}$$

follows. The BC (3.10c) implies

$$S_d^\top \tilde{e}(1,t) = -\int_0^1 S_d^\top \widetilde{A}_1(\zeta,t)\tilde{e}(\zeta,t)\mathrm{d}\zeta, \tag{3.24}$$

which is inserted into (3.23) to obtain

$$\begin{aligned}(\tilde{\theta}_1\tilde{e}(\cdot,t))(1) = &-\int_0^1 \Big(\widetilde{A}_1(\zeta,t) - S_r S_r^\top P(1,1,t) S_d S_d^\top \widetilde{A}_1(\zeta,t)\Big)\tilde{e}(\zeta,t)\mathrm{d}\zeta \\ &- S_r S_r^\top P(1,1,t) S_d \int_0^1 S_d^\top \widetilde{A}_1(\zeta,t)\tilde{e}(\zeta,t)\mathrm{d}\zeta \\ &+ \big(S_r\bar{Q}_1(t) + S_r S_r^\top P(1,1,t) S_r\big) S_r^\top \tilde{e}(1,t) \\ = &-\int_0^1 \widetilde{A}_1(\zeta,t)\tilde{e}(\zeta,t)\mathrm{d}\zeta \\ &+ \big(S_r\bar{Q}_1(t) + S_r S_r^\top P(1,1,t) S_r\big) S_r^\top \tilde{e}(1,t) \end{aligned} \tag{3.25}$$

To achieve the BC (3.10c), the term in parenthesis needs to vanish, which is ensured by (3.14e).

Now (3.9) and its second order spatial derivative with (3.17) are substituted into (3.8a) and the target system PDE (3.10a) into the time derivative of (3.9). Integration by parts is applied and the order of integration is changed for the expression resulting from the integral term, just like in Section 2.3. Subtracting the results yields

$$\begin{aligned} 0 = &\Big(\Lambda \mathrm{d}_z P(z,z,t) + \Lambda P_z(z,z,t) + P(z,z,t)\Lambda' + P_\zeta(z,z,t)\Lambda - A - \widetilde{A}_o\Big)\tilde{e} \\ &+ \Big(\Lambda P(z,z,t) - P(z,z,t)\Lambda\Big)\tilde{e}_z \\ &+ \int_0^z \Big(\Lambda P_{zz} - F + AP + \int_\zeta^z F(z,\bar{\zeta},t)P(\bar{\zeta},\zeta,t)\mathrm{d}\bar{\zeta} + P\widetilde{A}_o(\zeta,t) \\ &\qquad - \big(P\Lambda(\zeta)\big)_{\zeta\zeta} - P_t\Big)\tilde{e}(\zeta,t)\mathrm{d}\zeta \\ &+ \Big(-A_0 - LE_1E_1^\top P(0,0,t) + LE_2E_2^\top - P(z,0,t)\Lambda'(0) \\ &\quad - P_\zeta(z,0,t)\Lambda(0)\Big)\tilde{e}(0,t) + \Big(LE_1E_1^\top + P(z,0,t)\Lambda(0)\Big)\tilde{e}_z(0,t). \end{aligned} \tag{3.26}$$

With the BCs (3.14b) and (3.14c) as well as the PDE (3.14a), the first three summands vanish. For the remaining two, insert (3.19), leading to

$$\begin{aligned} 0 \overset{!}{=} &\Big(-A_0E_2 - LE_1E_1^\top P(0,0,t)E_2 + LE_2 - P(z,0,t)\Lambda'(0)E_2 \\ &- P_\zeta(z,0,t)\Lambda(0)E_2\Big)E_2^\top\tilde{e}(0,t) + \Big(LE_1 + P(z,0,t)\Lambda(0)E_1\Big)E_1^\top\tilde{e}_z(0,t), \end{aligned} \tag{3.27}$$

which is proved valid by inserting (3.15b) and (3.15a). ■

3.5 Solution of the observer kernel equations

In analogy to the controller gains, which depend on K in (2.28), the observer gains (3.15) depend on P, determined by the kernel equations (3.14). Consequently, their solvability is as essential for the design process as in the controller design.

Luckily, the solution of the observer kernel equations (3.14) turns out to be particularly simple because there exists the duality transformation

$$\breve{P}(z,\zeta,t) = \Lambda(1-z)P^\top(1-\zeta,1-z,T-t)\Lambda^{-1}(1-\zeta), \tag{3.28}$$

$T > t_0$[3] that maps them into the form of (2.28). This is stated in the following proposition.

Proposition 3.5.1 (Duality of kernel equations)**.** *The transformation* (3.28) *maps* (3.14) *into their* dual representation

$$\breve{\Lambda}\breve{P}_{zz} - (\breve{P}\breve{\Lambda}(\zeta))_{\zeta\zeta} = \breve{P}\breve{A}(\zeta,t) + \breve{A}_o\breve{P} - \breve{F} + \int_\zeta^z \breve{P}(z,\bar{\zeta})\breve{F}(\bar{\zeta},\zeta)\mathrm{d}\bar{\zeta} + \breve{P}_t \tag{3.29a}$$

$$\breve{\Lambda}\breve{P}(z,z,t) - \breve{P}(z,z,t)\breve{\Lambda} = 0 \tag{3.29b}$$

$$\breve{P}_\zeta(z,z,t)\breve{\Lambda} + \breve{\Lambda}\breve{P}(z,z,t)_z + \breve{\Lambda}\breve{P}_z(z,z,t) = -(\breve{A}+\breve{A}_o) - \breve{P}(z,z,t)\breve{\Lambda}' \tag{3.29c}$$

$$\breve{P}(z,0,t)\breve{\Lambda}(0)S_d = -\breve{A}_1 S_d \tag{3.29d}$$

$$\begin{aligned}\breve{P}(z,0,t)\breve{\Lambda}'(0)S_r + \breve{P}_\zeta(z,0,t)\breve{\Lambda}(0)S_r = \breve{P}(z,0,t)\breve{\Lambda}(0)S_r\breve{Q}(t)\\ - \breve{A}_1\Big(S_dS_d^\top\breve{P}(0,0,t)S_r - S_r\Big)\end{aligned} \tag{3.29e}$$

$$S_r^\top\breve{P}(0,0,t)S_r = \breve{Q}(t) \tag{3.29f}$$

[3] Note that the solvability of (2.28) according to Theorem 2.5.1 is only valid for each finite time interval $[t_0,T] = \mathcal{I} \subset \mathbb{R}^+_{t_0}$ with arbitrary $T \in (t_0,\infty)$ (see Lemma 2.5.8). Hence, it is no restriction to establish the duality only for that finite interval. Moreover, in practice, it is only possible to compute the kernel for a finite time range by principle.

with

$$\breve{\Lambda}(z) = \Lambda(1-z) \tag{3.30a}$$
$$\breve{A}(z,t) = \breve{\Lambda}(z)A^\top(1-z,T-t)\breve{\Lambda}^{-1}(z) \tag{3.30b}$$
$$\breve{A}_o(z,t) = \breve{\Lambda}(z)\widetilde{A}_o^\top(1-z,T-t)\breve{\Lambda}^{-1}(z) \tag{3.30c}$$
$$\breve{F}(z,\zeta,t) = \breve{\Lambda}(z)F^\top(1-\zeta,1-z,T-t)\breve{\Lambda}^{-1}(\zeta) \tag{3.30d}$$
$$\breve{A}_1(z,t) = \breve{\Lambda}(z)\widetilde{A}_1^\top(1-z,T-t) \tag{3.30e}$$
$$\breve{Q}(t) = -\bar{Q}_1^\top(T-t) = -\bar{Q}_1(T-t). \tag{3.30f}$$

The proof of this proposition can be found in Appendix B.3.

The form (3.29) is equal to (2.28), with the only difference that $A_0 \to 0$, $E_1 \to S_d$ and $E_2 \to S_r$. Note that even the not fully occupied matrices $\breve{A}_o$ in (3.29a) and $\breve{A}_1$ in (3.29d) have the same structure as their corresponding matrices $\widetilde{A}$ in (2.28a) and $\widetilde{A}_0$ in (2.28d) due to the fact that $\widetilde{A}_o$ and $\widetilde{A}_1$ have non-vanishing elements for those i,j for which $\lambda_i \geq \lambda_j$ (3.12) respectively $\lambda_i > \lambda_j$ (3.11). According to (3.30c) and (3.30e), the matrices $\breve{A}_o$ and $\breve{A}_1$ contain the transposed matrices $\widetilde{A}_o^\top$ and $\widetilde{A}_1^\top$, implying non-vanishing values for $\lambda_i \leq \lambda_j$ and $\lambda_i < \lambda_j$, respectively, just like $\widetilde{A}$ and $\widetilde{A}_0$.

Consequently, the methods for solving the kernel equations (2.28) directly apply for (3.29). The bounded map (3.28), respectively (B.45) imply the existence of a piecewise continuous solution of (3.14) according to Theorem 2.5.1.

Remark 3.5.2. In the case of a collocated measurement, i. e. at the same boundary as the actuation (see Remark 3.1.1), the resulting kernel equations are mapped into the controller form by the help of the change of coordinates $\bar{z} = \zeta$, $\bar{\zeta} = z$, $\bar{t} = T - t$. ◁

3.6 Stability of the observer error dynamics

Similar to Section 2.4, the stability of the observer error dynamics (3.8) is provided if the observer target system (3.10) is exponentially stable and the backstepping transformation (3.9) is boundedly invertible, i. e. (3.13) exists. The latter property ensures that (3.8) is boundedly mapped into (3.10) and is provided by Lemma 2.4.4 because of the duality of (2.28) and (3.14) (see Proposition 3.5.1). What remains to be shown is the stability of the target system (3.10) and is stated in the following proposition.

Proposition 3.6.1 (Stability of observer target system)**.** *Assume that $\widetilde{A}_o$ is chosen according to* (3.12) *and $\mu_o > \mu_{\max}$, where $\mu_{\max}$ is the largest eigenvalue*

of (3.10) *for* $\mu_o = 0$, $\widetilde{A}_1(z,t) \equiv 0$ *and* $\bar{A}_o(z,t) \equiv 0$. *Then, the observer target system* (3.10) *is well-posed and uniformly exponentially stable in the weighted* L_2*-norm* $\|h\| = \left(\int_0^1 \|\Lambda^{-\frac{1}{2}}(z)h(z)\|_{\mathbb{C}^n}^2 \mathrm{d}z\right)^{1/2}$, *i. e.*

$$\|\tilde{e}(t)\| \leq \widetilde{M} \mathrm{e}^{(\mu_{\max} - \mu_o + c)(t-t_0)} \|\tilde{e}(t_0)\|, \quad t \geq t_0 \tag{3.31}$$

for all $\tilde{e}(t_0) \in (L_2(0,1))^n$ *satisfying the BCs* (3.10b), (3.10c), *an* $\widetilde{M} \geq 1$, *any* $t_0 \geq 0$ *and any* $c > 0$, *i. e. the stability margin is* $\mu_o - \mu_{\max}$.

Proof. The proof follows the same idea as the proof of Lemma 2.4.2. However, as the couplings now appear in the boundary condition (3.10c), a homogenization is required for the coupled states.

The state vector is now permuted such that the diffusion coefficients are ordered ascending. The new state

$$\tilde{e}^*(z,t) = P\tilde{e}(z,t) \tag{3.32}$$

with $P^{-1} = P^\top \in \mathbb{R}^{n\times n}$ has the dynamics

$$\tilde{e}_t^*(z,t) = \Lambda^*(z)\tilde{e}_{zz}^*(z,t) - \mu_o\tilde{e}^*(z,t) - \bar{A}_o^*(z,t)\tilde{e}^*(z,t) \tag{3.33a}$$

$$P(\tilde{\theta}_0 P^\top \tilde{e}^*(t))(0) = (\tilde{\theta}_0^* \tilde{e}^*(t))(0) = 0 \tag{3.33b}$$

$$P(\tilde{\theta}_1 P^\top \tilde{e}^*(t))(1) = (\tilde{\theta}_1^* \tilde{e}^*(t))(1) = -\int_0^1 \widetilde{A}_1^*(\zeta,t)\tilde{e}^*(\zeta,t)\mathrm{d}\zeta, \tag{3.33c}$$

where the elements of $\Lambda^*(z) = P\Lambda P^\top = \mathrm{diag}(\lambda_i^*(z), \ldots, \lambda_n^*(z))$ suffice $\lambda_1^* \leq \ldots \leq \lambda_n^*$. This implies that the matrices $\bar{A}_o$ and $\widetilde{A}_1$ defined in (3.12b) and (3.11) become strictly lower triangular in the permuted system, i. e.

$$\bar{A}_o^*(z,t) = P\bar{A}_o(z,t)P^\top = \begin{bmatrix} 0 & \ldots & \ldots & 0 \\ \breve{A}_{o,21}^*(z,t) & \ddots & \ddots & \vdots \\ \vdots & \ddots & \ddots & \vdots \\ \breve{A}_{o,n1}^*(z,t) & \ldots & \breve{A}_{o,n\,n-1}^*(z,t) & 0 \end{bmatrix} \tag{3.34a}$$

$$\widetilde{A}_1^*(z,t) = P\widetilde{A}_1(z,t)P^\top = \begin{bmatrix} 0 & \ldots & \ldots & 0 \\ \widetilde{A}_{1,21}^*(z,t) & \ddots & \ddots & \vdots \\ \vdots & \ddots & \ddots & \vdots \\ \widetilde{A}_{1,n1}^*(z,t) & \ldots & \widetilde{A}_{1,n\,n-1}^*(z,t) & 0 \end{bmatrix}. \tag{3.34b}$$

Now the operators $\mathcal{A}_i - \mu_o I$ with

$$\mathcal{A}_i h = \lambda_i^* h'', \quad i = 1, \ldots, n, \tag{3.35a}$$

$$D(\mathcal{A}_i) = \{h \in H^2(0,1) \,|\, e_i^\top(\tilde{\theta}_0^* e_i h)(0) = e_i^\top(\tilde{\theta}_1^* e_i h)(1) = 0\} \tag{3.35b}$$

describe the homogeneous dynamics of the decoupled subsystems. Particularly, they have the same form and properties as in (2.47). Consequently, the abstract IVP

$$\dot{\tilde{e}}_1^*(t) = (\mathcal{A}_1 - \mu_o I)\tilde{e}_1^*(t), \quad t \in \mathbb{R}_{t_0}^+ \tag{3.36a}$$
$$\tilde{e}_1^*(t_0) = \tilde{e}_{01}^* \in D(\mathcal{A}_1) \tag{3.36b}$$

of the first state $\tilde{e}_1^*$ of the permuted target system (3.33) in the Hilbert space $L_2(0,1)$ is well-posed and, with the same argumentation as in the proof of Lemma 2.4.2, has the solution

$$\tilde{e}_1^*(t) = \mathcal{T}_1(t - t_0)\tilde{e}_1^*(t_0) \tag{3.37}$$

with the C_0-semigroup $\mathcal{T}_1(t)$ and the bound

$$\|\tilde{e}_1^*(t)\| \leq M_1 \mathrm{e}^{(\mu_{\max} - \mu_o)(t-t_0)} \|\tilde{e}_1^*(t_0)\|. \tag{3.38}$$

The IBVP of the second state reads

$$\tilde{e}_{2,t}^*(z,t) = \lambda_2^*(z)\tilde{e}_{2,zz}^*(z,t) - \mu_o \tilde{e}_2^*(z,t) - \breve{A}_{o,21}^*(z,t)\tilde{e}_1^*(z,t) \tag{3.39a}$$
$$e_2^\top P(\tilde{\theta}_0 P^\top \tilde{e}^*(t))(0) = 0 \tag{3.39b}$$
$$e_2^\top P(\tilde{\theta}_1 P^\top \tilde{e}^*(t))(1) = -\int_0^1 \widetilde{A}_{1,21}^*(\zeta,t)\tilde{e}_1^*(\zeta,t)\mathrm{d}\zeta. \tag{3.39c}$$

To be able to use the Riesz-spectral properties of the operators $\mathcal{A}_i - \mu_o I$ like in the proof of Lemma 2.4.2, this system with inhomogeneous BCs is now converted into an equivalent representation with homogeneous BCs.[4]

Rewriting the boundary operators with the help of (2.25) yields

$$e_2^\top P(\tilde{\theta}_0(P^\top \tilde{e}^*(t)))(0) = e_2^\top P E_1 E_1^\top P^\top \tilde{e}^*(0,t) + e_2^\top P E_2 E_2^\top P^\top \tilde{e}_z^*(0,t) \tag{3.40a}$$
$$e_2^\top P(\tilde{\theta}_1(P^\top \tilde{e}^*(t)))(1) = e_2^\top P S_d S_d^\top P^\top \tilde{e}^*(1,t) + e_2^\top P S_r S_r^\top P^\top \tilde{e}_z^*(1,t). \tag{3.40b}$$

[4] See [26, Ch. 3.3] for a system theoretic background to this procedure.

Knowing that

$$e_2^\top P E_1 E_1^\top P^\top = \begin{cases} e_2^\top, & j \leq m \\ 0, & j > m \end{cases} \tag{3.41a}$$

$$e_2^\top P E_2 E_2^\top P^\top = \begin{cases} 0, & j \leq m \\ e_2^\top, & j > m \end{cases} \tag{3.41b}$$

$$e_2^\top P S_d S_d^\top P^\top = \begin{cases} e_2^\top, & e_2^\top P S_d \neq 0^\top \\ 0, & e_2^\top P S_d = 0^\top \end{cases} \tag{3.41c}$$

$$e_2^\top P S_r S_r^\top P^\top = \begin{cases} 0, & e_2^\top P S_r = 0^\top \\ e_2^\top, & e_2^\top P S_r \neq 0^\top \end{cases}, \tag{3.41d}$$

i. e. the respective BC of a state can either be Dirichlet or Neumann type, the BCs can be written as

$$\underbrace{e_2^\top P E_1 E_1^\top P^\top e_2}_{s_1} \tilde{e}_2^*(0,t) + \underbrace{e_2^\top P E_2 E_2^\top P^\top e_2}_{s_2} \tilde{e}_{2,z}^*(0,t) = 0 \tag{3.42a}$$

$$\begin{aligned} &\underbrace{e_2^\top P S_d S_d^\top P^\top e_2}_{s_d} \tilde{e}_2^*(1,t) + \underbrace{e_2^\top P S_r S_r^\top P^\top e_2}_{s_r} \tilde{e}_{2,z}^*(1,t) \\ &\quad = \underbrace{-\int_0^1 \widetilde{A}_{1,21}^*(\zeta,t)\tilde{e}_1^*(\zeta,t)\mathrm{d}\zeta}_{=:w(t)}, \end{aligned} \tag{3.42b}$$

where one of s_1 and s_2 is always 1 and the other is 0 and the same for s_d and s_r.

Now introduce the homogeneous state

$$\varepsilon(z,t) = \tilde{e}_2^*(z,t) - h_2(z)w(t), \tag{3.43}$$

where $h_2(z)$ can always be determined in the form $a+bz+cz^2$ with constants a, b, c such that the dynamics of $\varepsilon(z,t)$ has homogeneous BCs. The conditions on $h_2(z)$ are determined by

$$\begin{aligned} &s_1\varepsilon(0,t) + s_2\varepsilon_z(0,t) \\ &\quad = \underbrace{s_1\tilde{e}_2^*(0,t) + s_2\tilde{e}_{2,z}^*(0,t)}_{\overset{(3.42a)}{=}0} - \underbrace{\big(s_1h_2(0) + s_2h_2'(0)\big)}_{\overset{!}{=}0} w(t) = 0 \end{aligned} \tag{3.44a}$$

$$\begin{aligned} &s_d\varepsilon(1,t) + s_r\varepsilon_z(1,t) \\ &\quad = \underbrace{s_d\tilde{e}_2^*(1,t) + s_r\tilde{e}_{2,z}^*(1,t)}_{\overset{(3.42b)}{=}w(t)} - \underbrace{\big(s_dh_2(1) + s_rh_2'(1)\big)}_{\overset{!}{=}1} w(t) = 0 \end{aligned} \tag{3.44b}$$

and solely depend on s_1, s_2, s_d and s_r.

To describe the dynamics of the homogeneous state, differentiate (3.43) w. r. t. t and insert (3.39a), leading to

$$\varepsilon_t = \lambda_2^* \tilde{e}_{2,zz}^* - \mu_o \tilde{e}_2^* - \breve{A}_{o,21}^* \tilde{e}_1^* - h_2 w_t, \tag{3.45}$$

where (3.43) solved for $\tilde{e}_2^*$ is inserted to obtain

$$\varepsilon_t = \lambda_2^* \varepsilon_{zz} - \mu_o \varepsilon + \lambda_2^* h_{2,zz} w - \mu_o h_2 w - \breve{A}_{o,21}^* \tilde{e}_1^* - h_2 w_t. \tag{3.46}$$

Differentiating w defined in (3.42b) w. r. t. t yields

$$w_t = -\int_0^1 \widetilde{A}_{1,21,t}^*(\zeta,t)\tilde{e}_1^*(\zeta,t)\mathrm{d}\zeta - \int_0^1 \widetilde{A}_{1,21}^*(\zeta,t)\tilde{e}_{1,t}^*(\zeta,t)\mathrm{d}\zeta, \tag{3.47}$$

where $\tilde{e}_{1,t}^*$ according to (3.33a) is substituted to get

$$\begin{aligned} -h_2 w_t = h_2 \int_0^1 \widetilde{A}_{1,21,t}^*(\zeta,t)\tilde{e}_1^*(\zeta,t)\mathrm{d}\zeta + h_2 \underbrace{\int_0^1 \widetilde{A}_{1,21}^*(\zeta,t)\lambda_1^*(\zeta)\tilde{e}_1^*(\zeta,t)_{\zeta\zeta}\mathrm{d}\zeta}_{(\star_5)} \\ \underbrace{-h_2 \int_0^1 \widetilde{A}_{1,21}^*(\zeta,t)\mu_o \tilde{e}_1^*(\zeta,t)\mathrm{d}\zeta}_{\mu_o h_2 w}. \end{aligned} \tag{3.48}$$

The term $(\star_5)$ is reformulated by applying integration by parts, yielding

$$\begin{aligned} (\star_5) = &\underbrace{-\widetilde{A}_{1,21}^*(0,t)\lambda^*(0)\tilde{e}_{1,z}^*(0,t) + \left(\widetilde{A}_{1,21}^*\lambda^*\right)_z(0,t)\tilde{e}_1^*(0,t)}_{\mathcal{E}_0(t)\tilde{e}_1^*(t)} \\ &+ \underbrace{\widetilde{A}_{1,21}^*(1,t)\lambda^*(1)\tilde{e}_{1,z}^*(1,t) - \left(\widetilde{A}_{1,21}^*\lambda^*\right)_z(1,t)\tilde{e}_1^*(1,t)}_{\mathcal{E}_1(t)\tilde{e}_1^*(t)} \\ &+ \int_0^1 \left(\widetilde{A}_{1,21}^*(\zeta,t)\lambda^*(\zeta)\right)_{\zeta\zeta}\tilde{e}_1^*(\zeta,t)\mathrm{d}\zeta. \end{aligned} \tag{3.49}$$

Inserting the previous equations subsequently into (3.46) finally leads to

$$\begin{aligned} \varepsilon_t = &\lambda_2^* \varepsilon_{zz} - \mu_o \varepsilon \\ &- \int_0^1 \underbrace{\left(\lambda_2^* h_{2,zz}\widetilde{A}_{1,21}^*(\zeta,t) - h_2 \widetilde{A}_{1,21,t}^*(\zeta,t) - h_2\left(\widetilde{A}_{1,21}^*(\zeta,t)\lambda^*(\zeta)\right)_{\zeta\zeta}\right)}_{k(\zeta,t)}\tilde{e}_1^*(\zeta,t)\mathrm{d}\zeta \\ &- \breve{A}_{o,21}^*\tilde{e}_1^* + h_2\mathcal{E}_0(t)\tilde{e}_1^*(t) + h_2\mathcal{E}_1(t)\tilde{e}_1^*(t). \end{aligned} \tag{3.50}$$

Together with the BCs (3.44), this is a time-invariant system with homogenous BCs, which is excited by $\tilde{e}_1^*$, and has the solution

$$\begin{aligned}\varepsilon(t) &= \mathcal{T}_2(t-t_0)\varepsilon(t_0) + \int_{t_0}^{t} \mathcal{T}_2(t-\tau)\Big(\breve{A}_{o,21}^*(\cdot,\tau)\mathcal{T}_1(\tau-t_0)\tilde{e}_1^*(t_0) \\ &\quad + h_2\mathcal{E}_0(\tau)[\mathcal{T}_1(\tau-t_0)\tilde{e}_1^*(t_0)] + h_2\mathcal{E}_1(\tau)[\mathcal{T}_1(\tau-t_0)\tilde{e}_1^*(t_0)] \\ &\quad - \int_0^1 k(\zeta,\tau)\big(\mathcal{T}_1(\tau-t_0)\tilde{e}_1^*(t_0)\big)(\zeta)\mathrm{d}\zeta\Big)\mathrm{d}\tau \qquad (3.51a) \\ &= \mathcal{T}_2(t-t_0)\varepsilon(t_0) + \int_{t_0}^{t} \mathcal{T}_2(t-\tau)R_2(\tau,t_0)\mathrm{d}\tau, \qquad (3.51b)\end{aligned}$$

with the abbreviation $R_2(t,t_0)$. The operators $\mathcal{E}_1(t)$ and $\mathcal{E}_2(t)$ according to (3.49) contain multiplications of a time-invariant boundary evaluation operator by bounded time dependent factors. Since the boundary evaluations are relatively bounded w. r. t. $\mathcal{A}_1 - \mu_o I$ according to Lemma A.1.1, their application to the analytic C_0-semigroup $\mathcal{T}_1(\tau-t_0)$ is a bounded linear operator with the same norm as the semigroup (see Lemma A.2.1) and consequently the same holds for $\mathcal{E}_1(t)$ and $\mathcal{E}_2(t)$. For that reason, the argumentation in the proof of Lemma 2.4.2 can be applied in the very same way, which shows

$$\|\varepsilon(t)\| \leq \widetilde{M}_2 \mathrm{e}^{(\mu_{\max}-\mu_o+c)(t-t_0)}\|\varepsilon(t_0)\| \qquad (3.52)$$

for some finite $\widetilde{M}_2 \geq 1$, any $t_0 \geq 0$ and any $c > 0$.

The bound for $\tilde{e}_2^*$ is obtained by solving (3.43) for it and inserting (3.52) and (3.38). In the result

$$\|\tilde{e}_2^*(t)\| \leq \widetilde{M}_2 \mathrm{e}^{\mu_{\max}-\mu_o+c}(t-t_0)\|\varepsilon(t_0)\| + \| \underbrace{h_2 \int_0^1 \widetilde{A}_{1,21}^*(\zeta,t)\tilde{e}_1^*(\zeta,t)\mathrm{d}\zeta}_{\mathcal{E}_I(t)\tilde{e}_1^*(t)} \|, \qquad (3.53)$$

$\varepsilon(t_0)$ is replaced by the help of (3.43), implying

$$\|\varepsilon(t_0)\| \leq \|\tilde{e}_2^*(t_0)\| + \| \underbrace{h_2 \int_0^1 \widetilde{A}_{1,21}^*(\zeta,t_0)\tilde{e}_1^*(\zeta,t_0)\mathrm{d}\zeta}_{\mathcal{E}_I(t_0)\tilde{e}_1^*(t_0)} \|. \qquad (3.54)$$

The operator $\mathcal{E}_I$ is a bounded linear operator, so that

$$\|\mathcal{E}_I(t)\tilde{e}_1^*(t)\| \leq \bar{c}\|\tilde{e}_1^*(t)\|, \qquad (3.55)$$

for some finite constant $\bar{c} > 0$ can be used in (3.53) and (3.54). Inserting (3.38) once more and with the same reasoning as in the proof of Lemma 2.4.2, the result

$$\|\tilde{e}_2^*(t)\| \leq M^* \mathrm{e}^{(\mu_{\max} - \mu_o + c)(t - t_0)} \|\tilde{e}^*(t_0)\| \tag{3.56}$$

is readily obtained for some finite M^*. Repeating this procedure for all states $\tilde{e}_i^*$, $i = 3, \ldots, n$, leads to the result of the proposition. Like in the proof of lemma 2.4.2, the analyticity of the generated C_0-semigroups $\mathcal{T}_i$, $i = 1, \ldots, n$ allows to consider ICs in $L_2(0,1)$ leading to a unique mild solution. ■

Remark 3.6.2. In the time-invariant case, the stability of the target system can be proved by using the duality between the target systems (2.23) and (3.10). In particular, the adjoint of the system-operator corresponding to (3.10) is exactly the system operator of (2.23). Then, the stability directly follows because the generated C_0-semigroups of an operator and its adjoint have the same norm [26, Lemma A.3.60]. The calculation of the adjoint system is shown in Appendix D, where the dependency on t is formally kept for integrity. In the time-dependent case, however, a further system theoretic analysis of the generated *mild evolution operators* [26, 38][5], the time-varying counterpart of the C_0-semigroups is required. ◁

Remark 3.6.3. For the stability analysis, the presented proof is sufficient. However, a more formal proof allowing further statements about the form of the solution is also possible and will be provided in Section 3.8.2. ◁

In view of the target system stability and the invertibility of (3.9), the stability of the observer error dynamics follows and is stated in the following theorem.

Theorem 3.6.4 (Stability of observer error dynamics)
Assume that the conditions of Proposition 3.6.1 hold. If the observer gains are chosen as (3.15) with $P(z, \zeta, t)$ being the solution of (3.14) then the observer error dynamics (3.8) is well-posed and uniformly exponentially stable in the weighted L_2-norm $\|h\| = \left(\int_0^1 \|\Lambda^{-\frac{1}{2}}(z) h(z)\|_{\mathbb{C}^n}^2 \mathrm{d}z\right)^{1/2}$, i. e.

$$\|e(t)\| \leq M \mathrm{e}^{(\mu_{\max} - \mu_o + c)(t - t_0)} \|e(t_0)\|, \quad t \geq t_0 \tag{3.57}$$

for all $e(t_0) \in (L_2(0,1))^n$ satisfying the BCs (3.8b), (3.8c), an $M \geq 1$, any $t_0 \geq 0$ and any $c > 0$, i. e. the stability margin is $\mu_o - \mu_{\max}$.

[5] In [38], they are called *evolution families*.

The proof follows with the very same argumentation as in the proof of Theorem 2.4.1.

Remark 3.6.5. As a result of Theorem 3.6.4, the observer reconstructs the actual state of the system with the prescribed observation dynamics in the sense of the L_2-norm. This means that in fact $e(z,t)$ may not converge at some point z in the sense of an element of a zero-set in L_2. However, Section 3.8.2 will show that the solution of (3.10) can be expressed by the help of analytic C_0-semigroups, implying that a point evaluation leads to an exponentially decaying signal with the same decay rate as the norm. Consequently, the observer indeed reconstructs the system state at each point z. ◁

3.7 Academic example

The functionality of the proposed backstepping observer is confirmed by simulations. To this end, the observer is applied to the system considered in Example 2.7.1.

Example 3.7.1 *(Observer simulation).*
The plant (2.21) with the parameters (2.224) of Example 2.7.1 is now equipped with a boundary measurement

$$y_m(t) = (\mathcal{C}_m x(t))(0) = \operatorname{col}(x_{1,z}(0,t), x_2(0,t), x_3(0,t)) \tag{3.58}$$

to obtain the system (3.5) for the observer design. Note that in case of diagonal boundary matrices, the measurement is the only difference between the system representations (2.21) and (3.5). An observer (3.6) is implemented to reconstruct the states of the system under state feedback control. Note that the controller still feeds back the actual states.

The observer is parameterized by $\widetilde{A}_o(z,t) = \mu_o I = 15I$ and the additional degrees of freedom $\boldsymbol{g}(\boldsymbol{\eta},t)$ and $K_{ij}^0(t)$ appearing during the solution of the kernel equations are set to zero like for the designed state feedback controller (see Example 2.7.1). The ICs $x_i(z,0) = \frac{3}{4}\sin(\pi z + 2\pi) + \frac{1}{4}\cos(3\pi z + \frac{\pi}{2})$, $i = 1,2,3$, of the plant lead to the initial measurement $y_m(0) = 0$, so that the observer IC is chosen to be $\hat{x}_0(z) = 0$ as the most intuitive choice. For the numerical computation of the kernel, the dual representation (3.29) of the kernel equations is solved by the methods of Section 2.5 and transformed into the original solution of (3.14) by (3.28). To this end, the kernel is dis-

cretized by 31 points in time and by 51 points[6] in each direction z, ζ. The remaining settings for the solution of the kernel equations are the same as in Example 2.7.1. Each step of the fixed-point iteration takes about 3 seconds of computing time and the tolerance (see Example 2.7.1) is reached after 20 iteration steps. The distributed observer gain $L(z,t)$ calculated by (3.15a) and (3.15b) is depicted in Figure 3.1.

The infinite-dimensional observer (3.6) is approximated by the same finite-elements method with linear basis functions as the plant but with a significantly lower order using 11 discretization points for each state.[7] This accounts for the fact that the observer actually needs to be realized on a hardware in practice, while the plant approximation is simply a model for the real system. The observer converges even with a lower order but the approximation error then leads to visible deviations from the desired behaviour. For the chosen order of approximation, almost no deviations are visible.

Figure 3.2 shows the reconstructed observer states $\hat{x}(z,t)$ as well as the observer error $e(z,t) = x(z,t) - \hat{x}(z,t)$. All states are reconstructed accurately and the observer error converges to zero, despite the comparably low observer order. The achieved decay rate $\|e(t)\| \leq M\mathrm{e}^{(\mu_{\max}-\mu_o+c)(t-t_0)}\|e(t_0)\| = M\mathrm{e}^{(-15+c)t}\|e(0)\|$, $\forall c > 0$, (see Theorem 3.6.4) is confirmed by Figure 3.3. To compare the observer error dynamics with the desired target system, the transformation (3.13), which is the inverse of (3.9), is determined by solving the reciprocity relation (2.64b) via fixed-point iteration. A comparison between the norms of the transformed observer error $\|\mathcal{T}_o(t)e(t)\|$ and the target system states $\|\tilde{e}(t)\|$ resulting from a simulation of (3.10) shows that the observer error attains the desired behaviour of the target system. ◁

3.8 Observer-based state feedback control

Besides using the observer presented in this chapter as an identification tool or for the purpose of diagnosis, an important field of interest is its usability in combination with a state feedback controller. This section answers the question of stability for the resulting control loop when using the backstepping controller of Chapter 2.

[6] Basically, sufficient accuracy can be obtained when using only 31 or fewer nodes. Even in the output-feedback case, which will be considered later, the high resolution is not needed. However, for an accurate simulation of the target system in the output-feedback case, the higher resolution is required.

[7] The finite-elements method is used because it is a very simple approximation method. Most likely, comparable results could be achieved with an observer of even lower order when using different approximation methods, like spectral approaches.

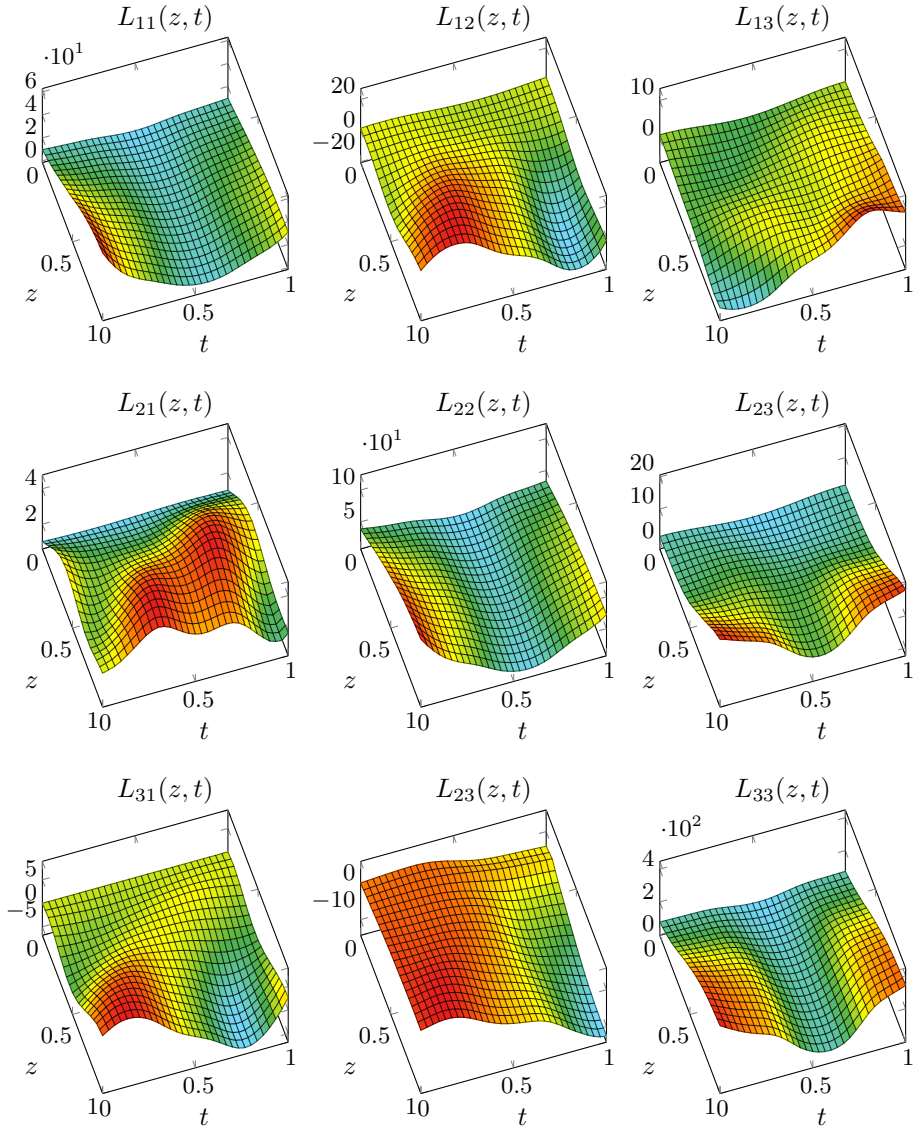

Figure 3.1: Distributed observer gain $L(z,t)$ for Example 3.7.1.

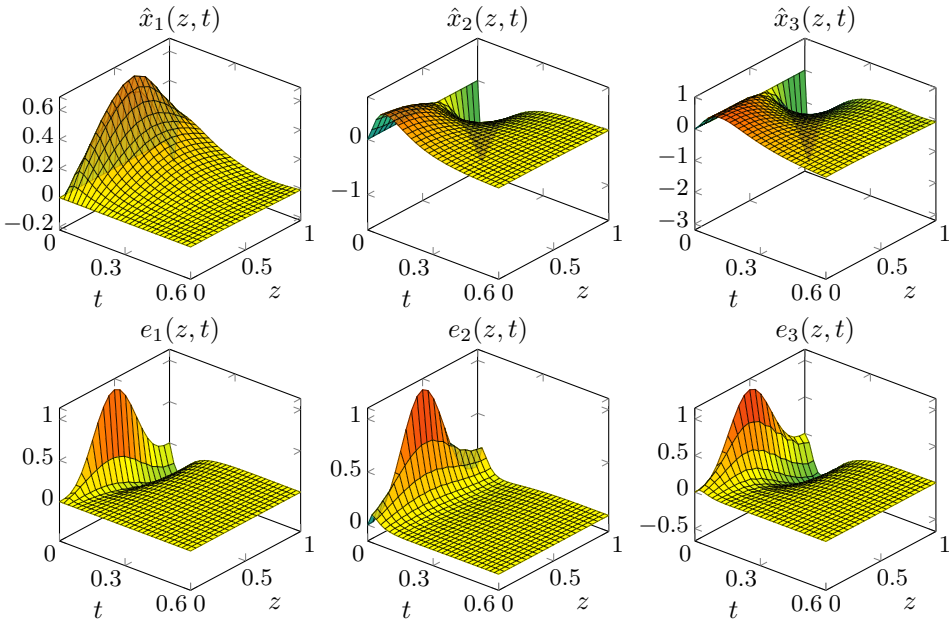

Figure 3.2: Reconstructed observer states $\hat{x}_i(z,t)$, $i = 1, \ldots, 3$ and corresponding observer errors $e_i(z,t)$ for the plant (2.21) with parameters (2.224) subject to the state feedback controller (2.27). The plant's ICs are $x_i(z,0) = \frac{3}{4}\sin(\pi z + 2\pi) + \frac{1}{4}\cos(3\pi z + \frac{\pi}{2})$. The observer uses the measurement (3.58) and has the ICs $\hat{x}_i(z,t) = 0$.

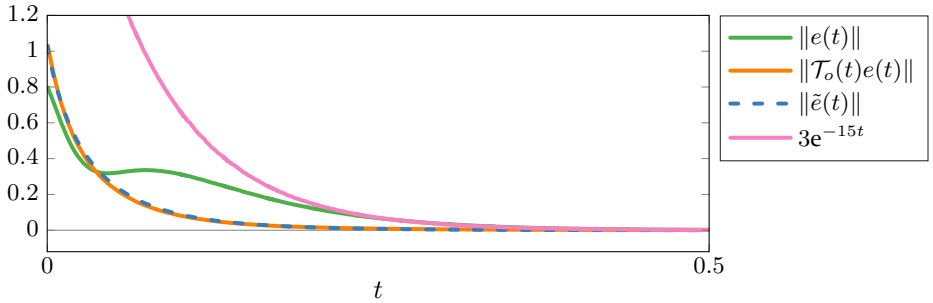

Figure 3.3: Weighted L_2-norms $\|e(t)\|$ of the observer error, the transformed error $\|\mathcal{T}_o(t)e(t)\|$ and the target system states $\|\tilde{e}(t)\|$. The pink curve is the desired decay rate $M\mathrm{e}^{(\mu_{\max}-\mu_o)t}$, which is achieved.

3.8.1 Problem formulation

To be able to realize the state feedback controller presented in Chapter 2 with the states reconstructed by the observer in Chapter 3, the boundary coupling matrices both must be diagonal. Thus, the output feedback controller applies for the system class

$$\begin{aligned} x_t(z,t) &= \Lambda(z)x_{zz}(z,t) + A(z,t)x(z,t) \\ &\quad + A_0(z,t)x(0,t) + \int_0^z F(z,\zeta,t)x(\zeta,t)\mathrm{d}\zeta \end{aligned} \tag{3.59a}$$

$$(\theta_0(t)x(t))(0) = 0 \tag{3.59b}$$

$$(\vartheta_1(t)x(t))(1) = u(t) \tag{3.59c}$$

$$y_m(t) = (\mathcal{C}_m x(t))(0) \tag{3.59d}$$

$$x(z,t_0) = x_0(z) \tag{3.59e}$$

with (3.59a) defined on $(z,t) \in (0,1) \times \mathbb{R}_{t_0}^+$, and

$$\theta_0(t)h = (E_1E_1^\top - E_2Q_0(t)E_2^\top)h + E_2E_2^\top h' \tag{3.60a}$$

$$\vartheta_1(t)h = \underbrace{(S_dS_d^\top - S_r\bar{Q}_1(t)S_r^\top)}_{\bar{B}_1^d}h + \underbrace{S_rS_r^\top}_{B_1^n}h', \tag{3.60b}$$

where $Q_0(t)$ and $\bar{Q}_1(t)$ are diagonal matrices (see (2.6b) and (3.4b)).

In this section the state feedback controller (2.27) is used with the states reconstructed by the observer (3.6). Thereby, the *output feedback controller*

$$\begin{aligned} u(t) = \mathcal{K}(t)\hat{x}(t) &= \big(\underbrace{\bar{B}_1^d(t) - \widetilde{B}_1^d}_{-S_r\bar{Q}_1(t)S_r^\top} + B_1^nK(1,1,t)\big)\hat{x}(1,t) \\ &\quad + \int_0^1 \big(B_1^nK_z(1,\zeta,t) + \widetilde{B}_1^dK(1,\zeta,t)\big)\hat{x}(\zeta,t)\mathrm{d}\zeta \end{aligned} \tag{3.61a}$$

$$\begin{aligned} \hat{x}_t(z,t) &= \Lambda(z)\hat{x}_{zz}(z,t) + A(z,t)\hat{x}(z,t) + A_0(z,t)\hat{x}(0,t) \\ &\quad + \int_0^z F(z,\zeta,t)\hat{x}(\zeta,t)\mathrm{d}\zeta + L(z,t)\Big(y_m(t) - (\mathcal{C}_m\hat{x}(t))(0)\Big) \end{aligned} \tag{3.61b}$$

$$(\theta_0(t)\hat{x}(t))(0) = L_0(t)\Big(y_m(t) - (\mathcal{C}_m\hat{x}(t))(0)\Big) \tag{3.61c}$$

$$(\vartheta_1(t)\hat{x}(t))(1) = u(t) \tag{3.61d}$$

$$\hat{x}(z,t_0) = \hat{x}_0(z) \tag{3.61e}$$

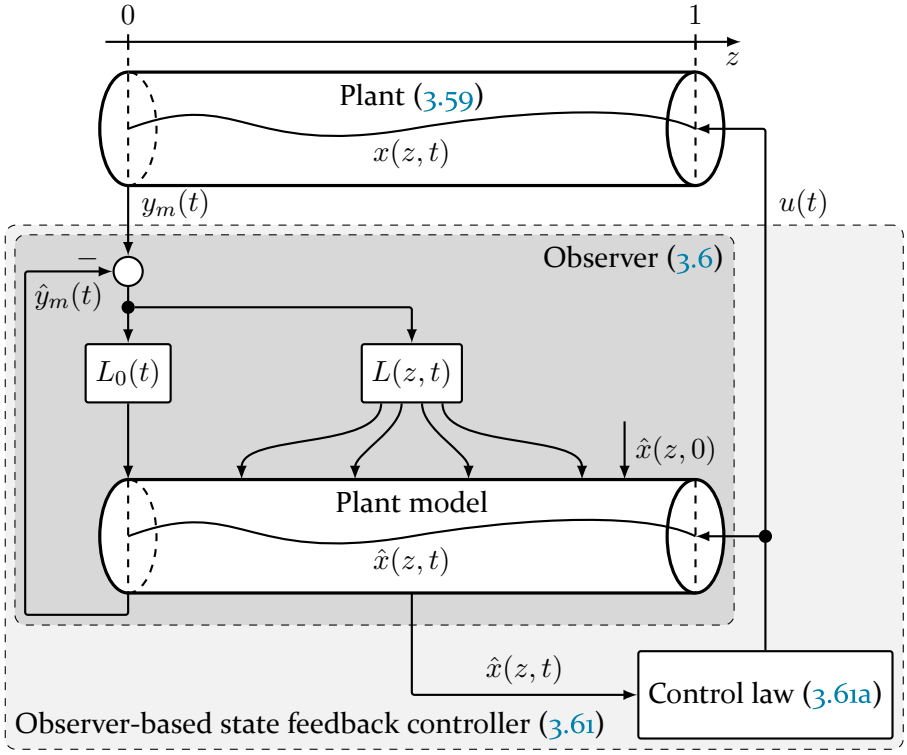

Figure 3.4: Systematic structure of the observer-based state feedback controller. Plant and observer are visualized as rods.

with $L(z,t)$, $L_0(t)$ according to (3.15) and $K(z,\zeta,t)$ being the solution of (2.28) as well as $P(z,\zeta,t)$ the solution of (3.14) is applied to the system. The principle of the resulting control loop is depicted in Figure 3.4, where both plant and observer are symbolized by a rod.

It has been shown in Section 2.4 that the state feedback controller stabilizes the system if the plant states are used for the feedback. The next section shows that this stability property is preserved when using the reconstructed states from the observer.

3.8.2 Stability of the output feedback control

If the dynamics of the closed-loop system consists of the dynamics of both subsystems, i. e. controlled plant dynamics and observer error dynamics, this is called *separation property* or *separation principle*. In particular, for finite dimensional systems, this principle is fulfilled if the spectrum of the

closed-loop system exactly consists of the eigenvalues of the controlled system without observer, complemented by the eigenvalues of the observer error dynamics.[8] Since the precise location of the eigenvalues is hard to determine for the considered system class, the separation principle is regarded as fulfilled if the stability margin of the closed-loop system is set by the smallest stability margin of both controlled system and observer error dynamics. This is a very strong property for the considered class of coupled parabolic systems with time-varying coefficients and the following theorem shows that it is achieved by the output feedback controller (3.61).

Theorem 3.8.1 (Stability of output feedback control)
The output feedback controller (3.61) with $L(z,t)$, $L_0(t)$ according to (3.15) and $K(z,\zeta,t)$ being the solution of (2.28) as well as $P(z,\zeta,t)$ being the solution of (3.14) uniformly exponentially stabilizes the system (3.59), i. e.,

$$\|x(t)\| \leq M\mathrm{e}^{(\mu_{\max}-\min(\mu_o,\mu_c)+c)(t-t_0)}\|x(t_0)\|, \quad t \geq t_0 \tag{3.62}$$

for all $x(t_0) \in (L_2(0,1))^n$ satisfying the BCs (3.59b), (3.59c), an $M \geq 1$, any $t_0 \geq 0$ and any $c > 0$, i. e. the stability margin is $\min(\mu_o, \mu_c) - \mu_{\max}$.

This theorem is proved in the sequel. To this end, the backstepping transformation (2.22) is applied to the controlled system with the control law (3.61a) and the observer error definition (3.7) with (3.9) is inserted, yielding the closed-loop system

$$\tilde{e}_t(z,t) = \Lambda(z)\tilde{e}_{zz}(z,t) - \widetilde{A}_o(z,t)\tilde{e}(z,t) \tag{3.63a}$$
$$(\tilde{\theta}_0\tilde{e}(t))(0) = 0 \tag{3.63b}$$
$$(\tilde{\theta}_1\tilde{e}(t))(1) = -\int_0^1 \widetilde{A}_1(\zeta,t)\tilde{e}(\zeta,t)\mathrm{d}\zeta \tag{3.63c}$$
$$\begin{aligned}\tilde{x}_t(z,t) = {}& \Lambda(z)\tilde{x}_{zz}(z,t) - \widetilde{A}(z,t)\tilde{x}(z,t) \\ & - \widetilde{A}_0(z,t)\big(E_1E_1^\top\tilde{x}_z(0,t) + E_2E_2^\top\tilde{x}(0,t)\big)\end{aligned} \tag{3.63d}$$
$$(\tilde{\theta}_0\tilde{x}(t))(0) = 0 \tag{3.63e}$$
$$(\tilde{\theta}_1\tilde{x}(t))(1) = \underbrace{-\mathcal{K}(t)\mathcal{T}_o^{-1}(t)\tilde{e}(t)}_{f_e(t)} \tag{3.63f}$$

[8] To be precise, this is called separation property [57] and is a special case of the separation principle, which is formulated for stochastic systems and covers more general statements [40].

in backstepping coordinates. For an exponentially stable closed-loop system, it is obvious that (3.63) needs this property.

Apparently, this system is a cascade of two exponentially stable systems (see Lemma 2.4.2 and Proposition 3.6.1) where the observer error dynamics $\tilde{e}$ excites the $\tilde{x}$-subsystem at its boundary. Therein, the operator $\mathcal{K}(t)$ contains a time-invariant boundary evaluation of its argument, multiplied by time dependent coefficients as can be seen in (3.61a). It is to be expected that this is a relatively bounded operator w. r. t. the system operator of the $\tilde{e}$-subsystem. But it is not known whether this operator is the generator of an analytic C_0-semigroup, nor is known whether the application of $\mathcal{T}_o^{-1}(t)$ leads to C_0-semigroups. The third problem is that the $\tilde{x}$-subsystem is excited at its boundary, leading to a generally unbounded actuation.

Due to these obstacles, the proof consists of the following steps.

1. Proving that the signal $\mathcal{K}(t)\mathcal{T}_o^{-1}(t)\tilde{e}(t)$ is bounded with exponentially decaying norm. In detail,
   a) showing that $\tilde{e}(t)$ and $\mathcal{T}_o^{-1}(t)\tilde{e}(t)$ can be expressed by the help of analytic C_0-semigroups and
   b) showing that the operator $\mathcal{K}(t)$ is relatively bounded w. r. t. the corresponding generators so that the result of its application has the same exponential decay.
2. Proving that the excitation of the $\tilde{x}$-subsystem at its boundary with the exponentially decaying signal leads to an exponentially decaying solution.

In Section 3.6 the autonomous system (3.63a)–(3.63c) has already been studied. It has been shown in Proposition 3.6.1 that it is exponentially stable but nothing more is known about the solution $\tilde{e}(t)$. Specifically, it was shown that the solutions of the state vector elements $\tilde{e}_i(t)$ are exponentially decaying, implying exponential stability of the state vector. To be able to prove Item 1, more knowledge about the solution is required.

During the proof of Proposition 3.6.1, the states $\tilde{e}(z,t)$ of the observer error target system (3.63a)–(3.63c) were permuted such that the diffusion coefficients were ordered ascending, which is always possible. To avoid further technical difficulties, and remove the necessity of this step, this ordering $\lambda_1 \leq \lambda_2 \leq \ldots \leq \lambda_n$ will be assumed in the following without loss of generality,

implying the matrices $\widetilde{A}_o(z,t)$ in (3.63a) and $\widetilde{A}_1(z,t)$ in (3.63c) to be strictly lower triangular. With this, the component form of (3.63a)–(3.63c) reads

$$\tilde{e}_{i,t}(z,t) = \lambda_i(z)\tilde{e}_{i,zz}(z,t) - \mu_o\tilde{e}_i(z,t) - \sum_{k=1}^{i-1} \breve{A}_{o,ik}(z,t)\tilde{e}_k(z,t) \tag{3.64a}$$

$$b_i^d\tilde{e}_i(0,t) + b_i^n\tilde{e}_{i,z}(0,t) = 0 \tag{3.64b}$$

$$s_i^d\tilde{e}_i(1,t) + s_i^n\tilde{e}_{i,z}(1,t) = \underbrace{-\int_0^1 \sum_{k=1}^{i-1} \widetilde{A}_{1,ik}(\zeta,t)\tilde{e}_k(\zeta,t)\mathrm{d}\zeta}_{w_i(t)}, \tag{3.64c}$$

for $i = 1,\dots,n$, where one of b_i^d, b_i^n is always 1 while the other is 0 and the same for s_i^d, s_i^n (cf. (3.64)). It is known from Section 3.6 that the homogeneous part of (3.64), i. e. without the couplings occurring due to the sums can be written in form of the abstract IVP

$$\dot{\tilde{e}}_i(t) = \underbrace{(\mathcal{A}_i - \mu_o I)}_{\widetilde{\mathcal{A}}_i}\tilde{e}_i(t), \quad t \in \mathbb{R}_{t_0}^+ \tag{3.65a}$$

$$\tilde{e}_i(t_0) = \tilde{e}_{0i} \in D(\mathcal{A}_i), \tag{3.65b}$$

where $\mathcal{A}_i$ is defined in (3.35). It has been shown that the operator $\widetilde{\mathcal{A}}_i$ is the generator of an exponentially stable analytic C_0-semigroup $\mathcal{T}_i(t)$ with

$$\|\mathcal{T}_i(t)h\| \le M_i \mathrm{e}^{(\mu_{\max}-\mu_o)t}\|h\|, \tag{3.66}$$

$h \in D(\mathcal{A}_i)$, for some finite M_i. Against this background it is possible to derive further properties of the solution of (3.64), which are stated in the following lemma.

Lemma 3.8.2. *The components $\tilde{e}_i(t) \in L_2(0,1)$, $i = 1,\dots,n$ of the solution $\tilde{e}(t)$ of (3.63a)–(3.63c) fulfil*

$$\tilde{e}_i(t) = \mathcal{T}_i(t-t_0)\tilde{e}_i(t_0) + \int_{t_0}^t \mathcal{T}_i(t-\tau)R_i(\tau,t_0)\mathrm{d}\tau + \mathcal{I}_i(t,t_0) \tag{3.67a}$$

with $R_i(t,t_0) \in L_2(0,1)$ and

$$\mathcal{I}_i(t,t_0) = \mathcal{T}_i(t-t_0)\mathcal{I}_i^a(t_0) + \mathcal{I}_i^b(t,t_0), \tag{3.67b}$$

where $\mathcal{I}_i^a(t_0), \mathcal{I}_i^b(t,t_0) \in C^\infty[0,1]$ are bounded and

$$\|R_i(t,t_0)\| \le M_i \mathrm{e}^{(\mu_{\max}-\mu_o+c)(t-t_0)} \tag{3.67c}$$

$$\|\mathcal{I}_i^b(t,t_0)\| \le M_i \mathrm{e}^{(\mu_{\max}-\mu_o+c)(t-t_0)} \tag{3.67d}$$

for some finite M_i and $t \ge t_0$.

Proof. First note that (3.67a) with (3.66), (3.67c) and (3.67d) yields the estimate

$$\|\tilde{e}_i(t)\| \leq M_i \mathrm{e}^{(\mu_{\max}-\mu_o)(t-t_0)}\|\tilde{e}_i(t_0)\| + \bar{c}\mathrm{e}^{(\mu_{\max}-\mu_o+c)(t-t_0)} \tag{3.68}$$

for some finite constant $\bar{c}$, or

$$\|\tilde{e}_i(t)\| \leq \underbrace{(M_i\|\tilde{e}_i(t_0)\| + \bar{c})}_{\bar{M}_i} \mathrm{e}^{(\mu_{\max}-\mu_o+c)(t-t_0)} \tag{3.69}$$

for some finite $\bar{M}_i$. Summing up all elements $k = 1, \ldots, i-1$ yields

$$\sum_{k=1}^{i-1} \|\tilde{e}_k(t)\| \leq \underbrace{\sum_{k=1}^{i-1} \bar{M}_k}_{\leq \widetilde{M}_i} \mathrm{e}^{(\mu_{\max}-\mu_o+c)(t-t_0)}, \tag{3.70}$$

which will be used later.

For $i = 1$, (3.37) shows the validity of (3.67) with $R_1(t,t_0) = 0$ and $\mathcal{I}_1(t,t_0) = 0$, obviously implying (3.67c), (3.67d). This is the base case for the following induction proof.

Now assume (3.67) to be valid for the indices $k = 1, \ldots, i-1$ which yields validity of (3.70). By analysing the solution $\tilde{e}_i(t)$ of (3.64) it will be shown that (3.67) then holds for i, too. By mathematical induction, it consequently holds for all $i = 1, \ldots, n$.

To determine the solution of (3.64), the system is converted into a representation with homogeneous BCs like in the proof of Proposition 3.6.1. The difference is that it is now done for a general index i. Introduce the *homogeneous state*

$$\varepsilon_i(z,t) = \tilde{e}_i(z,t) - h_i(z)w_i(t), \tag{3.71}$$

where an appropriate function $h_i \in C^\infty[0,1]$ can always be found in the form $a_i + b_i z + c_i z^2$ such that ε_i fulfils the homogeneous BCs

$$b_i^d \varepsilon_i(0,t) + b_i^n \varepsilon_{i,z}(0,t) = 0 \tag{3.72a}$$
$$s_i^d \varepsilon_i(1,t) + s_i^n \varepsilon_{i,z}(1,t) = 0. \tag{3.72b}$$

Following the same steps as in the proof of Proposition 3.6.1, the dynamics of the homogeneous state reads

$$\begin{aligned}\varepsilon_{i,t} &= \lambda_i \varepsilon_{i,zz} - \mu_o \varepsilon_i \\ &\quad \left.\begin{aligned} &- \int_0^1 \sum_{k=1}^{i-1} \Big(\lambda_i h_{i,zz} \widetilde{A}_{1,ik}(\zeta,t) - h_i \widetilde{A}_{1,ik,t}(\zeta,t) \\ &\qquad\qquad - h_i \big(\widetilde{A}_{1,ik}(\zeta,t)\lambda(\zeta) \big)_{\zeta\zeta} \Big) \tilde{e}_k(\zeta,t) \mathrm{d}\zeta \\ &- h_i \int_0^1 \sum_{k=1}^{i-1} \widetilde{A}_{1,ik} \sum_{j=1}^{k-1} \breve{A}_{o,kj}(\zeta,t) \tilde{e}_j(\zeta,t) \mathrm{d}\zeta \\ &- \sum_{k=1}^{i-1} \breve{A}_{o,ik} \tilde{e}_k - h_i \sum_{k=1}^{i-1} \mathcal{E}_{ik}^1 \tilde{e}_k) + h_i \sum_{k=1}^{i-1} \mathcal{E}_{ik}^0 \tilde{e}_k), \end{aligned} \right\} R_i(t,t_0) \end{aligned} \tag{3.73}$$

with the formal operators

$$\mathcal{E}_{ik}^1(t)h = (\widetilde{A}_{1,ik}(z,t)\lambda_k(z))_z(1,t)h(1) - \widetilde{A}_{1,ik}(1,t)\lambda_k(1)h'(1) \tag{3.74a}$$

$$\mathcal{E}_{ik}^0(t)h = (\widetilde{A}_{1,ik}(z,t)\lambda_k(z))_z(0,t)h(0) - \widetilde{A}_{1,ik}(0,t)\lambda_k(0)h'(0). \tag{3.74b}$$

Due to the triangular coupling structure, the expression $R_i(t,t_0)$ does not contain $\varepsilon_i(t)$. The homogeneous part, however, is exactly described by an abstract IVP of the form (3.65) so that the solution of (3.73) is given by

$$\varepsilon_i(t) = \mathcal{T}_i(t)\varepsilon_i(t_0) + \int_{t_0}^t \mathcal{T}_i(t-\tau) R_i(\tau,t_0) \mathrm{d}\tau. \tag{3.75}$$

Before proving (3.67a) with this result, the norm of $R_i(t,t_0)$ is calculated to prove (3.67c). Note that the spatial integrals appearing in $R_i(t,t_0)$ represent bounded operators on $\tilde{e}_k(t)$, so that their norm is $\leq \bar{c}\|\tilde{e}_k(t)\|$ for some constant $\bar{c}$. Consequently, the norm of $R_i(t,t_0)$ reads

$$\begin{aligned}\|R_i(t,t_0)\| &\leq \bar{c} \sum_{k=1}^{i-1} \|\tilde{e}_k(t)\| + \bar{c} \sum_{k=1}^{i-1} \sum_{j=1}^{k-1} \|\tilde{e}_j(t)\| \\ &\quad + \bar{c} \sum_{k=1}^{i-1} \|\mathcal{E}_{ik}^1(t)\tilde{e}_k(t))\| + \bar{c} \sum_{k=1}^{i-1} \|\mathcal{E}_{ik}^0(t)\tilde{e}_k(t))\|, \end{aligned} \tag{3.76}$$

where each $\bar{c}$ is a possibly different finite constant. However, as there exists a common finite bound for all those constants, they may be regarded as equal.

Now note that $k, j < i$ so that (3.67a) can be inserted for the solution $\tilde{e}_k(t)$. For the operators $\mathcal{E}_{ik}^{\nu}(t)$, $\nu = 0, 1$, this yields

$$\|\mathcal{E}_{ik}^{\nu}(t)\tilde{e}_k(t))\| \leq \|\mathcal{E}_{ik}^{\nu}(t)\mathcal{T}_k(t-t_0)\tilde{e}_k(t_0)\| + \int_{t_0}^{t} \|\mathcal{E}_{ik}^{\nu}(\tau)\mathcal{T}_k(t-\tau)R_k(\tau,t_0)\|\mathrm{d}\tau + \|\mathcal{E}_{ik}^{\nu}(t)\mathcal{I}_k(t,t_0)\|. \tag{3.77}$$

Since $\mathcal{E}_{ik}^{\nu}(t)$ defined in (3.74) contains time-dependent coefficients followed by a time-invariant boundary evaluation, it is relatively bounded w. r. t. $\widetilde{\mathcal{A}}_k$ according to Lemma A.1.1. Therefore, Lemma A.2.1 implies

$$\begin{aligned}\|\mathcal{E}_{ik}^{\nu}(t)\mathcal{T}_k(t-t_0)\tilde{e}_k(t_0)\| &\leq \bar{c}\|\mathcal{T}_k(t-t_0)\tilde{e}_k(t_0)\| \\ &\overset{(3.66)}{\leq} \bar{c}M_k\mathrm{e}^{(\mu_{\max}-\mu_o)(t-t_0)}\|\tilde{e}_k(t_0)\| \end{aligned} \tag{3.78a}$$

and

$$\begin{aligned}\|\mathcal{E}_{ik}^{\nu}(\tau)\mathcal{T}_k(t-\tau)R_k(\tau,t_0)\| &\leq \bar{c}\|\mathcal{T}_k(t-\tau)R_k(\tau,t_0)\| \\ &\leq \bar{c}M_k\mathrm{e}^{(\mu_{\max}-\mu_o)(t-\tau)}\|R_k(\tau,t_0)\| \\ &\overset{(3.67c)}{\leq} \bar{c}M_k\mathrm{e}^{(\mu_{\max}-\mu_o)(t-\tau)}\, M_k\mathrm{e}^{(\mu_{\max}-\mu_o+c)(\tau-t_0)} \\ &\leq \bar{c}M_k^2\mathrm{e}^{(\mu_{\max}-\mu_o+c)(t-t_0)} \end{aligned} \tag{3.78b}$$

for some finite constant $\bar{c}$. Moreover, applying $\mathcal{E}_{ik}^{\nu}(t)$ to $\mathcal{I}_k(t,t_0)$ yields

$$\|\mathcal{E}_{ik}^{\nu}(t)\mathcal{I}_k(t,t_0)\| \leq \|\mathcal{E}_{ik}^{\nu}\mathcal{T}_k(t-t_0)\mathcal{I}_k^a(t_0)\| + \|\mathcal{E}_{ik}^{\nu}(t)\mathcal{I}_k^b(t,t_0)\|. \tag{3.79}$$

Note that $\mathcal{I}_k^b(t,t_0) \in C^{\infty}[0,1]$[9] by assumption, where the application of $\mathcal{E}_{ik}^{\nu}(t)$ leads to a bounded result. This implies

$$\begin{aligned}\|\mathcal{E}_{ik}^{\nu}(t)\mathcal{I}_k(t,t_0)\| &\leq M_k\mathrm{e}^{(\mu_{\max}-\mu_o+c)(t-t_0)}\underbrace{\|\mathcal{I}_k^a(t_0)\|}_{\leq\bar{c}} + \bar{c}\|\mathcal{I}_k^b(t,t_0)\|. \\ &\overset{(3.67d)}{\leq} \widetilde{M}_k\mathrm{e}^{(\mu_{\max}-\mu_o+c)(t-t_0)} \end{aligned} \tag{3.80}$$

for some finite $\widetilde{M}_k$. Now the integration in (3.77) with (3.78b) and (2.57) is performed and the previous estimations are inserted. The result is substituted into (3.76) together with (3.70), leading to the bound (3.67c) for some finite M_i.

[9] $\mathcal{I}_k^b(t,t_0)$ solely contains $h_k \in C^{\infty}[0,1]$ as space dependent function, which will be seen later.

In order to prove (3.67a), the solution (3.75) is inserted into (3.71) with the definition of $w_i(t)$ in (3.64c) to obtain

$$\begin{aligned}\tilde{e}_i(t) = \mathcal{T}_i(t-t_0)\varepsilon_i(t_0) + \int_{t_0}^{t} \mathcal{T}_i(t-\tau)R_i(\tau,t_0)\mathrm{d}\tau \\ + \underbrace{h_i(z)\int_0^1 \sum_{k=1}^{i-1} \widetilde{A}_{1,ik}(\zeta,t)\tilde{e}_k(\zeta,t)\mathrm{d}\zeta}_{\mathcal{I}_i^b(t,t_0)},\end{aligned} \tag{3.81}$$

where (3.71) is inserted for $\varepsilon_i(t_0)$ to get

$$\begin{aligned}\tilde{e}_i(t) = \mathcal{T}_i(t-t_0)\tilde{e}_i(t_0) + \int_{t_0}^{t} \mathcal{T}_i(t-\tau)R_i(\tau,t_0)\mathrm{d}\tau \\ + \mathcal{T}_i(t-t_0)\underbrace{h_i(z)\int_0^1 \sum_{k=1}^{i-1} \widetilde{A}_{1,ik}(\zeta,t_0)\tilde{e}_k(\zeta,t_0)\mathrm{d}\zeta}_{\mathcal{I}_i^a(t_0)} + \mathcal{I}_i^b(t,t_0),\end{aligned} \tag{3.82}$$

proving the validity of (3.67a) for i. Obviously, $\mathcal{I}_i^a(t_0)$ is bounded in view of the boundedness of $\widetilde{A}_1$. Moreover, the only contained function depending on z in $\mathcal{I}_i^a$ and $\mathcal{I}_i^b$ is $h_i \in C^\infty[0,1]$ so that $\mathcal{I}_i^a(t_0), \mathcal{I}_i^b(t,t_0) \in C^\infty[0,1]$. To estimate the bound of $\mathcal{I}_i^b(t,t_0)$ note that the integration is a bounded operator, which allows to write

$$\|\mathcal{I}_i^b(t,t_0)\| \leq \|h_i(z)\|\bar{c}\sum_{k=1}^{i-1}\|\tilde{e}_k(t)\| \overset{(3.70)}{\leq} M_i \mathrm{e}^{(\mu_{\max}-\mu_o+c)(t-t_0)} \tag{3.83}$$

for some finite M_i, proving (3.67d) and thus the lemma. ■

It is already known from the proof of Proposition 3.6.1 that converting a boundary coupling into a distributed coupling involves the time derivative of the coupling term. Therefore, properties of the time derivative $\tilde{e}_{i,t}(z,t)$ of the solution will be needed, which are stated in the following lemma.

Lemma 3.8.3. *The time-derivative of* (3.67a) *has the form*

$$\begin{aligned}\tilde{e}_{i,t}(t) = \widetilde{\mathcal{A}}_i\mathcal{T}_i(t-t_0)\tilde{e}_i(t_0) + \int_{t_0}^{t}\widetilde{\mathcal{A}}_i\mathcal{T}_i(t-\tau)R_i(\tau,t_0)\mathrm{d}\tau + \widetilde{\mathcal{A}}_i\mathcal{T}_i(t-t_0)\mathcal{I}_i^a(t_0) \\ + \widetilde{\mathcal{I}}_i^b(t,t_0)\end{aligned} \tag{3.84a}$$

with

$$\|\widetilde{\mathcal{I}}_i^b(t,t_0)\| \leq M_i \mathrm{e}^{(\mu_{\max}-\mu_o+c)(t-t_0)} \tag{3.84b}$$

and

$$\|\tilde{e}_{i,t}(t)\| \leq M_i \mathrm{e}^{(\mu_{\max}-\mu_o+c)(t-t_0)} \tag{3.84c}$$

for some finite M_i and $t \geq t_0$.

Proof. Similar to Lemma 3.8.2, the proof is based on induction. Proving the validity of (3.84) for $i = 1$ is trivial by differentiating (3.67a). Then, it is assumed valid for $k = 1, \ldots, i-1$. Differentiating (3.67a) w. r. t. t yields

$$\begin{aligned}\tilde{e}_{i,t}(t) = \dot{\mathcal{T}}_i(t-t_0)\tilde{e}_i(t_0) + R_i(t,t_0) + \int_{t-0}^{t} \dot{\mathcal{T}}_i(t-\tau)R_i(\tau,t_0)\mathrm{d}\tau \\ + \dot{\mathcal{T}}_i(t-\tau)\mathcal{I}_i^a(t_0) + \mathcal{I}_{i,t}^b(t,t_0)\end{aligned} \tag{3.85a}$$

with

$$\begin{aligned}\mathcal{I}_{i,t}^b(t,t_0) = h_i(z)\int_0^1 \sum_{k=1}^{i-1} \widetilde{A}_{1,ik,t}(\zeta,t)\tilde{e}_k(\zeta,t)\mathrm{d}\zeta \\ + h_i(z)\int_0^1 \sum_{k=1}^{i-1} \widetilde{A}_{1,ik}(\zeta,t)\tilde{e}_{k,t}(\zeta,t)\mathrm{d}\zeta\end{aligned} \tag{3.85b}$$

for the index i. Because $\widetilde{\mathcal{A}}_i$ is the generator of $\mathcal{T}_i(t)$, it is $\dot{\mathcal{T}}_i(t)h = \widetilde{\mathcal{A}}_i\mathcal{T}_i(t)h$ for $h \in D(\mathcal{A})$ according to [26, Theorem 2.1.10]. Then, utilizing

$$\widetilde{\mathcal{I}}_i^b(t,t_0) = R_i(t,t_0) + \mathcal{I}_{i,t}^b(t,t_0), \tag{3.86}$$

(3.84a) is obtained for i and thus for all $i = 1, \ldots, n$ by induction. Recall that $\mathcal{T}_i(t)$ are analytic C_0-semigroups, implying that $\widetilde{\mathcal{A}}_i\mathcal{T}_i(t)$ is a bounded operator [26, Example 2.18]. This implies

$$\|\widetilde{\mathcal{A}}_i\mathcal{T}_i(t)h\| \leq \bar{M}_i \mathrm{e}^{(\mu_{\max}-\mu_o)t}\|h\| \tag{3.87}$$

for some finite $\bar{M}_i$, which is easy to see by the help of the semigroup property,

$$\begin{aligned}\|\widetilde{\mathcal{A}}_i\mathcal{T}_i(t)h\| &= \|\widetilde{\mathcal{A}}_i\mathcal{T}_i(\bar{t})\mathcal{T}_i(t-\bar{t})h\| \leq \bar{c}\|\mathcal{T}_i(t-\bar{t})h\| \\ &\leq \bar{c}M_i \mathrm{e}^{(\mu_{\max}-\mu_o)(t-\bar{t})}\|h\| \\ &\leq \underbrace{\bar{c}M_i \mathrm{e}^{-(\mu_{\max}-\mu_o)\bar{t}}}_{\bar{M}_i} \mathrm{e}^{(\mu_{\max}-\mu_o)t}\|h\|, \quad t_0 \leq \bar{t} \leq t.\end{aligned} \tag{3.88}$$

Considering the norm of (3.84a) with (3.87) and inserting (3.66), (3.67c) and (3.84b) proves (3.84c).

In the last step, since $k < i$, (3.84c) can be inserted into the norm of (3.85b) together with (3.69). This finally proves (3.84b) and the lemma. ■

Knowing that each state component has a solution of the form (3.67a) with (3.84a), the following corollary describes the properties of the application $\mathcal{K}(t)\mathcal{T}_o^{-1}(t)$ on the vector $\tilde{e}(z,t)$ and its time derivative.

Corollary 3.8.4. *The coupling term in* (3.63f) *has the properties*

$$\|\mathcal{T}_o^{-1}(t)\tilde{e}(t)\| \leq M\mathrm{e}^{(\mu_{\max}-\mu_o+c)(t-t_0)} \tag{3.89a}$$

$$\|\mathcal{K}(t)\mathcal{T}_o^{-1}(t)\tilde{e}(t)\| \leq M\mathrm{e}^{(\mu_{\max}-\mu_o+c)(t-t_0)} \tag{3.89b}$$

$$\|\left(\mathcal{K}(t)\mathcal{T}_o^{-1}(t)\tilde{e}(t)\right)_t\| \leq M\mathrm{e}^{(\mu_{\max}-\mu_o+c)(t-t_0)} \tag{3.89c}$$

for some finite M *and* $t \geq t_0$.

The proof can be found in Appendix B.4.

Now that the properties of the coupling term $f_e(t)$ in (3.63f) are known, its influence on the $\tilde{x}$-subsystem (3.63d)–(3.63f) can be analysed and is stated in the following lemma.

Lemma 3.8.5. *The system* (3.63d)–(3.63f) *is uniformly exponentially stable with stability margin* $\min(\mu_o, \mu_c) - \mu_{\max}$, *i. e.*

$$\|\tilde{x}(t)\| \leq \widetilde{M}\mathrm{e}^{(\mu_{\max}-\min(\mu_o,\mu_c)+c)(t-t_0)}\|\tilde{x}(t_0)\| \tag{3.90}$$

for some finite $\widetilde{M}$, *any* $t_0 \geq 0$ *and any* $c > 0$ *if*

$$\|f_e(t,t_0)\| \leq M\mathrm{e}^{(\mu_{\max}-\mu_o+c)(t-t_0)} \tag{3.91a}$$

$$\|f_{e,t}(t,t_0)\| \leq M\mathrm{e}^{(\mu_{\max}-\mu_o+c)(t-t_0)} \tag{3.91b}$$

for some finite M *and* $t \geq t_0$.

Proof. Like in the previous proofs, the $\tilde{x}$-subsystem is converted into a problem with homogeneous BCs. To this end

$$\bar{x}(z,t) = \tilde{x}(z,t) + H(z)f_e(t) \tag{3.92}$$

with the matrix-valued function $H(z) = \operatorname{diag}(h_1(z), \ldots, h_n(z)) \in \mathbb{R}^{n\times n}$ is introduced. Assuming $h_i(z) = a_i + b_i z + c_i z^2$ with constants a_i, b_i, c_i allows to find them in a way such that $\bar{x}(z,t)$ fulfils the homogeneous BCs

$$(\tilde{\theta}_0\bar{x}(t))(0) = 0 \tag{3.93a}$$

$$(\tilde{\theta}_1\bar{x}(t))(1) = 0. \tag{3.93b}$$

After inserting (3.63d) into the time-derivative of (3.92), it reads

$$\begin{aligned}\bar{x}_t &= \Lambda\tilde{x}_{zz} - \widetilde{A}\tilde{x} - \widetilde{A}_0\big(E_1E_1^\top\tilde{x}_z(0,t) + E_2E_2^\top\tilde{x}(0,t)\big) + Hf_{e,t}(t)\\ &= \Lambda\bar{x}_{zz} - \widetilde{A}\bar{x} - \widetilde{A}_0\big(E_1E_1^\top\bar{x}_z(0,t) + E_2E_2^\top\bar{x}(0,t)\big)\\ &\quad - \Lambda H_{zz}f_e(t) + \widetilde{A}Hf_e(t) + Hf_{e,t}(t)\\ &\quad + \widetilde{A}_0\big(E_1E_1^\top H_z(0) + E_2E_2^\top H(0)\big)f_e(t)\\ &= \Lambda\bar{x}_{zz} - \widetilde{A}\bar{x} - \widetilde{A}_0\big(E_1E_1^\top\bar{x}_z(0,t) + E_2E_2^\top\bar{x}(0,t)\big) + \tilde{f}_e(z,t), \qquad (3.94)\end{aligned}$$

with the formal excitation $\tilde{f}_e(z,t)$. Considering the norm of $\tilde{f}_e(z,t)$ with the assumptions (3.91), directly shows

$$\|\tilde{f}_e(z,t)\| \leq M\mathrm{e}^{(\mu_{\max}-\mu_o+c)(t-t_0)}. \qquad (3.95)$$

It is known from Lemma 2.4.2 that the homogeneous part in (3.94) with the BCs (3.44) is exponentially stable. Now it is excited by the signal $\tilde{f}_e(z,t)$. Consequently the solution of a state component $\bar{x}_i(t)$ reads

$$\bar{x}_i(t) = \bar{x}_{i,h}(t) + \int_{t_0}^{t}\mathcal{T}_i(t-\tau)e_i^\top\tilde{f}_e(\tau)\mathrm{d}\tau, \qquad (3.96)$$

where $\bar{x}_{i,h}(t)$ is the i^{th} component of the solution of the homogeneous part of (3.94), of which it is known that

$$\|\bar{x}_{i,h}(t)\| \leq M_i\mathrm{e}^{(\mu_{\max}-\mu_c+c)(t-t_0)}\|\bar{x}_i(t_0)\| \qquad (3.97)$$

for some finite M_i. After inserting this with (3.95) into the norm of (3.96), the solution is bounded by

$$\begin{aligned}\|\bar{x}_i(t)\| &\leq \|\bar{x}_{i,h}(t)\| + \int_{t_0}^{t}\|\mathcal{T}_i(t-\tau)e_i^\top f_e(\tau)\|\mathrm{d}\tau\\ &\leq M_i\mathrm{e}^{(\mu_{\max}-\mu_c+c)(t-t_0)}\|\bar{x}_i(t_0)\|\\ &\quad + \int_{t_0}^{t}M_i\mathrm{e}^{(\mu_{\max}-\mu_c)(t-\tau)}\bar{M}\mathrm{e}^{(\mu_{\max}-\mu_o+c)(\tau-t_0)}\mathrm{d}\tau\\ &\leq M_i\mathrm{e}^{(\mu_{\max}-\mu_c+c)(t-t_0)}\|\bar{x}_i(t_0)\|\\ &\quad + M_i\bar{M}\mathrm{e}^{(\mu_{\max}+c)(t-t_0)}\mathrm{e}^{-\mu_c t}\mathrm{e}^{\mu_o t_0}\int_{t_0}^{t}\mathrm{e}^{(-\mu_o+\mu_c)(\tau)}\mathrm{d}\tau. \qquad (3.98)\end{aligned}$$

For the integral, the cases $\mu_c = \mu_o$ and $\mu_c \neq \mu_o$ need to be considered separately. In the first case,

$$\begin{aligned}\|\bar{x}_i(t)\| &\leq M_i\mathrm{e}^{(\mu_{\max}-\mu_c+c)(t-t_0)}\|\bar{x}_i(t_0)\| + M_i\bar{M}\mathrm{e}^{(\mu_{\max}-\mu_c+c)(t-t_0)}\\ &\leq \widetilde{M}_i\mathrm{e}^{(\mu_{\max}-\mu_c+c)(t-t_0)}\|\bar{x}(t_0)\| \qquad (3.99)\end{aligned}$$

follows for some finite $\widetilde{M}_i$.

In the second case $\mu_c \neq \mu_o$,

$$\begin{aligned}\|\bar{x}_i(t)\| &\leq M_i \mathrm{e}^{(\mu_{\max}-\mu_c+c)(t-t_0)}\|\bar{x}_i(t_0)\| \\ &\quad + \frac{M_i\bar{M}}{-\mu_o+\mu_c}\mathrm{e}^{(\mu_{\max}+c)(t-t_0)}\mathrm{e}^{-\mu_c t}\mathrm{e}^{\mu_o t_0}\left(\mathrm{e}^{(-\mu_o+\mu_c)t}-\mathrm{e}^{(-\mu_o+\mu_c)t_0}\right) \\ &= M_i \mathrm{e}^{(\mu_{\max}-\mu_c+c)(t-t_0)}\|\bar{x}_i(t_0)\| \\ &\quad + \frac{M_i\bar{M}}{-\mu_o+\mu_c}\left(\mathrm{e}^{(\mu_{\max}-\mu_o+c)(t-t_0)}-\mathrm{e}^{(\mu_{\max}-\mu_c+c)(t-t_0)}\right) \\ &\leq \widetilde{M}_i \mathrm{e}^{(\mu_{\max}-\min(\mu_c,\mu_o)+c)(t-t_0)}\|\bar{x}(t_0)\| \end{aligned} \tag{3.100}$$

for some finite $\widetilde{M}_i$. Considering all states $\bar{x}_i(t)$ shows that in total (3.90) holds, proving the lemma. ■

Now the following proof is simple.

Proof of Theorem 3.8.1. With Corollary 3.8.4, the conditions of Lemma 3.8.5 are fulfilled, showing that the $\tilde{x}$-subsystem (3.63d)–(3.63f) is exponentially stable. Since the same holds for the $\tilde{e}$-subsystem (3.63a)–(3.63c) according to Proposition 3.6.1, the closed-loop system (3.63) in backstepping coordinates is exponentially stable, too. Due to the bounded invertibility of the applied transformations (2.22) and (3.9) (see Lemma 2.4.4 and Proposition 3.5.1), the stability of the closed-loop system in original coordinates readily follows with the same argumentation as in the proof of Theorem 2.4.1. Like in the proofs of Lemma 2.4.2 and Proposition 3.6.1, the analyticity of the involved C_0-semigroups allows the consideration of L_2-ICs. ■

3.8.3 Academic example

To validate the results of this chapter, simulations are performed combining the state feedback controller in Example 2.7.1 with the observer in Example 3.7.1.

Example 3.8.6 *(Output feedback controller).*
Consider the plant (2.21) with the parameters (2.224) and the measurement (3.58), which is a system of the form (3.59). Now, the output feedback controller (3.61) is applied to the system. Controller and observer are parameterized like in Example 2.7.1 and Example 3.7.1 with the decay parameters $\mu_c = 8$ and $\mu_o = 15$ (see Theorem 2.4.1 and Theorem 3.6.4) leading to a total decay rate of $\|x(t)\| \leq M\mathrm{e}^{(-8+c)t}\|x(0)\|$, $\forall c > 0$, according to Theorem 3.8.1. The

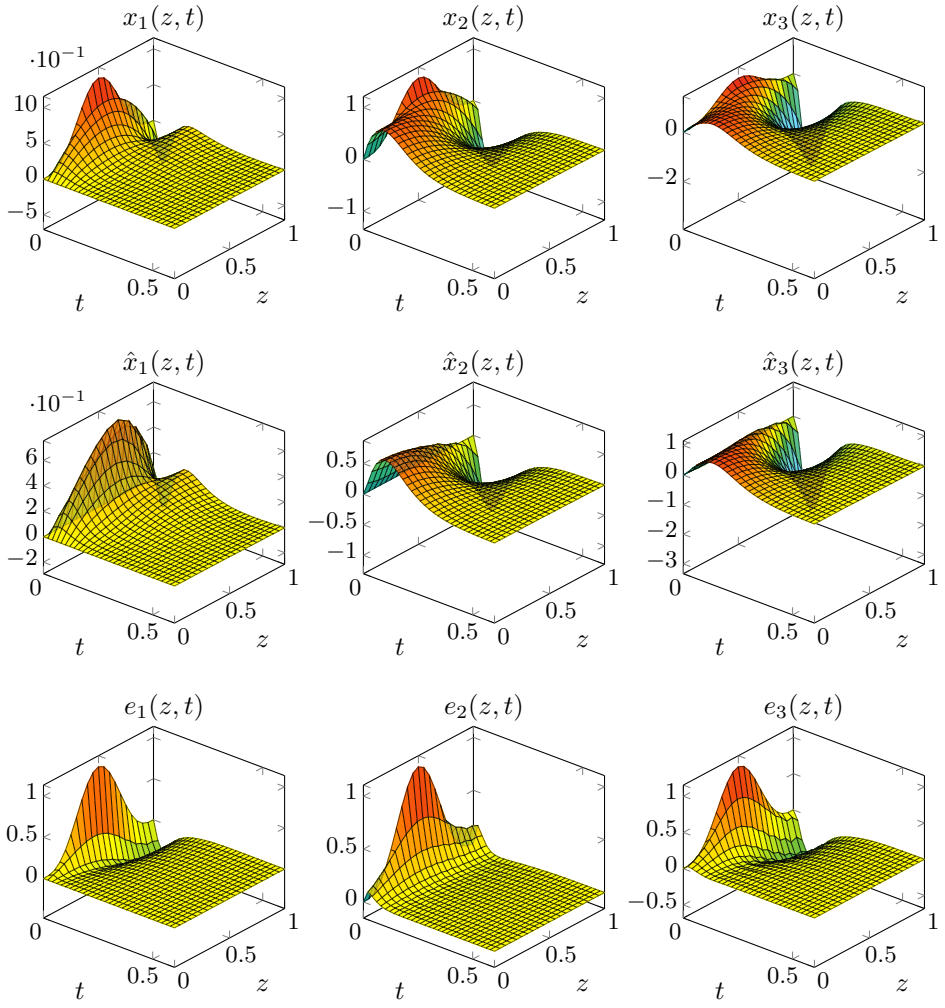

Figure 3.5: Closed-loop state profiles $x_i(z,t)$, $i = 1, \ldots, 3$ for the plant (2.21) with parameters (2.224) and ICs $x_i(z,0) = \frac{3}{4}\sin(\pi z + 2\pi) + \frac{1}{4}\cos(3\pi z + \frac{\pi}{2})$ subject to the output feedback controller (3.61), the corresponding observer states $\hat{x}_i(z,t)$ and the observer errors $e_i(z,t)$.

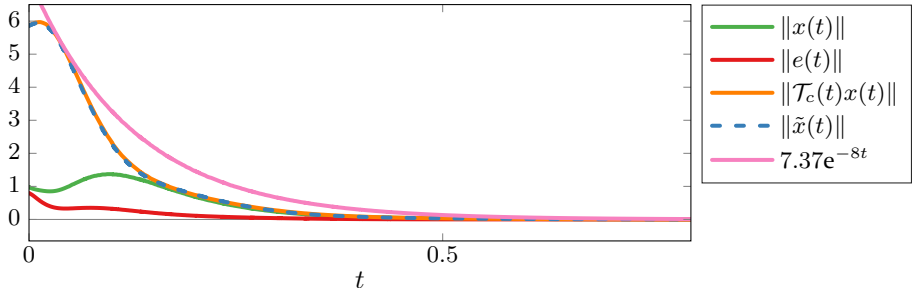

Figure 3.6: Weighted L_2-norms $\|x(t)\|$ and $\|e(t)\|$ of the states and the observer error as well as the transformed states $\|\mathcal{T}_c(t)x(t)\|$ and the target system states $\|\tilde{x}(t)\|$. The pink curve is the desired decay rate $M\mathrm{e}^{(\mu_{\max}-\min(\mu_o,\mu_c))t}$, which is achieved.

observer is implemented by a finite-elements approximation with 11 nodes per state like in Example 3.7.1.

Figure 3.5 shows the resulting state profiles $x(z,t)$, the reconstructed states $\hat{x}(z,t)$ as well as the corresponding observer errors $e(z,t)$. Obviously, the output feedback controller is able to stabilize the system with the desired decay rate and the observer states $\hat{x}(z,t)$ converge to the actual system states $x(z,t)$.

This is confirmed by the resulting weighted L_2-norms of the state $\|x(t)\|$, the transformed state $\|\mathcal{T}_c(t)x(t)\|$ and the target system state $\|\tilde{x}(t)\|$ together with the desired decay rate $M\mathrm{e}^{-8t}$ in Figure 3.6. Moreover, the comparison of the transformed states and the target system states shows that the closed-loop system indeed attains the dynamics (3.63). Note that the observer error's target system dynamics now couples into the state's target system dynamics according to (3.63), leading to different results as in Figure 2.17. The observer converges faster than the plant due to the faster parameterization with $\mu_o > \mu_c$. ◁

3.9 Concluding remarks

With the backstepping method, a systematic observer design for coupled parabolic PIDEs with space and time dependent coefficients and boundary measurements is possible. The observer is constructed as a model of the plant with time dependent correction terms in the PIDE and the left BC. The target system of the observer backstepping transformation is equipped with an integral coupling term in the right boundary condition, leading to a cascaded system of time-invariant subsystems with time dependent couplings, whose decay rate is set by the user. To determine the observer

gains, the observer kernel equations need to be solved. Utilizing a duality transformation, they are mapped into the form of those appearing in the state feedback controller design so that existing methods for their solution can be applied. The functionality of the observer was confirmed in a simulation, which shows the uniform exponential convergence with the desired decay rate even with an approximated observer of comparably low order.

The backstepping state feedback controller for boundary actuation presented in Chapter 2 can be realized for coupled parabolic PIDEs with space and time dependent coefficients and a boundary measurement with the help of a backstepping observer presented in Chapter 3. The separation property holds despite the time dependency of the system parameters and can be shown due to the time-invariance of the appearing target systems' subsystems. The resulting output feedback controller (3.61) is able to uniformly exponentially stabilize the system with a prescribed rate of convergence even with a comparably low order of the observer approximation, which was confirmed by a simulation.

Therefore, the presented output feedback controller is a powerful tool for the stabilization of a wide class of coupled parabolic systems and comes with a systematic design method.

The usage of the state feedback controller of Chapter 2 is not restricted to boundary observers, but is expected to be applicable in combination with arbitrary observers which exponentially reconstruct the system states. Depending on the observer error dynamics, a new analysis of the closed-loop stability might though be required. Analogously, the boundary observer of Section 3.8 may not only be implemented for the realization of a state feedback controller, but can be utilized to reconstruct states of an arbitrarily controlled or uncontrolled coupled parabolic system.

4 Bilateral backstepping control for coupled parabolic PDEs

The previous chapters dealt with systems classified by their *unilateral* characteristics, which means that the actuation and the measurements are located at one single boundary of the system. In practice, however, there may be the possibility to place actuators or sensors at both ends of the domain, which is known as *bilateral* case. For the controller design, using this additional degree of freedom, it is to be expected that the control effort for achieving comparable results as in the unilateral case, can be significantly reduced. Analogously, observers incorporating measurements at both ends of the domain can get along with smaller observer gains, increasing their robustness and reducing noise amplification.

For this reason, it is of paramount interest to extend the backstepping method to bilateral systems. The starting points to these considerations were provided by [97], which presented the backstepping method for parabolic PDEs on arbitrary dimensional balls with actuation on the whole boundary. Since in one dimension, the ball actually is an interval, this included bilateral control of 1D parabolic systems. Therefore, [96] focused on this, included further system classes and described two basic concepts to deal with bilateral control. The first concept is to adjust the applied integral transformation leading to a symmetric backstepping transformation, which was applied in [97]. This approach is also utilized in [11] for the bilateral stabilization and observer design of a viscous Hamilton-Jacobi PDE. By the help of a Hopf-Cole-transformation, this semilinear parabolic system is mapped into a linear representation so that the results of [97] can be applied. The other concept proposed in [96] is to reformulate the problem by suitable transformations to achieve unilateral actuation. To this end, the spatial domain is folded at a folding point inside the domain, with the aim to get a system representation which is similar to the classic unilateral problem so that existing results can be utilized. This is applied in [41] for the observer design of a parabolic PDE with constant coefficients, where measurements are available at both boundaries

and in-domain, which allows to design two independent observers for the different parts of the domain. For hyperbolic 2×2 systems with spatially varying coefficients, [107] considers the minimum time observer design.

In addition to the capability of dealing with bilateral actuation and sensing, the folding approach introduces the possibility to handle in-domain actuation and measurements, since the chosen folding point is mapped to a boundary in the folded domain. For this reason, this chapter covers two topics, the design of a bilateral backstepping state feedback controller and the design of a backstepping observer using in-domain measurements, both for coupled parabolic systems with space and time dependent parameters.

For in-domain actuation, [103, 104, 108] introduced the backstepping method for scalar parabolic systems with constant coefficients using a method quite similar to the folding technique.

Utilizing the folding approach to handle bilateral actuation leads to new challenges in the controller design. In particular, folding a scalar parabolic system leads to a system with two states coupled via special folding boundary conditions (BCs), which need to be introduced to ensure the regularity of the solution. In [96], the folding point is chosen to be the centre of the spatial domain. With constant parameters, this leads to equal diffusion coefficients in the folded system. This was extended by [19, 20] to the case where the folding point can be chosen arbitrarily as a design parameter to freely distribute the control effort between the available boundary inputs. However, this leads to different diffusion coefficients in the folded system, requiring the addition of coupling terms, the so-called well-posedness terms, in the target system to ensure the well-posedness of the kernel equations. This challenge is tackled by introducing a second, Fredholm-type integral transformation to eliminate the couplings and to obtain a target system whose stability is easy to show.

The folding BCs also appear in [88], where the backstepping method is applied to a scalar parabolic system with a discontinuous, piecewise constant diffusion coefficient. By separating the system into two parts, a coupled system of two PDEs with boundary coupling and constant diffusion is obtained with the same coupling BC as in the folding case. That problem is solved by using an approach with piecewise defined kernels. The stability of the target system, which is similar to the one in the folding case, is stated but the proof is omitted for lack of space.

The results of this chapter have been published in [117] for the special case of time-invariant PDEs and sorted, distinct diffusion coefficients as well as Robin-BCs. In the following, these results are generalized to the

time dependent case with general diffusion coefficients and general BCs. Since the procedure is nevertheless very similar to the contents of [117], some paragraphs are equal.

The next section introduces the considered system class. The folding transformation is presented in Section 4.2, followed by the utilized integral transformations. After determining the stabilizing control law, the closed-loop stability is analysed in Section 4.6. The subsequent sections present the conversion of the appearing kernel equations into integral equations, which are solved by the method of successive approximations. The derivatives of the kernels required for the control law are derived without numerical differentiation in Section 4.10. The observer design for in-domain measurements is briefly presented before the chapter is closed with some numerical examples, including both state feedback and output feedback control.

4.1 Problem formulation

Consider the following system of coupled parabolic PDEs with *bilateral* actuation

$$w_t(\check{z},t) = \check{\Lambda}(\check{z})w_{\check{z}\check{z}}(\check{z},t) + \check{A}(\check{z},t)w(\check{z},t) \tag{4.1a}$$

$$(\check{\theta}_0(t)w(t))(0) = u_0(t) \tag{4.1b}$$

$$(\check{\theta}_1(t)w(t))(1) = u_1(t), \tag{4.1c}$$

with the state $w(\check{z},t) \in \mathbb{R}^n$, $w(\check{z},t_0) = w_0(\check{z}) \in \mathbb{R}^n$, the diffusion matrix $\check{\Lambda}(\check{z}) = \operatorname{diag}(\check{\lambda}_1(\check{z}),\dots,\check{\lambda}_n(\check{z})) \in \mathbb{R}^{n\times n}$, $\check{\lambda}_i(\check{z}) > 0$, the reaction matrix $\check{A}(\check{z},t) \in \mathbb{R}^{n\times n}$ as well as the left and right inputs $u_0(t), u_1(t) \in \mathbb{R}^n$. The PDE (4.1a) is defined on $(\check{z},t) \in [0,1] \times \mathbb{R}^+_{t_0}$. The formal boundary operators $\check{\theta}_i(t)$, $i = 0,1$, can represent arbitrary combinations of Dirichlet and Robin or Neumann BCs, which, in analogy to the previous chapters, is written as

$$\check{\theta}_i(t)h = (S_d^i S_d^{i\top} - S_r^i Q_i(t) S_r^{i\top})h + S_r^i S_r^{i\top} h_z, \quad i = 0,1. \tag{4.2}$$

Therein, S_d^i and S_r^i are the selection matrices to select states with Dirichlet and Robin BCs, respectively, at the corresponding boundary and fulfil $S_d^i S_d^{i\top} + S_r^i S_r^{i\top} = I$. The Robin matrices $Q_i(t) \in \mathbb{R}^{n\times n}$ can have an arbitrary structure, since they can directly be eliminated by the corresponding input.

Like in Section 2.1, this system might result from the Hopf-Cole-transformation of a system with diagonal advection matrix. It is assumed that $\check{A}(z,t)$ and $\check{\lambda}_i$ fulfil the respective conditions in Assumption 2.1.5 and Assumption 2.1.6.

In the following sections, a stabilizing state feedback controller is determined for the inputs $u_0(t)$, $u_1(t)$ by utilizing the backstepping method. To this end, a *folding transformation* is applied, leading to a system representation with one-sided, or *unilateral* actuation. Then, the classical backstepping transformation can be applied, leading to the control law and the kernel equations to be solved. However, unfolding the target system back to the original system reveals that the achieved system has an involved structure, which hinders the stability analysis. Therefore, a second transformation step is required. By utilizing a mixed *Volterra-Fredholm integral transformation*, the resulting target system is a cascade of exponentially stable parabolic systems, allowing to explicitly prescribe the uniform stability margin.

The kernel equations for both transformations are converted into integral equations and solved by the method of successive approximations.

4.2 Folding transformation

As proposed by [19, 20, 96], a *folding transformation* is applied to the system (4.1). To this end, the spatial domain is folded at a *folding point* $\check{z}_0$, which is a design parameter. Then, the new spatial coordinate

$$z = z(\check{z}) = \begin{cases} (\check{z}_0 - \check{z})/\check{z}_0, & \check{z} < \check{z}_0 \\ (\check{z} - \check{z}_0)/(1 - \check{z}_0), & \check{z} \geq \check{z}_0 \end{cases} \tag{4.3}$$

is introduced with the new state $x(z,t) = \operatorname{col}(x^l(z,t), x^r(z,t)) \in \mathbb{R}^{2n}$, $z \in [0,1]$, $t \geq t_0$, where $x^l(z,t)$ and $x^r(z,t)$ describe the left and right part w. r. t. $\check{z}_0$, respectively. The new state vector reads

$$x(z,t) = \begin{bmatrix} x^l(z,t) \\ x^r(z,t) \end{bmatrix} = \begin{bmatrix} x_1(z,t) \\ \vdots \\ x_{2n}(z,t) \end{bmatrix} = \begin{bmatrix} w_1(\check{z}_0 - \check{z}_0 z, t) \\ \vdots \\ w_n(\check{z}_0 - \check{z}_0 z, t) \\ w_1(\check{z}_0 + (1-\check{z}_0)z, t) \\ \vdots \\ w_n(\check{z}_0 + (1-\check{z}_0)z, t) \end{bmatrix}. \tag{4.4}$$

Figure 4.1 visualizes the utilized folding transformation. Differentiating (4.4)

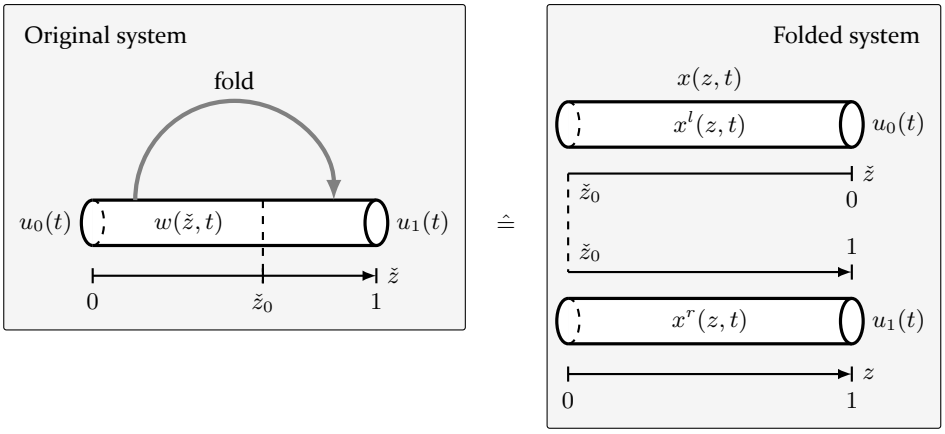

Figure 4.1: The utilized folding transformation, mapping the system with bilateral actuation into a system representation with unilateral actuation. The left boundary of the folded system is subject to the special folding BCs ensuring the regularity of the solution.

w. r. t. t and inserting (4.1a) yields

$$x_t(z,t) = \begin{bmatrix} w_t(\check{z}_0 - \check{z}_0 z, t) \\ w_t(\check{z}_0 + (1-\check{z}_0)z, t) \end{bmatrix} = \begin{bmatrix} \check{\Lambda}(\check{z}_0 - \check{z}_0 z) w_{\check{z}\check{z}}(\check{z}_0 - \check{z}_0 z, t) \\ \check{\Lambda}(\check{z}_0 + (1-\check{z}_0)z) w_{\check{z}\check{z}}(\check{z}_0 + (1-\check{z}_0)z, t) \end{bmatrix} + \begin{bmatrix} \check{A}(\check{z}_0 - \check{z}_0 z, t) w(\check{z}_0 - \check{z}_0 z, t) \\ \check{A}(\check{z}_0 + (1-\check{z}_0)z, t) w(\check{z}_0 + (1-\check{z}_0)z, t) \end{bmatrix}. \tag{4.5}$$

The spatial derivatives of (4.4) read

$$x_z(z,t) = \begin{bmatrix} -w_{\check{z}}(\check{z}_0 - \check{z}_0 z, t)\check{z}_0 \\ w_{\check{z}}(\check{z}_0 + (1-\check{z}_0)z, t)(1-\check{z}_0) \end{bmatrix} \tag{4.6a}$$

$$x_{zz}(z,t) = \begin{bmatrix} w_{\check{z}\check{z}}(\check{z}_0 - \check{z}_0 z, t)\check{z}_0^2 \\ w_{\check{z}\check{z}}(\check{z}_0 + (1-\check{z}_0)z, t)(1-\check{z}_0)^2 \end{bmatrix}, \tag{4.6b}$$

which is inserted into (4.5) to obtain

$$x_t(z,t) = \Lambda(z) x_{zz}(z,t) + A(z,t) x(z,t) \tag{4.7}$$

with

$$\begin{aligned} \Lambda(z) &= \begin{bmatrix} \check{\Lambda}(\check{z}_0 - \check{z}_0 z)/\check{z}_0^2 & \\ & \check{\Lambda}\big(\check{z}_0 + (1-\check{z}_0)z\big)/(1-\check{z}_0)^2 \end{bmatrix} \\ &= \operatorname{bdiag}(\Lambda^l(z), \Lambda^r(z)) = \operatorname{diag}(\lambda_1(z), \dots, \lambda_{2n}(z)), \end{aligned} \tag{4.8a}$$

$$A(z,t) = \begin{bmatrix} \check{A}(\check{z}_0 - \check{z}_0 z, t) & \\ & \check{A}(\check{z}_0 + (1-\check{z}_0)z, t) \end{bmatrix} = \operatorname{bdiag}(A^l(z,t), A^r(z,t)). \tag{4.8b}$$

To be able to apply the backstepping method of Chapter 2, the diffusion coefficients must fulfil Assumption 2.1.6. Consequently, the folding point $\check{z}_0$ must be chosen appropriately in view of (4.8a). However, due to the different scaling with $1/\check{z}_0^2$ and $1/(1-\check{z}_0)^2$ in (4.8a), an appropriate $\check{z}_0$ can always be found to fulfil Assumption 2.1.6, both small and large enough, which is important to freely distribute the control effort between the two inputs, as will be seen later.

Since the system parameters have a diagonal structure, the PDE (4.7) describes two decoupled subsystems. However, the solution of the original system (4.1) must be continuously differentiable w. r. t. z so that the weak second-order derivative can exist. Consequently, the continuity of the solution and its first derivative at the folding point,

$$\lim_{\check{z}\to\check{z}_0^-} w(\check{z},t) = \lim_{\check{z}\to\check{z}_0^+} w(\check{z},t) \tag{4.9a}$$

$$\lim_{\check{z}\to\check{z}_0^-} w_{\check{z}}(\check{z},t) = \lim_{\check{z}\to\check{z}_0^+} w_{\check{z}}(\check{z},t), \tag{4.9b}$$

are additional conditions to ensure the same properties for the original and the folded system, which are implicitly included in the original system (4.1). Applying the transformation (4.4) with (4.3) to (4.9) leads to

$$x^l(0,t) = x^r(0,t) \tag{4.10a}$$

$$x_z^l(0,t) = -\underbrace{\frac{\check{z}_0}{1-\check{z}_0}}_{\tilde{z}_0} x_z^r(0,t). \tag{4.10b}$$

Finally, applying the folding transformation with (4.6a) to the BCs (4.1b) and (4.1c) leads to

$$\underbrace{\begin{bmatrix} S_d^0 S_d^{0\top} & \\ & S_d^1 S_d^{1\top} \end{bmatrix}}_{B_1^d} x(1,t) + \underbrace{\begin{bmatrix} S_r^0 S_r^{0\top} & \\ & S_r^1 S_r^{1\top} \end{bmatrix}}_{B_1^n} x_z(1,t) = \underbrace{\begin{bmatrix} (S_d^0 S_d^{0\top} - \check{z}_0 S_r^0 S_r^{0\top})u_0(t) - \check{z}_0 S_r^0 Q_0(t) S_r^{0\top} w(0,t) \\ (S_d^1 S_d^{1\top} + (1-\check{z}_0) S_r^1 S_r^{1\top})u_1(t) + (1-\check{z}_0) S_r^1 Q_1(t) S_r^{1\top} w(1,t) \end{bmatrix}}_{u(t)} \tag{4.11}$$

with the new input $u(t) \in \mathbb{R}^{2n}$.

To sum up, the folded system representation reads

$$x_t(z,t) = \Lambda(z)x_{zz}(z,t) + A(z,t)x(z,t) \tag{4.12a}$$
$$x^l(0,t) = x^r(0,t) \tag{4.12b}$$
$$x^l_z(0,t) = -\tilde{z}_0 x^r_z(0,t) \tag{4.12c}$$
$$B_1^d x(1,t) + B_1^n x_z(1,t) = u(t). \tag{4.12d}$$

This system is subject to the usual, unilateral actuation. Hence, the standard backstepping transformation can be applied. This is used in the following to determine a feedback law for the new input $u(t)$. By its definition (4.11), the corresponding control law for the original inputs $u_0(t)$, $u_1(t)$ is easy to determine then.

In contrast to the system (2.21) considered in Chapter 2, the folded system (4.12) is subject to the special *folding BCs* (4.12b), (4.12c), which lead to new challenges in the backstepping design.

Remark 4.2.1. An intuitive extension of the presented folding method is to use different folding points for each state to get additional degrees of freedom. However, by doing so, coupling terms like

$$x_{i,t}(z,t) = \ldots + a_{ij}(z,t)x_j(f_{ij}(z),t) + \ldots \tag{4.13}$$

naturally arise, where $f_{ij}(z)$ is the coordinate transformation from the spatial domain of state i to the one of state j. Hence, the folded system can no more described by a PDE of the form (4.12a), which prevents the usage of the usual backstepping transformation. ◁

4.3 Backstepping transformation

To design the state feedback controller for (4.12), the boundedly invertible backstepping transformation

$$\tilde{x}(z,t) = x(z,t) - \int_0^z K(z,\zeta,t)x(\zeta,t)\mathrm{d}\zeta = (\mathcal{T}_c(t)x(t))(z), \tag{4.14}$$

with the kernel $K(z,\zeta,t) \in \mathbb{R}^{2n\times 2n}$ (see (2.22)), is applied with the intermediate control law

$$\begin{aligned} u(t) = {} & B_1^n K(1,1,t)x(1,t) \\ & + \int_0^1 \big(B_1^n K_z(1,\zeta,t) + B_1^d K(1,\zeta,t)\big)x(\zeta,t)\mathrm{d}\zeta + \tilde{u}(t) \end{aligned} \tag{4.15}$$

(see (2.27)) and the new input $\tilde{u}(t) = \mathrm{col}(0, \tilde{u}^r(t)) \in \mathbb{R}^{2n}$ with $\tilde{u}^r(t) \in \mathbb{R}^n$ to map the system (4.12) into the *intermediate target system*

$$\tilde{x}_t(z,t) = \Lambda(z)\tilde{x}_{zz}(z,t) - \mu_c\tilde{x}(z,t) - \widetilde{A}_0(z,t)\tilde{x}(0,t) - \widetilde{A}_1(z,t)\tilde{x}_z(0,t) \tag{4.16a}$$

$$\tilde{x}^l(0,t) = \tilde{x}^r(0,t) \tag{4.16b}$$

$$\tilde{x}^l_z(0,t) = -\tilde{z}_0\tilde{x}^r_z(0,t) \tag{4.16c}$$

$$B_1^d\tilde{x}(1,t) + B_1^n\tilde{x}_z(1,t) = \tilde{u}(t) \tag{4.16d}$$

with the new state $\tilde{x}(z,t) = \mathrm{col}(\tilde{x}^l(z,t), \tilde{x}^r(z,t)) \in \mathbb{R}^{2n}$. In (4.16a) defined on $(z,t) \in (0,1) \times \mathbb{R}^+_{t_0}$, μ_c is the design parameter to influence the decay rate of the system. The matrices $\widetilde{A}_0(z,t) = [\widetilde{A}_{0,ij}(z,t)] \in \mathbb{R}^{2n\times 2n}$, $\widetilde{A}_1(z,t) = [\widetilde{A}_{1,ij}(z,t)] \in \mathbb{R}^{2n\times 2n}$ have the same structure as $\widetilde{A}_0(z,t)$ in (2.23a), given by (2.24) and are introduced to ensure the well-posedness of the kernel equations. After a suitable reordering of the states (see Section 2.4.1), they can be represented by

$$\widetilde{A}_i(z,t) = \begin{bmatrix} \widetilde{A}_i^l(z,t) & 0 \\ \widetilde{A}_i^{lr}(z,t) & \widetilde{A}_i^r(z,t) \end{bmatrix}, \tag{4.17}$$

$i = 0, 1$, which shows that they lead to a coupling between the left and right subsystem via $\widetilde{A}_i^{lr}(z)$, which will be eliminated in the next step. To simplify the presentation in the following chapters, note that by inserting (2.23b) and (2.23c) into the coupling terms in (2.23a), the PDE (2.23a) can be rewritten in the form

$$\tilde{x}_t(z,t) = \Lambda(z)\tilde{x}_{zz}(z,t) - \mu\tilde{x}(z,t) - \bar{A}_0(z,t)\tilde{x}(0,t) - \bar{A}_1(z,t)\tilde{x}_z(0,t) \tag{4.18}$$

with

$$\bar{A}_i(z,t) = \begin{bmatrix} \widetilde{A}_i^l(z,t) & 0 \\ \bar{A}_i^{lr}(z,t) & 0 \end{bmatrix}, \quad i = 0, 1. \tag{4.19}$$

Remark 4.3.1. Like in (2.23a), a matrix $\widetilde{A}(z,t)$ according to (2.41) is possible instead of the scalar μ_c in (4.16a). However, to simplify the presentation, $\widetilde{A}(z,t) = \mu_c I$ is assumed in this chapter. ◁

Due to the folding BCs (4.16b), (4.16c), the intermediate target system (4.16) loses its cascade structure compared to (2.23). This significantly impedes the stability analysis. To achieve a cascaded target system, another transformation is applied in the next step.

Remark 4.3.2. The utilized backstepping transformation (4.14) can be expressed in the original coordinates by unfolding the states, i. e. inserting (4.4) in (4.14) and an equal transformation for $\tilde{x}$. Calling the unfolded target system states $\tilde{w}(\check{z},t)$, this results in

$$\tilde{w}(\check{z},t) = w(\check{z},t) - \int_{\check{\zeta}_l(\check{z})}^{\check{z}} \check{K}(\check{z},\check{\zeta},t) w(\check{\zeta},t) \mathrm{d}\check{\zeta} \tag{4.20}$$

with

$$\check{\zeta}_l(\check{z}) = \begin{cases} \check{z}_0 + \frac{1-\check{z}_0}{\check{z}_0}(\check{z}_0 - \check{z}), & \check{z} < \check{z}_0 \\ \check{z}_0 - \frac{\check{z}_0}{1-\check{z}_0}(\check{z} - \check{z}_0), & \check{z} \geq \check{z}_0. \end{cases} \tag{4.21}$$

The unfolded kernel $\check{K}(\check{z},\check{\zeta},t)$ corresponds to the original kernel

$$K(z,\zeta,t) = \begin{bmatrix} K^{11}(z,\zeta,t) & K^{12}(z,\zeta,t) \\ K^{21}(z,\zeta,t) & K^{22}(z,\zeta,t) \end{bmatrix} \tag{4.22}$$

with the blocks $K^{ij}(z,\zeta,t) \in \mathbb{R}^{n\times n}$, $i,j = 1,2$, by

$$\check{K}(\check{z},\check{\zeta},t) = \begin{cases} & \check{z} < \check{z}_0: & \check{z} \geq \check{z}_0: \\ \check{\zeta} < \check{z}_0: & \frac{-1}{\check{z}_0} K^{11}(\frac{\check{z}_0-\check{z}}{\check{z}_0}, \frac{\check{z}_0-\check{\zeta}}{\check{z}_0}, t) & \frac{1}{\check{z}_0} K^{21}(\frac{\check{z}-\check{z}_0}{1-\check{z}_0}, \frac{\check{z}_0-\check{\zeta}}{\check{z}_0}, t) \\ \check{\zeta} \geq \check{z}_0: & \frac{-1}{1-\check{z}_0} K^{12}(\frac{\check{z}_0-\check{z}}{\check{z}_0}, \frac{\check{\zeta}-\check{z}_0}{1-\check{z}_0}, t) & \frac{1}{1-\check{z}_0} K^{22}(\frac{\check{z}-\check{z}_0}{1-\check{z}_0}, \frac{\check{\zeta}-\check{z}_0}{1-\check{z}_0}, t). \end{cases} \tag{4.23}$$

Figure 4.2 visualizes the backstepping transformation for the unfolded system.

In [96], the bilateral control design problem in the case $n = 1$ is tackled by utilizing a symmetric backstepping transformation

$$\tilde{w}(\check{z},t) = w(\check{z},t) - \int_{-\check{z}}^{\check{z}} k(\check{z},\xi) w(\xi,t) \mathrm{d}\xi \tag{4.24}$$

if the original state $w(\check{z},t)$ is defined on the symmetric spatial coordinate $\check{z} \in [-1,1]$. This is included in (4.20) as a special case with the folding point $\check{z}_0 = 0.5$, when mapping $\check{z} \in [0,1] \to \check{z} \in [-1,1]$ and $\check{\zeta} \in [0,1] \to \xi \in [-1,1]$. The symmetric approach with central folding point leads to the hourglass-shaped spatial domain $(\check{z},\xi) \in [-1,1] \times [-|x|,|x|]$ depicted in Figure 4.3. The resulting kernel equations contain BCs on the pink lines $\check{z} = \xi$ and $\check{z} = -\xi$. In the representation of the folded transformation (2.22), these correspond to

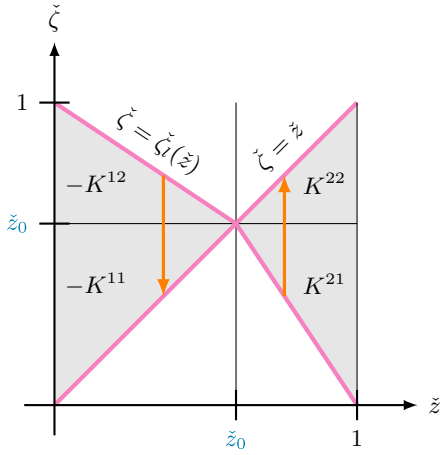

Figure 4.2: Spatial domain and direction of integration in the unfolded representation (4.20) of the backstepping transformation. The pink lines represent the boundaries of the integration, whose path is symbolized by the orange arrows.

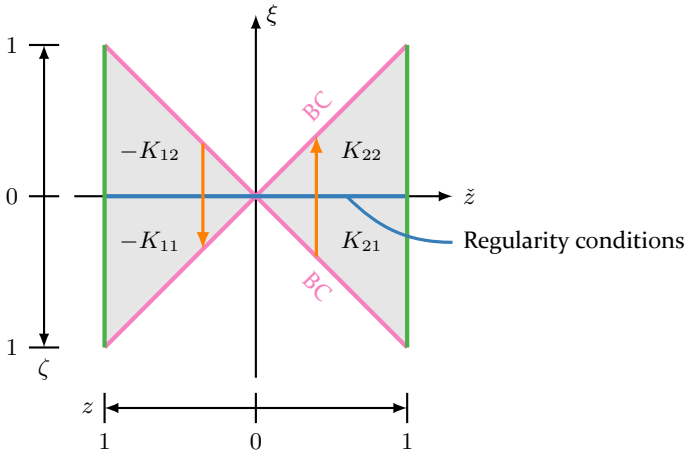

Figure 4.3: Domain of the kernel $K(\check{z},\xi)$ of a symmetric backstepping transformation on the coordinates $(\check{z},\xi)$. Applying the folding transformation, the resulting coordinates (z,ζ) separate the domain into the four parts K_{ij} of the matrix-valued kernel appearing in the folding approach. The coloured boundaries correspond the ones in the left picture of Figure 2.1. A BC on the pink line results from the two-sided backstepping approach, whereas regularity conditions need to be imposed on the blue line when separating the kernel.

the boundary (z, z). From Figure 4.3, it becomes apparent that the elements K_{ij} of the kernel must fulfil regularity conditions at the blue border in order to ensure that both kernels result in the same transformation, leading to the conditions

$$K_{i1}(z,0) = K_{i2}(z,0) \tag{4.25a}$$
$$K_{i1,\zeta}(z,0) = -K_{i2,\zeta}(z,0), \quad i = 1,2, \tag{4.25b}$$

which is nothing else than (4.45e), (4.45f) in the scalar case with constant diffusion. In fact, the two approaches for the bilateral backstepping transformation are supposed to be equivalent.

To be able to apply the standard backstepping transformation, all appearing terms in (4.12a) must be in a form referred to as *strict-feedback* form in [63, Ch. 4.10]. Therefore, the integral term must be of the same form as the applied backstepping transformation (cf. (2.21a) and (2.22)). For this reason, the integral term and the local coupling term in (2.21a) are not allowed in in (4.1a), since they would lose this property due to the folding. Instead, however, the PDE (4.1a) could contain terms of the form $\int_{\check{\zeta}_l(\check{z})}^{\check{\bar{z}}} \check{F}(\check{z},\check{\zeta},t)w(\check{\zeta},t)\mathrm{d}\check{\zeta}$ with $\check{\zeta}_l(\check{z})$ in (4.21) implied by (4.20) and $\check{A}_{\check{z}_0}(\check{z},t)w(\check{z}_0,t)$ leading to the usual, spatially causal integral and local term in the folded PDE (4.12a). Since these terms do not change the basic design procedure, they are not included in the following to increase the readability. Nevertheless, it is basically possible to extend the class of systems that can be handled by backstepping due to these terms compared to the unilateral case. ◁

4.4 Decoupling transformation

To simplify the presentation, it is assumed that the diffusion coefficients λ_i of the folded system are sorted, leading to $\lambda_j^l \geq \lambda_i^r$, $i, j = 1, \ldots, n$ in all sections concerning the decoupling transformation. This can always be achieved by a suitable reordering of the states of the original system (4.1) as well as the folded system (4.12). To be generic, the other sections do not assume this sorting.

Due to the coupling BCs and the well-posed matrices $\widetilde{A}_0(z)$, $\widetilde{A}_1(z)$, the intermediate target system (2.23) has an involved structure, which hinders the stability analysis. To facilitate this problem, the boundedly invertible *Volterra-Fredholm-type decoupling transformation*

$$\bar{x}^l(z,t) = \tilde{x}^l(z,t) \tag{4.26}$$

$$\bar{x}^r(z,t) = \tilde{x}^r(z,t) - \int_0^z Q(z,\zeta,t)\tilde{x}^r(\zeta,t)\mathrm{d}\zeta - \int_0^1 P(z,\zeta,t)\tilde{x}^l(\zeta,t)\mathrm{d}\zeta \tag{4.27}$$

abbreviated

$$\bar{x}(z,t) = (\mathcal{T}_d(t)\tilde{x}(t))(z) \tag{4.28}$$

with the new state $\tilde{x}(z,t) = \mathrm{col}(\bar{x}^l(z,t), \bar{x}^r(z,t)) \in \mathbb{R}^{2n}$ and the kernels $P(z,\zeta,t)$, $Q(z,\zeta,t) \in \mathbb{R}^{n\times n}$ is applied to the $\tilde{x}^r$-system and the additional state feedback

$$\tilde{u}^r(t) = \int_0^1 \tilde{R}_f(\zeta,t)\tilde{x}(\zeta,t)\mathrm{d}\zeta \tag{4.29}$$

with

$$\tilde{R}_f(\zeta,t) = \begin{bmatrix}\tilde{R}_f^l(\zeta,t) & \tilde{R}_f^r(\zeta,t)\end{bmatrix} \in \mathbb{R}^{n\times 2n} \tag{4.30a}$$

$$\tilde{R}_f^l(\zeta,t) = S_r^1 S_r^{1\top} P_z(1,\zeta,t) + S_d^1 S_d^{1\top} P(1,\zeta,t) \tag{4.30b}$$

$$\tilde{R}_f^r(\zeta,t) = S_r^1 S_r^{1\top} Q_z(1,\zeta,t) + S_d^1 S_d^{1\top} Q(1,\zeta,t) \tag{4.30c}$$

is utilized. They map (2.23) into the *final target system*

$$\tilde{x}_t^l(z,t) = \Lambda_l(z)\tilde{x}_{zz}^l(z,t) - \mu_c\tilde{x}^l(z,t) - \widetilde{A}_0^l(z,t)\tilde{x}^l(0,t) - \widetilde{A}_1^l(z,t)\tilde{x}_z^l(0,t) \tag{4.31a}$$

$$\bar{x}_t^r(z,t) = \Lambda_r(z)\bar{x}_{zz}^r(z,t) - \mu_c\bar{x}^r(z,t) - \check{A}_0^r(z,t)\bar{x}^r(0,t) - \check{A}_1^r(z,t)\bar{x}_z^r(0,t) \tag{4.31b}$$

$$\tilde{x}^l(0,t) = \bar{x}^r(0,t) \tag{4.31c}$$

$$\tilde{x}_z^l(0,t) = -\tilde{z}_0\bar{x}_z^r(0,t) \tag{4.31d}$$

$$\tilde{x}_z^l(1,t) = \bar{x}_z^r(1,t) = 0, \tag{4.31e}$$

with the strictly lower triangular coupling matrices $\check{A}_i^r(z) \in \mathbb{R}^{n\times n}$, $i = 0, 1$, in which the coupling of the right and left states is removed in the PDEs. This will result in a cascade of parabolic PDEs after unfolding.

4.5 The stabilizing control law

To be able to realize (4.29), the backstepping transformation (4.14) needs to be inserted for the intermediate target system state $\tilde{x}(z,t)$. After changing the order of integration, the additional state feedback then reads

$$\tilde{u}^r(t) = \int_0^1 \underbrace{\left(\tilde{R}_f(\zeta,t) - \int_\zeta^1 \tilde{R}_f(z,t)K(z,\zeta,t)\mathrm{d}z\right)}_{\check{R}_f(\zeta,t)} x(\zeta,t)\mathrm{d}\zeta \tag{4.32}$$

and after inserting into (4.15),

$$u(t) = B_1^n K(1,1,t)x(1,t) + \int_0^1 \underbrace{\Big(B_1^n K_z(1,\zeta,t) + B_1^d K(1,\zeta,t) + \operatorname{col}\big(0, \check{R}_f(\zeta,t)\big)\Big)}_{R_f(\zeta,t)} x(\zeta,t)\mathrm{d}\zeta \tag{4.33}$$

is the final state feedback in terms of the folded state $x(z,t)$.

With the definition of the new input $u(t)$ according to (4.11) and the control law (4.33), the state feedback controller for the original inputs is obtained as

$$S_d^{0\top} u_0(t) = \int_0^1 \begin{bmatrix} S_d^{0\top} & 0 \end{bmatrix} R_f(\zeta,t)x(\zeta,t)\mathrm{d}\zeta \tag{4.34a}$$

$$S_d^{1\top} u_1(t) = \int_0^1 \begin{bmatrix} 0 & S_d^{1\top} \end{bmatrix} R_f(\zeta,t)x(\zeta,t)\mathrm{d}\zeta \tag{4.34b}$$

$$\begin{aligned} S_r^{0\top} u_0(t) = &- Q_0(t) S_r^{0\top} w(0,t) - \frac{1}{\check{z}_0}\Big(\begin{bmatrix} S_r^{0\top} & 0 \end{bmatrix} K(1,1,t)x(1,t) \\ &+ \int_0^1 \begin{bmatrix} S_r^{0\top} & 0 \end{bmatrix} R_f(\zeta,t)x(\zeta,t)\mathrm{d}\zeta\Big) \end{aligned} \tag{4.34c}$$

$$\begin{aligned} S_r^{1\top} u_1(t) = &- Q_1(t) S_r^{1\top} w(1,t) + \frac{1}{1-\check{z}_0}\Big(\begin{bmatrix} 0 & S_r^{1\top} \end{bmatrix} K(1,1,t)x(1,t) \\ &+ \int_0^1 \begin{bmatrix} 0 & S_r^{1\top} \end{bmatrix} R_f(\zeta,t)x(\zeta,t)\mathrm{d}\zeta\Big), \end{aligned} \tag{4.34d}$$

which can be summed up to

$$\begin{aligned} &\underbrace{(S_d^0 S_d^{0\top} + S_r^0 S_r^{0\top})}_{I} u_0(t) \\ &= -S_r^0 Q_0(t) S_r^{0\top} w(0,t) - \frac{1}{\check{z}_0}\begin{bmatrix} S_r^0 S_r^{0\top} & 0 \end{bmatrix} K(1,1,t)x(1,t) \\ &\quad + \int_0^1 \Big(\begin{bmatrix} S_d^0 S_d^{0\top} & 0 \end{bmatrix} R_f(\zeta,t) - \begin{bmatrix} \frac{1}{\check{z}_0} S_r^0 S_r^{0\top} & 0 \end{bmatrix} R_f(\zeta,t)x(\zeta,t)\Big)\mathrm{d}\zeta \end{aligned} \tag{4.35a}$$

$$\begin{aligned} &\underbrace{(S_d^1 S_d^{1\top} + S_r^1 S_r^{1\top})}_{I} u_1(t) \\ &= -S_r^1 Q_1(t) S_r^{1\top} w(1,t) + \frac{1}{1-\check{z}_0}\begin{bmatrix} 0 & S_r^1 S_r^{1\top} \end{bmatrix} K(1,1,t)x(1,t) \\ &\quad + \int_0^1 \Big(\begin{bmatrix} 0 & S_d^1 S_d^{1\top} \end{bmatrix} R_f(\zeta,t) + \begin{bmatrix} 0 & \frac{1}{1-\check{z}_0} S_r^1 S_r^{1\top} \end{bmatrix}\Big) R_f(\zeta,t)x(\zeta,t)\mathrm{d}\zeta. \end{aligned} \tag{4.35b}$$

In compact vector notation, this reads

$$\begin{aligned}\begin{bmatrix}u_0(t)\\u_1(t)\end{bmatrix} = &-\begin{bmatrix}S_r^0 Q_0(t) S_r^{0\top} w(0,t)\\ S_r^1 Q_1(t) S_r^{1\top} w(1,t)\end{bmatrix} + \begin{bmatrix}\frac{-1}{\check{z}_0} I_n & \\ & \frac{1}{1-\check{z}_0} I_n\end{bmatrix}\\ &\cdot \left(\begin{bmatrix}S_r^0 S_r^{0\top} & \\ & S_r^1 S_r^{1\top}\end{bmatrix} K(1,1,t) x(1,t)\right.\\ &\left. + \int_0^1 \begin{bmatrix}S_r^0 S_r^{0\top} & \\ & S_r^1 S_r^{1\top}\end{bmatrix} R_f(\zeta,t) x(\zeta,t) \mathrm{d}\zeta\right)\\ &+ \int_0^1 \begin{bmatrix}S_d^0 S_d^{0\top} & \\ & S_d^1 S_d^{1\top}\end{bmatrix} R_f(\zeta,t) x(\zeta,t) \mathrm{d}\zeta. \end{aligned} \tag{4.36}$$

Inserting the folding definition (4.4), the *control law* in terms of the original states finally reads

$$\begin{aligned}\begin{bmatrix}u_0(t)\\u_1(t)\end{bmatrix} = &-\begin{bmatrix}S_r^0 Q_0(t) S_r^{0\top} w(0,t)\\ S_r^1 Q_1(t) S_r^{1\top} w(1,t)\end{bmatrix} + \begin{bmatrix}\frac{-1}{\check{z}_0} I_n & \\ & \frac{1}{1-\check{z}_0} I_n\end{bmatrix}\\ &\cdot \left(R_0(t) w(0,t) + R_1(t) w(1,t) + \int_0^1 \check{R}_n(\check{\zeta},t) w(\check{\zeta},t) \mathrm{d}\check{\zeta}\right)\\ &+ \int_0^1 \check{R}_d(\check{\zeta},t) w(\check{\zeta},t) \mathrm{d}\check{\zeta} \end{aligned} \tag{4.37a}$$

with $R_b(t) = [R_{b,ij}(t)] \in \mathbb{R}^{2n\times n}$, $b = 0, 1$, $\check{R}_n(\check{\zeta},t) = [\check{R}_{n,ij}(\check{\zeta},t)] \in \mathbb{R}^{2n\times n}$, $\check{R}_d(\check{\zeta},t) = [\check{R}_{d,ij}(\check{\zeta},t)] \in \mathbb{R}^{2n\times n}$, and

$$R_{0,ij}(t) = e_i^\top \begin{bmatrix}S_r^0 S_r^{0\top} & \\ & S_r^1 S_r^{1\top}\end{bmatrix} K(1,1,t) e_j \tag{4.37b}$$

$$R_{1,ij}(t) = e_i^\top \begin{bmatrix}S_r^0 S_r^{0\top} & \\ & S_r^1 S_r^{1\top}\end{bmatrix} K(1,1,t) e_{j+n} \tag{4.37c}$$

$$\check{R}_{n,ij}(\check{\zeta},t) = \begin{cases} \frac{1}{\check{z}_0} e_i^\top \begin{bmatrix}S_r^0 S_r^{0\top} & \\ & S_r^1 S_r^{1\top}\end{bmatrix} R_f(\frac{\check{z}_0-\check{\zeta}}{\check{z}_0},t) e_j, & \check{\zeta} < \check{z}_0\\ \frac{1}{1-\check{z}_0} e_i^\top \begin{bmatrix}S_r^0 S_r^{0\top} & \\ & S_r^1 S_r^{1\top}\end{bmatrix} R_f(\frac{\check{\zeta}-\check{z}_0}{1-\check{z}_0},t) e_{j+n}, & \check{\zeta} \geq \check{z}_0\end{cases} \tag{4.37d}$$

$$\check{R}_{d,ij}(\check{\zeta},t) = \begin{cases} \frac{1}{\check{z}_0} e_i^\top \begin{bmatrix}S_d^0 S_d^{0\top} & \\ & S_d^1 S_d^{1\top}\end{bmatrix} R_f(\frac{\check{z}_0-\check{\zeta}}{\check{z}_0},t) e_j, & \check{\zeta} < \check{z}_0\\ \frac{1}{1-\check{z}_0} e_i^\top \begin{bmatrix}S_d^0 S_d^{0\top} & \\ & S_d^1 S_d^{1\top}\end{bmatrix} R_f(\frac{\check{\zeta}-\check{z}_0}{1-\check{z}_0},t) e_{j+n}, & \check{\zeta} \geq \check{z}_0\end{cases}, \tag{4.37e}$$

for $i = 1, \dots, 2n$, $j = 1, \dots, n$.

4.6 Closed-loop stability

In analogy to Section 2.4, the stability of the closed-loop system is present if the target system (4.31) is exponentially stable and the utilized transformations (4.14) and (4.27) exist and are boundedly invertible.

To prove the first property, (4.31) is unfolded back to the original representation utilizing

$$\tilde{w}(\check{z},t) = \begin{cases} \tilde{x}^l((\check{z}_0 - \check{z})/\check{z}_0, t), & \check{z} < \check{z}_0 \\ \bar{x}^r((\check{z} - \check{z}_0)/(1-\check{z}_0), t), & \check{z} \geq \check{z}_0 \end{cases} \tag{4.38}$$

leading to

$$\tilde{w}_t(\check{z},t) = \check{\Lambda}(\check{z})\tilde{w}_{\check{z}\check{z}}(\check{z},t) - \mu_c\tilde{w}(\check{z},t) - A_0(\check{z},t)\tilde{w}(\check{z}_0,t) - A_1(\check{z},t)\tilde{w}_{\check{z}}(\check{z}_0,t) \tag{4.39a}$$

$$S_r^0 S_r^{0\top}\tilde{w}_{\check{z}}(0,t) + S_d^0 S_d^{0\top}\tilde{w}(0,t) = 0 \tag{4.39b}$$

$$S_r^1 S_r^{1\top}\tilde{w}_{\check{z}}(1,t) + S_d^1 S_d^{1\top}\tilde{w}(1,t) = 0, \tag{4.39c}$$

where $A_b(\check{z},t) = [A_{b,ij}(\check{z},t)]$, $b = 0, 1$, $i, j = 1, \dots, n$, with

$$A_{0,ij}(\check{z},t) = \begin{cases} \widetilde{A}^l_{0,ij}(z,t), & \check{z} < \check{z}_0 \\ \check{A}^r_{0,ij}(z,t), & \check{z} \geq \check{z}_0 \end{cases} \tag{4.40a}$$

$$A_{1,ij}(\check{z},t) = \begin{cases} -\check{z}_0\widetilde{A}^l_{1,ij}(z,t), & \check{z} < \check{z}_0 \\ (1-\check{z}_0)\check{A}^r_{1,ij}(z,t), & \check{z} \geq \check{z}_0 \end{cases} \tag{4.40b}$$

and (4.3) are strictly lower triangular matrices. Therefore, the unfolded target system (4.39) has the same structure as (2.23), i. e. it is a cascade of exponentially stable parabolic PDEs. The difference that the coupling due to $A_i(\check{z},t)$, $i = 0, 1$, occurs at the folding point $\check{z}_0$ rather than at the left boundary does not change the reasoning in the proof of Lemma 2.4.2 so that the following lemma is valid with the same argumentation.

Lemma 4.6.1 (Stability of the unfolded target system)**.** *Assume that $\mu_c > \mu_{\max}$, where $\mu_{\max}$ is the largest eigenvalue of (4.39) for $\mu_c = 0$, $A_0(z,t) \equiv 0$ and $A_1(z,t) \equiv 0$. Then, the the unfolded target system (4.39) is well-posed and exponentially stable in the weighted L_2-norm $\|h\| = (\int_0^1 \|\check{\Lambda}^{-\frac{1}{2}}(\check{z})h(\check{z})\|^2_{\mathbb{C}^n}\mathrm{d}\check{z})^{1/2}$, i. e.*

$$\|\tilde{w}(t)\| \leq \widetilde{M}\mathrm{e}^{(\mu_{\max}-\mu_c+c)(t-t_0)}\|\tilde{w}(t_0)\|, \quad t \geq t_0 \tag{4.41}$$

for all $\tilde{w}(t_0) \in (L_2(0,1))^n$*, any* $t_0 \geq 0$*, an* $\widetilde{M} \geq 1$*, and any* $c > 0$*, i. e. the stability margin is* $\mu_c - \mu_{\max}$*.*

Proof. The proof immediately follows from the proof of Lemma 2.4.2. ■

Note that the decoupling of the left and right subsystems by (4.27) leads to a significant simplification of the target system structure so that the stability margin can be explicitly assigned, like in the unilateral case.

To ensure that the stability property of the target system (4.16) is inherited by the original closed-loop system resulting from (4.1) when applying (4.37), the bounded invertibility of (4.14) and (4.27) needs to be guaranteed. This, of course presumes that the transformations (4.14) and (4.27) exist, which will be shown in Section 4.9.

The backsteping transformation (4.14) is inherently invertible due the Volterra-type of the integral operator with the same reasoning as in Section 2.4.2. To show that (4.27) is invertible, write it as

$$\bar{x}^r(z,t) = (\mathcal{T}_v(t)\tilde{x}^r(t))(z) - \int_0^1 P(z,\zeta,t)\tilde{x}^l(\zeta,t)\mathrm{d}\zeta, \tag{4.42}$$

where $\mathcal{T}_v(t)$ is a Volterra-type integral operator. Hence, the inverse transformation reads

$$\tilde{x}^r(z,t) = \Big(\mathcal{T}_v^{-1}(t)\big(\bar{x}^r(\cdot,t) + \int_0^1 P(\cdot,\zeta,t)\tilde{x}^l(\zeta,t)\mathrm{d}\zeta\big)\Big)(z), \tag{4.43}$$

which solely requires the inversion of the Volterra-type integral operator $\mathcal{T}_v(t)$. The existence of this inverse follows from the same reasoning as for (4.14).

Therefore, the stability of the unfolded target system (4.39) according to Lemma 4.6.1 implies the stability of the closed-loop folded system (4.12) with (4.33). After unfolding back to the system representation of (4.1), this directly leads to the following theorem.

Theorem 4.6.2 (Closed-loop stability with bilateral actuation) Assume that $\mu_c > \mu_{\max}$, where $\mu_{\max}$ is the largest eigenvalue of (4.31) for $A_0(z,t) \equiv 0$ and $A_1(z,t) \equiv 0$. Then, the closed-loop system (4.1) with (4.37) is well-posed and uniformly exponentially stable in the weighted L_2-norm $\|h\| = \big(\int_0^1 \|\check{\Lambda}^{-\frac{1}{2}}(z)h(z)\|_{\mathbb{C}^n}^2 \mathrm{d}z\big)^{1/2}$, i. e.

$$\|x(t)\| \leq M\mathrm{e}^{(\mu_{\max}-\mu_c+c)(t-t_0)}\|x(t_0)\|, \quad t \geq t_0 \tag{4.44}$$

for all $x(t_0) \in (L_2(0,1))^n$, an $M \geq 1$, any $t_0 \geq 0$ and any $c > 0$, i. e. the stability margin is $\mu_c - \mu_{\max}$.

For the calculation of (4.37b)–(4.37e), the kernels $K(z,\zeta,t)$ and $P(z,\zeta,t)$, $Q(z,\zeta,t)$ of the transformations (4.14) and (4.27) need to be determined. In both cases, this can be done by converting the corresponding kernel equations into integral equations and solving them with the method of successive approximations. The next sections present the conversion into integral equations, followed by their solution in Section 4.9.

4.7 Volterra-kernel integral equations

Like in the previous chapters, the short form notation omitting independent variables is used in the following. This means, if no independent variables are written, the reader needs to insert the variables over which the dependent variable is defined.

Performing similar steps as in Section 2.3, the *kernel equations*

$$\Lambda K_{zz} - (K\Lambda(\zeta))_{\zeta\zeta} = K(A(\zeta,t) + \mu_c I) + K_t \tag{4.45a}$$

$$\Lambda K(z,z,t) - K(z,z,t)\Lambda = 0 \tag{4.45b}$$

$$K_\zeta(z,z,t)\Lambda + \Lambda \mathrm{d}_z K(z,z,t) + \Lambda K_z(z,z,t) = -(A + \mu_c I) - K(z,z,t)\Lambda' \tag{4.45c}$$

$$K(0,0,t) = 0 \tag{4.45d}$$

$$K(z,0,t)\Lambda(0)S_1 + \widetilde{A}_1(z,t)S_1 = 0 \tag{4.45e}$$

$$K_\zeta(z,0,t)\Lambda(0)S_2 + K(z,0,t)\Lambda'(0)S_2 - \widetilde{A}_0(z,t)S_2 = 0 \tag{4.45f}$$

with (4.45a) defined on $0 < \zeta < z < 1$, $t \in \mathbb{R}^+_{t_0}$ and

$$S_1 = \begin{bmatrix} -\tilde{z}_0 I_n \\ I_n \end{bmatrix}, \quad S_2 = \begin{bmatrix} I_n \\ I_n \end{bmatrix}, \tag{4.46}$$

need to be fulfilled to map (4.12) into (4.16). They have the same form as (2.28) except for the new folding BCs (4.45e), (4.45f), requiring significant modifications of the solution procedure.

4.7.1 Canonical kernel equations

Like in Section 2.5, the solution of (4.45) is based on a transformation into integral equations. To this end, their component form is transformed into

canonical coordinates which allow the conversion into integral equations by formal integrations. Since the novelty of (4.45) are the BCs (4.45e), (4.45f), they will attain special attention in the following.

The component form $\boldsymbol{K}(z,\zeta,t) = K_{ij}(z,\zeta,t)$ of (4.45e) reads

$$\widetilde{A}_{1,ij} - \frac{1}{\tilde{z}_0}\widetilde{A}_{1,ij+n} = \underbrace{-\boldsymbol{K}(z,0,t)\lambda_j(0) + \frac{1}{\tilde{z}_0}K_{ij+n}(z,0,t)\lambda_{j+n}(0)}_{=:\mathcal{K}_j^1} \tag{4.47}$$

for $j \leq n$, which shows that the respective left ($j \leq n$) and right ($j > n$) elements of the kernel K and the matrix $\widetilde{A}_1$ are coupled. The short form $\mathcal{K}_j^1$ is introduced as abbreviation for later usage.

Similarly, the component form of (4.45f) reads

$$\begin{aligned}\widetilde{A}_{0,ij} + \widetilde{A}_{0,ij+n} &= \boldsymbol{K}_\zeta(z,0,t)\lambda_j(0) + \boldsymbol{K}(z,0,t)\lambda_j'(0)\\ &\quad + K_{ij+n,\zeta}(z,0,t)\lambda_{j+n}(0) + K_{ij+n}(z,0,t)\lambda_{j+n}'(0) =: \mathcal{K}_j^0,\end{aligned} \tag{4.48}$$

for $j \leq n$ with the abbreviation $\mathcal{K}_j^0$.

The coupling matrices $\widetilde{A}_0$ and $\widetilde{A}_1$ are needed to ensure well-posedness of the kernel equations, like the matrix $\widetilde{A}_0$ in (2.23). Their task is to fulfil the BCs (4.47) and (4.48) for some indices so that no condition on the respective kernel element results. Yet, they can only cover so many conditions that they attain a cascade structure, i. e. $\widetilde{A}_{k,ij} = 0$, $k = 0, 1$, for $\lambda_i \geq \lambda_j$ (see (2.24)), which is important for the stability of the target system. In the unilateral case in Section 2.5, $\widetilde{A}_0$ needs to remove the BC at the lower boundary $(z, 0)$ for all kernel elements with $\lambda_i < \lambda_j$.

In the folding case, it is important that the folding BCs (4.47) and (4.48) only couple kernel elements for which $s = 1$ according to (2.131). This is essential to ensure that the coupling at the boundary $\Gamma_2 : (z, 0)$ (see Figure 2.1) belongs to the same canonical coordinates $\widetilde{\Gamma}_2 : (\boldsymbol{\eta}, \boldsymbol{\eta})$ in the coordinate systems of the coupled elements, as can be seen in Figure 2.2 and Figure 2.3. In other words, for $j \leq n$, (4.47) and (4.48) must only imply a condition on the kernel elements if $\lambda_i \geq \lambda_j$ and $\lambda_i \geq \lambda_{j+n}$. In turn, this means that $\widetilde{A}_b$, $b = 0, 1$, need to remove the BCs for both the cases $\lambda_i < \lambda_j$ and $\lambda_i < \lambda_{j+n}$, $j \leq n$.

Removing the BC (4.47) for elements $K_{ij}(z, 0, t)$ with $\lambda_i < \lambda_j$, $j \leq n$, for example by choosing

$$\widetilde{A}_{1,ij+n} = 0 \tag{4.49a}$$

$$\widetilde{A}_{1,ij} = \mathcal{K}_j^1 \tag{4.49b}$$

also removes the BC for the element $K_{ij+n}(z,0,t)$ due to the coupling. But it must also be removed in the case $\lambda_i < \lambda_{j+n}$, $j \leq n$, where no degree of freedom is available at first glance if simultaneously $\lambda_i \geq \lambda_j$ holds, because in this case, $\widetilde{A}_{1,ij} = 0$ due to the cascade structure. However, specifying

$$\frac{1}{\tilde{z}_0}\widetilde{A}_{1,ij+n} = \widetilde{A}_{1,ij} - \mathcal{K}_j^1 \tag{4.50}$$

for $\lambda_i < \lambda_{j+n}$, $j \leq n$, rather than (4.49a) solves this problem. In the case $(\lambda_i < \lambda_j) \wedge (\lambda_i < \lambda_{j+n})$, (4.50) automatically implies (4.49a) due to (4.49b) and in the case $(\lambda_i \geq \lambda_j) \wedge (\lambda_i < \lambda_{j+n})$, where $\widetilde{A}_{1,ij} = 0$, (4.50) fulfils the BC (4.47). Proceeding the same way for $i > n$ and for (4.48) finally leads to the choices

$$\begin{array}{lll} & \lambda_i < \lambda_j : & \lambda_i < \lambda_{j+n} : \\ i \leq n : & \widetilde{A}_{1,ij} = \mathcal{K}_j^1 & \widetilde{A}_{1,ij+n} = \tilde{z}_0\widetilde{A}_{1,ij} - \tilde{z}_0\mathcal{K}_j^1 \\ & \widetilde{A}_{0,ij} = \mathcal{K}_j^0 & \widetilde{A}_{0,ij+n} = -\widetilde{A}_{0,ij} + \mathcal{K}_j^0 \\ i > n : & \widetilde{A}_{1,ij+n} = -\tilde{z}_0\mathcal{K}_j^1 & \widetilde{A}_{1,ij} = \frac{1}{\tilde{z}_0}\widetilde{A}_{1,ij+n} + \mathcal{K}_j^1 \\ & \widetilde{A}_{0,ij+n} = \mathcal{K}_j^0 & \widetilde{A}_{0,ij} = -\widetilde{A}_{0,ij+n} + \mathcal{K}_j^0. \end{array} \tag{4.51}$$

for $j \leq n$. Remember that for all cases not included in (4.51), $\widetilde{A}_{0,ij} = 0$ and $\widetilde{A}_{1,ij} = 0$ holds to ensure the cascade structure. With (4.51) the remaining BCs for the kernel resulting from (4.47) and (4.48) only need to be fulfilled in the case $(\lambda_i \geq \lambda_j) \wedge (\lambda_i \geq \lambda_{j+n})$, $j \leq n$ and read

$$\boldsymbol{K}(z,0,t)\lambda_j(0)\tilde{z}_0 = K_{ij+n}(z,0,t)\lambda_{j+n}(0) \tag{4.52a}$$

$$\begin{aligned} &\boldsymbol{K}_\zeta(z,0,t)\lambda_j(0) + \boldsymbol{K}(z,0,t)\lambda_j'(0) \\ &\qquad = -K_{ij+n,\zeta}(z,0,t)\lambda_{j+n}(0) - K_{ij+n}(z,0,t)\lambda_{j+n}'(0). \end{aligned} \tag{4.52b}$$

Together, (4.52) are two BCs for the kernel elements with $j \leq n$ and $j > n$, which both appear in each BC. Since each kernel element may only have one BC at this boundary $(z,0)$, it is helpful to interpret one as a condition for the left elements ($j \leq n$) and one for the right elements ($j > n$). To this end, (4.52a) is reformulated by an index shift $j \to j+n$, resulting in

$$\boldsymbol{K}(z,0,t)\lambda_j(0) = K_{ij-n}(z,0,t)\lambda_{j-n}(0)\tilde{z}_0 \tag{4.53}$$

for $j \geq n$, $(\lambda_i \geq \lambda_{j-n}) \wedge (\lambda_i \geq \lambda_j)$. Then, (4.53) is considered as a BC for the right elements ($j > n$), whereas (4.52b) is a BC for the left elements ($j \leq n$).

The component form of the PDE (4.45a) and of the remaining BCs follows the same way as in Section 2.5.1. In total, the resulting component form of the kernel equations reads

$$\lambda_i \boldsymbol{K}_{zz} - (\lambda_j(\zeta)\boldsymbol{K})_{\zeta\zeta} = \sum_{k=1}^{2n} K_{ik} A_{kj}(\zeta,t) + \mu_c \boldsymbol{K} + \boldsymbol{K}_t \tag{4.54a}$$

defined on $0 < \zeta < z < 1$, $t \in \mathbb{R}_{t_0}^+$ with the BCs

$$[\boldsymbol{K}(z,z,t) = 0]_{\lambda_i \neq \lambda_j} \tag{4.54b}$$

$$[\boldsymbol{K}_z(z,z,t) = \frac{\boldsymbol{A}}{\lambda_j - \lambda_i}]_{\lambda_i \neq \lambda_j} \tag{4.54c}$$

$$\left[\boldsymbol{K}(z,z,t) = -\int_0^z \frac{\boldsymbol{A}(\zeta,t) + \mu_c \delta_{ij}}{2\sqrt{\lambda_i(\zeta)\lambda_i(z)}} \mathrm{d}\zeta\right]_{\lambda_i = \lambda_j} \tag{4.54d}$$

$$[\boldsymbol{K}(z,0,t)\lambda_j(0) = K_{ij-n}(z,0,t)\lambda_{j-n}(0)\tilde{z}_0]_{\substack{j > n \\ \lambda_i \geq \lambda_j \\ \lambda_i \geq \lambda_{j-n}}} \tag{4.54e}$$

$$\begin{aligned}&[\boldsymbol{K}_\zeta(z,0,t)\lambda_j(0) + \boldsymbol{K}(z,0,t)\lambda_j'(0) \\ &\quad = -K_{ij+n,\zeta}(z,0,t)\lambda_{j+n}(0) - K_{ij+n}(z,0,t)\lambda_{j+n}'(0)]_{\substack{j \leq n \\ \lambda_i \geq \lambda_j \\ \lambda_i \geq \lambda_{j+n}}}\end{aligned} \quad . \tag{4.54f}$$

To get a better overview on how (4.54e), (4.54f) and (4.51) cover all matrix elements to fulfil (4.45e) and (4.45f), the simpler special case of sorted diffusion coefficients $\lambda_1 > \ldots > \lambda_{2n}$ is considered. Then, the condition $\lambda_i \geq \lambda_j$ is changed into $i \leq j$ and $\lambda_i < \lambda_j$ is turned to $i > j$, accordingly. The choice (4.51) simplifies to

$$\begin{aligned} i > j,\, i-n \leq j \leq n: \qquad & i > j > n: \\ \widetilde{A}_{1,ij} &= \mathcal{K}_j^1 & \widetilde{A}_{1,ij} &= -\tilde{z}_0 \mathcal{K}_{j-n}^1 \\ \widetilde{A}_{0,ij} &= \mathcal{K}_j^0 & \widetilde{A}_{0,ij} &= \mathcal{K}_{j-n}^0. \end{aligned} \tag{4.55}$$

For this simpler case, Figure 4.4 provides a graphical overview of the related index combinations for the kernel BCs and the coupling matrix elements needed to fulfil (4.47) and (4.48). Note that with the choice (4.51), the matrices $\widetilde{A}_0$ and $\widetilde{A}_1$ both have an occupancy resulting in a cascade structure, like (2.24). In particular, for the special case $\lambda_1 > \ldots > \lambda_{2n}$, the choice (4.55) leads to the structure

$$\widetilde{A}^k = \begin{bmatrix} \widetilde{A}^k_{\searrow 1} & 0 \\ \widetilde{A}^k_{\swarrow} & \widetilde{A}^k_{\searrow 2} \end{bmatrix}, \quad k = 0, 1, \tag{4.56}$$

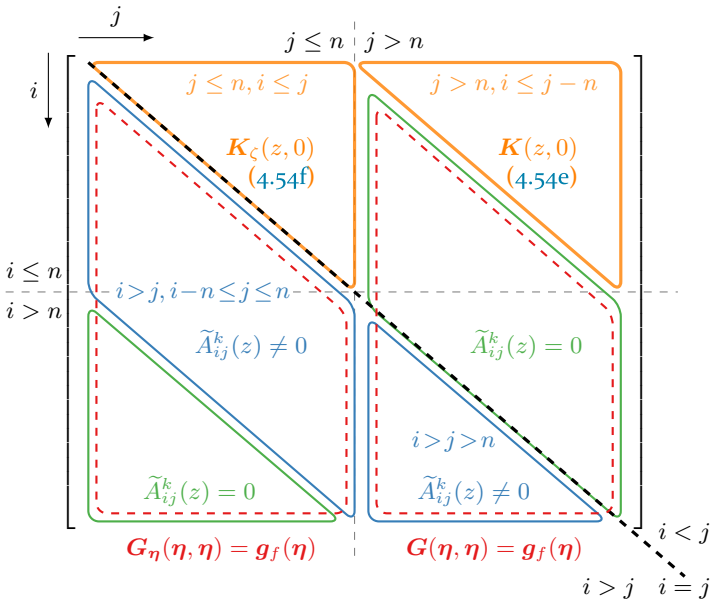

Figure 4.4: Index combinations $i, j = 1, \dots, 2n$, for which the BCs (4.47), (4.48) are either fulfilled by the kernel BCs or the choice of the coupling matrix elements $\widetilde{A}_{0,ij}$, $\widetilde{A}_{1,ij}$ in the special case $\lambda_1 > \dots > \lambda_{2n}$. The orange triangles mark the index combinations for which the kernel elements must fulfil the coupling BCs (4.54e) and (4.54f), the blue areas represent the indices where $\widetilde{A}_{k,ij} \neq 0$, $k = 0, 1$, to fulfil (4.55). For the green regions, $\widetilde{A}_{k,ij} = 0$ but (4.47) and (4.48) are fulfilled due to the appearing coupling, i. e. by the blue counterparts w. r. t. the line $j = n$. The parts where artificial BCs (4.58g), (4.58h) need to be introduced are marked by the red dashed borders.

where $\widetilde{A}^k_{\diagdown 1}$ and $\widetilde{A}^k_{\diagdown 2}$ are strictly lower triangular matrices and $\widetilde{A}^k_{\diagup}$ is an upper triangular matrix so that in total, $\widetilde{A}_0$ and $\widetilde{A}_1$ are strictly lower triangular (blue regions in Figure 4.4). Note that even in the general case of unsorted and possibly equal diffusion coefficients, the states can always be reordered to ensure $\lambda_1 \geq \dots \geq \lambda_{2n}$. Then, (4.56) is the maximal occupancy of the permuted matrices $\widetilde{A}_0$ and $\widetilde{A}_1$, i. e. they can only have less entries, but not more.

Applying the change of coordinates (2.136) derived in Section 2.5.3 with the introduction of the canonical kernel elements

$$\boldsymbol{G}(\boldsymbol{\xi}, \boldsymbol{\eta}, t) = \lambda_j(\boldsymbol{\zeta}(\boldsymbol{\xi}, \boldsymbol{\eta}))\boldsymbol{K}(\boldsymbol{z}(\boldsymbol{\xi}, \boldsymbol{\eta}), \boldsymbol{\zeta}(\boldsymbol{\xi}, \boldsymbol{\eta}), t), \tag{4.57}$$

which is (2.140) with (2.97), the component form (4.54) is mapped into the canoncial kernel equations

$$\boldsymbol{G}_{\boldsymbol{\xi}\boldsymbol{\eta}} = \underbrace{\frac{\boldsymbol{s}}{4}\sum_{k=1}^{2n}\Big(\frac{\lambda_j(\zeta)}{\lambda_k(\zeta)}G_{ik}A_{kj}(\zeta,t)\Big)\Big|_{\zeta=\boldsymbol{\zeta}(\boldsymbol{\xi},\boldsymbol{\eta})}}_{\boldsymbol{\mathcal{A}}[G](\boldsymbol{\xi},\boldsymbol{\eta},t)} + \frac{\boldsymbol{s}\mu_c}{4}\boldsymbol{G} - \frac{1}{4}\bar{\boldsymbol{a}}_{\Delta}\boldsymbol{G}_{\boldsymbol{\xi}} + \frac{\boldsymbol{s}}{4}\bar{\boldsymbol{a}}_{\Sigma}\boldsymbol{G}_{\boldsymbol{\eta}} + \frac{\boldsymbol{s}}{4}\boldsymbol{G}_t =: \boldsymbol{F}[G,\boldsymbol{G}_{\boldsymbol{\xi}},\boldsymbol{G}_{\boldsymbol{\eta}}] \tag{4.58a}$$

with the BCs

$$\Big[\boldsymbol{G}(\boldsymbol{\xi},0,t) = \bar{\boldsymbol{c}}^4(\boldsymbol{\xi},t)\Big]_{\lambda_i=\lambda_j} \tag{4.58b}$$

$$[\boldsymbol{G}(\boldsymbol{\xi},\boldsymbol{\eta}_l(\boldsymbol{\xi}),t) = 0]_{\lambda_i\neq\lambda_j} \tag{4.58c}$$

$$\Bigg[\boldsymbol{s}\boldsymbol{G}_{\boldsymbol{\xi}}(\boldsymbol{\xi},\boldsymbol{\eta}_l(\boldsymbol{\xi}),t) + \boldsymbol{G}_{\boldsymbol{\eta}}(\boldsymbol{\xi},\boldsymbol{\eta}_l(\boldsymbol{\xi}),t) = \underbrace{\frac{\boldsymbol{A}\lambda_j\sqrt{\lambda_i}}{\lambda_j-\lambda_i}}_{\bar{\boldsymbol{c}}^5(\boldsymbol{\xi},t)}\Bigg]_{\substack{\lambda_i\neq\lambda_j\\ z=\boldsymbol{z}(\boldsymbol{\xi},\boldsymbol{\eta}_l(\boldsymbol{\xi}))}} \tag{4.58d}$$

$$[\boldsymbol{G}(\boldsymbol{\eta},\boldsymbol{\eta},t) = \tilde{z}_0 G_{ij-n}(\boldsymbol{\eta},\boldsymbol{\eta},t)]_{\substack{j>n\\ \lambda_i\geq\lambda_j\\ \lambda_i\geq\lambda_{j-n}}} \tag{4.58e}$$

$$\Big[\big(\boldsymbol{G}_{\boldsymbol{\eta}}(\boldsymbol{\eta},\boldsymbol{\eta},t) - \boldsymbol{G}_{\boldsymbol{\xi}}(\boldsymbol{\eta},\boldsymbol{\eta},t)\big)\tilde{z}_0 = G_{ij+n,\xi}(\boldsymbol{\eta},\boldsymbol{\eta},t) - G_{ij+n,\eta}(\boldsymbol{\eta},\boldsymbol{\eta},t)\Big]_{\substack{j\leq n\\ \lambda_i\geq\lambda_j\\ \lambda_i\geq\lambda_{j+n}}} \tag{4.58f}$$

$$[\boldsymbol{G}(\boldsymbol{\eta},\boldsymbol{\eta},t) = \boldsymbol{g}(\boldsymbol{\eta},t)]_{\substack{j>n\\ (\lambda_i<\lambda_j)\vee(\lambda_i<\lambda_{j-n})\\ \boldsymbol{\eta}\geq 0}} \tag{4.58g}$$

$$[\boldsymbol{G}_{\boldsymbol{\eta}}(\boldsymbol{\eta},\boldsymbol{\eta},t) = \boldsymbol{g}(\boldsymbol{\eta},t)]_{\substack{j\leq n\\ (\lambda_i<\lambda_j)\vee(\lambda_i<\lambda_{j+n})\\ \boldsymbol{\eta}\geq 0}}, \tag{4.58h}$$

in which $\bar{\boldsymbol{c}}^4(\boldsymbol{\xi},t) = \boldsymbol{c}^4(\boldsymbol{z}(\boldsymbol{\xi},0),t)$ with $\boldsymbol{K}_0 = 0$ (see (2.150c)), $\bar{\boldsymbol{a}}_{\Delta}$, $\bar{\boldsymbol{a}}_{\Sigma}$ are defined in (2.149), $\boldsymbol{s}$ can be found in (2.131) and $\boldsymbol{\eta}_l(\boldsymbol{\xi})$ given by (2.123) and (2.128) is the lower boundary of the spatial domain depicted in Figures 2.2 and 2.3. In (4.58e) and (4.58f), the fact that $\xi_{ij+n}(\boldsymbol{\eta},\boldsymbol{\eta}) = \eta_{ij+n}(\boldsymbol{\eta},\boldsymbol{\eta}) = \boldsymbol{\eta}$ for $j\leq n$, $\lambda_i\geq\lambda_j$ and $\lambda_i\geq\lambda_{j+n}$, as well as $\sqrt{\frac{\lambda_{j+n}(0)}{\lambda_j(0)}} = \tilde{z}_0$ was utilized.

The *artificial BCs* (4.58g), (4.58h) have been introduced to fully determine the kernel and contain the degrees of freedom $\boldsymbol{g} = g_{ij}$, $i,j = 1,\dots,2n$,

$g_{ij}(\cdot, t) \in C[0, \bar{\boldsymbol{\eta}}]$, where $\bar{\boldsymbol{\eta}} = \phi_i(1)$ for $\lambda_i \geq \lambda_j$ and $\bar{\boldsymbol{\eta}} = \phi_j(1)$ for $\lambda_i < \lambda_j$ and $g_{ij}(z, \cdot) \in G_\alpha(\mathbb{R}^+_{t_0})$, $\alpha \in [1, 2)$. Their introduction as Dirichlet respectively Neumann BCs is defined by the way the equations will be converted into integral equations in the next step. In the case of descending diffusion coefficients, the indices for which they are provided are depicted by the red dashed areas in Figure 4.4. Note that in contrast to the unilateral case, there also exist artificial BCs for $\lambda_i \geq \lambda_j$.

The steps to convert the kernel equations (4.45) into their canoncial form (4.58) have been similar to Section 2.5.4. In the next step, they are converted into integral equations which will require significant modifications compared to Section 2.5.5 due to the coupling BCs (4.58e), (4.58f).

4.7.2 Conversion into integral equations

To account for the different types of BCs (4.58f) for $j \leq n$ and (4.58e) for $j > n$, a different order of integration is required for the formal integration of (4.58a) in these cases.

The BC (4.58e) is of the same form as (2.143f) and (2.143g). Hence, the same method as in Section 2.5.5 can be used to convert (4.58a) into integral equations for the elements $j > n$. However, it is not possible to convert (4.58f) into the same form without including the unknown derivative $\boldsymbol{G}_{\boldsymbol{\eta}}$ of one of the elements $\boldsymbol{G}$ or G_{ij+n}, from the view of $j \leq n$. Therefore, this derivative must be determined by an integral equation, like the derivative $\boldsymbol{G}_{\boldsymbol{\xi}} = \boldsymbol{H}$ in Section 2.5.5.

Due to the second order nature of the PDE (4.58a), it is possible to first integrate w. r. t. $\boldsymbol{\eta}$ and then w. r. t. $\boldsymbol{\xi}$ leading to

$$\boldsymbol{G}_{\boldsymbol{\xi}} = \boldsymbol{G}_{\boldsymbol{\xi}}(\boldsymbol{\xi}, \boldsymbol{\eta}_l(\boldsymbol{\xi}), t) + \int_{\boldsymbol{\eta}_l(\boldsymbol{\xi})}^{\boldsymbol{\eta}} \boldsymbol{F}[G, \boldsymbol{G}_{\boldsymbol{\xi}}, \boldsymbol{G}_{\boldsymbol{\eta}}] \mathrm{d}\bar{\eta} \tag{4.59a}$$

$$\boldsymbol{G} = \boldsymbol{G}(\boldsymbol{\xi}_l(\boldsymbol{\eta}), \boldsymbol{\eta}, t) + \int_{\boldsymbol{\xi}_l(\boldsymbol{\eta})}^{\boldsymbol{\xi}} \boldsymbol{G}_{\boldsymbol{\xi}}(\bar{\xi}, \boldsymbol{\eta}, t) \mathrm{d}\bar{\xi}, \tag{4.59b}$$

which is done in Section 2.5.5 to obtain (2.143a) with (2.143b), or to interchange this order of integration. Then,

$$\boldsymbol{G}_{\boldsymbol{\eta}} = \boldsymbol{G}_{\boldsymbol{\eta}}(\boldsymbol{\xi}_l(\boldsymbol{\eta}), \boldsymbol{\eta}, t) + \int_{\boldsymbol{\xi}_l(\boldsymbol{\eta})}^{\boldsymbol{\xi}} \boldsymbol{F}[G, \boldsymbol{G}_{\boldsymbol{\xi}}, \boldsymbol{G}_{\boldsymbol{\eta}}](\bar{\xi}, \boldsymbol{\eta}, t) \mathrm{d}\bar{\xi} \tag{4.60a}$$

$$\boldsymbol{G} = \boldsymbol{G}(\boldsymbol{\xi}, \boldsymbol{\eta}_l(\boldsymbol{\xi}), t) + \int_{\boldsymbol{\eta}_l(\boldsymbol{\xi})}^{\boldsymbol{\eta}} \boldsymbol{G}_{\boldsymbol{\eta}}(\boldsymbol{\xi}, \bar{\eta}, t) \mathrm{d}\bar{\eta}, \tag{4.60b}$$

is obtained, where $\boldsymbol{G}_{\boldsymbol{\eta}}$ can be determined as the solution of the integral equation (4.60a). In both cases, the BCs must be of the correct form to replace the boundary terms. Since for $j > n$ they have the same form as in Section 2.5.5,

$$\boldsymbol{H} = \boldsymbol{G}_{\boldsymbol{\xi}} \tag{4.61}$$

can be introduced to use (4.59), which then reads

$$\boldsymbol{H} = \boldsymbol{H}(\boldsymbol{\xi}, \boldsymbol{\eta}_l(\boldsymbol{\xi}), t) + \int_{\boldsymbol{\eta}_l(\boldsymbol{\xi})}^{\boldsymbol{\xi}} \boldsymbol{F}[G, \boldsymbol{H}, \boldsymbol{G}_{\boldsymbol{\eta}}] \mathrm{d}\bar{\eta} \tag{4.62a}$$

$$\boldsymbol{G} = \boldsymbol{G}(\boldsymbol{\xi}_l(\boldsymbol{\eta}), \boldsymbol{\eta}, t) + \int_{\boldsymbol{\xi}_l(\boldsymbol{\eta})}^{\boldsymbol{\xi}} \boldsymbol{H}(\bar{\xi}, \boldsymbol{\eta}, t) \mathrm{d}\bar{\xi}, \tag{4.62b}$$

for which the BCs (4.58b), (4.58c) and (4.58d) are reformulated as conditions for $\boldsymbol{H}(\boldsymbol{\xi}, \boldsymbol{\eta}_l(\boldsymbol{\xi}), t)$ like it was done in Section 2.5.4. Together with (4.58e) and (4.58g), the boundary terms in (4.62) are all given. In a last step, integration by parts is applied in (4.62a) to eliminate the unknown derivative $\boldsymbol{G}_{\boldsymbol{\eta}}$ like shown in Section 2.5.5.

For the left elements with $j \leq n$,

$$\boldsymbol{J} = \boldsymbol{G}_{\boldsymbol{\eta}} \tag{4.63}$$

is introduced to use (4.60) for the conversion into integral equations, which then read

$$\boldsymbol{J}(\boldsymbol{\xi}, \boldsymbol{\eta}, t) = \boldsymbol{J}(\boldsymbol{\xi}_l(\boldsymbol{\eta}), \boldsymbol{\eta}, t) + \int_{\boldsymbol{\xi}_l(\boldsymbol{\eta})}^{\boldsymbol{\xi}} \boldsymbol{F}[G, \boldsymbol{G}_{\boldsymbol{\xi}}, \boldsymbol{J}](\bar{\xi}, \boldsymbol{\eta}, t) \mathrm{d}\bar{\xi} \tag{4.64a}$$

$$\boldsymbol{G}(\boldsymbol{\xi}, \boldsymbol{\eta}, t) = \boldsymbol{G}(\boldsymbol{\xi}, \boldsymbol{\eta}_l(\boldsymbol{\xi}), t) + \int_{\boldsymbol{\eta}_l(\boldsymbol{\xi})}^{\boldsymbol{\eta}} \boldsymbol{J}(\boldsymbol{\xi}, \bar{\eta}, t) \mathrm{d}\bar{\eta}. \tag{4.64b}$$

To substitute the boundary terms in (4.64), (4.58b) and (4.58c) can directly be inserted for $\boldsymbol{G}(\boldsymbol{\xi}, \boldsymbol{\eta}_l(\boldsymbol{\xi}), t)$. The BCs (4.58d) and (4.58f), however, need to be formulated as conditions for $\boldsymbol{J} = \boldsymbol{G}_{\boldsymbol{\eta}}$. To this end, (4.58c) is differentiated w. r. t. $\boldsymbol{\xi}$, leading to

$$\boldsymbol{G}_{\boldsymbol{\xi}}(\boldsymbol{\xi}, \boldsymbol{\eta}_l(\boldsymbol{\xi}), t) + \boldsymbol{G}_{\boldsymbol{\eta}}(\boldsymbol{\xi}, \boldsymbol{\eta}_l(\boldsymbol{\xi}), t) \boldsymbol{\eta}_l'(\boldsymbol{\xi}) = 0, \quad \lambda_i \neq \lambda_j \tag{4.65}$$

(see (2.152)). Now, solving (4.58d) for $\boldsymbol{G}_{\boldsymbol{\xi}}(\boldsymbol{\xi}, \boldsymbol{\eta}_l(\boldsymbol{\xi}), t)$ and inserting the result into (4.65) yields

$$\boldsymbol{J}(\boldsymbol{\xi}_l(\boldsymbol{\eta}), \boldsymbol{\eta}, t) = \underbrace{\frac{\bar{c}^5(\boldsymbol{\xi}_l(\boldsymbol{\eta}), t)}{1 - s\boldsymbol{\eta}_l'(\boldsymbol{\xi}_l(\boldsymbol{\eta}))}}_{\bar{c}^6(\boldsymbol{\eta}, t)}, \quad \lambda_i \neq \lambda_j \tag{4.66}$$

in the case $\boldsymbol{\eta} < 0$ after the substitution $\boldsymbol{\xi} = \boldsymbol{\xi}_l(\boldsymbol{\eta})$ and in view of (4.63). Since the denominator in (2.153) cannot be zero, the same holds for the one in (4.66). Note that it is either possible to convert the BC (4.58d) into a condition for $\boldsymbol{G}_{\boldsymbol{\xi}}$ like in (2.153), or into a condition for $\boldsymbol{G}_{\boldsymbol{\eta}}$ as in (4.66).

For $\boldsymbol{\eta} \geq 0$, (4.58e) is differentiated w. r. t. $\boldsymbol{\eta}$ yielding

$$\begin{aligned}[\boldsymbol{G}_{\boldsymbol{\xi}}(\boldsymbol{\eta},\boldsymbol{\eta},t) + \boldsymbol{G}_{\boldsymbol{\eta}}(\boldsymbol{\eta},\boldsymbol{\eta},t) \\ = \tilde{z}_0 G_{ij-n,\xi}(\boldsymbol{\eta},\boldsymbol{\eta},t) + \tilde{z}_0 G_{ij-n,\eta}(\boldsymbol{\eta},\boldsymbol{\eta},t)]_{\substack{j>n \\ \lambda_i \geq \lambda_j \\ \lambda_j \geq \lambda_{j-n}}}\end{aligned}, \tag{4.67}$$

or from the perspective of the elements $j \leq n$,

$$\begin{aligned}[G_{ij+n,\xi}(\boldsymbol{\eta},\boldsymbol{\eta},t) + G_{ij+n,\eta}(\boldsymbol{\eta},\boldsymbol{\eta},t) \\ = \tilde{z}_0 \boldsymbol{G}_{\boldsymbol{\xi}}(\boldsymbol{\eta},\boldsymbol{\eta},t) + \tilde{z}_0 \boldsymbol{G}_{\boldsymbol{\eta}}(\boldsymbol{\eta},\boldsymbol{\eta},t)]_{\substack{j\leq n \\ \lambda_i \geq \lambda_{j+n} \\ \lambda_j \geq \lambda_j}}\end{aligned}, \tag{4.68}$$

when keeping in mind that $\xi_{ij-n}(\boldsymbol{\eta},\boldsymbol{\eta}) = \eta_{ij-n}(\boldsymbol{\eta},\boldsymbol{\eta}) = \boldsymbol{\eta}$. Solving (4.68) for $G_{ij+n,\eta}(\boldsymbol{\eta},\boldsymbol{\eta},t)$ and inserting the result into (4.58f) leads to

$$\left[\boldsymbol{J}(\boldsymbol{\eta},\boldsymbol{\eta},t) = \frac{1}{\tilde{z}_0} G_{ij+n,\xi}(\boldsymbol{\eta},\boldsymbol{\eta},t)\right]_{\substack{j\leq n \\ \lambda_i \geq \lambda_{j+n} \\ \lambda_j \geq \lambda_j \\ \boldsymbol{\eta} \geq 0}}. \tag{4.69}$$

Finally, (4.66), (4.69) and (4.58h) can replace $\boldsymbol{J}(\boldsymbol{\xi}_l(\boldsymbol{\eta}),\boldsymbol{\eta},t)$ in (4.64).

The last unknown in (4.64) is the derivative $\boldsymbol{G}_{\boldsymbol{\xi}}$ appearing in (4.69) and the right-hand side of (4.64a). Rather than applying integration by parts for its elimination, it is possible to use (4.62a) for its determination. Basically, this equation is only required in the case $j > n$ for the determination of $\boldsymbol{G}$ according to (4.62b). However, it may also be used in the case $j \leq n$, since the utilized BCs (4.58b)–(4.58d) are valid for all $j = 1,\ldots,2n$. Therefore, both $\boldsymbol{G}_{\boldsymbol{\xi}}(\boldsymbol{\eta},\boldsymbol{\eta},t) = \boldsymbol{H}(\boldsymbol{\eta},\boldsymbol{\eta},t)$ and $G_{ij+n,\xi}(\boldsymbol{\eta},\boldsymbol{\eta},t) = H_{ij+n}(\boldsymbol{\eta},\boldsymbol{\eta},t)$ in (4.69) can be replaced by (4.62a). Figure 4.5 shows the two different approaches for converting (4.58a) into integral equations in the cases $j \leq n$ and $j > n$. Due to the different order of integrations, the coupling of the kernel elements originating from the BCs (4.45e), (4.45f) is formulated as a coupling between solution-elements of the resulting integral equations (4.62) and (4.64). This coupling is equivalent to the coupling introduced by the reaction matrix A in the PDE (4.45a). Hence, the determined integral equations can be handled with the same method as in the unilateral case.

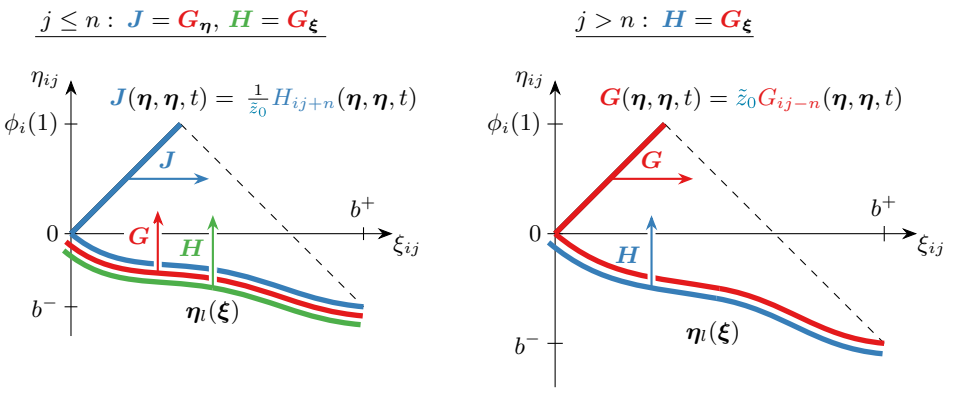

Figure 4.5: The spatial domains of the kernel equations (4.58) in the canonical coordinate systems $(\boldsymbol{\xi},\boldsymbol{\eta})$ for $\lambda_i > \lambda_j$ with the different directions of integration in the cases $j \leq n$ (left) leading to (4.64) and $j > n$ (right) resulting in (4.62) to account for the coupling BCs at $(\boldsymbol{\eta},\boldsymbol{\eta})$. The spatial domain is characterized by $b^- = \phi_i(1) - \phi_j(1)$, $b^+ = \phi_i(1) + \phi_j(1)$ and $\boldsymbol{\eta}_l(\boldsymbol{\xi})$. The bold coloured lines represent the BCs and the coloured arrows the respective directions of integration for the corresponding variables. Herein, the blue and red arrows symbolize the first and second integration, respectively, which highlights the reversal of the integration order for $j \leq n$ and $j > n$. For the left elements, the BC for $\boldsymbol{J}(\boldsymbol{\eta},\boldsymbol{\eta},t)$ depends on $H_{ij+n}(\boldsymbol{\eta},\boldsymbol{\eta},t)$ and for $j > n$, $\boldsymbol{G}(\boldsymbol{\eta},\boldsymbol{\eta},t)$ depends on $G_{ij-n}(\boldsymbol{\eta},\boldsymbol{\eta},t)$ for which both the respective integral equation can be substituted. In this way, the kernel equations can be converted into proper integral equations.

Inserting the BCs like described and introducing

$$\boldsymbol{H} = \boldsymbol{H}_1 + \int_{\boldsymbol{\eta}_l(\boldsymbol{\xi})}^{\boldsymbol{\eta}} \frac{\boldsymbol{s}}{4} \boldsymbol{G}_t(\boldsymbol{\xi},\bar{\eta},t)\mathrm{d}\bar{\eta} \tag{4.70}$$

$$\boldsymbol{J} = \boldsymbol{J}_1 + \int_{\boldsymbol{\xi}_l(\boldsymbol{\eta})}^{\boldsymbol{\xi}} \frac{\boldsymbol{s}}{4} \boldsymbol{G}_t(\boldsymbol{\xi},\bar{\eta},t)\mathrm{d}\bar{\eta} + \Big[\frac{1}{4\tilde{z}_0} \int_{\eta_{l,ij+n}(\boldsymbol{\eta})}^{\boldsymbol{\eta}} G_{ij+n,t}(\boldsymbol{\eta},\bar{\eta},t)\mathrm{d}\bar{\eta}\Big]_{\substack{\lambda_i \geq \lambda_j \\ \lambda_i \geq \lambda_{j+n} \\ \boldsymbol{\eta} \geq 0}}, \tag{4.71}$$

to produce double integrals for the time derivative of the kernel like in Section 2.5.5, the resulting *kernel integral equations* finally read

$$\boldsymbol{G} = \boldsymbol{G}_0 + \boldsymbol{F}_G[\boldsymbol{H}_1, J_1] \tag{4.72a}$$

$$\boldsymbol{H}_1 = \boldsymbol{H}_0 + \boldsymbol{F}_H[G, \boldsymbol{H}_1, J_1] \tag{4.72b}$$

$$j \leq n: \quad \boldsymbol{J}_1 = \boldsymbol{J}_0 + \boldsymbol{F}_J[G, H_1, J_1] \tag{4.72c}$$

with

$$\boldsymbol{G}_0 = \big[\bar{\boldsymbol{c}}^4(\boldsymbol{\xi},t)\big]_{\substack{\lambda_i=\lambda_j\\ j\le n}} + [\boldsymbol{g}(\boldsymbol{\eta},t)]_{\substack{j>n\\ (\lambda_i<\lambda_j)\vee(\lambda_i<\lambda_{j-n})\\ \boldsymbol{\eta}\ge 0}} + \big[\tilde{z}_0\bar{c}^4_{ij-n}(\boldsymbol{\eta},t)\big]_{\substack{j>n\\ \lambda_i\ge\lambda_j\\ \lambda_i=\lambda_{j-n}\\ \boldsymbol{\eta}\ge 0}} \tag{4.73a}$$

$$\begin{aligned}\boldsymbol{H}_0 = H_{0,ij} = [\tfrac{\bar{a}_\Sigma(\boldsymbol{\xi},\boldsymbol{\eta})}{4}\bar{\boldsymbol{c}}^4(\boldsymbol{\xi},t)]_{\substack{j\le n\\ \lambda_i=\lambda_j}} &+ [\bar{\boldsymbol{c}}^2(\boldsymbol{\xi},t)]_{\lambda_i=\lambda_j}\\ - [\tfrac{\bar{a}_\Sigma(\boldsymbol{\xi},0)}{4}\bar{\boldsymbol{c}}^4(\boldsymbol{\xi},t)]_{\lambda_i=\lambda_j} &+ [\tfrac{s\bar{a}_\Sigma(\boldsymbol{\xi},\boldsymbol{\eta})}{4}\boldsymbol{g}(\boldsymbol{\eta},t)]_{\substack{j>n\\ (\lambda_i<\lambda_{j-n})\vee(\lambda_i<\lambda_j)\\ \boldsymbol{\eta}\ge 0}}\\ + [\bar{\boldsymbol{c}}^1(\boldsymbol{\xi},t)]_{\lambda_i\ne\lambda_j} &+ [\tfrac{\bar{a}_\Sigma(\boldsymbol{\xi},\boldsymbol{\eta})}{4}\tilde{z}_0\bar{c}^4_{ij-n}(\boldsymbol{\eta},t)]_{\substack{\lambda_i\ge\lambda_j\\ \lambda_i=\lambda_{j-n}\\ \boldsymbol{\eta}\ge 0}}\end{aligned} \tag{4.73b}$$

$$\begin{aligned}\boldsymbol{J}_0 = [\bar{\boldsymbol{c}}^6(\boldsymbol{\eta},t)]_{\substack{i\ne j\\ \boldsymbol{\eta}<0}}&\\ + [\frac{1}{\tilde{z}_0}H_{0,ij+n}(\boldsymbol{\eta},\boldsymbol{\eta},t)]_{\substack{\lambda_i\ge\lambda_j\\ \lambda_i\ge\lambda_{j+n}\\ \boldsymbol{\eta}\ge 0}} &+ [\boldsymbol{g}(\boldsymbol{\eta},t)]_{\substack{(\lambda_i<\lambda_j)\vee(\lambda_i<\lambda_{j+n})\\ \boldsymbol{\eta}\ge 0}},\end{aligned} \tag{4.73c}$$

where $\bar{\boldsymbol{c}}^2(\boldsymbol{\xi},t) = \boldsymbol{c}^2(\boldsymbol{z}(\boldsymbol{\xi},0),t)$ with $\boldsymbol{K}_0(t) = 0$ (see (2.150c)) and $\bar{\boldsymbol{c}}^1(\boldsymbol{\xi},t) = \boldsymbol{c}^1(\boldsymbol{z}(\boldsymbol{\xi},\boldsymbol{\eta}_l(\boldsymbol{\xi})),t)$ (see (2.143d)), as well as

$$\begin{aligned}\boldsymbol{F}_G[\boldsymbol{H}_1,J_1] = \Big[\int_{\boldsymbol{\eta}_l(\boldsymbol{\xi})}^{\boldsymbol{\eta}}\boldsymbol{J}(\boldsymbol{\xi},\bar{\eta},t)\mathrm{d}\bar{\eta}\Big]_{j\le n} &+ \Big[\int_{\boldsymbol{\xi}_l(\boldsymbol{\eta})}^{\boldsymbol{\xi}}\boldsymbol{H}(\bar{\xi},\boldsymbol{\eta},t)\mathrm{d}\bar{\xi}\Big]_{j>n}\\ + \Big[\tilde{z}_0\int_{\eta_{l,ij-n}(\boldsymbol{\eta})}^{\boldsymbol{\eta}}J_{ij-n}(\boldsymbol{\eta},\bar{\eta},t)\mathrm{d}\bar{\eta}\Big]_{\substack{j>n\\ \lambda_i\ge\lambda_j\\ \lambda_i\ge\lambda_{j-n}\\ \boldsymbol{\eta}\ge 0}}&\end{aligned} \tag{4.74a}$$

$$\begin{aligned}\boldsymbol{F}_H[G,\boldsymbol{H}_1,J_1] = F_{H,ij}[G,\boldsymbol{H}_1,J_1] = \int_{\boldsymbol{\eta}_l(\boldsymbol{\xi})}^{\boldsymbol{\eta}}\Big(-\tfrac{\bar{a}_\triangle(\boldsymbol{\xi},\bar{\eta})}{4}\boldsymbol{H}(\boldsymbol{\xi},\bar{\eta},t)&\\ + \tfrac{s}{4}\big(\tilde{\boldsymbol{a}}(\boldsymbol{z}(\boldsymbol{\xi},\bar{\eta}),\boldsymbol{\zeta}(\boldsymbol{\xi},\bar{\eta}))+\mu\big)\boldsymbol{G}(\boldsymbol{\xi},\bar{\eta},t) + [\tfrac{s\bar{a}_\Sigma(\boldsymbol{\xi},\boldsymbol{\eta})}{4}\boldsymbol{J}(\boldsymbol{\xi},\bar{\eta},t)]_{j\le n}&\end{aligned}$$

$$+\tfrac{s}{4}\boldsymbol{\mathcal{A}}[G](\boldsymbol{\xi},\bar{\eta},t)\Big)\mathrm{d}\bar{\eta}+\Big[\tfrac{s\bar{a}_\Sigma(\boldsymbol{\xi},\boldsymbol{\eta})}{4}\int_{\boldsymbol{\xi}_l(\boldsymbol{\eta})}^{\boldsymbol{\xi}}\boldsymbol{H}(\bar{\xi},\boldsymbol{\eta},t)\mathrm{d}\bar{\xi}\Big]_{j>n}$$
$$+\Big[\tfrac{\bar{a}_\Sigma(\boldsymbol{\xi},\boldsymbol{\eta})\tilde{z}_0}{4}\int_{\eta_{l,ij-n}(\boldsymbol{\eta})}^{\boldsymbol{\eta}}J_{ij-n}(\boldsymbol{\eta},\bar{\eta},t)\mathrm{d}\bar{\eta}\Big]_{\substack{j>n\\ \lambda_i\geq\lambda_j\\ \lambda_i\geq\lambda_{j-n}\\ \boldsymbol{\eta}\geq 0}} \tag{4.74b}$$

$$\boldsymbol{F}_J[G,H_1,J_1]=\int_{\boldsymbol{\xi}_l(\boldsymbol{\eta})}^{\boldsymbol{\xi}}\Big(\tfrac{s\bar{a}_\Sigma(\bar{\xi},\boldsymbol{\eta})}{4}\boldsymbol{J}(\bar{\xi},\boldsymbol{\eta},t)-\tfrac{\bar{a}_\Delta(\bar{\xi},\boldsymbol{\eta})}{4}\boldsymbol{H}(\bar{\xi},\boldsymbol{\eta},t)$$
$$+\tfrac{s}{4}\boldsymbol{\mathcal{A}}[G](\bar{\xi},\boldsymbol{\eta},t)+\mu\boldsymbol{G}(\bar{\xi},\boldsymbol{\eta},t)\Big)\mathrm{d}\bar{\xi}$$
$$+\Big[+\frac{1}{\tilde{z}_0}F_{H,ij+n}[G,H_{1,ij+n},J](\boldsymbol{\eta},\boldsymbol{\eta},t)\Big]_{\substack{\lambda_i\geq\lambda_j\\ \lambda_i\geq\lambda_{j+n}\\ \boldsymbol{\eta}\geq 0}}, \tag{4.74c}$$

where $\boldsymbol{H}$ and $\boldsymbol{J}$ still need to be replaced by (4.71) and $\tilde{a}$ is given in (2.166). Note that $\boldsymbol{F}_G$ and $\boldsymbol{F}_H$ only contain J_{ij} with $j\leq n$, which is determined by (4.72c).

4.8 Volterra-Fredholm-kernel integral equations

By performing similar calculation as for the derivation of (4.45), it can be shown that (2.23) is mapped into the final target system (4.31) if the kernels $P(z,\zeta,t)$ and $Q(z,\zeta,t)$ are the solution of the *kernel equations*

$$\Lambda_r P_{zz}-(P\Lambda_l(\zeta))_{\zeta\zeta}=P_t \tag{4.75a}$$
$$(P_\zeta(z,1,t)\Lambda_l(1)+P(z,1,t)\Lambda_l'(1))S_r^0=0 \tag{4.75b}$$
$$P(z,1,t)\Lambda_l(1)S_d^0=0 \tag{4.75c}$$
$$P(0,\zeta,t)=0 \tag{4.75d}$$
$$P_z(0,\zeta,t)=0 \tag{4.75e}$$

$$\Lambda_r Q_{zz}-(Q\Lambda_r(\zeta))_{\zeta\zeta}=Q_t \tag{4.75f}$$
$$Q_\zeta(z,z,t)\Lambda_r+Q(z,z,t)\Lambda_r'+\Lambda_r Q'(z,z,t)\quad+\Lambda_r Q_z(z,z,t)=0 \tag{4.75g}$$
$$\Lambda_r Q(z,z,t)-Q(z,z,t)\Lambda_r=0 \tag{4.75h}$$
$$Q(0,0,t)=0 \tag{4.75i}$$

with the coupling BCs

$$P(z,0,t)\Lambda_l(0) - \tfrac{1}{z_0}Q(z,0,t)\Lambda_r(0) = \bar{A}_1^{lr} - \int_0^z Q\bar{A}_1^{lr}(\zeta,t)\mathrm{d}\zeta - \int_0^1 P\widetilde{A}_1^{l}(\zeta,t)\mathrm{d}\zeta + \tfrac{1}{z_0}\check{A}_1^{r}, \tag{4.75j}$$

$$Q_\zeta(z,0,t)\Lambda_r(0) + Q(z,0,t)\Lambda_r'(0) + P_\zeta(z,0,t)\Lambda_l(0) + P(z,0,t)\Lambda_l'(0) = -\bar{A}_0^{lr} + \int_0^z Q\bar{A}_0^{lr}(\zeta,t)\mathrm{d}\zeta + \int_0^1 P\widetilde{A}_0^{l}(\zeta,t)\mathrm{d}\zeta + \check{A}_0^{r}, \tag{4.75k}$$

in which $P(z,\zeta,t)$ is defined on the rectangular spatial domain $0 \leq z \leq 1$, $0 \leq \zeta \leq 1$ and $Q(z,\zeta,t)$ is defined on the triangular domain $0 \leq \zeta \leq z \leq 1$. Since the kernel equations for $P(z,\zeta,t)$ and $Q(z,\zeta,t)$ are coupled via the BCs (4.75j) and (4.75k), they cannot be solved independently, but a solution method needs to be derived allowing a simultaneous determination of both kernels. This challenging problem of solving coupled Fredholm-Volterra kernel equations is new in the backstepping framework and provides a general extension of the corresponding transformation presented in [20].

Since both PDEs (4.75a) and (4.75f) have the same spatial differential operator as (4.45a), the approach to solve (4.75) is the same as for the solution of (4.45). The main difference is that (4.75a) is now defined on a rectangular domain and that the coupling between the kernel elements only appears in the coupling BCs. Therefore, the component forms of the equations for both kernels are transformed into canonical coordinates in the next step, which can then be converted into integral equations.

4.8.1 Canonical kernel equations

The equivalent *component form* of (4.75) for the matrix elements $\boldsymbol{P}(z,\zeta,t) = P_{ij}(z,\zeta,t)$, $i,j = 1,\ldots,n$, reads

$$\lambda_i^r \boldsymbol{P}_{zz} - (\lambda_j^l(\zeta)\boldsymbol{P})_{\zeta\zeta} = \boldsymbol{P}_t \tag{4.76a}$$

$$(\lambda_j^l(1)\boldsymbol{P}_\zeta(z,1,t) + \lambda_j^{l\prime}(1)\boldsymbol{P}(z,1,t))S_r^0 = 0 \tag{4.76b}$$

$$\boldsymbol{P}(z,1,t)\lambda_j^l(1)S_d^0 = 0 \tag{4.76c}$$

$$\boldsymbol{P}(0,\zeta,t) = 0 \tag{4.76d}$$

$$\boldsymbol{P}_z(0,\zeta,t) = 0 \tag{4.76e}$$

and for $\boldsymbol{Q}(z,\zeta,t) = Q_{ij}(z,\zeta,t)$, $i,j = 1,\dots,n$,

$$\lambda_i^r \boldsymbol{Q}_{zz} - (\lambda_j^r(\zeta)\boldsymbol{Q})_{\zeta\zeta} = \boldsymbol{Q}_t \tag{4.77a}$$
$$\boldsymbol{Q}_\zeta(z,z,t)\lambda_j^r + \boldsymbol{Q}(z,z,t)\lambda_j^{r\prime} + \lambda_i^r \boldsymbol{Q}'(z,z,t) + \lambda_i^r \boldsymbol{Q}_z(z,z,t) = 0 \tag{4.77b}$$
$$(\lambda_i^r - \lambda_j^r)\boldsymbol{Q}(z,z,t) = 0 \tag{4.77c}$$
$$\boldsymbol{Q}(0,0,t) = 0. \tag{4.77d}$$

The coupling BCs for (4.76) and (4.77) are

$\underline{i \le j:}$

$$\begin{aligned}&\lambda_j^l(0)\boldsymbol{P}(z,0,t) - \tfrac{1}{\tilde{z}_0}\lambda_j^r(0)\boldsymbol{Q}(z,0,t)\\ &\quad = \bar{A}^{lr}_{1,ij} - \sum_{k=1}^n \int_0^z Q_{ik}\bar{A}^{lr}_{1,kj}(\zeta,t)\mathrm{d}\zeta\\ &\qquad - \sum_{k=1}^n \int_0^1 P_{ik}\widetilde{A}^{l}_{1,kj}(\zeta,t)\mathrm{d}\zeta\end{aligned} \tag{4.78a}$$

$$\begin{aligned}&\lambda_j^r(0)\boldsymbol{Q}_\zeta(z,0,t) + \lambda_j^{r\prime}\boldsymbol{Q}(z,0,t) + \lambda_j^l(0)\boldsymbol{P}_\zeta(z,0,t) + \lambda_j^{l\prime}(0)\boldsymbol{P}(z,0,t)\\ &\quad = -\bar{A}^{lr}_{0,ij} + \sum_{k=1}^n \int_0^z Q_{ik}\bar{A}^{lr}_{0,kj}(\zeta,t)\mathrm{d}\zeta + \sum_{k=1}^n \int_0^1 P_{ik}\widetilde{A}^{l}_{0,kj}(\zeta,t)\mathrm{d}\zeta\end{aligned} \tag{4.78b}$$

if the components of $\check{A}_i^r(z,t)$, $i = 0,1$, are chosen to be zero for $i \le j$ and

$\underline{i > j:}$

$$\begin{aligned}\check{A}^r_{0,ij}(z,t) &= \lambda_j^r(0)\boldsymbol{Q}_\zeta(z,0,t) + \lambda_j^{r\prime}(0)\boldsymbol{Q}(z,0,t) + \lambda_j^l(0)\boldsymbol{P}_\zeta(z,0,t)\\ &\quad + \lambda_j^{l\prime}(0)\boldsymbol{P}(z,0,t) + \bar{A}^{lr}_{0,ij} - \sum_{k=1}^n \int_0^z Q_{ik}\bar{A}^{lr}_{0,kj}(\zeta,t)\mathrm{d}\zeta\\ &\quad - \sum_{k=1}^n \int_0^1 P_{ik}\widetilde{A}^{l}_{0,kj}(\zeta,t)\mathrm{d}\zeta\end{aligned} \tag{4.79a}$$

$$\begin{aligned}\check{A}^r_{1,ij} &= \tilde{z}_0\Big(\lambda_j^l(0)\boldsymbol{P}(z,0,t) - \tfrac{1}{\tilde{z}_0}\lambda_j^r(0)\boldsymbol{Q}(z,0,t) - \bar{A}^{lr}_{1,ij}\\ &\quad + \sum_{k=1}^n \int_0^z Q_{ik}\bar{A}^{lr}_{1,kj}(\zeta,t)\mathrm{d}\zeta + \sum_{k=1}^n \int_0^1 P_{ik}\widetilde{A}^{l}_{1,kj}(\zeta,t)\mathrm{d}\zeta\Big).\end{aligned} \tag{4.79b}$$

Note that this degree of freedom is needed to ensure the well-posedness of the kernel equations for the Volterra-kernel $Q(z,\zeta,t)$, just like it was for

the backstepping kernel $K(z,\zeta.t)$ (see Section 4.7.1). Since both kernels of the second transformation (4.27) are of dimension $n \times n$, the strictly lower triangular well-posedness terms defined by (4.79) are enough to ensure well-posedness of the kernel equations. This is a simplification compared to the first transformation with Figure 4.4.

While the BVP (4.76a)–(4.76e) is already in the form which can be transformed into canonical coordinates, a further simplification is required for (4.77a)–(4.77d). In contrast to (4.45), the BVP for $\boldsymbol{Q}(z,\zeta,t)$ contains no inhomogeneity except in the coupling BCs (4.78a), (4.78b). Thus, (4.77b) can be rewritten for $\lambda_i^r = \lambda_j^r$ to obtain

$$\boldsymbol{Q}'(z,z,t) = -\frac{\lambda_i^{r\prime}}{2\lambda_i^r}\boldsymbol{Q}(z,z,t) \tag{4.80}$$

with the solution $\boldsymbol{Q}(z,z,t) = 0$ following from (4.77d). Due to (4.77c), $\boldsymbol{Q}(z,z,t) = 0$ also holds in the case $\lambda_i^r \neq \lambda_j^r$. Hence, the BVP (4.77a)–(4.77d) can be represented in simplified *component form* as

$$\lambda_i^r \boldsymbol{Q}_{zz} - (\lambda_j^r(\zeta)\boldsymbol{Q})_{\zeta\zeta} = \boldsymbol{Q}_t \tag{4.81a}$$
$$\boldsymbol{Q}(z,z,t) = 0 \tag{4.81b}$$
$$[\boldsymbol{Q}_z(z,z) = 0]_{\lambda_i^r \neq \lambda_j^r} \tag{4.81c}$$

complemented by the coupling BCs (4.78a), (4.78b).

To convert the kernel equations into their canonical form, the *canonical coordinates*

$$\xi_{ij}^P(z,\zeta) = \phi_i^r(z) + \phi_j^l(\zeta) \tag{4.82a}$$
$$\eta_{ij}^P(z,\zeta) = \phi_i^r(z) - \phi_j^l(\zeta) \tag{4.82b}$$
$$\xi_{ij}^Q(z,\zeta) = \tfrac{1}{2}(1-s)(\phi_i^r(1) + \phi_j^r(1)) + s(\phi_i^r(z) + \phi_j^r(\zeta)) \tag{4.82c}$$
$$\eta_{ij}^Q(z,\zeta) = -\tfrac{1}{2}(1-s)(\phi_i^r(1) - \phi_j^r(1)) + \phi_i^r(z) - \phi_j^r(\zeta) \tag{4.82d}$$

with

$$\phi_i^r(z) = \int_0^z \frac{\mathrm{d}\zeta}{\sqrt{\lambda_i^r(\zeta)}}, \quad \phi_i^l(z) = \int_0^z \frac{\mathrm{d}\zeta}{\sqrt{\lambda_i^l(\zeta)}}, \tag{4.83a}$$

$i = 1,\ldots,n$ and the corresponding inverses

$$z^P(\boldsymbol{\xi},\boldsymbol{\eta}) = (\phi_i^r)^{-1}(\tfrac{1}{2}(\boldsymbol{\xi}+\boldsymbol{\eta})) \tag{4.84a}$$
$$\zeta^P(\boldsymbol{\xi},\boldsymbol{\eta}) = (\phi_j^l)^{-1}(\tfrac{1}{2}(\boldsymbol{\xi}-\boldsymbol{\eta})) \tag{4.84b}$$

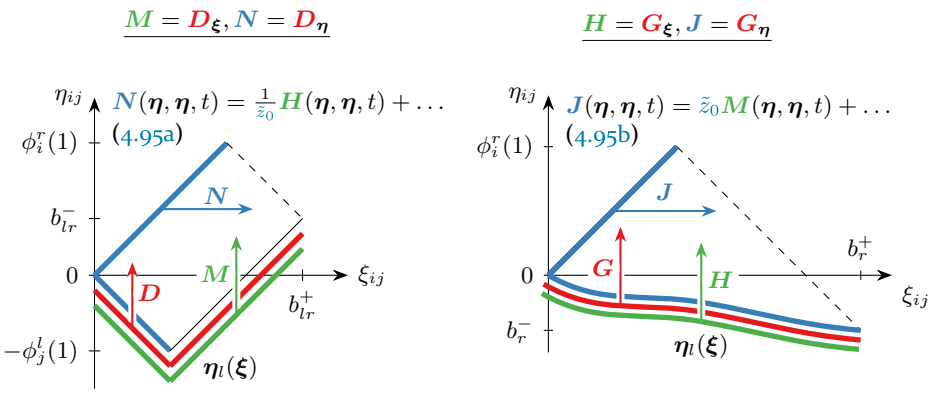

Figure 4.6: The spatial domains of the canonical kernel equations (4.89), (4.90) and (4.95) in the canonical coordinate systems (ξ, η) for $i \leq j$ with the utilized directions of integration. The spatial domains are characterized by $b_{lr}^- = \phi_i^r(1) - \phi_j^l(1)$, $b_{lr}^+ = \phi_i^r(1) + \phi_j^l(1)$, $b^- = \phi_i^r(1) - \phi_j^r(1)$, $b^+ = \phi_i^r(1) + \phi_j^r(1)$. In the left picture, the lower boundary $\eta_l(\xi)$ is given by (4.87). In the right picture, it is determined the same way as in Figure 4.5. The thick coloured lines represent the BCs and the coloured arrows the respective directions of integration for the corresponding variables. Herein, the blue and red arrows symbolize the first and second integration, respectively. For the left elements, the BC for $N(\eta,\eta,t)$ depends on $H(\eta,\eta,t)$ for which the respective integral equation can be substituted, which is symbolized by the green arrow. On the other hand, $J(\eta,\eta,t)$ depends on $M(\eta,\eta,t)$ for which again the corresponding integral equation can be substituted.

as well as

$$z^Q(\xi,\eta) = (\phi_i^r)^{-1}(\tfrac{1}{2}(s\xi+\eta) + \tfrac{1}{2}(1-s)\phi_i^r(1)) \tag{4.85a}$$
$$\zeta^Q(\xi,\eta) = (\phi_j^r)^{-1}(\tfrac{1}{2}(s\xi-\eta) + \tfrac{1}{2}(1-s)\phi_j^r(1)), \tag{4.85b}$$

respectively, are introduced along with the new kernel elements

$$\boldsymbol{D}(\xi,\eta,t) = D_{ij}(\xi^P(z,\zeta),\eta^P(z,\zeta),t) = \lambda_j^l(\zeta)\boldsymbol{P}(z,\zeta,t) \tag{4.86a}$$
$$\boldsymbol{G}(\xi,\eta,t) = G_{ij}(\xi^Q(z,\zeta),\eta^Q(z,\zeta),t) = \lambda_j^r(\zeta)\boldsymbol{Q}(z,\zeta,t). \tag{4.86b}$$

With the change of coordinates (4.82a), (4.82b), the boundaries of the original Fredholm-domain of $P(z,\zeta,t)$ are mapped as $(z,0) \to (\eta,\eta)$, $(0,\zeta) \to (\eta,-\eta)$, $(z,1) \to (\xi,\xi-2\phi_j^l(1))$ and $(1,\zeta) \to (\xi,2\phi_i^r(1)-\xi)$. Hence the lower boundary

$$\eta_l(\xi) = \eta_l^D(\xi) = \begin{cases} -\xi, & \xi \leq \phi_j^l(1) \\ \xi - 2\phi_j^l(1), & \xi > \phi_j^l(1) \end{cases} \tag{4.87}$$

consists of two parts in this case. Of course, the same is valid for the left boundary

$$\boldsymbol{\xi}_l(\boldsymbol{\eta}) = \boldsymbol{\xi}_l^D(\boldsymbol{\eta}) = \begin{cases} \boldsymbol{\eta}, & \boldsymbol{\eta} \geq 0 \\ -\boldsymbol{\eta}, & \boldsymbol{\eta} < 0. \end{cases} \tag{4.88}$$

The resulting spatial domains for $\boldsymbol{D}$ and $\boldsymbol{G}$ are depicted in Figure 4.6. Due to the fact that (4.81a) only contains the diffusion coefficients of the right subsystem, specifying the matrices $\check{A}_i^r(z,t)$, $i = 0, 1$, as strictly lower triangular according to (4.79) leads to a solvable BVP for $\boldsymbol{Q}(z,\zeta,t)$. To ensure the same shape of the spatial domain for all i, j (see Figure 4.5), s_{ij} according to (2.131) is introduced in the transformation (4.82c), (4.82d) like it was applied in (2.136). In contrast to that, (4.76a) contains λ_i^l and λ_j^r. In this case, $\lambda_i^r \leq \lambda_j^l$ for all $i, j = 1, \ldots, n$ due to the assumed sorting of the diffusion coefficients. Hence the resulting spatial domains for all kernel elements $\boldsymbol{D}$, i. e. the Fredholm part, already have a similar shape. Moreover, due to the types of BCs, it can be seen from the transformation into integral equations that the simple change of coordinates (4.82c), (4.82d) is sufficient for the Fredholm kernel.

Together, (4.82), (4.86) lead to the *canonical kernel equations*

$$\boldsymbol{D}_{\boldsymbol{\xi}\boldsymbol{\eta}} = \underbrace{-\frac{\bar{\boldsymbol{a}}_{\Delta}^{lr}}{4}\boldsymbol{D}_{\boldsymbol{\xi}} + \frac{\bar{\boldsymbol{a}}_{\Sigma}^{lr}}{4}\boldsymbol{D}_{\boldsymbol{\eta}}}_{\boldsymbol{\mathcal{A}}_{\boldsymbol{D}}[\boldsymbol{D}_{\xi},\boldsymbol{D}_{\eta}](\boldsymbol{\xi},\boldsymbol{\eta},t)} + \frac{1}{4}\boldsymbol{D}_t \tag{4.89a}$$

$$\boldsymbol{D}(\boldsymbol{\eta}, -\boldsymbol{\eta}, t) = 0 \tag{4.89b}$$

$$\boldsymbol{D}_{\boldsymbol{\eta}}(\boldsymbol{\eta}, -\boldsymbol{\eta}, t) = 0 \tag{4.89c}$$

$$\boldsymbol{D}_{\boldsymbol{\xi}}(\boldsymbol{\eta}, -\boldsymbol{\eta}, t) = 0 \tag{4.89d}$$

$$\left[\boldsymbol{D}_{\boldsymbol{\xi}}(\boldsymbol{\xi}, \boldsymbol{\xi} - 2\phi_j^l(1), t) = \boldsymbol{D}_{\boldsymbol{\eta}}(\boldsymbol{\xi}, \boldsymbol{\xi} - 2\phi_j^l(1), t)\right]_{\substack{\boldsymbol{\xi} > \phi_j^l(1) \\ S_r^0 e_j \neq 0}} \tag{4.89e}$$

$$\left[\boldsymbol{D}_{\boldsymbol{\xi}}(\boldsymbol{\xi}, \boldsymbol{\xi} - 2\phi_j^l(1), t) = -\boldsymbol{D}_{\boldsymbol{\eta}}(\boldsymbol{\xi}, \boldsymbol{\xi} - 2\phi_j^l(1), t)\right]_{\substack{\boldsymbol{\xi} > \phi_j^l(1) \\ S_d^0 e_j \neq 0}} \tag{4.89f}$$

and

$$\boldsymbol{G}_{\boldsymbol{\xi}\boldsymbol{\eta}} = \underbrace{-\frac{\bar{\boldsymbol{a}}_{\Delta}^{r}}{4}\boldsymbol{G}_{\boldsymbol{\xi}} + \frac{\boldsymbol{s}\bar{\boldsymbol{a}}_{\Sigma}^{r}}{4}\boldsymbol{G}_{\boldsymbol{\eta}}}_{\boldsymbol{\mathcal{A}}_{\boldsymbol{G}}[\boldsymbol{G}_{\xi},\boldsymbol{G}_{\eta}](\boldsymbol{\xi},\boldsymbol{\eta},t)} + \frac{\boldsymbol{s}}{4}\boldsymbol{G}_t \tag{4.90a}$$

$$\boldsymbol{G}(\boldsymbol{\xi}, \boldsymbol{\eta}_l(\boldsymbol{\xi}), t) = 0 \tag{4.90b}$$

$$\boldsymbol{G}_{\boldsymbol{\xi}}(\boldsymbol{\xi}, \boldsymbol{\eta}_l(\boldsymbol{\xi}), t) = 0 \tag{4.90c}$$

$$\left[\boldsymbol{G}_{\boldsymbol{\eta}}(\boldsymbol{\xi}_l(\boldsymbol{\eta}), \boldsymbol{\eta}, t) = 0\right]_{\boldsymbol{\eta} < 0} \tag{4.90d}$$

with the coupling BCs

$$\underline{\lambda_i^r \geq \lambda_j^r:}$$

$$\begin{aligned}\boldsymbol{D}(\boldsymbol{\eta},\boldsymbol{\eta},t) &= \tfrac{1}{\tilde{z}_0}\boldsymbol{G}(\boldsymbol{\eta},\boldsymbol{\eta},t) + \bar{\boldsymbol{A}}_1^{lr}(z^P(\boldsymbol{\eta},\boldsymbol{\eta}),t)\\ &- \int_0^{z^P(\boldsymbol{\eta},\boldsymbol{\eta})} \frac{1}{\lambda_k^r(\zeta)} G_{ik}((\xi_{ik}^Q,\eta_{ik}^Q)(z^P(\boldsymbol{\eta},\boldsymbol{\eta}),\zeta),t)\bar{A}_{1,kj}^{lr}(\zeta,t)\mathrm{d}\zeta\\ &- \int_0^1 \frac{1}{\lambda_k^l(\zeta)} D_{ik}((\xi_{ik}^P,\eta_{ik}^P)(z^P(\boldsymbol{\eta},\boldsymbol{\eta}),\zeta),t)\widetilde{A}_{1,kj}^{l}(\zeta,t)\mathrm{d}\zeta \end{aligned} \tag{4.91a}$$

$$\begin{aligned}\boldsymbol{G}_{\boldsymbol{\xi}}(\boldsymbol{\eta},\boldsymbol{\eta},t) - \boldsymbol{G}_{\boldsymbol{\eta}}(\boldsymbol{\eta},\boldsymbol{\eta},t) &= -\tilde{z}_0(\boldsymbol{D}_{\boldsymbol{\xi}}(\boldsymbol{\eta},\boldsymbol{\eta},t) - \boldsymbol{D}_{\boldsymbol{\eta}}(\boldsymbol{\eta},\boldsymbol{\eta},t))\\ &+ \int_0^{z^Q(\boldsymbol{\eta},\boldsymbol{\eta})} \frac{\sqrt{\lambda_j^r(0)}}{\lambda_k^r(\zeta)} G_{ik}((\xi_{ik}^Q,\eta_{ik}^Q)(z^Q(\boldsymbol{\eta},\boldsymbol{\eta}),\zeta),t)\bar{A}_{0,kj}^{lr}(\zeta,t)\mathrm{d}\zeta\\ &+ \int_0^1 \frac{\sqrt{\lambda_j^r(0)}}{\lambda_k^l(\zeta)} D_{ik}((\xi_{ik}^P,\eta_{ik}^P)(z^P(\boldsymbol{\eta},\boldsymbol{\eta}),\zeta),t)\widetilde{A}_{0,kj}^{l}(\zeta,t)\mathrm{d}\zeta\\ &- \sqrt{\lambda_j^r(0)}\bar{\boldsymbol{A}}_0^{lr}(z^P(\boldsymbol{\eta},\boldsymbol{\eta}),t), \end{aligned} \tag{4.91b}$$

where

$$\bar{\boldsymbol{a}}_\Delta^{lr} = \bar{\boldsymbol{a}}_\Delta^{lr}(\boldsymbol{\xi},\boldsymbol{\eta}) = \frac{\lambda_j^{l\prime}(\zeta)}{2\sqrt{\lambda_j^l(\zeta)}} - \frac{\lambda_i^{r\prime}(z)}{\sqrt{\lambda_i^r(z)}} \tag{4.92a}$$

$$\bar{\boldsymbol{a}}_\Sigma^{lr} = \bar{\boldsymbol{a}}_\Sigma^{lr}(\boldsymbol{\xi},\boldsymbol{\eta}) = \frac{\lambda_j^{l\prime}(\zeta)}{2\sqrt{\lambda_j^l(\zeta)}} + \frac{\lambda_i^{r\prime}(z)}{\sqrt{\lambda_i^r(z)}} \tag{4.92b}$$

and (z,ζ) are substituted by (4.84) as well as

$$\bar{\boldsymbol{a}}_\Delta^{r} = \bar{\boldsymbol{a}}_\Delta^{r}(\boldsymbol{\xi},\boldsymbol{\eta}) = \frac{\lambda_j^{r\prime}(\zeta)}{2\sqrt{\lambda_j^r(\zeta)}} - \frac{\lambda_i^{r\prime}(z)}{\lambda_i^r(z)} \tag{4.93a}$$

$$\bar{\boldsymbol{a}}_\Sigma^{r} = \bar{\boldsymbol{a}}_\Sigma^{r}(\boldsymbol{\xi},\boldsymbol{\eta}) = \frac{\lambda_j^{r\prime}(\zeta)}{2\sqrt{\lambda_j^r(\zeta)}} + \frac{\lambda_i^{r\prime}(z)}{\lambda_i^r(z)}, \tag{4.93b}$$

in which (z,ζ) are substituted by (4.85). To simplify the notation, the *summation convention*

$$\sum_{k=1}^{n}(c_k A_{ik} B_{kj}) =: c_k A_{ik} B_{kj} \tag{4.94}$$

is introduced in (4.91), which means that all expressions having k as an index, are summed from 1 to n. To be able to convert the canonical kernel equations into integral equations, the coupling BCs (4.91) require an additional

reformulation. To this end, (4.91a) is differentiated w. r. t. $\boldsymbol{\eta}$. The result is utilized in (4.91b) to obtain the BCs

$$\underline{i \leq j:}$$

$$\begin{aligned}\boldsymbol{D}_{\boldsymbol{\eta}}(\boldsymbol{\eta},\boldsymbol{\eta},t) = {}& \tfrac{1}{\tilde{z}_0}\boldsymbol{G}_{\boldsymbol{\xi}}(\boldsymbol{\eta},\boldsymbol{\eta},t) - \tfrac{1}{2\tilde{z}_0}\int_0^z \frac{\sqrt{\lambda_j^r(0)}}{\lambda_k^r(\zeta)} G_{ik}\bar{A}^{lr}_{0,kj}(\zeta,t)\mathrm{d}\zeta \\ & - \tfrac{1}{2\tilde{z}_0}\int_0^1 \frac{\sqrt{\lambda_j^r(0)}}{\lambda_k^l(\zeta)} D_{ik}\widetilde{A}^{l}_{0,kj}(\zeta,t)\mathrm{d}\zeta - \int_0^z \frac{s_{ik}G_{ik,\xi}+G_{ik,\eta}}{2\lambda_k^r(\zeta)}\bar{A}^{lr}_{1,kj}(\zeta,t)\mathrm{d}\zeta \\ & - \int_0^1 \frac{D_{ik,\xi}+D_{ik,\eta}}{2\lambda_k^l(\zeta)}\widetilde{A}^{l}_{1,kj}(\zeta,t)\mathrm{d}\zeta - \frac{\sqrt{\lambda_j^r(0)}}{2\tilde{z}_0}\bar{\boldsymbol{A}}_0^{lr} + \frac{\sqrt{\lambda_i^r(z)}}{2}(\bar{\boldsymbol{A}}_1^{lr})'\end{aligned} \tag{4.95a}$$

$$\begin{aligned}\boldsymbol{G}_{\boldsymbol{\eta}}(\boldsymbol{\eta},\boldsymbol{\eta},t) = {}& \tilde{z}_0\boldsymbol{D}_{\boldsymbol{\xi}}(\boldsymbol{\eta},\boldsymbol{\eta},t) - \int_0^z \frac{\sqrt{\lambda_j^r(0)}}{2\lambda_k^r(\zeta)} G_{ik}\bar{A}^{lr}_{0,kj}(\zeta,t)\mathrm{d}\zeta \\ & - \int_0^1 \frac{\sqrt{\lambda_j^r(0)}}{2\lambda_k^l(\zeta)} D_{ik}\widetilde{A}^{l}_{0,kj}(\zeta,t)\mathrm{d}\zeta + \int_0^z \frac{\tilde{z}_0(s_{ik}G_{ik,\xi}+G_{ik,\eta})}{2\lambda_k^r(\zeta)}\bar{A}^{lr}_{1,kj}(\zeta,t)\mathrm{d}\zeta \\ & + \int_0^1 \frac{\tilde{z}_0(D_{ik,\xi}+D_{ik,\eta})}{2\lambda_k^l(\zeta)}\widetilde{A}^{l}_{1,kj}(\zeta,t)\mathrm{d}\zeta + \frac{\sqrt{\lambda_j^r(0)}}{2}\bar{\boldsymbol{A}}_0^{lr} - \frac{\sqrt{\lambda_i^r(z)}}{2}(\bar{\boldsymbol{A}}_1^{lr})'.\end{aligned} \tag{4.95b}$$

In (4.95a) $z = z^P(\boldsymbol{\eta},\boldsymbol{\eta})$, G_{ik} and its derivatives are equipped with the spatial argument $(\xi_{ik}^Q,\eta_{ik}^Q)(z^P(\boldsymbol{\eta},\boldsymbol{\eta}),\zeta)$ and D_{ik} and its derivatives are evaluated at $(\xi_{ik}^P,\eta_{ik}^P)(z^P(\boldsymbol{\eta},\boldsymbol{\eta}),\zeta)$. In (4.75k) $z = z^Q(\boldsymbol{\eta},\boldsymbol{\eta})$, G_{ik} and its derivatives have the spatial argument $(\xi_{ik}^Q,\eta_{ik}^Q)(z^Q(\boldsymbol{\eta},\boldsymbol{\eta}),\zeta)$, and D_{ik} and its derivatives are evaluated at $(\xi_{ik}^P,\eta_{ik}^P)(z^Q(\boldsymbol{\eta},\boldsymbol{\eta}),\zeta)$.

By mapping $(\bar{\boldsymbol{A}}_1^{lr})'(z)$ in (4.49b) (see (4.17)) into canonical coordinates, it can be shown that it is a piecewise continuous function.

To uniquely determine the kernels, the BCs are complemented by the *artificial BCs*

$$\underline{i > j:}$$

$$\boldsymbol{D}_{\boldsymbol{\eta}}(\boldsymbol{\eta},\boldsymbol{\eta},t) = \boldsymbol{g}_D(\boldsymbol{\eta},t) \tag{4.96a}$$

$$\boldsymbol{G}_{\boldsymbol{\eta}}(\boldsymbol{\eta},\boldsymbol{\eta},t) = \boldsymbol{g}_G(\boldsymbol{\eta},t) \tag{4.96b}$$

(see (4.58g), (4.58h)) with the degrees of freedom $\boldsymbol{g}_D = g_{D,ij}$, $\boldsymbol{g}_G = g_{G,ij}$, $i,j = 1,\dots,n$, $g_{D,ij}(\cdot,t), g_{G,ij}(\cdot,t) \in C[0,\phi_i^r(1)]$ and $g_{D,ij}(z,\cdot), g_{G,ij}(z,\cdot) \in G_\alpha(\mathbb{R}^+_{t_0})$, $\alpha \in [1,2)$.

4.8.2 Kernel integral equations

Similar to Section 4.7.2, the canonical kernel equations (4.89), (4.90) with (4.95), (4.96) are converted into integral equations by formally integrating the PDEs (4.89a), (4.90a) w. r. t. $\boldsymbol{\xi}$ and $\boldsymbol{\eta}$. A BC at $(\boldsymbol{\xi}, \boldsymbol{\eta}) = (\boldsymbol{\eta}, \boldsymbol{\eta})$ for the respective derivative w. r. t. $\boldsymbol{\eta}$ is available for both $\boldsymbol{D}$ and $\boldsymbol{G}$ by (4.95). Together with (4.89c), (4.90d) and (4.91), $\boldsymbol{D}_{\boldsymbol{\eta}}(\boldsymbol{\xi}_l(\boldsymbol{\eta}), \boldsymbol{\eta}, t)$ and $\boldsymbol{G}_{\boldsymbol{\eta}}(\boldsymbol{\xi}_l(\boldsymbol{\eta}), \boldsymbol{\eta}, t)$ are known at the whole left boundary $\boldsymbol{\xi}_l(\boldsymbol{\eta})$ of the respective spatial domain (see Figure 4.6).

To get the BC for $\boldsymbol{D}$ and $\boldsymbol{G}$ on the lower boundary, note that $\boldsymbol{D}'(\boldsymbol{\xi}, \boldsymbol{\xi} - 2\phi_j^l(1), t) = \boldsymbol{D}_{\boldsymbol{\xi}}(\boldsymbol{\xi}, \boldsymbol{\xi} - 2\phi_j^l(1), t) + \boldsymbol{D}_{\boldsymbol{\eta}}(\boldsymbol{\xi}, \boldsymbol{\xi} - 2\phi_j^l(1), t)$. Inserting (4.89e) and integrating w. r. t. $\boldsymbol{\xi}$ then yields

$$\begin{aligned}\big[\boldsymbol{D}(\boldsymbol{\xi}, \boldsymbol{\xi} - 2\phi_j^l(1), t) = \underbrace{\boldsymbol{D}(\phi_j^l(1), -\phi_j^l(1), t)}_{\overset{(4.89c)}{=} 0} \\ + \int_{\phi_j^l(1)}^{\boldsymbol{\xi}} 2\boldsymbol{D}_{\boldsymbol{\eta}}(\bar{\xi}, \bar{\xi} - 2\phi_j^l(1), t)\mathrm{d}\bar{\xi}\big]_{\boldsymbol{\xi} > \phi_j^l(1)}. \quad (4.97)\end{aligned}$$

Together with (4.89c) and (4.90b), BCs $\boldsymbol{D}(\boldsymbol{\xi}, \boldsymbol{\eta}_l(\boldsymbol{\xi}), t)$ and $\boldsymbol{G}(\boldsymbol{\xi}, \boldsymbol{\eta}_l(\boldsymbol{\xi}), t)$ are available at the whole lower boundary $\boldsymbol{\eta}_l(\boldsymbol{\xi})$ of the respective spatial domain (see Figure 4.6).

Furthermore, note that even for the respective derivatives $\boldsymbol{D}_{\boldsymbol{\xi}}$ and $\boldsymbol{G}_{\boldsymbol{\xi}}$, a BC on the whole lower boundary of the domains is determined by (4.89d), (4.89e) and (4.90c).

Hence, introducing the variables

$$\boldsymbol{N}(\boldsymbol{\xi}, \boldsymbol{\eta}, t) = N_{ij}(\boldsymbol{\xi}, \boldsymbol{\eta}, t) \coloneqq \boldsymbol{D}_{\boldsymbol{\eta}}(\boldsymbol{\xi}, \boldsymbol{\eta}, t) \quad (4.98a)$$

$$\boldsymbol{J}(\boldsymbol{\xi}, \boldsymbol{\eta}, t) = J_{ij}(\boldsymbol{\xi}, \boldsymbol{\eta}, t) \coloneqq \boldsymbol{G}_{\boldsymbol{\eta}}(\boldsymbol{\xi}, \boldsymbol{\eta}, t) \quad (4.98b)$$

and

$$\boldsymbol{M}(\boldsymbol{\xi}, \boldsymbol{\eta}, t) = M_{ij}(\boldsymbol{\xi}, \boldsymbol{\eta}, t) \coloneqq \boldsymbol{D}_{\boldsymbol{\xi}}(\boldsymbol{\xi}, \boldsymbol{\eta}, t) \quad (4.99a)$$

$$\boldsymbol{H}(\boldsymbol{\xi}, \boldsymbol{\eta}, t) = G_{ij}(\boldsymbol{\xi}, \boldsymbol{\eta}, t) \coloneqq \boldsymbol{G}_{\boldsymbol{\xi}}(\boldsymbol{\xi}, \boldsymbol{\eta}, t), \quad (4.99b)$$

and inserting the BCs (4.89b)–(4.89e), (4.90b)–(4.90d), (4.97), (4.95) and (4.96), the *kernel integral equations* finally read

$$\boldsymbol{N} = \boldsymbol{N}_0 + \boldsymbol{F}_N[N, D, M, J, G, H] \tag{4.100a}$$
$$\boldsymbol{D} = \boldsymbol{D}_0 + \boldsymbol{F}_D[\boldsymbol{N}] \tag{4.100b}$$
$$\boldsymbol{M} = \boldsymbol{M}_0 + \boldsymbol{F}_M[N, D, M, J, G, H] \tag{4.100c}$$
$$\boldsymbol{J} = \boldsymbol{J}_0 + \boldsymbol{F}_J[N, D, M, J, G, H] \tag{4.100d}$$
$$\boldsymbol{G} = \boldsymbol{G}_0 + \boldsymbol{F}_G[\boldsymbol{J}] \tag{4.100e}$$
$$\boldsymbol{H} = \boldsymbol{H}_0 + \boldsymbol{F}_H[\boldsymbol{J}, \boldsymbol{H}] \tag{4.100f}$$

with

$$\boldsymbol{N}_0(\boldsymbol{\eta}, t) = [\boldsymbol{g}_D]_{\substack{i>j \\ \boldsymbol{\eta}\geq 0}} + \Big[\frac{\sqrt{\lambda_j^r(0)}}{2\tilde{z}_0}\bar{\boldsymbol{A}}_0^{lr} + \frac{\sqrt{\lambda_i^r}}{2}(\bar{\boldsymbol{A}}_1^{lr})'\Big]_{\substack{i\leq j \\ z=z^P(\boldsymbol{\eta},\boldsymbol{\eta}) \\ \boldsymbol{\eta}\geq 0}} \tag{4.101a}$$

$$\boldsymbol{D}_0(\boldsymbol{\xi}, t) = \Big[\int_{\phi_j^l(1)}^{\boldsymbol{\xi}} 2\boldsymbol{N}_0(\boldsymbol{\eta}_l(\bar{\xi}), t)\mathrm{d}\bar{\xi}\Big]_{\boldsymbol{\xi} > \phi_j^l(1)} \tag{4.101b}$$

$$\boldsymbol{M}_0(\boldsymbol{\xi}, t) = [\boldsymbol{N}_0(\boldsymbol{\eta}_l(\boldsymbol{\xi}), t)]_{\boldsymbol{\xi} > \phi_j^l(1)} \tag{4.101c}$$

$$\boldsymbol{J}_0(\boldsymbol{\eta}, t) = [\boldsymbol{g}_G]_{\substack{i>j \\ \boldsymbol{\eta}\geq 0}} + \Big[\tilde{z}_0\boldsymbol{M}_0(\boldsymbol{\eta}, t) + \frac{\sqrt{\lambda_j^r(0)}}{2}\bar{\boldsymbol{A}}_0^{lr} - \frac{\tilde{z}_0\sqrt{\lambda_i^r}}{2}(\bar{\boldsymbol{A}}_1^{lr})'\Big]_{\substack{i\leq j \\ z=z^Q(\boldsymbol{\eta},\boldsymbol{\eta}) \\ \boldsymbol{\eta}\geq 0}} \tag{4.101d}$$

$$\boldsymbol{G}_0 = \boldsymbol{H}_0 = 0 \tag{4.101e}$$

and

$$\begin{aligned}\boldsymbol{F}_N[N, D, M, J, G, H] = \Big[&\frac{1}{\tilde{z}_0}\int_{\boldsymbol{\eta}_l(\boldsymbol{\eta})}^{\boldsymbol{\eta}} \big(\boldsymbol{\mathcal{A}}_{\boldsymbol{G}}[\boldsymbol{H}, \boldsymbol{J}](\boldsymbol{\eta}, \bar{\eta}, t) + \frac{\boldsymbol{s}}{4}\boldsymbol{G}_t(\boldsymbol{\eta}, \bar{\eta}, t)\big)\mathrm{d}\bar{\eta} \\ &- \frac{1}{2\tilde{z}_0}\int_0^z \frac{\sqrt{\lambda_j^r(0)}}{\lambda_k^r(\zeta)} G_{ik}\bar{A}_{0,kj}^{lr}(\zeta, t)\mathrm{d}\zeta - \frac{1}{2\tilde{z}_0}\int_0^1 \frac{\sqrt{\lambda_j^r(0)}}{\lambda_k^l(\zeta)} D_{ik}\widetilde{A}_{0,kj}^{l}(\zeta, t)\mathrm{d}\zeta \\ &- \int_0^z \frac{s_{ik}H_{ik} + J_{ik}}{2\lambda_k^r(\zeta)}\bar{A}_{1,kj}^{lr}(\zeta, t)\mathrm{d}\zeta - \int_0^1 \frac{M_{ik} + N_{ik}}{2\lambda_k^l(\zeta)}\widetilde{A}_{1,kj}^{l}(\zeta, t)\mathrm{d}\zeta\Big]_{\substack{i\leq j \\ z=z^P(\boldsymbol{\eta},\boldsymbol{\eta}) \\ \boldsymbol{\eta}\geq 0}} \\ &+ \int_{\boldsymbol{\xi}_l(\boldsymbol{\eta})}^{\boldsymbol{\xi}} \big(\boldsymbol{\mathcal{A}}_{\boldsymbol{D}}[\boldsymbol{M}, \boldsymbol{N}](\bar{\xi}, \boldsymbol{\eta}, t) + \frac{1}{4}\boldsymbol{D}_t(\bar{\xi}, \boldsymbol{\eta}, t)\big)\mathrm{d}\bar{\xi}\end{aligned} \tag{4.102a}$$

$$\boldsymbol{F}_D[\boldsymbol{N}] = \int_{\boldsymbol{\eta}_l(\boldsymbol{\xi})}^{\boldsymbol{\eta}} \boldsymbol{N}(\boldsymbol{\xi}, \bar{\eta}, t)\mathrm{d}\bar{\eta} + \Big[\int_{\phi_j^l(1)}^{\boldsymbol{\xi}} 2\boldsymbol{F}_N(\bar{\xi}, \boldsymbol{\eta}_l(\bar{\xi}), t)\mathrm{d}\bar{\xi}\Big]_{\boldsymbol{\xi} > \phi_j^l(1)} \tag{4.102b}$$

$$\boldsymbol{F}_M[N,D,M,J,G,H] = [\boldsymbol{F}_N(\boldsymbol{\xi},\boldsymbol{\eta}_l(\boldsymbol{\xi}),t)]_{\boldsymbol{\xi}>\phi_j^l(1)} + \int_{\boldsymbol{\eta}_l(\boldsymbol{\xi})}^{\boldsymbol{\eta}} \big(\boldsymbol{\mathcal{A}_D}[\boldsymbol{M},\boldsymbol{N}](\boldsymbol{\xi},\bar{\eta},t) + \frac{1}{4}\boldsymbol{D}_t(\boldsymbol{\xi},\bar{\eta},t)\big)\mathrm{d}\bar{\eta} \tag{4.102c}$$

$$\begin{aligned}\boldsymbol{F}_J[N,D,M,J,G,H] = \Big[&\tilde{z}_0\boldsymbol{F}_M(\boldsymbol{\eta},\boldsymbol{\eta},t) - \frac{1}{2}\int_0^z \frac{\sqrt{\lambda_j^r(0)}}{\lambda_k^r(\zeta)} G_{ik}\bar{A}^{lr}_{0,kj}(\zeta,t)\mathrm{d}\zeta \\ &- \frac{1}{2}\int_0^1 \frac{\sqrt{\lambda_j^r(0)}}{\lambda_k^l(\zeta)} D_{ik}\widetilde{A}^{l}_{0,kj}(\zeta,t)\mathrm{d}\zeta + \int_0^z \frac{\tilde{z}_0(s_{ik}H_{ik}+J_{ik})}{2\lambda_k^r(\zeta)}\bar{A}^{lr}_{1,kj}(\zeta,t)\mathrm{d}\zeta \\ &+ \int_0^1 \frac{\tilde{z}_0(M_{ik}+N_{ik})}{2\lambda_k^l(\zeta)}\widetilde{A}^{l}_{1,kj}(\zeta,t)\mathrm{d}\zeta\Big]_{\substack{i\le j\\ z=z^Q(\boldsymbol{\eta},\boldsymbol{\eta})\\ \boldsymbol{\eta}\ge 0}} \\ &+ \int_{\boldsymbol{\xi}_l(\boldsymbol{\eta})}^{\boldsymbol{\xi}} \big(\boldsymbol{\mathcal{A}_G}[\boldsymbol{H},\boldsymbol{J}](\bar{\xi},\boldsymbol{\eta},t) + \frac{\boldsymbol{s}}{4}\boldsymbol{G}_t(\bar{\xi},\boldsymbol{\eta},t)\big)\mathrm{d}\bar{\xi}\end{aligned} \tag{4.102d}$$

$$\boldsymbol{F}_G[\boldsymbol{J}] = \int_{\boldsymbol{\eta}_l(\boldsymbol{\xi})}^{\boldsymbol{\eta}} \boldsymbol{J}(\boldsymbol{\xi},\bar{\eta},t)\mathrm{d}\bar{\eta} \tag{4.102e}$$

$$\boldsymbol{F}_H[\boldsymbol{J},\boldsymbol{H}] = \int_{\boldsymbol{\eta}_l(\boldsymbol{\xi})}^{\boldsymbol{\eta}} \big(\boldsymbol{\mathcal{A}_G}[\boldsymbol{H},\boldsymbol{J}](\boldsymbol{\xi},\bar{\eta},t) + \frac{\boldsymbol{s}}{4}\boldsymbol{G}_t(\boldsymbol{\xi},\bar{\eta},t)\big)\mathrm{d}\bar{\eta}. \tag{4.102f}$$

Therein, the integral equation (4.100a) has been utilized in (4.89e) and (4.97). Moreover, the arguments of D_{ik} and its derivatives as well as G_{ik} and its derivatives are the same as in (4.95).

Like in Section 4.7.2, the integral equations need to be reformulated in a way such that the time derivatives only appear under double integrals, which is important for the convergence proof, like in Section 2.5.6. To this end, the definitions

$$\boldsymbol{N} = \boldsymbol{N}_1 + \Big[\frac{\boldsymbol{s}}{4\tilde{z}_0}\int_{\boldsymbol{\eta}_l(\boldsymbol{\eta})}^{\boldsymbol{\eta}} \boldsymbol{G}_t(\boldsymbol{\eta},\bar{\eta},t)\mathrm{d}\bar{\eta}\Big]_{\substack{i\le j\\ \boldsymbol{\eta}\ge 0}} + \frac{1}{4}\int_{\boldsymbol{\xi}_l(\boldsymbol{\eta})}^{\boldsymbol{\xi}} \boldsymbol{D}_t(\bar{\xi},\boldsymbol{\eta},t)\mathrm{d}\bar{\xi} \tag{4.103a}$$

$$\begin{aligned}\boldsymbol{M} = \boldsymbol{M}_1 &+ \Big[\frac{\boldsymbol{s}}{4\tilde{z}_0}\int_{\boldsymbol{\eta}_l(\boldsymbol{\eta}_l(\boldsymbol{\xi}))}^{\boldsymbol{\eta}_l(\boldsymbol{\xi})} \boldsymbol{G}_t(\boldsymbol{\eta}_l(\boldsymbol{\xi}),\bar{\eta},t)\mathrm{d}\bar{\eta}\Big]_{\substack{i\le j\\ \boldsymbol{\eta}_l(\boldsymbol{\xi})\ge 0\\ \boldsymbol{\xi}>\phi_j^l(1)}} \\ &+ \Big[\frac{1}{4}\int_{\boldsymbol{\xi}_l(\boldsymbol{\eta}_l(\boldsymbol{\xi}))}^{\boldsymbol{\xi}} \boldsymbol{D}_t(\bar{\xi},\boldsymbol{\eta}_l(\boldsymbol{\xi}),t)\mathrm{d}\bar{\xi}\Big]_{\boldsymbol{\xi}>\phi_j^l(1)} + \frac{1}{4}\int_{\boldsymbol{\eta}_l(\boldsymbol{\xi})}^{\boldsymbol{\eta}} \boldsymbol{D}_t(\boldsymbol{\xi},\bar{\eta},t)\mathrm{d}\bar{\eta}\end{aligned} \tag{4.103b}$$

$$\boldsymbol{J} = \boldsymbol{J}_1 + \frac{\boldsymbol{s}}{4}\int_{\boldsymbol{\xi}_l(\boldsymbol{\eta})}^{\boldsymbol{\xi}} \boldsymbol{G}_t(\bar{\xi},\boldsymbol{\eta},t)\mathrm{d}\bar{\xi} + \Big[\frac{\boldsymbol{s}}{4}\int_{\boldsymbol{\eta}_l(\boldsymbol{\eta}_l(\boldsymbol{\eta}))}^{\boldsymbol{\eta}_l(\boldsymbol{\eta})} \boldsymbol{G}_t(\boldsymbol{\eta}_l(\boldsymbol{\eta}),\bar{\eta},t)\mathrm{d}\bar{\eta}\Big]_{\substack{i\le j\\ \boldsymbol{\eta}_l(\boldsymbol{\eta})\ge 0\\ \boldsymbol{\xi}>\phi_j^l(1)}}$$
$$+\Big[\frac{\tilde{z}_0}{4}\int_{\boldsymbol{\xi}_l(\boldsymbol{\eta}_l(\boldsymbol{\eta}))}^{\boldsymbol{\eta}} \boldsymbol{D}_t(\bar{\xi},\boldsymbol{\eta}_l(\boldsymbol{\eta}),t)\mathrm{d}\bar{\xi}\Big]_{\substack{i\le j\\ \boldsymbol{\eta}\ge 0\\ \boldsymbol{\xi}>\phi_j^l(1)}} \Big[+\frac{\tilde{z}_0}{4}\int_{\boldsymbol{\eta}_l(\boldsymbol{\eta})}^{\boldsymbol{\eta}} \boldsymbol{D}_t(\boldsymbol{\eta},\bar{\eta},t)\mathrm{d}\bar{\eta}\Big]_{\substack{i\le j\\ \boldsymbol{\eta}\ge 0}} \tag{4.103c}$$

$$\boldsymbol{H} = \boldsymbol{H}_1 + \int_{\boldsymbol{\eta}_l(\boldsymbol{\xi})}^{\boldsymbol{\eta}} \frac{\boldsymbol{s}}{4}\boldsymbol{G}_t(\boldsymbol{\xi},\bar{\eta},t)\mathrm{d}\bar{\eta} \tag{4.103d}$$

need to be inserted into (4.102) in a last step. Since this step does not change the types of spatial integrals appearing in the integral equations, the result is not written down here.

4.9 Successive approximations

The integral equations (4.72)–(4.74) and (4.100)– (4.102) are of a similar form as (2.170) and (2.171) and can now be solved by the *method of successive approximations*, i. e. by applying fixed-point iteration. This will finally lead to the following theorem.

Theorem 4.9.1 (Folding kernel equations)
The kernel equations (4.45) and (4.75) have a piecewise continuous solution with $K(z,\zeta,t)$ and $Q(z,\zeta,t)$ defined on $0 \le \zeta \le z \le 1$, $t \in \mathbb{R}_{t_0}^+$ and $P(z,\zeta,t)$ defined on $0 \le \zeta \le 1$, $0 \le z \le 1$, $t \in \mathbb{R}_{t_0}^+$.

Proof. To solve the integral equations via fixed-point iteration, the solutions are represented by

$$\boldsymbol{G} = \sum_{l=0}^{\infty}\Delta\boldsymbol{G}^l, \quad \boldsymbol{H}_1 = \sum_{l=0}^{\infty}\Delta\boldsymbol{H}_1^l, \quad \boldsymbol{J}_1 = \sum_{l=0}^{\infty}\Delta\boldsymbol{J}_1^l \tag{4.104}$$

$$\boldsymbol{D} = \sum_{l=0}^{\infty}\Delta\boldsymbol{D}^l, \quad \boldsymbol{M}_1 = \sum_{l=0}^{\infty}\Delta\boldsymbol{M}_1^l, \quad \boldsymbol{N}_1 = \sum_{l=0}^{\infty}\Delta\boldsymbol{N}_1^l \tag{4.105}$$

with $\Delta X^l = [\Delta X_{ij}^l]$, $X \in \{G, H_1, J_1, D, M_1, N_1\}$, which are calculated by the update law

$$\Delta\boldsymbol{X}^{l+1} = \boldsymbol{F}_X, \qquad \Delta\boldsymbol{X}^0 = \boldsymbol{X}_0, \tag{4.106}$$

$X \in \{G, H_1, J_1, D, M_1, N_1\}$ (see (2.178)), where the starting values $\boldsymbol{X}_0$ are given by (4.73), (4.101) and the iteration laws are given by (4.74) and (4.102), where the insertion of (4.103) is presumed.

Of course, the integral equations (4.72)–(4.74) and (4.100)–(4.102) differ from (2.170) and (2.171) due to the coupling BCs (4.45e), (4.45f) and (4.95). However, the types of the appearing terms in the integral operators (4.74) are the same as in (2.170c) and (2.171c), except for the terms with the Fredholm integrals and the boundary integral

$$\int_{\phi_j^l(1)}^{\xi} \dots \mathrm{d}\bar{\xi}. \tag{4.107}$$

Noting that inside the Fredholm integrals, $z = z(\boldsymbol{\eta}, \boldsymbol{\eta})$ always holds allows to derive similar estimates as in (B.12) for the new integral types. In addition, since

$$\max_{\lambda_i<\lambda_j} \max_{z} \sqrt{\frac{\lambda_i(z)}{\lambda_j(z)}} \geq \max_{\lambda_i^r<\lambda_j^r} \max_{z} \sqrt{\frac{\lambda_i^r(z)}{\lambda_j^r(z)}} \tag{4.108}$$

holds, the choice (2.191) is also sufficient for the decoupling kernel $\boldsymbol{G}(\boldsymbol{\xi}, \boldsymbol{\eta}, t)$ in (4.90), whose spatial domain only depends on the right diffusion coefficients λ_i^r. Consequently, uniform convergence of the series (4.104) follows by the same reasoning as the proof of Proposition 2.5.6 in Section 2.5.6.

Therefore, (4.104) provides the piecewise continuous solution of the integral equations (4.72) and the corresponding kernel equations. ■

Remark 4.9.2. The applied solvability proof provides the smoothness of the obtained solutions w. r. t. t in view of (2.190). However, it does not prove the Gevrey-property w. r. t. t, since (2.193) is only proved for $p = 0$. However, since evaluations of the kernel $K(z, \zeta, t)$ of (4.14) in the form of $\widetilde{A}_1(z, t)$ and $\widetilde{A}_0(z, t)$ serve as input parameters for the second transformation kernels (see (4.27)) in (4.95), this property is required for the convergence proof of the Volterra-Fredholm-transformation. In the scalar case, [100] proves this property. The application of these ideas to the present case, however, is beyond the scope of this thesis. ◁

4.10 Computation of the kernel derivatives

Similar to the unilateral case, the realization of the control law (4.37) requires the calculation of the derivatives $K_z(1, \zeta, t)$, $P_z(1, \zeta, t)$ and $Q_z(1, \zeta, t)$

according to (4.33), (4.32) and (4.30). In analogy to Section 2.6, they may be computed without performing a numerical differentiation.

Expressing the derivatives of the kernels in the canonical coordinates leads to (2.220) for $K(z,\zeta,t)$ as well as

$$\boldsymbol{Q}_z(z,\zeta,t) = \frac{\boldsymbol{s}}{\sqrt{\lambda_i^r(z)\lambda_j^r(\zeta)}}\boldsymbol{G}_{\boldsymbol{\xi}}(\boldsymbol{\xi},\boldsymbol{\eta},t) + \frac{1}{\sqrt{\lambda_i^r(z)\lambda_j^r(\zeta)}}\boldsymbol{G}_{\boldsymbol{\eta}}(\boldsymbol{\xi},\boldsymbol{\eta},t) \tag{4.109a}$$

$$\begin{aligned}\boldsymbol{Q}_\zeta(z,\zeta,t) = &-\frac{\lambda_j^{r\prime}(\zeta)}{\lambda_j^r(\zeta)}\boldsymbol{Q}(z,\zeta,t) + \frac{\boldsymbol{s}}{(\lambda_j^r)^{3/2}(\zeta)}\boldsymbol{G}_{\boldsymbol{\xi}}(\boldsymbol{\xi},\boldsymbol{\eta},t)\\ &-\frac{1}{(\lambda_j^r)^{3/2}(\zeta)}\boldsymbol{G}_{\boldsymbol{\eta}}(\boldsymbol{\xi},\boldsymbol{\eta},t)\end{aligned} \tag{4.109b}$$

and

$$\boldsymbol{P}_z(z,\zeta,t) = \frac{1}{\sqrt{\lambda_i^r(z)\lambda_j^l(\zeta)}}\boldsymbol{D}_{\boldsymbol{\xi}}(\boldsymbol{\xi},\boldsymbol{\eta},t) + \frac{1}{\sqrt{\lambda_i^r(z)\lambda_j^l(\zeta)}}\boldsymbol{D}_{\boldsymbol{\eta}}(\boldsymbol{\xi},\boldsymbol{\eta},t) \tag{4.110a}$$

$$\begin{aligned}\boldsymbol{P}_\zeta(z,\zeta,t) = &-\frac{\lambda_j^{l\prime}(\zeta)}{\lambda_j^l(\zeta)}\boldsymbol{P}(z,\zeta,t) + \frac{1}{(\lambda_j^l)^{3/2}(\zeta)}\boldsymbol{D}_{\boldsymbol{\xi}}(\boldsymbol{\xi},\boldsymbol{\eta},t)\\ &-\frac{1}{(\lambda_j^l)^{3/2}(\zeta)}\boldsymbol{D}_{\boldsymbol{\eta}}(\boldsymbol{\xi},\boldsymbol{\eta},t).\end{aligned} \tag{4.110b}$$

For the decoupling kernels (4.109) and (4.110), all kernel derivatives, $\boldsymbol{G}_{\boldsymbol{\xi}} = \boldsymbol{H}$, $\boldsymbol{D}_{\boldsymbol{\xi}} = \boldsymbol{M}$, $\boldsymbol{G}_{\boldsymbol{\eta}} = \boldsymbol{J}$ and $\boldsymbol{D}_{\boldsymbol{\eta}} = \boldsymbol{N}$ are available as the solution of the fixed-point iteration (4.104) and thus can directly be inserted.

For the backstepping kernel $\boldsymbol{K}(z,\zeta,t)$, the derivative $\boldsymbol{G}_{\boldsymbol{\xi}} = \boldsymbol{H}$ is available as the solution of the fixed-point iteration. Moreover, $\boldsymbol{G}_{\boldsymbol{\eta}} = \boldsymbol{J}$ is a result of the fixed-point iteration for $j \leq n$. Only for $j > n$, it still needs to be determined.

With the same approach as in Section 2.6, a formal integration of the PDE (4.58a) w. r. t. $\boldsymbol{\xi}$ leads to an integral equation for the unknown $\boldsymbol{G}_{\boldsymbol{\eta}}(\boldsymbol{\xi},\boldsymbol{\eta},t)$ and introduces the boundary terms $\boldsymbol{G}_{\boldsymbol{\eta}}(\boldsymbol{\xi}_l(\boldsymbol{\eta}),\boldsymbol{\eta},t)$. To substitute them by BCs, solve (4.67) for $\boldsymbol{G}_{\boldsymbol{\eta}}(\boldsymbol{\eta},\boldsymbol{\eta},t)$ to obtain

$$\Big[\boldsymbol{G}_{\boldsymbol{\eta}}(\boldsymbol{\eta},\boldsymbol{\eta},t) = \big(H_{ij-n}(\boldsymbol{\eta},\boldsymbol{\eta},t) + J_{ij-n}(\boldsymbol{\eta},\boldsymbol{\eta},t)\big)\tilde{z}_0 - \boldsymbol{H}(\boldsymbol{\eta},\boldsymbol{\eta},t)\Big]_{\substack{j\leq n\\ \lambda_i\geq\lambda_j\\ \lambda_i\geq\lambda_{j+n}\\ \boldsymbol{\eta}\geq 0}}, \tag{4.111}$$

where all terms on the right-hand side are available as solutions of the integral equations (4.72), except $J_{ij-n}(\boldsymbol{\eta},\boldsymbol{\eta},t)$ for which (4.69) is substituted.

Moreover, differentiating (4.58g) w. r. t. $\boldsymbol{\eta}$ yields

$$\Big[\boldsymbol{G}_{\boldsymbol{\eta}}(\boldsymbol{\eta},\boldsymbol{\eta},t)=\boldsymbol{g}_{\boldsymbol{\eta}}(\boldsymbol{\eta},t)-\boldsymbol{H}(\boldsymbol{\eta},\boldsymbol{\eta},t)\Big]_{\substack{j>n\\(\lambda_i<\lambda_j)\vee(\lambda_i<\lambda_{j-n})\\ \boldsymbol{\eta}\geq 0}} \tag{4.112}$$

after solving for $\boldsymbol{G}_{\boldsymbol{\eta}}(\boldsymbol{\eta},\boldsymbol{\eta},t)$. For $\boldsymbol{\eta}<0$, (4.66) can directly be inserted.

Finally, the following integral equation to determine $\boldsymbol{J}(\boldsymbol{\xi},\boldsymbol{\eta},t)$ for $j>n$ is obtained.

$$\boldsymbol{G}_{\boldsymbol{\eta}}=\boldsymbol{G}^0_{\boldsymbol{\eta}}+\boldsymbol{F}_{\boldsymbol{G}_{\boldsymbol{\eta}}}[\boldsymbol{G}_{\boldsymbol{\eta}}] \tag{4.113}$$

with

$$\begin{aligned}\boldsymbol{G}^0_{\boldsymbol{\eta}}=&\Big[\tilde{z}_0 H_{ij-n}(\boldsymbol{\eta},\boldsymbol{\eta},t)-\boldsymbol{H}(\boldsymbol{\eta},\boldsymbol{\eta},t)\Big]_{\substack{j\leq n\\ \lambda_i\geq\lambda_j\\ \lambda_i\geq\lambda_{j+n}\\ \boldsymbol{\eta}\geq 0}}\\
&+\Big[\big(-c^*_{1,ij-n}H_{ij-n}(\boldsymbol{\eta},\boldsymbol{\eta},t)+c^*_{2,ij-n}\boldsymbol{H}(\boldsymbol{\eta},\boldsymbol{\eta},t)\big)\tilde{z}_0\Big]_{\substack{j\leq n\\ \lambda_i\geq\lambda_j\\ \lambda_i\geq\lambda_{j+n}\\ \boldsymbol{\eta}\geq 0}}\\
&+\Big[\boldsymbol{g}_{\boldsymbol{\eta}}(\boldsymbol{\eta},t)-\boldsymbol{H}(\boldsymbol{\eta},\boldsymbol{\eta},t)\Big]_{\substack{j>n\\(\lambda_i<\lambda_j)\vee(\lambda_i<\lambda_{j-n})\\ \boldsymbol{\eta}\geq 0}}+[\bar{\boldsymbol{c}}^6(\boldsymbol{\eta},t)]_{\substack{\lambda_i\neq\lambda_j\\ \boldsymbol{\eta}<0}}\\
&+\int_{\boldsymbol{\xi}_l(\boldsymbol{\eta})}^{\boldsymbol{\xi}}\Big(\frac{\boldsymbol{s}}{4}\boldsymbol{\mathcal{A}}[G](\bar{\xi},\boldsymbol{\eta},t)-\frac{\bar{\boldsymbol{a}}_\Delta(\bar{\xi},\boldsymbol{\eta})}{4}\boldsymbol{H}(\bar{\xi},\boldsymbol{\eta},t)+\frac{\boldsymbol{s}}{4}\boldsymbol{G}_t(\bar{\xi},\boldsymbol{\eta},t)\Big)\mathrm{d}\bar{\xi}\end{aligned} \tag{4.114a}$$

and

$$\boldsymbol{F}_{\boldsymbol{G}_{\boldsymbol{\eta}}}[\boldsymbol{G}_{\boldsymbol{\eta}}]=\int_{\boldsymbol{\xi}_l(\boldsymbol{\eta})}^{\boldsymbol{\xi}}\frac{\boldsymbol{s}\bar{\boldsymbol{a}}_\Sigma(\bar{\xi},\boldsymbol{\eta},t)}{4}\boldsymbol{G}_{\boldsymbol{\eta}}(\bar{\xi},\boldsymbol{\eta},t)\mathrm{d}\bar{\xi}. \tag{4.114b}$$

Like in Section 2.6, this integral equation can be solved by fixed-point iteration, which can be shown to converge with the same methods as in Section 2.5.6, allowing a systematic computation of the kernel derivatives.

4.11 Backstepping observer design for in-domain measurements

In addition to the state feedback controller design, the folding technique is also applicable for the observer design. In particular, assuming bilateral

sensing, i. e. an available measurement at each boundary of the domain, applying the folding transformation of Section 4.2 leads to a system with unilateral measurement. The corresponding observer design is equal to the presented observer design method in Chapter 3.

Besides converting the bilateral actuation and sensing to one boundary, the folding transformation maps the folding point to a boundary, too. This allows to apply the method to systems with appropriate in-domain actuation or measurement. Depending on the type of interaction, this leads to a more or less complicated problem. In particular, if only the state w or its spatial derivative $w_{\check{z}}$ can be set or measured at a point, the folding approach leads to an underactuated problem for the resulting coupled PDEs which needs further investigations. A similar case has been studied in [103, 104, 108], where a scalar parabolic system has an in-domain actuation specifying a discontinuity of the spatial derivative. In this case, applying a Fredholm-type integral transformation allows to transform the in-domain input into a boundary actuation. On the other hand, [20] presented the observer design for a scalar parabolic system with a collocated in-domain measurement, i. e. both w and $w_{\check{z}}$ are measured at a point $\check{z}_m$ inside the domain. In this case, folding the system introduces no folding BCs and two independent observers can be designed for the left and right part w. r. t. $\check{z}_m$.

This design procedure can be applied for coupled parabolic PDEs as well and is therefore briefly presented in this section. To this end, consider the system (4.1) equipped with the measurement

$$y_m(t) = \begin{bmatrix} w(\check{z}_m, t) \\ w_{\check{z}}(\check{z}_m, t) \end{bmatrix}, \tag{4.115a}$$

where $\check{z}_m \in (0, 1)$ is the location of the measurement. Applying the folding transformation (4.4) with (4.3) and setting $\check{z}_0 = \check{z}_m$ leads to the folded representation

$$x_t(z,t) = \Lambda(z) x_{zz}(z,t) + A(z,t) x(z,t) \tag{4.116a}$$

$$x^l(0,t) = x^r(0,t) \tag{4.116b}$$

$$x^l_z(0,t) = -\check{z}_0 x^r_z(0,t) \tag{4.116c}$$

$$B_1^d x(1,t) + B_1^n x_z(1,t) = u(t) \tag{4.116d}$$

$$y_m(t) = \begin{bmatrix} y_{m,1}(t) \\ y_{m,2}(t) \end{bmatrix} = \begin{bmatrix} x^l(0,t) \\ \frac{-1}{\check{z}_0} x^l_z(0,t) \end{bmatrix} = \begin{bmatrix} x^r(0,t) \\ \frac{1}{1-\check{z}_0} x^r_z(0,t) \end{bmatrix} \tag{4.116e}$$

with Λ and A given in (4.8). Note that (4.116e) allows to write

$$x_z^l(0,t) = -\check{z}_0 y_{m,2}(t) \tag{4.117a}$$
$$x_z^r(0,t) = (1-\check{z}_0) y_{m,2}(t) \tag{4.117b}$$
$$x^l(0,t) = x^r(0,t) = y_{m,1}(t). \tag{4.117c}$$

Due to the block diagonal structure of A it is now possible to design two separate observers for the states x^l and x^r. Each observer is realized as

$$\hat{x}_t^b(z,t) = \Lambda^b(z)\hat{x}_{zz}^b(z,t) + A^b(z,t)\hat{x}(z,t) + L^b(z,t)(x_z^b(0,t) - \hat{x}_z^b(0,t)) \tag{4.118a}$$
$$x^b(0,t) = y_{m,1}(t) \tag{4.118b}$$
$$E^{b\top} B_1^d x(1,t) + E^{b\top} B_1^n x_z(1,t) = E^{b\top} u(t), \tag{4.118c}$$

$b \in \{l, r\}$, where $x_z^b(0,t)$ is replaced by the measurement according to (4.117),

$$E^{b\top} = \begin{cases} \begin{bmatrix} I & 0 \end{bmatrix}, & b = l \\ \begin{bmatrix} 0 & I \end{bmatrix}, & b = r \end{cases} \tag{4.119}$$

and $L^b(z,t) \in \mathbb{R}^{n\times n}$ are the observer gains to be determined.

Introducing the observer error $e^b(z,t) = x^b(z,t) - \hat{x}^b(z,t)$, $b \in \{l, r\}$ leads to the *observer error dynamics*

$$e_t^b(z,t) = \Lambda^b(z) e_{zz}^b(z,t) + A^b(z,t) e^b(z,t) - L^b(z,t) e_z^b(0,t) \tag{4.120a}$$
$$e^b(0,t) = 0 \tag{4.120b}$$
$$e^b(1,t) = 0. \tag{4.120c}$$

This is exactly the same as the observer error dynamics (3.8) derived in the unilateral case. Hence, the two observers (4.118) can be designed uniformly exponentially stable by the methods presented in Chapter 3.

4.12 Output feedback control

Section 3.8 has shown that an unilateral backstepping state feedback controller (2.27) can be combined with an unilateral backstepping observer (3.6) to a uniformly exponentially stable output feedback controller. The same is applicable when utilizing the bilateral controller (4.37) or the bilateral observers (4.118) or even both of them. In detail, the proof of the separation property shown in Section 3.8.2 still holds, since the dynamics of the closed-loop

system in backstepping coordinates is of the form (3.63)[1] in all cases. Note that in the case that both observer and controller are designed by the folding technique, the chosen folding point $\check{z}_0$ and the point of measurement $\check{z}_m$, which is the folding point for the observer design, are mutually independent. While in the controller design for bilateral actuation, it is a design parameter to distribute the control effort between the inputs, it is set by the sensor location in the case of an observer with in-domain measurement.

4.13 Academic examples

The following simulations demonstrate the effectiveness of the proposed folding approach.

Example 4.13.1 *(Bilateral state feedback controller).*
Consider a system (4.1) with the parameters

$$\check{\Lambda}(\check{z}) = \begin{bmatrix} \check{z}^2 + 2 & 0 \\ 0 & \mathrm{e}^{-\check{z}} + \frac{1}{2} \end{bmatrix} \tag{4.121a}$$

$$\check{A}(\check{z}, t) = \begin{bmatrix} 4.5 - 6\theta_{1.25}(t) & 2 + \cos(2\pi(\check{z} + t)) \\ (2 + \sin(2\pi(\check{z} + t))) & 3 - 4\theta_{1.25}(t), \end{bmatrix} \tag{4.121b}$$

$$t_0 = 0 \tag{4.121c}$$

where θ_ω is defined in (2.225) and the Neumann actuations

$$(\check{\theta}_0 w(t))(0) = w_{\check{z}}(0, t) = u_0(t) \tag{4.122a}$$

$$(\check{\theta}_1 w(t))(1) = w_{\check{z}}(1, t) = u_1(t), \tag{4.122b}$$

which is open-loop unstable. For this system, both an unilateral (2.27) and a bilateral (4.37) backstepping controller are designed with $\widetilde{A}(z, t) = \mu_c I = 8$ (see (2.23), (4.31)). In the unilateral case, only $u_1(t)$ is used as input, i. e. $u_0(t) = 0$ is set.

For the design of the bilateral controller, a numerical analysis of the possible folding points to ensure Assumption 2.1.6 reveals the intervals $\check{z}_0 \in I_i$, $I_1 = (0, 0.412)$, $I_2 = (0.424, 0488)$, $I_3 = (0.568, 0.596)$, $I_4 = (0.604, 1)$. The bilateral controller (4.37) is designed with the folding point $\check{z}_0 = 0.375$, which leads to descending diffusion coefficients $\lambda_1 > \ldots > \lambda_4$ in the folded system (4.12). In both uni- and bilateral cases, the additional degrees of freedom

[1] In particular, in the case of a bilateral backstepping controller, the PDE (3.63d) is replaced by (4.39a), i. e. the coupling term looks slightly different and the observer error dynamics enters the target system dynamics at both boundaries, but this has no impact on the proof.

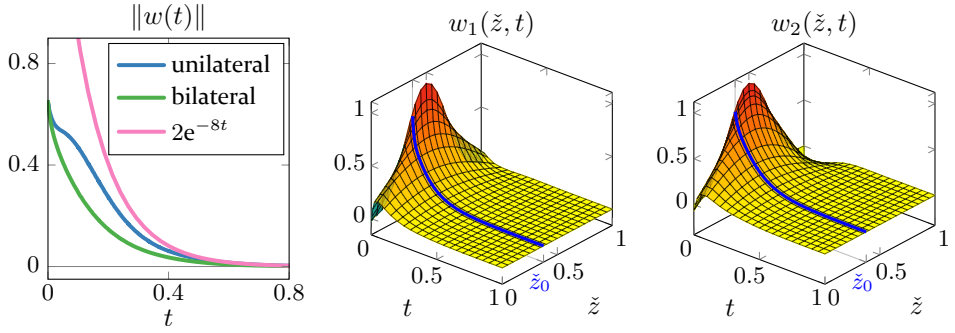

Figure 4.7: Weighted L_2-norms $\|w(t)\|$ of the closed-loop states with the unilateral and the bilateral controller and state profiles $w_i(\check{z},t)$, $i=1,2$ in the bilateral case. The pink curve is the desired decay rate $Me^{(\mu_{\max}-\mu_c)t}$ of the unilateral controller. The blue line in the state profiles marks the folding point $\check{z}_0=0.375$.

$\boldsymbol{g}(\boldsymbol{\eta},t)$ (see (2.150f), (4.58g) and (4.58h)) as well as $\boldsymbol{g}_D(\boldsymbol{\eta},t)$, $\boldsymbol{g}_G(\boldsymbol{\eta},t)$ (see (4.96)) are set to zero for simplicity.

The simulations are performed with the ICs $w_i(z,0)=\frac{3}{4}\sin(\pi z+2\pi)+\frac{1}{4}\cos(3\pi z+\frac{\pi}{2})$, $i=1,2$, which are compatible to the BCs.

The kernel equations (2.28), (4.45), (4.75) are discretized with 31 grid points in each direction z,ζ,t in the time interval $t\in[0,1]$ and the resulting canonical coordinates $(\boldsymbol{\xi},\boldsymbol{\eta})$ are resampled to have a maximum number of 80 nodes in $\boldsymbol{\xi}$-direction and the same tick length in $\boldsymbol{\eta}$. The fixed-point iterations (2.178) with (2.182) and (4.104) with (4.106), respectively, are stopped as soon as the maximum absolute increment drops below 10^{-5} (see Example 2.7.1), which occurs after 16 iteration steps in the unilateral case. In the bilateral case, the iteration terminates after 15 steps for (4.14) and after 18 steps for (4.27). Figure 4.7 shows the resulting weighted L_2-norms $\|w(t)\|$ of the closed-loop system's state in both cases together with the state profiles $w_i(\check{z},t)$, $i=1,2$ for the bilateral controller. With both controllers, the desired decay rate is achieved.

The corresponding control efforts are depicted in Figure 4.8. Obviously, the amplitude of the right input $u_1(t)$ can significantly be reduced by utilizing the bilateral controller.

It has been shown in [20] that by the choice of the folding point $\check{z}_0$, the distribution of the control efforts between the inputs can be adjusted. To verify this, Figure 4.9 shows the resulting control efforts for two different choices of $\check{z}_0=0.2$ and $\check{z}_0=0.85$. In the latter case, a reordering of the states of the folded system is required to achieve sorted diffusion coefficients. Moving the folding point to one end of the spatial domain decreases the

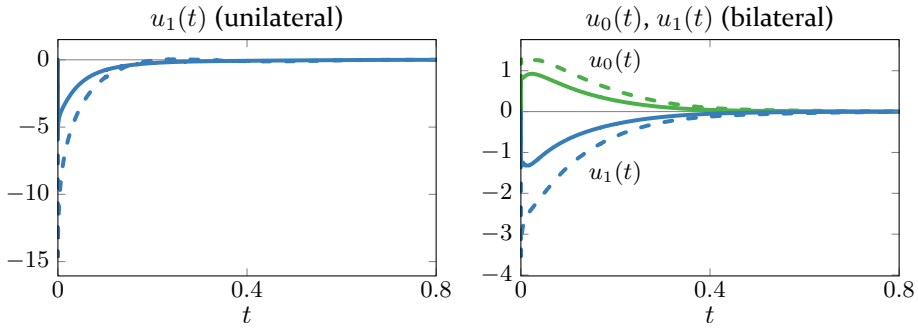

Figure 4.8: Control efforts of the unilateral controller (left) compared to the bilateral controller (right). The solid line corresponds to the first component $e_1^\top u_i(t)$, $i = 0, 1$ of the respective input and the dashed line to the second element $e_2^\top u_i(t)$, while the right input $u_1(t)$ is depicted in blue and the left input $u_0(t)$ in green.

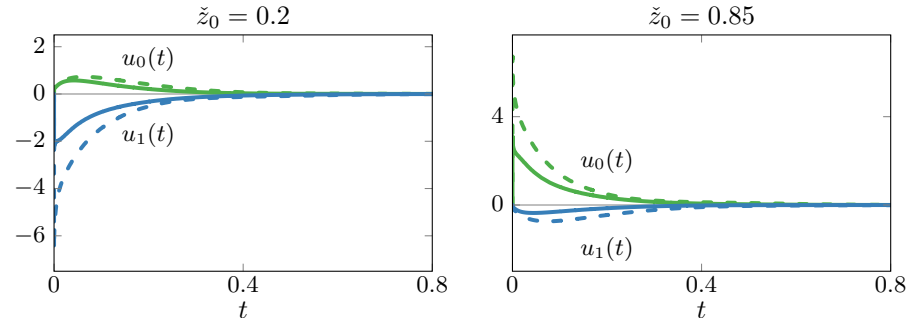

Figure 4.9: Control efforts for the different choices of $\check{z}_0 = 0.2$ (left) and $\check{z}_0 = 0.85$ (right). The solid lines correspond to the first components $e_1^\top u_i(t)$, $i = 0, 1$ of the respective input and the dashed lines to the second elements $e_2^\top u_i(t)$, while the right input $u_1(t)$ is depicted in blue and the left input $u_0(t)$ in green color.

control effort of the corresponding input and increases the one on the other side. Note that due to the space dependency of the system parameters, no symmetric behaviour w. r. t. $\check{z} = 0.5$ is expected. The corresponding state profiles $w_i(\check{z}, t)$, $i = 1, 2$, for the different folding points are depicted in Figure 4.10. It is verified that the folding point has a significant influence on the closed-loop state profiles. In [20] it is shown that the limit when moving the folding point to one boundary, e. g. $\check{z}_0 \to 0$ leads to the same controller as the unilateral design. In the present case, the control efforts resulting from the simulations suggest that this could hold as well. ◁

To verify the functionality of the folding observer introduced in Section 4.11, it is combined with the controller of Example 4.13.1 in the following example.

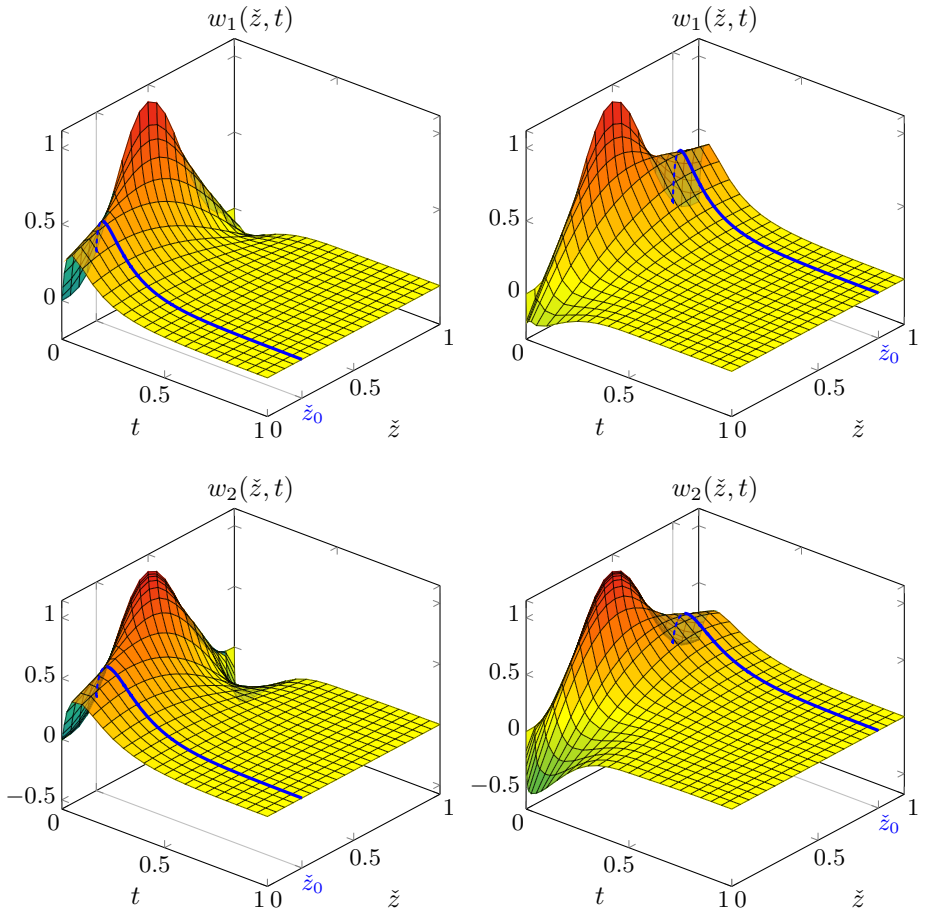

Figure 4.10: Closed-loop state profiles $w_i(\check{z},t)$, $i=1,2$, with the bilateral controller (4.37) and the two different folding points $\check{z}_0 = 0.2$ (left) and $\check{z}_0 = 0.85$ (right) in Example 4.13.1.

Example 4.13.2 *(Bilateral output feedback control).*
Consider the system (4.1) with the parameters (4.121), (4.122), introduced in Example 4.13.1. Now, an in-domain measurement

$$y_m(t) = (\theta_m w(t))(\check{z}_m) = \begin{bmatrix} w(0.7,t) \\ w_{\check{z}}(0.7,t) \end{bmatrix} \tag{4.123}$$

is available for the design of two observers according to (4.118). To this end, the decay parameter is set to $\widetilde{A}_o(z,t) = 16I$, i. e. $\mu_o = 16$ (see (3.10a) and (3.12)). The further degrees of freedom are set to zero for simplicity. The numerical parameters for the solution of the kernel equations are the same

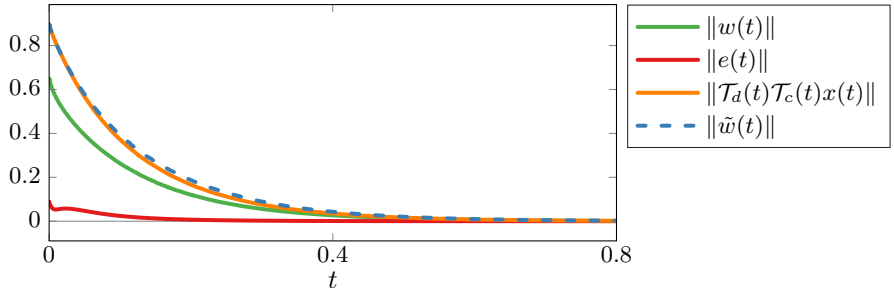

Figure 4.11: Weighted L_2-norms $\|w(t)\|$ and $\|e(t)\|$ of the closed-loop states and the observer error as well as the transformed states $\|\mathcal{T}_d(t)\mathcal{T}_c(t)x(t)\|$ and the target system states $\|\tilde{w}(t)\|$.

as in Example 4.13.1. Both observers are approximated with 11 points for each state. Not that due to the folding, twice the observer order compared to the unilateral observer in Chapter 3 results.

With the plant ICs $w_i(\check{z},0) = \frac{3}{4}\sin(\pi\check{z}+2\pi) + \frac{1}{4}\cos(3\pi\check{z}+\frac{\pi}{2})$, $i=1,2$, the initial measurement $y_m(0) \neq 0$. Therefore, the IC of the observer is set to

$$\hat{x}(z,0) = (2w_0 + w_0')z^3 - (3w_0 - 2w_0')z^2 + w_0'z + w_0 \tag{4.124a}$$

$$w_0 = \begin{bmatrix} y_{m,1}(0) \\ y_{m,1}(0) \end{bmatrix} \tag{4.124b}$$

$$w_0' = \begin{bmatrix} -\check{z}_m y_{m,2}(0) \\ (1-\check{z}_m) y_{m,2}(0) \end{bmatrix}, \tag{4.124c}$$

compatible to the measurement and the BCs.

For a proper validation of the simulation results, a simulation of the target system is performed. To this end, the closed-loop target dynamics (cf. (3.63), (4.31)) are simulated. The resulting weighted L_2-norms of the closed-loop state $\|w(t)\|$, the observer error $\|e(t)\|$, as well as the transformed folded system states $\|\mathcal{T}_d(t)\mathcal{T}_c(t)x(t)\|$ and the target system's state $\|\tilde{w}(t)\|$ are depicted in Figure 4.11. Therein, the observer error $e(z,t)$ is a vector containing the observer errors $e^b(z,t)$, $b \in \{l,r\}$ of both observers. Like in Example 3.8.6, the observer converges faster than the system states due to its faster parameterization. Due to the observer IC, the observer error amplitude is comparably low. Despite the usage of the observer, the closed-loop system is uniformly exponentially stabilized and the closed-loop dynamics in backstepping coordinates coincides with the desired dynamics except for numerical deviations, despite the comparably low observer order.

Depending on the location of the measurement, the observer error has a different spatial distribution. Intuitively, the observer error at a certain point gets smaller as its distance to the measurement point $\check{z}_m$ gets smaller. Hence, if the measurement point $\check{z}_m$ can be chosen freely, a small observer error can be achieved in a desired region around $\check{z}_m$. To validate this, a further simulation with a measurement at $\check{z}_m = 0.3$ is performed. Figure 4.12 shows the resulting reconstructed observer states $\hat{w}(\check{z}, t)$ in both cases. They are obtained by unfolding the reconstructed states $\hat{x}(z, t)$. Due to the fast parameterization of the observers with $\mu_o = 16$, both converge to the actual states quite fast so that their profiles look similar. To see the difference, Figure 4.13 shows the corresponding observer errors $\bar{e}(w, t) = w(\check{z}, t) - \hat{w}(\check{z}, t)$ for $t \in [0, 0.2]$. As expected, the observer error at the measurement point is exactly zero. Moreover, the observer error in the smaller part of the domain is a lot smaller than in the larger part. ◁

Remark 4.13.3. Though it looks like the observer error $\bar{e}(\check{z}, t)$ might have a defect of differentiability at the point of the measurement $\check{z}_m$, this is only a matter of resolution. In detail, selecting higher orders for the observer-approximation and higher printing-resolutions, the smoothness of the solution becomes apparent. Since low-order observers are desirable in practice, the observer functionality is demonstrated with the low order of 11 nodes per observer state. ◁

4.14 Concluding remarks

By utilizing the folding-technique, a system with bilateral actuation can be transformed into a representation with unilateral actuation, allowing to apply the usual backstepping transformation. Due to the special folding-BCs ensuring the regularity of the solution, the kernel equations get an additional boundary coupling, which requires a new solution strategy. Using a different sequence of integration for the coupled solution elements allows to transform the kernel equations into integral equations with usual couplings. Thus, they can be solved by the method of successive approximations like in the unilateral case.

To obtain a target system where the uniform stability margin can explicitly be assigned like in the unilateral case, a second, Volterra-Fredholm-type transformation is utilized. The appearing coupled kernel equations can be converted into integral equations again and solved by fixed-point iteration.

The choice of the folding point is restricted to ensure non-intersecting diffusion coefficients in the folded system. In any case, there exist suitable

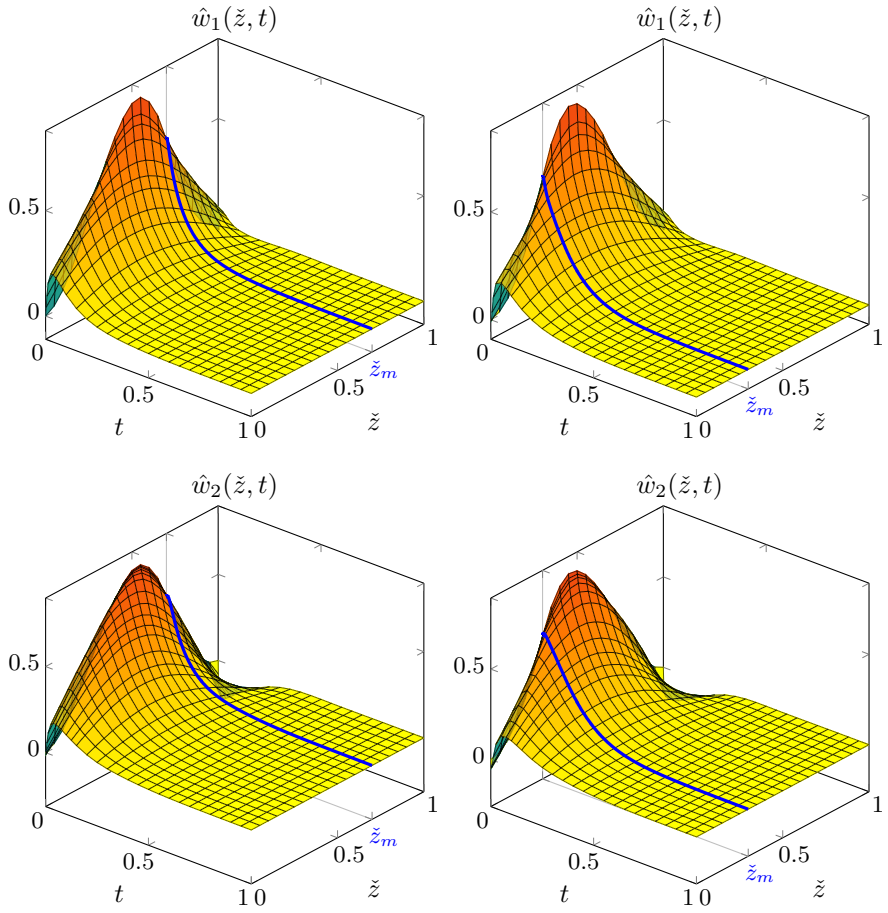

Figure 4.12: Reconstructed observer states $\hat{w}(\check{z},t)$ for two different measurement points $\check{z}_m = 0.7$ and $\check{z}_m = 0.3$.

folding points both small and large enough so that the distribution of the control effort between left and right inputs can be adjusted by the choice of the folding point. Though the restriction will be rather small in most cases (see Example 4.13.1), it can be completely removed once the backstepping method is established for intersecting diffusion coefficients, which is an interesting topic for future research.

By the help of the folding technique, it is possible to design observers for systems with bilateral or in-domain sensing. If both the state and its spatial derivative are available as in-domain measurement, the latter case leads to the design of two independent backstepping observers where the results of the

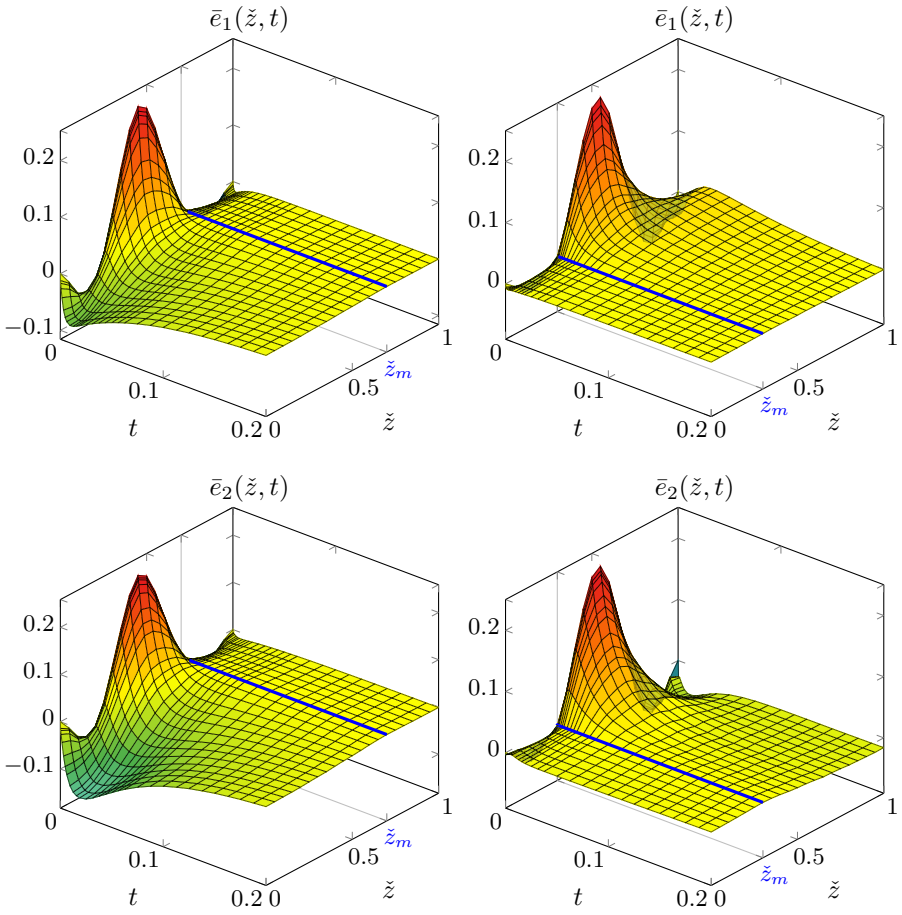

Figure 4.13: Corresponding observer errors $\bar{e}(\check{z},t)$ for two different measurement points $\check{z}_m = 0.7$ and $\check{z}_m = 0.3$.

unilateral case can be applied. For future research, it is of particular interest if the observer design is possible with only a single in-domain measurement, possibly by applying the ideas of [103, 108].

In the utilized implementation, both observers (4.118) are realized with the same approximation order. For the original domain $\check{z}$, this means that the left and right part w. r. t. $\check{z}_m$ implicitly have different resolutions. The effect of using different observer approximation orders for both parts of the domain, for instance in relation of the size of the domains, could further be investigated.

Simulation results confirm the applicability of the proposed design method and the possibility to reduce the control effort for one input compared to unilateral actuation.

5 Further research topics

The presented systematic design methods for the boundary control of coupled parabolic systems with space and time dependent coefficients and both uni- and bilateral actuation can be the starting point for plenty of further research. While observer-based output regulation [114] and robust output regulation by state feedback control [115] have already been considered in the time-invariant case, their extension to time-varying parameters could rise new obstacles. On the other hand, there is a large field of control techniques that have not even been considered for coupled parabolic systems. For instance adaptive control, which is already combined with backstepping in the scalar case [82]. Another interesting field are coupled parabolic PDEs on higher-dimensional spatial domains, for which the results in [72] are of interest. The backstepping method for coupled parabolic systems with arbitrarily intersecting diffusion coefficients could utilize [88] as a starting point. A very active research topic are systems where a certain type of PDE is either coupled by one ore more ODEs, or even a different type of PDE. So far, there are only a few results for coupled parabolic PDEs in this direction [31] without consideration of time-varying coefficients.

The extension of the flatness-based trajectory planning and its combination with backstepping to flatness-based tracking control [73] to coupled parabolic systems should directly be possible due to the simple structure of the target system, at least in the unilateral case.

Another very interesting open research field are *underactuated* systems. That means that the number of inputs is less than the number of PDEs and occurs for example in chemical reactors with higher reaction order. When applying the backstepping method in this case, it is no more possible to prescribe a cascaded target system. Instead, a boundary coupling must be allowed due to the missing control inputs. Though this coupling is different to the one in the folding case, the obtained results may be utilized for further investigations.

A Relatively bounded operators

Considering abstract IVPs

$$\dot{x}(t) = \mathcal{A}x(t), \quad x(0) = x_0 \in D(\mathcal{A}) \tag{A.1}$$

with the operator $\mathcal{A}$ on the domain $D(\mathcal{A}) \subset X$ requires to choose a suitable state space X which is a Hilbert space. For parabolic systems, $X = L_2(0,1)$ turns out to be the correct choice to ensure a well-posed IVP. Consequently, convergence properties like for exponentially stable systems

$$\|x(t)\| \leq M\mathrm{e}^{-\mu t}\|x_0\| \tag{A.2}$$

are only stated in terms of the norm induced by the inner product in X. The L_2-norm, however, is invariant w. r. t. changes in zero-sets of the functions. That is, there are infinitely many functions having the same L_2-norm but may have different values at single points of their domain. For this reason, the exponential stability in the L_2-norm allows no deduction of the state's value at a single point z_0. In practice, it is known that parabolic systems, particularly the diffusion operator has a smoothing effect on the solution. Therefore, it is intuitive that if the system is stable, it will also be pointwise stable. The proof of this is in general a challenging task, but turns out to be simple if the system operator is analytic, as is mostly the case when considering parabolic systems. This will be shown in Appendix A.2.

In the case of distributed parameters systems, the system operator is in general unbounded, which leads to many differences in the mathematical treatment compared to finite-dimensional systems.

Hereby, an operator is called unbounded, if it is not bounded according to the following definition [26, Definition A.3.8].

Definition A.1 (Bounded operators). An operator $\mathcal{B} : D(\mathcal{B}) \subset X \to Y$, where X and Y are normed linear spaces is called *bounded*, if there exists a $\bar{c} \in \mathbb{R}$ such that

$$\|\mathcal{B}x\| \leq \bar{c}\|x\| \tag{A.3}$$

for all $x \in D(\mathcal{B})$. ◀

An important subclass of unbounded operators are those which are *relatively bounded* w. r. t. an unbounded operator $\mathcal{A}$. They can be imagined as being less or equally „unbounded“ as $\mathcal{A}$. In most cases, a general statement concerning all unbounded operators is hardly possible. Luckily, the majority of interesting operators (such as the point evaluation) turn out to be at least relatively bounded w. r. t. the system operator. This property is stated in the following definition [59].

Definition A.2 (Relatively bounded operators). An operator $\mathcal{B}$ is relatively bounded w. r. t. $\mathcal{A}$, or simply $\mathcal{A}$-bounded ($D(\mathcal{A}) \subset D(\mathcal{B})$) if there exist non-negative numbers a, $b \in \mathbb{R}$ such that

$$\|\mathcal{B}h\| \leq a\|\mathcal{A}h\| + b\|h\|, \quad h \in D(\mathcal{A}). \tag{A.4}$$

The greatest lower bound of all a for which (A.4) holds, is called $\mathcal{A}$-bound of $\mathcal{B}$. ◀

Remark A.3. Even if an operator has the relative bound 0, there is a big difference to a bounded operator. In particular, it is not possible to write (A.3) because typically b in (A.4) tends to infinity as a tends to zero. ◁

A.1 Relative boundedness of evaluation operators

In the framework of control, point measurements either at the boundaries or in the domain appear frequently, either during the observer design (point measurement) or the output regulation (point-like control outputs) as well as in form of the coupling between subsystems. It turns out that both the evaluation of a function at a specific point $h(z_0)$, $z_0 \in [0, 1]$ and the evaluation of the spatial derivative at a specific point $h'(z_0)$, $z_0 \in [0, 1]$ correspond to relatively bounded operators w. r. t. the diffusion-reaction-operator, which is stated in the following lemma.

Lemma A.1.1. *Let*

$$\mathcal{B}_1 h = h(z_0), \quad \mathcal{B}_2 h = h'(z_0), \quad z_0 \in D(h) \tag{A.5}$$

and

$$\mathcal{A}h = \lambda h'' - \mu h, \quad \lambda(z) > 0,\ \mu \in \mathbb{R} \tag{A.6}$$

with $D(\mathcal{A}) \subset D(\mathcal{B}_1)$, $D(\mathcal{A}) \subset D(\mathcal{B}_2)$ and $h \in D(\mathcal{A})$ on $z \in [0, 1]$. The operators $\mathcal{B}_1$ and $\mathcal{B}_2$ are $\mathcal{A}$-bounded with $\mathcal{A}$-bound zero.

Proof. In [59, Chap. IV, Sec. 1], it is shown that with the equality

$$h' = Gh'' + Hh, \tag{A.7}$$

the first order derivative can be expressed dependent on the second order derivative and the actual function by means of the (bounded) integral operators G and H. Thereby, (A.7) holds for all z over which h is defined so that it can also be evaluated at a certain point z_0. The result

$$h'(z_0) = \widetilde{G}h'' + \widetilde{H}h \tag{A.8}$$

again contains (bounded) integral operators $\widetilde{G}$ and $\widetilde{H}$, which depend on a positive number n. Thus, $|h'(z_0)|$ can be estimated by

$$\begin{aligned} |h'(z_0)| &= |\widetilde{G}h'' + \widetilde{H}h| \\ &\leq |\widetilde{G}h''| + |\widetilde{H}h| \\ &= \|\widetilde{G}h''\| + \|\widetilde{H}h\| \\ &\leq \|\widetilde{G}\|\|h''\| + \|\widetilde{H}\|\|h\|, \end{aligned} \tag{A.9}$$

where

$$\|\widetilde{G}\| \leq \frac{1}{n-1} \tag{A.10a}$$

$$\|\widetilde{H}\| \leq \frac{2n(n+1)}{n-1} \tag{A.10b}$$

for arbitrary $n > 1$ follows from [59]. Rather than evaluating (A.7) at a point z_0, it is also possible to consider its norm

$$\begin{aligned} \|h'\| &= \|Gh'' + Hh\| \\ &\leq \|G\|\|h''\| + \|H\|\|h\|, \end{aligned} \tag{A.11}$$

where G and H have the same bounds (A.10). In summary,

$$|h'(z_0)| \leq \frac{1}{n-1}\|h''\| + \frac{2n(n+1)}{n-1}\|h\| \tag{A.12a}$$

$$\|h'\| \leq \underbrace{\frac{1}{n-1}}_{a}\|h''\| + \underbrace{\frac{2n(n+1)}{n-1}}_{b}\|h\| \tag{A.12b}$$

holds for arbitrary $n > 1$. Since the limit of a for $n \to \infty$ is zero, the first-order differential operator itself and the point-evaluation $\mathcal{B}_2$ of the first order

derivative are relatively bounded w. r. t. the second order differential operator with relative bound zero.

Moreover, it is shown in [59, Chap. IV, Sec. 1] that the point evaluation operator satisfies

$$|h(z_0)| \leq \frac{1}{(2n+3)^{\frac{1}{2}}}\|h'\| + \frac{n+1}{(2n+1)^{\frac{1}{2}}}\|h\| \tag{A.13}$$

for arbitrary $n > 0$. Obviously, it is relatively bounded w. r. t. the first order differential operator. Combining (A.12) and (A.13) leads to the result

$$|h(z_0)| \leq \underbrace{\frac{1}{(2n+3)^{\frac{1}{2}}(n-1)}}_{a}\|h''\| + \underbrace{\left(\frac{2n(n+1)}{(2n+3)^{\frac{1}{2}}(n-1)} + \frac{n+1}{(2n+1)^{\frac{1}{2}}}\right)}_{b}\|h\|. \tag{A.14}$$

Again, a can be made arbitrarily small by a sufficiently large n, which implies that the relative bound of the point evaluation $\mathcal{B}_1$ w. r. t. the second order differential operator (diffusion operator) is zero.

For parabolic systems, the system operator often is a diffusion-reaction operator, namely (A.6). This rises the question whether an operator $\mathcal{B}$ which is relatively bounded w. r. t. the diffusion operator, is also relatively bounded w. r. t. $\mathcal{A}$. To this end, (A.6) is divided by λ to obtain

$$\underbrace{\frac{\mathcal{A}h}{\lambda}}_{\widetilde{\mathcal{A}}h} = h'' - \frac{\mu}{\lambda}h. \tag{A.15}$$

Due to the relative boundedness of $\mathcal{B}$ w. r. t. the diffusion operator,

$$\begin{aligned}
\|\mathcal{B}h\| &\leq a\|h''\| + b\|h\| \\
&\leq a\|h''\| - a\|\frac{\mu}{\lambda}h\| + b\|h\| + a\|\frac{\mu}{\lambda}h\| && \text{(A.16)} \\
&\leq a\|h'' - \frac{\mu}{\lambda}h\| + \tilde{b}\|h\| = a\|\widetilde{\mathcal{A}}h\| + \tilde{b}\|h\| && \text{(A.17)}
\end{aligned}$$

holds for some $\tilde{b}$, showing that $\mathcal{B}$ is relatively bounded w. r. t. $\widetilde{\mathcal{A}}$ with relative bound zero. What remains to be shown is that the $\widetilde{\mathcal{A}}$-bounded operator is also $\mathcal{A}$-bounded. To this end note that

$$\begin{aligned}
\|\mathcal{B}h\| &\leq a\|\widetilde{\mathcal{A}}h\| + \tilde{b}\|h\| \\
&= a\|\frac{\mathcal{A}h}{\lambda}\| + \tilde{b}\|h\| \\
&\leq a\|\frac{1}{\lambda}\|\|\mathcal{A}h\| + \tilde{b}\|h\|. && \text{(A.18)}
\end{aligned}$$

Consequently, $\mathcal{B}$ is $\mathcal{A}$-bounded with $\mathcal{A}$-bound zero, proving the lemma. ■

To simplify the notation when dealing with time dependent operators, the following definition is useful.

Definition A.1.2. A time dependent operator $\mathcal{B}(t)$ of the form $\mathcal{B}(t) = B(t)\mathcal{B}_c$ with a uniformly bounded $B(t) \in X$, where X is a finite dimensional vector space, is called relatively bounded w. r. t. an operator $\mathcal{A}$ (or $\mathcal{A}$-bounded) if the operator $\mathcal{B}_c$ is $\mathcal{A}$-bounded. ◀

A.2 Norms of relatively bounded operators

With the property of relative boundedness, the following lemma allows to determine the norm of the application of such an operator to an analytic C_0-semigroup.

Lemma A.2.1. *Let the linear operator $\mathcal{A}$ be the generator of an exponentially stable analytic C_0-semigroup $\mathcal{T}(t)$ with decay rate μ, i. e. $\|\mathcal{T}(t)h\| \leq M\mathrm{e}^{-\mu t}\|h\|$, $h \in D(\mathcal{A})$, $M \geq 1$. Assume that $\mathcal{B}$ is an $\mathcal{A}$-bounded operator with $D(\mathcal{B}) \supset D(\mathcal{A})$. Then, the operator $\mathcal{B}\mathcal{T}(t)$ is a bounded linear operator with*

$$\|\mathcal{B}\mathcal{T}(t)h\| \leq M\mathrm{e}^{-\mu t}\|h\|, \quad h \in D(\mathcal{A}), \tag{A.19}$$

for some positive constant M.

Proof. It is helpful to first recover some properties of analytic C_0-semigroups. Assume $\mathcal{A}$ is the generator of an analytic C_0-semigroup $\mathcal{T}(t)$ (which is a bounded linear operator). Then $\forall h \in D(\mathcal{A})$, according to [26, Example 2.18]

1. $\mathcal{T}(t)h \in D(\mathcal{A})$ (the semigroup maps elements of the domain into elements of the domain.)
2. $\mathcal{A}\mathcal{T}(t)$ is a bounded linear operator.

Now let $\mathcal{B}$ be an $\mathcal{A}$-bounded operator with $D(\mathcal{B}) \supset D(\mathcal{A})$. This means that there exist non-negative constants a, b such that

$$\|\mathcal{B}h\| \leq a\|\mathcal{A}h\| + b\|h\|, \quad \forall h \in D(A). \tag{A.20}$$

According to 1., h may be the result of an application $\mathcal{T}(t)\tilde{h}$, $\tilde{h} \in D(\mathcal{A})$, so that this can be inserted for h in (A.20) giving

$$\|\mathcal{B}\mathcal{T}(t)\tilde{h}\| \leq a\|\mathcal{A}\mathcal{T}(t)\tilde{h}\| + b\|\mathcal{T}(t)\tilde{h}\|. \tag{A.21}$$

Using 2. and the fact that $\mathcal{T}(t)$ is a bounded linear operator yields

$$\|\mathcal{A}\mathcal{T}(t)\tilde{h}\| \leq \bar{c}\|\tilde{h}\| \quad \text{and} \quad \|\mathcal{T}(t)\tilde{h}\| \leq \bar{d}\|\tilde{h}\| \tag{A.22}$$

for some positive constants $\bar{c}, \bar{d}$. Inserting this in (A.21), leads to

$$\|\mathcal{B}\mathcal{T}(t)\tilde{h}\| \leq (a\bar{c} + b\bar{d})\|\tilde{h}\|. \tag{A.23}$$

In a last step, using the semigroup property $\mathcal{T}(t) = \mathcal{T}(t_0)\mathcal{T}(t-t_0)$, $t > t_0 > 0$ and the growth bound $\|\mathcal{T}(t)h\| \leq M\mathrm{e}^{-\mu t}\|h\|$, the result

$$\begin{aligned}\|\mathcal{B}\mathcal{T}(t)\tilde{h}\| &= \|\mathcal{B}\mathcal{T}(t_0)\mathcal{T}(t-t_0)\tilde{h}\| \leq (a\bar{c} + b\bar{d})\|\mathcal{T}(t-t_0)\tilde{h}\| \\ &\leq (ac + bd)M\mathrm{e}^{-\mu(t-t_0)}\|\tilde{h}\| \leq \underbrace{(a\bar{c} + b\bar{d})M\mathrm{e}^{\mu t_o}}_{\widetilde{M}} e^{-\mu t}\|\tilde{h}\|\end{aligned} \tag{A.24}$$

proves the lemma. ■

B Proofs

B.1 BCs of the inverse kernel equations

To show that the inverse kernel equations (2.61) indeed have the same number of conditions for L as the original kernel equations (2.28) pose on K, it needs to be shown that the choice of $\widetilde{A}_0$ according to (2.24) also fulfils the BCs (2.61d) and (2.61e) for the corresponding elements of the inverse kernel.

To this end, insert (2.28d) into (2.61d) to get

$$K(z,0,t)\Lambda(0)E_1 + \int_0^z LK(\zeta,0,t)\Lambda(0)E_1 \mathrm{d}\zeta = L(z,0,t)\Lambda(0)E_1 \tag{B.1}$$

and use (2.64b) with $\zeta = 0$ yielding

$$\int_0^z LK(\zeta,0,t)\mathrm{d}\zeta = \int_0^z LK(\zeta,0,t)\mathrm{d}\zeta. \tag{B.2}$$

For the Robin BCs, apply (2.22) on (2.61f), and subtract the result from (2.28e). This leads to

$$\begin{aligned}
&\underbrace{\Big(K(z,0,t) - L(z,0,t) + \int_0^z KL(\zeta,0,t)\mathrm{d}\zeta\Big)}_{\overset{(2.64a)}{=}0}\Lambda'(0)E_2 \\
&+ \Big(K_\zeta(z,0,t) - L_\zeta(z,0,t) + \int_0^z KL_\zeta(z,0,t)\mathrm{d}\zeta\Big)\Lambda(0)E_2 \\
&= -K(z,0,t)\Lambda(0)E_2Q_0(t) + \widetilde{A}_0E_1E_1^\top K(0,0,t)E_2.
\end{aligned} \tag{B.3}$$

Taking the derivative of (2.64a) w. r. t. ζ yields

$$L_\zeta(z,\zeta,t) = K_\zeta(z,\zeta,t) + K(z,\zeta,t)L(\zeta,\zeta,t) + \int_\zeta^z K(z,\bar{\zeta},t)L_\zeta(\bar{\zeta},\zeta,t)\mathrm{d}\bar{\zeta} \tag{B.4a}$$

$$L_\zeta(z,0,t) = K_\zeta(z,0,t) + K(z,0,t)L(0,0,t) + \int_0^z K(z,\zeta,t)L_\zeta(\zeta,0,t)\mathrm{d}\zeta, \tag{B.4b}$$

which is solved for $K(z,0,t)L(0,0,t)$ revealing that (B.3) can be written as

$$K(z,0,t)L(0,0,t)\Lambda(0)E_2 = K(z,0,t)\Lambda(0)E_2Q_0(t) - \widetilde{A}_0E_1E_1^\top K(0,0,t)E_2. \tag{B.5}$$

Now (2.28d) is inserted for $\widetilde{A}_0E_1$ to obtain

$$\begin{aligned} K(z,0,t)L(0,0,t)\Lambda(0)E_2 = K(z,0,t)\Lambda(0)E_2Q_0(t) \\ + K(z,0,t)\Lambda(0)E_1^\top K(0,0,t)E_2. \end{aligned} \tag{B.6}$$

With $L(0,0,t) = K(0,0,t)$ (see (2.64)), it remains to check whether

$$K(0,0,t)\Lambda(0)E_2 = \Lambda(0)E_2Q_0(t) + \Lambda(0)E_1^\top K(0,0,t)E_2. \tag{B.7}$$

The easiest way for this is to look at the components of (B.7) by multiplying with $e_i^\top$, $i = 1,\dots,n$, from left, and with $E_2^\top e_j$, $j = m+1,\dots,n$, from right, giving

$$\begin{aligned} e_i^\top K(0,0,t)\Lambda(0)e_j &= e_i^\top\Lambda(0)E_2Q_0(t)E_2^\top e_j + e_i^\top\Lambda(0)E_1E_1^\top K(0,0,t)E_2E_2^\top e_j \\ e_i^\top K(0,0,t)e_j\lambda_j(0) &= \lambda_i(0)e_i^\top e_jq_j(t) + \lambda_i(0)e_i^\top E_1E_1^\top K(0,0,t)e_j \\ K_{ij}(0,0,t)\lambda_j(0) &= \lambda_i(0)\delta_{ij}q_j(t) + \lambda_i(0)e_i^\top E_1E_1^\top K(0,0,t)e_j, \end{aligned} \tag{B.8}$$

where

$$\delta_{ij} = \begin{cases} 1, & i = j \\ 0, & i \neq j \end{cases} \tag{B.9}$$

is the Kronecker delta. Now, two different cases need to be considered. For $i > m$, the last term in (B.8) vanishes, as $e_i^\top E_1 = 0$. Thus,

$$K_{ij}(0,0,t)\lambda_j(0) = \lambda_i(0)q_j(t)\delta_{ij}, \quad i > m,\ j > m \tag{B.10}$$

is obtained. This condition is fulfilled according to (2.92).

For $i \leq m$, $\delta_{ij} = 0$ because $j \geq m$ and $e_i^\top E_1E_1^\top = e_i^\top$. Therefore,

$$K_{ij}(0,0,t)\lambda_j(0) = \lambda_i(0)K_{ij}(0,0,t), \quad i \leq m,\ j > m \tag{B.11}$$

needs to be fulfilled. Considering (2.92) shows that $K_{ij}(0,0,t)$ can only have non-zero values if $\lambda_i = \lambda_j$. Consequently, (B.11) is also fulfilled.

B.2 Integral estimates

In order to prove convergence of the fixed-point iteration, the growth assumption (2.190) needs to be inserted into the integral equations an the appearing integrals must be evaluated. This is not possible in closed-form but the following Lemma shows suitable estimates for them.

Lemma B.2.1. *The following integral estimates hold if* $\gamma \in (\bar{\lambda}, 1)$*:*

$$\int_{\boldsymbol{\xi}_l(\boldsymbol{\eta})}^{\boldsymbol{\xi}} \bar{\boldsymbol{f}}^l(\bar{\xi}, \boldsymbol{\eta}) \mathrm{d}\bar{\xi} \leq \frac{c_2}{(l+1)} \bar{\boldsymbol{f}}^{l+1}(\boldsymbol{\xi}, \boldsymbol{\eta}) \tag{B.12a}$$

$$\int_{\boldsymbol{\eta}_l(\boldsymbol{\xi})}^{\boldsymbol{\eta}} \bar{\boldsymbol{f}}^l(\boldsymbol{\xi}, \bar{\eta}) \mathrm{d}\bar{\eta} \leq \frac{2}{(l+1)} \bar{\boldsymbol{f}}^{l+1}(\boldsymbol{\xi}, \boldsymbol{\eta}) \tag{B.12b}$$

$$\int_{0}^{\boldsymbol{\eta}} \bar{\boldsymbol{f}}^l(\bar{\eta}, \bar{\eta}) \mathrm{d}\bar{\eta} \leq \frac{c_3}{l+1} \bar{\boldsymbol{f}}^{l+1}(\boldsymbol{\xi}, \boldsymbol{\eta}) \tag{B.12c}$$

$$\int_{0}^{\boldsymbol{z}(\boldsymbol{\eta},\boldsymbol{\eta})} \boldsymbol{f}^l(z, \bar{\zeta}) \mathrm{d}\bar{\zeta} \leq \frac{c_4}{(l+1)} \bar{\boldsymbol{f}}^{l+1}(\boldsymbol{\eta}, \boldsymbol{\eta}), \quad \lambda_i \geq \lambda_j,\ \boldsymbol{\eta} \geq 0 \tag{B.12d}$$

$$\int_{\zeta}^{z} \boldsymbol{f}^l(z, \bar{\zeta}) \mathrm{d}\bar{\zeta} \leq \frac{c_4}{l+1} \boldsymbol{f}^{l+1}(z, \zeta), \tag{B.12e}$$

$$\int_{\boldsymbol{\eta}_l(\boldsymbol{\xi})}^{\boldsymbol{\eta}} f_k^l(\boldsymbol{z}(\boldsymbol{\xi}, \bar{\eta}), \boldsymbol{\zeta}(\boldsymbol{\xi}, \bar{\eta})) \mathrm{d}\bar{\eta} \leq \frac{c_5}{l+1} \bar{\boldsymbol{f}}^{l+1}(\boldsymbol{\xi}, \boldsymbol{\eta}), \quad \lambda_i \leq \lambda_k \tag{B.12f}$$

for some finite $c_2, \ldots, c_5$ *as well as* $\forall (z, \zeta) \in \bar{\mathcal{D}} \leftrightarrow (\boldsymbol{\xi}, \boldsymbol{\eta}) \in \bar{\boldsymbol{\mathcal{D}}}_c$ *if not stated else.*

Proof. To get a bound for the integrals over $\boldsymbol{f}^l(z, \zeta) = \bar{\boldsymbol{f}}^l(\boldsymbol{\xi}, \boldsymbol{\eta})$ defined in (2.190), it is helpful to start with the corresponding derivatives.[1] Differentiating $\bar{\boldsymbol{f}}(\boldsymbol{\xi}, \boldsymbol{\eta})$ with the help of (2.137) w. r. t. $\boldsymbol{\xi}$ and $\boldsymbol{\eta}$ shows

$$(\bar{\boldsymbol{f}}(\boldsymbol{\xi}, \boldsymbol{\eta}))_{\boldsymbol{\xi}} = \phi_i'(z) \Big(\phi_i^{-1}\big(w_{ij}(\boldsymbol{\xi}, \boldsymbol{\eta})\big) \Big)_{\boldsymbol{\xi}} - \gamma \phi_i'(\zeta) \Big(\phi_j^{-1}\big(v_{ij}(\boldsymbol{\xi}, \boldsymbol{\eta})\big) \Big)_{\boldsymbol{\xi}} \tag{B.13a}$$

$$(\bar{\boldsymbol{f}}(\boldsymbol{\xi}, \boldsymbol{\eta}))_{\boldsymbol{\eta}} = \phi_i'(z) \Big(\phi_i^{-1}\big(w_{ij}(\boldsymbol{\xi}, \boldsymbol{\eta})\big) \Big)_{\boldsymbol{\eta}} - \gamma \phi_i'(\zeta) \Big(\phi_j^{-1}\big(v_{ij}(\boldsymbol{\xi}, \boldsymbol{\eta})\big) \Big)_{\boldsymbol{\eta}}. \tag{B.13b}$$

[1] The reader needs to keep in mind that the points z, ζ and $\boldsymbol{\xi}, \boldsymbol{\eta}$ are always related by the maps (2.136), respectively (2.137).

To express the derivative of the inverse function ϕ_i^{-1}, keep in mind that $w_{ij}(\boldsymbol{\xi}, \boldsymbol{\eta}) = w_{ij}(\xi_{ij}(z,\zeta), \eta_{ij}(z,\zeta)) = w_i(z) = \phi_i(z)$ holds as well as $v_{ij}(\boldsymbol{\xi}, \boldsymbol{\eta}) = v_{ij}(\xi_{ij}(z,\zeta), \eta_{ij}(z,\zeta)) = v_j(\zeta) = \phi_j(\zeta)$ (see Figure 2.4). Consequently,

$$(\phi_i^{-1})'(\phi_i(z)) = \frac{1}{\phi_i'(z)} \overset{(2.104)}{=} \sqrt{\lambda_i(z)} \tag{B.14a}$$

$$(\phi_j^{-1})'(\phi_j(\zeta)) = \frac{1}{\phi_j'(\zeta)} \overset{(2.104)}{=} \sqrt{\lambda_j(\zeta)} \tag{B.14b}$$

with (2.104) can be inserted into (B.13) to get

$$(\bar{\boldsymbol{f}}(\boldsymbol{\xi}, \boldsymbol{\eta}))_{\boldsymbol{\xi}} = (\boldsymbol{f}(z,\zeta))_{\boldsymbol{\xi}} = \sqrt{\frac{\lambda_i(z)}{\lambda_i(z)}} w_{ij,\boldsymbol{\xi}} - \gamma \sqrt{\frac{\lambda_j(\zeta)}{\lambda_i(\zeta)}} v_{ij,\boldsymbol{\xi}} \tag{B.15a}$$

$$(\bar{\boldsymbol{f}}(\boldsymbol{\xi}, \boldsymbol{\eta}))_{\boldsymbol{\eta}} = (\boldsymbol{f}(z,\zeta))_{\boldsymbol{\eta}} = \sqrt{\frac{\lambda_i(z)}{\lambda_i(z)}} w_{ij,\boldsymbol{\eta}} - \gamma \sqrt{\frac{\lambda_j(\zeta)}{\lambda_i(\zeta)}} v_{ij,\boldsymbol{\eta}}, \tag{B.15b}$$

for which (2.135) is differentiated w. r. t. $\boldsymbol{\xi}$ and $\boldsymbol{\eta}$ as

$$w_{ij,\boldsymbol{\xi}} = v_{ij,\boldsymbol{\xi}} = \frac{s}{2} \tag{B.16a}$$

$$w_{ij,\boldsymbol{\eta}} = \frac{1}{2}, \quad v_{ij,\boldsymbol{\eta}} = -\frac{1}{2}, \tag{B.16b}$$

finally yielding

$$(\boldsymbol{f}(z,\zeta))_{\boldsymbol{\xi}} = \frac{s}{2} \left(1 - \gamma \sqrt{\frac{\lambda_j(\zeta)}{\lambda_i(\zeta)}} \right) \tag{B.17a}$$

$$(\boldsymbol{f}(z,\zeta))_{\boldsymbol{\eta}} = \frac{1}{2} \left(1 + \gamma \sqrt{\frac{\lambda_j(\zeta)}{\lambda_i(\zeta)}} \right). \tag{B.17b}$$

With this result, the derivatives

$$(\boldsymbol{f}^{l+1}(z,\zeta))_{\boldsymbol{\xi}} = (l+1)\boldsymbol{f}^l(z,\zeta)(\boldsymbol{f}(z,\zeta))_{\boldsymbol{\xi}} \tag{B.18a}$$

$$(\boldsymbol{f}^{l+1}(z,\zeta))_{\boldsymbol{\eta}} = (l+1)\boldsymbol{f}^l(z,\zeta)(\boldsymbol{f}(z,\zeta))_{\boldsymbol{\eta}} \tag{B.18b}$$

can be determined to

$$(\boldsymbol{f}^{l+1}(z,\zeta))_{\boldsymbol{\xi}} = (l+1)\boldsymbol{f}^l(z,\zeta)\frac{s}{2} \left(1 - \gamma \sqrt{\frac{\lambda_j(\zeta)}{\lambda_i(\zeta)}} \right) \tag{B.19a}$$

$$(\boldsymbol{f}^{l+1}(z,\zeta))_{\boldsymbol{\eta}} = (l+1)\boldsymbol{f}^l(z,\zeta)\frac{1}{2} \left(1 + \gamma \sqrt{\frac{\lambda_j(\zeta)}{\lambda_i(\zeta)}} \right). \tag{B.19b}$$

Now note that according to (2.191),

$$\gamma \in \left(\overline{\lambda}, 1\right), \tag{B.20}$$

where

$$\overline{\lambda} = \max_{\lambda_i<\lambda_j} \max_{z} \sqrt{\frac{\lambda_i(z)}{\lambda_j(z)}} \tag{B.21}$$

is the maximal quotient of all diffusion coefficients for $\lambda_i < \lambda_j$.[2] This choice ensures that

$$\boldsymbol{f}(z,\zeta) > 0^{3} \tag{B.22}$$

and with the definition of s according to (2.131),

$$s\left(1-\gamma\sqrt{\frac{\lambda_j(\zeta)}{\lambda_i(\zeta)}}\right) = \left|1-\gamma\sqrt{\frac{\lambda_j(\zeta)}{\lambda_i(\zeta)}}\right| > 0 \tag{B.23}$$

which leads to

$$(\boldsymbol{f}(z,\zeta))_{\boldsymbol{\xi}} = (\bar{\boldsymbol{f}}(\boldsymbol{\xi},\boldsymbol{\eta}))_{\boldsymbol{\xi}} > 0, \quad (\boldsymbol{f}(z,\zeta))_{\boldsymbol{\eta}} = (\bar{\boldsymbol{f}}(\boldsymbol{\xi},\boldsymbol{\eta}))_{\boldsymbol{\eta}} > 0 \tag{B.24}$$

with (B.17). In other words, $\boldsymbol{f}(z,\zeta) = \bar{\boldsymbol{f}}(\boldsymbol{\xi},\boldsymbol{\eta})$ is strictly monotonically increasing in $\boldsymbol{\xi}$ and $\boldsymbol{\eta}$ so that the relation

$$0 \leq \frac{\bar{\boldsymbol{f}}(\xi^*,\eta^*)}{\bar{\boldsymbol{f}}(\boldsymbol{\xi},\boldsymbol{\eta})} \leq 1 \tag{B.25a}$$

holds for all points $\boldsymbol{\xi}_l(\boldsymbol{\eta}) \leq \xi^* \leq \boldsymbol{\xi}$ and $\boldsymbol{\eta}_l(\boldsymbol{\xi}) \leq \eta^* \leq \boldsymbol{\eta}$ inside the canonical spatial domain $\bar{\boldsymbol{\mathcal{D}}}_c$.

Remark B.2.2. In contrast to [113], (B.19a) contains the quotient $\frac{\lambda_j(\zeta)}{\lambda_i(\zeta)}$, where both coefficients are evaluated at the same point. Thus, the choice (B.20) of γ indeed is sufficient for (B.23). ◁

Utilizing (B.23), (B.19a) can be written as

$$(\boldsymbol{f}^{l+1}(z,\zeta))_{\boldsymbol{\xi}} = (l+1)\boldsymbol{f}^{l}(z,\zeta)\underbrace{\frac{1}{2}\left|1-\gamma\sqrt{\frac{\lambda_j(\zeta)}{\lambda_i(\zeta)}}\right|}_{\geq\frac{1}{c_2}} \tag{B.26a}$$

$$(\bar{\boldsymbol{f}}^{l+1}(\boldsymbol{\xi},\boldsymbol{\eta}))_{\boldsymbol{\xi}} \geq \frac{(l+1)}{c_2}\bar{\boldsymbol{f}}^{l}(\boldsymbol{\xi},\boldsymbol{\eta}) \tag{B.26b}$$

[2] If all diffusion coefficients are equal, i. e. there is no $\lambda_i < \lambda_j$, (B.21) returns $\overline{\lambda} = 0$.
[3] Because $\gamma < 1$, $\zeta \leq z$ and ϕ_i beeing strictly monotonically increasing.

with some finite $c_2 > 0$. Integrating (B.26b) w. r. t. $\boldsymbol{\xi}$, starting from the left boundary yields

$$\begin{aligned}\int_{\boldsymbol{\xi}_l(\boldsymbol{\eta})}^{\boldsymbol{\xi}} \bar{\boldsymbol{f}}^l(\bar{\xi},\boldsymbol{\eta})\mathrm{d}\bar{\xi} &\leq \frac{c_2}{(l+1)}\big(\bar{\boldsymbol{f}}^{l+1}(\boldsymbol{\xi},\boldsymbol{\eta}) - \bar{\boldsymbol{f}}^{l+1}(\boldsymbol{\xi}_l(\boldsymbol{\eta}),\boldsymbol{\eta})\big)\\ &= \frac{c_2}{(l+1)}\bar{\boldsymbol{f}}^{l+1}(\boldsymbol{\xi},\bar{\eta})\Bigg(1 - \underbrace{\left(\frac{\bar{\boldsymbol{f}}(\boldsymbol{\xi}_l(\boldsymbol{\eta}),\boldsymbol{\eta})}{\bar{\boldsymbol{f}}(\boldsymbol{\xi},\boldsymbol{\eta})}\right)^{l+1}}_{(\star_6)}\Bigg). \qquad \text{(B.27)}\end{aligned}$$

Since $\boldsymbol{\xi}_l(\boldsymbol{\eta})$ is the left boundary of the spatial domain (see Figure 2.2), obviously $\boldsymbol{\xi}_l(\boldsymbol{\eta}) \leq \boldsymbol{\xi}$ holds for all $\boldsymbol{\xi}, \boldsymbol{\eta}$, so that (B.25a) gives $0 \leq (\star_6) \leq 1$. Consequently, $0 \leq 1 - (\star_6) \leq 1$, implying (B.12a).

To prove (B.12b), inserting $1 + \gamma\sqrt{\frac{\lambda_j(\zeta)}{\lambda_i(\zeta)}} \geq 1$ into (B.19b), yields

$$\bar{\boldsymbol{f}}^l(\boldsymbol{\xi},\boldsymbol{\eta}) \leq \frac{2}{l+1}\big(\bar{\boldsymbol{f}}^{l+1}(\boldsymbol{\xi},\boldsymbol{\eta})\big)_{\boldsymbol{\eta}}, \qquad \text{(B.28)}$$

which is integrated w. r. t. $\boldsymbol{\eta}$ starting from the lower boundary of the spatial domain and leading to

$$\begin{aligned}\int_{\boldsymbol{\eta}_l(\boldsymbol{\xi})}^{\boldsymbol{\eta}} \bar{\boldsymbol{f}}^l(\boldsymbol{\xi},\bar{\eta})\mathrm{d}\bar{\eta} &\leq \frac{2}{l+1}\big(\bar{\boldsymbol{f}}^{l+1}(\boldsymbol{\xi},\boldsymbol{\eta}) - \bar{\boldsymbol{f}}^{l+1}(\boldsymbol{\xi},\boldsymbol{\eta}_l(\boldsymbol{\xi}))\big)\\ &= \frac{2}{l+1}\bar{\boldsymbol{f}}^{l+1}(\boldsymbol{\xi},\bar{\eta})\left(1 - \left(\frac{\bar{\boldsymbol{f}}(\boldsymbol{\xi},\boldsymbol{\eta}_l(\boldsymbol{\xi}))}{\bar{\boldsymbol{f}}(\boldsymbol{\xi},\boldsymbol{\eta})}\right)^{l+1}\right). \qquad \text{(B.29)}\end{aligned}$$

Again, $\boldsymbol{\eta}_l(\boldsymbol{\xi}) \leq \boldsymbol{\eta}$ is valid for all $\boldsymbol{\xi}, \boldsymbol{\eta}$, so that (B.25a) renders the expression in braces between 0 and 1. Therefore, (B.12b) directly follows.

Differentiating $\bar{\boldsymbol{f}}^{l+1}(\boldsymbol{\eta},\boldsymbol{\eta})$ w. r. t. $\boldsymbol{\eta}$ yields

$$\begin{aligned}\big(\bar{\boldsymbol{f}}^{l+1}(\boldsymbol{\eta},\boldsymbol{\eta})\big)_{\boldsymbol{\eta}} &= (l+1)\bar{\boldsymbol{f}}^l(\boldsymbol{\eta},\boldsymbol{\eta})\Bigg(\frac{1}{\sqrt{\lambda_i(z)}}\big(\frac{\boldsymbol{s}}{2}\sqrt{\lambda_i(z)} + \frac{1}{2}\sqrt{\lambda_i(z)}\big)\\ &\qquad - \frac{\gamma}{\sqrt{\lambda_i(\zeta)}}\big(\frac{\boldsymbol{s}}{2}\sqrt{\lambda_j(\zeta)} - \frac{1}{2}\sqrt{\lambda_j(\zeta)}\big)\Bigg)\\ &= (l+1)\bar{\boldsymbol{f}}^l(\boldsymbol{\eta},\boldsymbol{\eta})\Bigg(\underbrace{\frac{1}{2}\boldsymbol{s}\Big(1 - \gamma\sqrt{\frac{\lambda_j(\zeta)}{\lambda_i(\zeta)}}\Big)}_{\frac{1}{2}\left|1-\gamma\sqrt{\frac{\lambda_j(\zeta)}{\lambda_i(\zeta)}}\right| \geq \frac{1}{c_2}} + \frac{1}{2}\Big(1 + \gamma\sqrt{\frac{\lambda_j(\zeta)}{\lambda_i(\zeta)}}\Big)\Bigg)\\ &\geq \frac{(l+1)}{c_3}\bar{\boldsymbol{f}}^l(\boldsymbol{\eta},\boldsymbol{\eta}) \qquad \text{(B.30)}\end{aligned}$$

for some finite $c_3 > 0$. Just as before, integrating both sides w. r. t. $\boldsymbol{\eta}$ for $\boldsymbol{\eta} \geq 0$ leads to

$$\begin{aligned}\int_0^{\boldsymbol{\eta}} \bar{\boldsymbol{f}}^l(\bar{\eta},\bar{\eta})\mathrm{d}\bar{\eta} &\leq \frac{c_3}{l+1}\Big(\bar{\boldsymbol{f}}^{l+1}(\boldsymbol{\eta},\boldsymbol{\eta}) - \bar{\boldsymbol{f}}^{l+1}(0,0)\Big) \\ &= \frac{c_3}{l+1}\bar{\boldsymbol{f}}^{l+1}(\boldsymbol{\xi},\boldsymbol{\eta})\Bigg(\Big(\underbrace{\frac{\bar{\boldsymbol{f}}(\boldsymbol{\eta},\boldsymbol{\eta})}{\bar{\boldsymbol{f}}(\boldsymbol{\xi},\boldsymbol{\eta})}}_{0\leq\cdot\leq 1}\Big)^{l+1} - \Big(\underbrace{\frac{\bar{\boldsymbol{f}}(0,0)}{\bar{\boldsymbol{f}}(\boldsymbol{\xi},\boldsymbol{\eta})}}_{0\leq\cdot\leq 1}\Big)^{l+1}\Bigg). \end{aligned} \tag{B.31}$$

For the expressions in braces, (B.25a) directly applies because $\boldsymbol{\eta} \geq 0$. As result, (B.12c) is deduced.

For the next two estimates, differentiate $\boldsymbol{f}^{l+1}(z,\zeta)$ w. r. t. ζ to obtain

$$(\boldsymbol{f}^{l+1}(z,\zeta))_\zeta = (l+1)\boldsymbol{f}^l(z,\zeta)\boldsymbol{f}_\zeta(z,\zeta) \tag{B.32}$$

where, by the help of (2.104),

$$\boldsymbol{f}_\zeta(z,\zeta) = -\gamma\frac{1}{\sqrt{\lambda_i(\zeta)}} \leq -\frac{1}{c_4} < 0 \tag{B.33}$$

for some finite $c_4 > 0$. Inserting (B.33) into (B.32) and integrating both sides from $z_l \leq z$ to z w. r. t. ζ yields

$$\begin{aligned}\int_{z_l}^{z} \boldsymbol{f}^l(z,\bar{\zeta})\mathrm{d}\bar{\zeta} &\leq \frac{-c_4}{l+1}(\boldsymbol{f}^{l+1}(z,z) - \boldsymbol{f}^{l+1}(z,z_l)) \\ &= \frac{c_4}{l+1}\boldsymbol{f}^{l+1}(z,\zeta)\left(\left(\frac{\boldsymbol{f}(z,z_l)}{\boldsymbol{f}(z,\zeta)}\right)^{l+1} - \left(\frac{\boldsymbol{f}(z,z)}{\boldsymbol{f}(z,\zeta)}\right)^{l+1}\right). \end{aligned} \tag{B.34}$$

for all $\zeta \leq z$. To prove (B.12d), insert $z_l = 0$ and consider a point $\boldsymbol{\xi} = \boldsymbol{\eta}$ so that $z = \boldsymbol{z}(\boldsymbol{\eta},\boldsymbol{\eta})$ for $\lambda_i \geq \lambda_j$. According to the inverse map (2.137b), $\zeta = \boldsymbol{\zeta}(\boldsymbol{\eta},\boldsymbol{\eta}) = 0$, so that $f(z,\zeta) = f(z,0)$. Consequently,

$$\int_0^{z(\boldsymbol{\eta},\boldsymbol{\eta})} \boldsymbol{f}^l(z,\bar{\zeta})\mathrm{d}\bar{\zeta} \leq \frac{c_4}{l+1}\bar{\boldsymbol{f}}^{l+1}(\boldsymbol{\eta},\boldsymbol{\eta})\left(\left(\underbrace{\frac{\boldsymbol{f}(z,0)}{\boldsymbol{f}(z,0)}}_{=1}\right)^{l+1} - \left(\underbrace{\frac{\boldsymbol{f}(z,z)}{\boldsymbol{f}(z,0)}}_{0\leq\cdot\leq 1}\right)^{l+1}\right) \tag{B.35}$$

is obtained. Due to the strictly monotonic decrease of $\boldsymbol{f}(z,\zeta)$ w. r. t. ζ according to (B.33) and $z \geq 0$, the last term in braces is between 0 and 1 so that (B.12d) is implied.

For (B.12e), insert $z_l = \zeta$ into (B.34), yielding

$$\int_\zeta^z \boldsymbol{f}^l(z,\bar\zeta)\mathrm{d}\bar\zeta \leq \frac{c_4}{l+1}\boldsymbol{f}^{l+1}(z,\zeta)\Bigg(\Big(\underbrace{\frac{\boldsymbol{f}(z,\zeta)}{\boldsymbol{f}(z,\zeta)}}_{=1}\Big)^{l+1} - \Big(\underbrace{\frac{\boldsymbol{f}(z,z)}{\boldsymbol{f}(z,\zeta)}}_{0\leq\cdot\leq 1}\Big)^{l+1}\Bigg), \tag{B.36}$$

where again (B.33) implies the bound of the last brace. Analogously to the previous cases, (B.12e) follows.

The remaining estimate is proven the same way. The derivative

$$(f_k^{l+1}(z,\zeta))_{\boldsymbol{\eta}} = (l+1)f_k(z,\zeta)\underbrace{\frac{1}{2}\Big(\sqrt{\frac{\lambda_i(z)}{\lambda_k(z)}} + \gamma\sqrt{\frac{\lambda_j(\zeta)}{\lambda_k(\zeta)}}\Big)}_{\geq\frac{1}{c_5}} \geq 0 \tag{B.37}$$

for some finite $c_5 > 0$ allows to integrate both sides w. r. t. $\boldsymbol{\eta}$, yielding

$$\begin{aligned}\int_{\boldsymbol{\eta}_l(\boldsymbol{\xi})}^{\boldsymbol{\eta}} f_k^l(\boldsymbol{z}(\boldsymbol{\xi},\bar\eta),\boldsymbol{\zeta}(\boldsymbol{\xi},\bar\eta))\mathrm{d}\bar\eta &\leq \frac{c_5}{l+1}\Big(f_k^{l+1}(z,\zeta) - f_k^{l+1}(z,\zeta)|_{\boldsymbol{\eta}_l(\boldsymbol{\xi})}\Big)\\ &\leq \frac{c_5}{l+1}\bar{\boldsymbol{f}}^{l+1}(\boldsymbol{\xi},\boldsymbol{\eta})\underbrace{\Bigg(\Big(\frac{f_k(z,\zeta)}{\boldsymbol{f}(z,\zeta)}\Big)^{l+1} - \Big(\frac{f_k(z,\zeta)|_{\boldsymbol{\eta}_l(\boldsymbol{\xi})}}{\boldsymbol{f}(z,\zeta)}\Big)^{l+1}\Bigg)}_{(\star_7)}.\end{aligned} \tag{B.38}$$

To obtain a bounded and positive $(\star_7)$, $f_k^{l+1}(z,\zeta)|_{\boldsymbol{\eta}_l(\boldsymbol{\xi})} \leq f_k^{l+1}(z,\zeta)$ and

$$\frac{f_k(z,\zeta)}{\boldsymbol{f}(z,\zeta)} = \frac{\phi_k(z)-\gamma\phi_k(\zeta)}{\phi_i(z)-\gamma\phi_i(\zeta)} \overset{!}{\leq} 1 \tag{B.39}$$

need to hold. The first condition is obviously fulfilled because of $\boldsymbol{\eta}_l(\boldsymbol{\xi}) \leq \boldsymbol{\eta}$ and the positiveness of (B.37). For (B.39), note that

$$\phi_i(z)-\gamma\phi_i(\zeta) = \phi_i(z)-\phi_i(\zeta)+(1-\gamma)\phi_i(\zeta) \overset{(2.96)}{=} \int_\zeta^z \frac{1}{\sqrt{\lambda_i(\bar z)}}\mathrm{d}\bar z + (1-\gamma)\phi_i(\zeta), \tag{B.40}$$

which is why (B.39) can be written as

$$\frac{f_k(z,\zeta)}{\boldsymbol{f}(z,\zeta)} = \frac{\int_\zeta^z \frac{1}{\sqrt{\lambda_k(\bar z)}}\mathrm{d}\bar z + (1-\gamma)\phi_k(\zeta)}{\int_\zeta^z \frac{1}{\sqrt{\lambda_i(\bar z)}}\mathrm{d}\bar z + (1-\gamma)\phi_i(\zeta)}. \tag{B.41}$$

In the relevant case $\lambda_i \leq \lambda_k$, the relation $\int_\zeta^z \frac{1}{\sqrt{\lambda_k(\bar z)}}\mathrm{d}\bar z \leq \int_\zeta^z \frac{1}{\sqrt{\lambda_i(\bar z)}}\mathrm{d}\bar z$ holds and (2.96) implies $\phi_k(\zeta) \leq \phi_i(\zeta)$ so that (B.39) is valid. Consequently, $0 \leq (\star_7) \leq 1$ in (B.38) showing that (B.12f) holds for $\lambda_i \leq \lambda_k$, which proves the lemma. ∎

B.3 Duality of the kernel equations (proof of Proposition 3.5.1)

Solving (3.28) for $P(1-\zeta, 1-z, T-t)$ yields its inverse

$$P(1-\zeta,1-z,T-t) = \underbrace{\Lambda(1-\zeta)}_{\breve{\Lambda}(\zeta)} \breve{P}^\top(z,\zeta,t) \underbrace{\Lambda^{-1}(1-z)}_{\breve{\Lambda}^{-1}(z)}. \tag{B.42}$$

Introducing the inverted coordinates

$$\breve{z} = 1-\zeta, \qquad \breve{\zeta} = 1-z, \tag{B.43a}$$

as well as

$$\breve{t} = T-t \tag{B.43b}$$

this can also be expressed as

$$P(\breve{z},\breve{\zeta},\breve{t}) = \Lambda(\breve{z})\breve{P}^\top(1-\breve{\zeta},1-\breve{z},T-\breve{t})\Lambda^{-1}(\breve{\zeta}). \tag{B.44}$$

However, as $0 \le \breve{\zeta} \le \breve{z} \le 1$ following from (B.43a) and $0 \le \zeta \le z \le 1$ as well as $t_0 \le \breve{t} \le T$ since $t_0 \le t \le T$, the variables may be renamed $\breve{z} \to z$, $\breve{\zeta} \to \zeta$, $\breve{t} \to t$ so that

$$P(z,\zeta,t) = \Lambda(z)\breve{P}^\top(1-\zeta,1-z,T-t)\Lambda^{-1}(\zeta) \tag{B.45}$$

is also valid, implying

$$P_t(z,\zeta,t) = -\Lambda(z)\breve{P}_t^\top(1-\zeta,1-z,T-t)\Lambda^{-1}(\zeta). \tag{B.46}$$

Now differentiate (B.42) twice w. r. t. ζ to obtain

$$\begin{aligned}
\big(P(1-\zeta,1-z,T-t)\big)_{\zeta\zeta} &= \big(\breve{\Lambda}(\zeta)\breve{P}^\top(z,\zeta,t)\breve{\Lambda}^{-1}(z)\big)_{\zeta\zeta} \\
\big(-P_z(1-\zeta,1-z,T-t)\big)_{\zeta} &= \Big(\big(\breve{\Lambda}(\zeta)\breve{P}^\top(z,\zeta,t)\big)_{\zeta}\breve{\Lambda}^{-1}(z)\Big)_{\zeta} \\
P_{zz}(1-\zeta,1-z,T-t) &= \big(\breve{\Lambda}(\zeta)\breve{P}^\top(z,\zeta,t)\big)_{\zeta\zeta}\breve{\Lambda}^{-1}(z) \\
P_{zz}(\breve{z},\breve{\zeta},\breve{t}) &= \big(\breve{\Lambda}(\zeta)\breve{P}^\top(z,\zeta,T-t)\big)_{\zeta\zeta}\Big|_{\substack{z=1-\breve{\zeta}\\ \zeta=1-\breve{z}}}\breve{\Lambda}^{-1}(1-\breve{\zeta}).
\end{aligned} \tag{B.47}$$

Insert (B.45) into $(P(z,\zeta,t)\Lambda(\zeta))$ and differentiate twice w. r. t. ζ to get

$$\begin{aligned}\big(P(z,\zeta,t)\Lambda(\zeta)\big)_{\zeta\zeta} &= \Big(\Lambda(z)\breve{P}^\top(1-\zeta,1-z,T-t)\Big)_{\zeta\zeta}\\ &= \Big(-\Lambda(z)\breve{P}_z^\top(1-\zeta,1-z,T-t)\Big)_{\zeta}\\ &= \Lambda(z)\breve{P}_{zz}^\top(1-\zeta,1-z,T-t). \end{aligned} \tag{B.48}$$

Now, (3.14a) is considered at the points $(\breve{z},\breve{\zeta},\breve{t})$. Then, (B.44) as well as (B.46)–(B.48) are inserted. This yields

$$\begin{aligned}&\Lambda(\breve{z})\big(\breve{\Lambda}(\zeta)\breve{P}^\top(z,\zeta,T-\breve{t})\big)_{\zeta\zeta}\Big|_{\substack{z=1-\breve{\zeta}\\ \zeta=1-\breve{z}}}\breve{\Lambda}^{-1}(1-\breve{\zeta})\\ &\quad-\Lambda(\breve{z})\breve{P}_{zz}^\top(1-\breve{\zeta},1-\breve{z},T-\breve{t})\\ &=-\Lambda(\breve{z})\breve{P}^\top(1-\breve{\zeta},1-\breve{z},t-\breve{t})\Lambda^{-1}(\breve{\zeta})\widetilde{A}_o(\breve{\zeta},\breve{t})\\ &\quad-\Lambda(\breve{z})\breve{P}_t^\top(1-\breve{\zeta},1-\breve{z},T-\breve{t})\Lambda^{-1}(\breve{\zeta})\\ &\quad-A(\breve{z},\breve{t})\Lambda(\breve{z})\breve{P}^\top(1-\breve{\zeta},1-\breve{z},T-\breve{t})\Lambda^{-1}(\breve{\zeta})+F(\breve{z},\breve{\zeta},\breve{t})\\ &\qquad-\int_{\breve{\zeta}}^{\breve{z}}F(\breve{z},\bar{\zeta},\breve{t})\Lambda(\bar{\zeta})\breve{P}^\top(1-\breve{\zeta},1-\bar{\zeta},T-\breve{t})\Lambda^{-1}(\breve{\zeta})\mathrm{d}\bar{\zeta}. \end{aligned} \tag{B.49}$$

Inserting (B.43) simplifies the expression to

$$\begin{aligned}&\Lambda(1-\zeta)\big(\breve{\Lambda}(\zeta)\breve{P}^\top(z,\zeta,t)\big)_{\zeta\zeta}\breve{\Lambda}^{-1}(z)-\Lambda(1-\zeta)\breve{P}_{zz}^\top(z,\zeta,t)\\ &=-\Lambda(1-\zeta)\breve{P}^\top(z,\zeta,t)\Lambda^{-1}(1-z)\widetilde{A}_o(1-z,T-t)\\ &\quad-\Lambda(1-\zeta)\breve{P}_t^\top(z,\zeta,t)\Lambda^{-1}(1-z)\\ &\quad-A(1-\zeta,T-t)\Lambda(1-\zeta)\breve{P}^\top(z,\zeta,t)\Lambda^{-1}(1-z)+F(1-\zeta,1-z,T-t)\\ &\quad-\int_{1-z}^{1-\zeta}F(1-\zeta,\bar{\zeta},T-t)\Lambda(\bar{\zeta})\breve{P}^\top(z,1-\bar{\zeta},t)\Lambda^{-1}(1-z)\mathrm{d}\bar{\zeta}. \end{aligned} \tag{B.50}$$

To reformulate the integral, substitute $\tilde{\zeta}=1-\bar{\zeta}$ with $\mathrm{d}\bar{\zeta}=-\mathrm{d}\tilde{\zeta}$, which yields

$$\begin{aligned}&-\int_{1-z}^{1-\zeta}F(1-\zeta,\bar{\zeta},T-t)\Lambda(\bar{\zeta})\breve{P}^\top(z,1-\bar{\zeta},t)\Lambda^{-1}(1-z)\mathrm{d}\bar{\zeta}\\ &=\int_{z}^{\zeta}F(1-\zeta,1-\tilde{\zeta},T-t)\Lambda(1-\tilde{\zeta})\breve{P}^\top(z,\tilde{\zeta},t)\Lambda^{-1}(1-z)\mathrm{d}\tilde{\zeta}\\ &=-\int_{\zeta}^{z}F(1-\zeta,1-\tilde{\zeta},T-t)\breve{\Lambda}(\tilde{\zeta})\breve{P}^\top(z,\tilde{\zeta},t)\breve{\Lambda}^{-1}(z)\mathrm{d}\tilde{\zeta}. \end{aligned} \tag{B.51}$$

In the next step, (B.50) with (B.51) is premultiplied by $\Lambda^{-1}(1-\zeta) = \breve{\Lambda}^{-1}(\zeta)$ and postmultiplied by $\Lambda(1-z) = \breve{\Lambda}(z)$. Then, transposing the equation and inverting the signs leads to

$$\begin{aligned}
&\breve{\Lambda}(z)\breve{P}_{zz} - \big(\breve{P}\breve{\Lambda}(\zeta)\big)_{\zeta\zeta} \\
&= \underbrace{\breve{\Lambda}(z)\widetilde{A}_o^\top(1-z,T-t)\breve{\Lambda}^{-1}(z)}_{\breve{A}_o(z,t)}\breve{P} + \breve{P}\underbrace{\breve{\Lambda}(\zeta)A^\top(1-\zeta,T-t)\breve{\Lambda}^{-1}(\zeta)}_{\breve{A}(\zeta,t)} + \breve{P}_t \\
&- \underbrace{\breve{\Lambda}(z)F^\top(1-\zeta,1-z,T-t)\breve{\Lambda}^{-1}(\zeta)}_{\breve{F}(z,\zeta,t)} \\
&+ \int_\zeta^z \breve{P}(z,\tilde{\zeta})\underbrace{\breve{\Lambda}(\tilde{\zeta})F^\top(1-\zeta,1-\tilde{\zeta},T-t)\breve{\Lambda}^{-1}(\zeta)}_{\breve{F}(\tilde{\zeta},\zeta,t)}\mathrm{d}\tilde{\zeta},
\end{aligned} \tag{B.52}$$

which is (3.29a).

To derive the BCs, first insert (B.45) into (3.14b) and substitute $t - T \to t$, yielding

$$\Lambda\breve{P}^\top(1-z,1-z,t)\Lambda^{-1}\Lambda - \Lambda\Lambda\breve{P}^\top(1-z,1-z,t)\Lambda^{-1} = 0,$$

which, after premultiplying Λ^{-1}, postmultiplying Λ and transposing, reads

$$\Lambda\breve{P}(1-z,1-z,t) - \breve{P}(1-z,1-z,t)\Lambda. \tag{B.53}$$

Substituting $1-z \to z$ finally results in (3.29b).

For the remaining BCs, differentiating (B.45) w. r. t. ζ and w. r. t. z leads to the expressions

$$\begin{aligned}
P_\zeta = &-\Lambda\breve{P}_z^\top(1-\zeta,1-z,T-t)\Lambda^{-1}(\zeta) \\
&-\Lambda\breve{P}^\top(1-\zeta,1-z,T-t)\Lambda^{-2}(\zeta)\Lambda'(\zeta)
\end{aligned} \tag{B.54a}$$

$$P_z = \Lambda'\breve{P}^\top(1-\zeta,1-z,T-t)\Lambda^{-1}(\zeta) - \Lambda\breve{P}_\zeta^\top(1-\zeta,1-z,T-t)\Lambda^{-1}(\zeta). \tag{B.54b}$$

To insert this into (3.14c), note that

$$\Lambda\big(P(z,z,t)\big)_z = \Lambda P_z(z,z,t) + \Lambda P_\zeta(z,z,t), \tag{B.55}$$

so that (3.14c) reads

$$\begin{aligned}
&-\Lambda\breve{P}_z^\top - \Lambda\breve{P}^\top\Lambda^{-1}\Lambda' - \Lambda^2\breve{P}_z^\top\Lambda^{-1} - \Lambda^2\breve{P}_z^\top\Lambda^{-2}\Lambda' \\
&+ 2\Lambda\Lambda'\breve{P}^\top\Lambda^{-1} - 2\Lambda^2\breve{P}_\zeta^\top\Lambda^{-1} = A + \widetilde{A}_o - \Lambda\breve{P}^\top\Lambda^{-1}\Lambda',
\end{aligned} \tag{B.56}$$

where $\breve{P}^\top$ and its derivatives are evaluated at $(1-z, 1-z, T-t)$. Premultiplying by Λ^{-1} and postmultiplying by Λ as well as transposing the equation,

$$-\Lambda\breve{P}_z - \breve{P}_z\Lambda - 2\breve{P}_\zeta\Lambda - \Lambda'\Lambda^{-1}\breve{P}\Lambda + 2\breve{P}\Lambda' = \Lambda(A^\top + \widetilde{A}_o^\top)\Lambda^{-1} - \Lambda'\breve{P} \tag{B.57}$$

follows. Now $1-z \to z$ and $T-t \to t$ is substituted with $\breve{\Lambda}'(z) = -\Lambda'(1-z)$, yielding

$$\begin{aligned}
&-\breve{\Lambda}\breve{P}_z(z,z,t) - \breve{P}(z,z,t)_z\breve{\Lambda} - \breve{P}_\zeta(z,z,t)\breve{\Lambda} \\
&+\breve{\Lambda}'\breve{\Lambda}^{-1}\breve{P}(z,z,t)\breve{\Lambda} - 2\breve{P}(z,z,t)\breve{\Lambda}' \\
&\quad= \underbrace{\breve{\Lambda}A^\top(1-z,T-t)\breve{\Lambda}^{-1}}_{\breve{A}(z,t)} + \underbrace{\breve{\Lambda}\widetilde{A}_o^\top(1-z,T-t)\breve{\Lambda}^{-1}}_{\breve{A}_o(z,t)}.
\end{aligned} \tag{B.58}$$

In a last step, insert

$$\breve{\Lambda}'\breve{\Lambda}^{-1}\breve{P}(z,z,t)\breve{\Lambda} \overset{(3.29b)}{=} \breve{\Lambda}'\breve{\Lambda}^{-1}\breve{\Lambda}\breve{P}(z,z,t) = \breve{\Lambda}'\breve{P}(z,z,t), \tag{B.59}$$

so that (3.29c) directly follows.

To reformulate (3.14d), insert the definition of ϑ_1 according to (3.4b) to get

$$\begin{aligned}
&(S_dS_d^\top - S_r\bar{Q}_1S_r^\top)P(1,\zeta,t) + S_rS_r^\top P_z(1,\zeta,t) \\
&\quad= -\widetilde{A}_1(\zeta,t) + S_rS_r^\top P(1,1,t)S_dS_d^\top\widetilde{A}_1(\zeta,t),
\end{aligned} \tag{B.60}$$

where (B.45) and (B.54) are inserted to obtain

$$\begin{aligned}
&(S_dS_d^\top - S_r\bar{Q}_1S_r^\top)\Lambda(1)\breve{P}^\top(1-\zeta,0,T-t)\Lambda^{-1}(\zeta) + S_rS_r^\top \\
&\cdot\Big(\Lambda'(1)\breve{P}^\top(1-\zeta,0,T-t)\Lambda^{-1}(\zeta) - \Lambda(1)\breve{P}_\zeta^\top(1-\zeta,0,T-t)\Lambda^{-1}(\zeta)\Big) \\
&\quad= -\widetilde{A}_1(\zeta,t) + S_rS_r^\top P(1,1,t)S_dS_d^\top\widetilde{A}_1(\zeta,t).
\end{aligned} \tag{B.61}$$

Postmultiplying by $\Lambda(\zeta)$, substituting $1-\zeta \to z$, $T-t \to t$ and transposing the result yields

$$\begin{aligned}
&\breve{P}(z,0,t)\breve{\Lambda}(0)(S_dS_d^\top - S_r\bar{Q}_1^\top S_r^\top) - \breve{P}(z,0,t)\breve{\Lambda}'(0)S_rS_r^\top - \breve{P}_\zeta(z,0,t)\breve{\Lambda}(0)S_rS_r^\top \\
&= -\underbrace{\breve{\Lambda}(z)\widetilde{A}_1^\top(1-z,T-t)}_{\breve{A}_1(z,t)} \\
&\quad+ \breve{\Lambda}(z)\widetilde{A}_1^\top(1-z,T-t)S_dS_d^\top\breve{\Lambda}^{-1}(0)\breve{P}(0,0,t)\breve{\Lambda}(0)S_rS_r^\top,
\end{aligned} \tag{B.62}$$

where $\Lambda'(1) = -\breve{\Lambda}'(0)$ was used. Now note that (3.29b) implies

$$\begin{aligned} \breve{\Lambda}^{-1}\breve{P}(z,z,t)\breve{\Lambda} &= \breve{P}(z,z,t) \\ \breve{\Lambda}^{-1}(0)\breve{P}(0,0,t)\breve{\Lambda}(0) &= \breve{P}(0,0,t) \end{aligned} \tag{B.63}$$

and postmultiply (B.62) by each S_d and S_r, leading to (3.29d) and (3.29e).

For the last condition, insert (B.45) into (3.14e) to get

$$S_r^\top \Lambda(1)\breve{P}^\top(0,0,T-t)\Lambda^{-1}(1)S_r = -\bar{Q}_1(t) \tag{B.64}$$

$$S_r^\top \breve{\Lambda}^{-1}(0)\breve{P}(0,0,t)\breve{\Lambda}(0)S_r = \underbrace{(-\bar{Q}_1^\top(t-T))}_{\breve{Q}(t)}. \tag{B.65}$$

With (B.63), this yields (3.29f).

B.4 Coupling term properties (proof of Corollary 3.8.4)

To describe the solution vector $\tilde{e}(z,t) = \operatorname{col}(\tilde{e}_1(z,t),\dots,\tilde{e}_n(z,t))$, (3.67a) is inserted into the vector, yielding

$$\tilde{e}(t) = \underbrace{\operatorname{diag}(\mathcal{T}_i(t-t_0))}_{\mathcal{T}(t-t_0)} \underbrace{\begin{bmatrix} \tilde{e}_1(t_0) \\ \vdots \\ \tilde{e}_n(t_0) \end{bmatrix}}_{\tilde{e}(t_0)} + \int_{t_0}^{t} \mathcal{T}(t-\tau) \underbrace{\begin{bmatrix} R_1(\tau,t_0) \\ \vdots \\ R_n(\tau,t_0) \end{bmatrix}}_{R(\tau,t_0)} \mathrm{d}\tau + \underbrace{\begin{bmatrix} \mathcal{I}_1(t,t_0) \\ \vdots \\ \mathcal{I}_n(t,t_0) \end{bmatrix}}_{\mathcal{I}(t,t_0)}, \tag{B.66}$$

where

$$\mathcal{I}(t,t_0) = \mathcal{T}(t,t_0) \underbrace{\begin{bmatrix} \mathcal{I}_1^a(t_0) \\ \vdots \\ \mathcal{I}_n^a(t_0) \end{bmatrix}}_{\mathcal{I}^a(t_0)} + \underbrace{\begin{bmatrix} \mathcal{I}_1^b(t,t_0) \\ \vdots \\ \mathcal{I}_n^b(t,t_0) \end{bmatrix}}_{\mathcal{I}^b(t,t_0)}. \tag{B.67}$$

With (3.69) and the definition of the Euclidean norm,

$$\begin{aligned} \|\tilde{e}(t)\| &= \Big(\sum_{i=1}^{n} \|\tilde{e}_i(t)\|^2\Big)^{\frac{1}{2}} \le \Big(\sum_{i=1}^{n} \bar{M}_i^2 \mathrm{e}^{2(\mu_{\max}-\mu_o+c)(t-t_0)}\Big)^{\frac{1}{2}} \\ &= \underbrace{\Big(\sum_{i=1}^{n} \bar{M}_i^2\Big)^{\frac{1}{2}}}_{\bar{M}} \mathrm{e}^{(\mu_{\max}-\mu_o+c)(t-t_0)} \end{aligned} \tag{B.68}$$

follows.

Now apply the backstepping transformation (3.9) to (B.66), giving

$$\mathcal{T}_o^{-1}(t)\tilde{e}(t) = \tilde{e}(t) - \int_0^z P(z,\zeta,t)\Big(\big(\mathcal{T}(t-t_0)\tilde{e}(t_0)\big)(\zeta) - \int_{t_0}^t \big(\mathcal{T}(t-\tau)R(\tau,t_0)\mathrm{d}\tau\big)(\zeta)\Big)\mathrm{d}\zeta - \int_0^z P(z,\zeta,t)\mathcal{I}(t,t_0)(\zeta)\mathrm{d}\zeta. \tag{B.69}$$

Since the appearing spatial integrals in (B.69) are bounded operators, it is possible to write

$$\|\mathcal{T}_o^{-1}(t)\tilde{e}(t)\| \leq \bar{M}\mathrm{e}^{(\mu_{\max}-\mu_o+c)(t-t_0)} + \bar{c}\|\mathcal{T}(t-t_0)\tilde{e}(t_0)\| + \bar{c}\int_{t_0}^t \|\mathcal{T}(t-\tau)R(\tau,t_0)\|\mathrm{d}\tau + \bar{c}\|\mathcal{I}(t,t_0)\|. \tag{B.70}$$

after the substitution of (B.68). The diagonality of $\mathcal{T}$ as well as the bounds (3.66) and (3.67d) then directly lead to the result (3.89a).

Prior to applying $\mathcal{K}(t)$ on $\mathcal{T}_o^{-1}(t)\tilde{e}(t)$, note that according to its definition in (3.61a), it can be expressed in the form

$$\mathcal{K}(t)h = \overbrace{\underbrace{\big(-S_r\bar{Q}_1(t)S_r^\top + B_1^n K(1,1,t)\big)}_{=:K_1(t)}h(1)}^{=:\mathcal{K}_1(t)h} + \mathcal{K}_b(t)h, \quad h \in L_2(0,1) \tag{B.71}$$

where $\mathcal{K}_b(t)$ is a bounded integral operator and $\mathcal{K}_1(t)$ is an unbounded operator containing a time-dependent matrix multiplication and a time-invariant boundary evaluation. Thus, for the norm estimation

$$\|\mathcal{K}(t)\mathcal{T}_o^{-1}(t)\tilde{e}(t)\| \leq \|\mathcal{K}_1(t)\mathcal{T}_o^{-1}(t)\tilde{e}(t)\| + \underbrace{\|\mathcal{K}_b(t)\mathcal{T}_o^{-1}(t)\tilde{e}(t)\|}_{\leq\bar{c}\|\mathcal{T}_o^{-1}(t)\tilde{e}(t)\|} \tag{B.72}$$

it suffices to analyse the application of $\mathcal{K}_1(t)$ to (B.69) in view of (3.89a). After the insertion of (B.66), this reads

$$\begin{aligned}\mathcal{K}_1(t)\mathcal{T}_o^{-1}(t)\tilde{e}(t) = \ & \mathcal{K}_1(t)\mathcal{T}(t-t_0)\tilde{e}(t_0) + \int_{t_0}^{t} \mathcal{K}_1(t)\mathcal{T}(t-\tau)R(\tau,t_0)\mathrm{d}\tau \\ & - \mathcal{K}_1(t)\mathcal{I}(t,t_0) - K_1(t)\int_0^1 P(z,\zeta,t)\Big(\big(\mathcal{T}(t-t_0)\tilde{e}(t_0)\big)(\zeta) \\ & - \int_{t_0}^{t}\big(\mathcal{T}(t-\tau)R(\tau,t_0)\mathrm{d}\tau\big)(\zeta)\Big)\mathrm{d}\zeta - K_1(t)\int_0^1 P(z,\zeta,t)\mathcal{I}(t,t_0)(\zeta)\mathrm{d}\zeta.\end{aligned} \tag{B.73}$$

As the spatial integrals are bounded operators, what remains to be investigated is the application of $\mathcal{K}_1(t)$ to $\mathcal{T}(t-t_0)$ and to $\mathcal{I}(t,t_0)$. However, due to the diagonality of $\mathcal{T}$, $\mathcal{K}_1$ performs boundary evaluations on $\mathcal{T}_i(t-t_0)$. Exploiting the analyticity of $\mathcal{T}_i$, the relative boundedness of $\mathcal{K}_1$ leads to $\|\mathcal{K}_1(t)\mathcal{T}(t-t_0)h\| \leq \bar{c}\|\mathcal{T}(t-t_0)h\|$ (see Appendix A.2). Inserting $\mathcal{I}(t,t_0) = \mathcal{T}(t-t_0)\mathcal{I}^a(t_0) + \mathcal{I}^b(t,t_0)$ and the fact that the components $\mathcal{I}_i^b(t,t_0)$ are in $C^\infty[0,1]$, where $\mathcal{K}_1(t)$ is a bounded operator, yields

$$\|\mathcal{K}_1(t)\mathcal{I}(t,t_0)\| \leq \bar{c}\|\mathcal{T}(t-t_0)\mathcal{I}^a(t_0)\| + \bar{c}\|\mathcal{I}^b(t,t_0)\|. \tag{B.74}$$

After inserting (3.66), (3.67c), (3.67d) and performing the same steps as done before, the estimate (3.89b) readily follows.

To prove (3.89c), differentiate $\mathcal{K}(t)\mathcal{T}_o^{-1}(t)\tilde{e}(t)$ w. r. t. t, yielding

$$\begin{aligned}\big(\mathcal{K}(t)\mathcal{T}_o^{-1}(t)\tilde{e}(t)\big)_t = \ & K_{1,t}(t)(\mathcal{T}_o^{-1}(t)\tilde{e}(t))(1) + K_1(t)\big((\mathcal{T}_o^{-1}(t)\tilde{e}(t))(1)\big)_t \\ & + \int_0^1 \big(B_1^n K_{zt}(1,\zeta,t) + \widetilde{B}_1^d K_t(1,\zeta,t)\big)(\mathcal{T}_o^{-1}(t)\tilde{e}(t))(\zeta)\mathrm{d}\zeta \\ & + \int_0^1 \big(B_1^n K_z(1,\zeta,t) + \widetilde{B}_1^d K(1,\zeta,t)\big)\big((\mathcal{T}_o^{-1}(t)\tilde{e}(t))(\zeta)\big)_t\mathrm{d}\zeta.\end{aligned} \tag{B.75}$$

The derivative of (3.9) w. r. t. t is

$$\big(\mathcal{T}_o^{-1}(t)\tilde{e}(t)\big)_t = \tilde{e}_t(t) - \int_0^z P_t(z,\zeta,t)\tilde{e}(\zeta,t)\mathrm{d}\zeta - \int_0^z P(z,\zeta,t)\tilde{e}_t(\zeta,t)\mathrm{d}\zeta, \tag{B.76}$$

which is evaluated for $z = 1$ and inserted into (B.75), where the integrals are bounded operators again. Then, considering the norm after substituting (B.68) as well as

$$\|\tilde{e}_t(t)\| \leq \bar{M}\mathrm{e}^{(\mu_{\max}-\mu_o+c)(t-t_0)}, \tag{B.77}$$

which is induced by (3.84c) for some finite $\bar{M}$ with the same argumentation as in (B.68), directly leads to (3.89c), proving the corollary.

C Useful theorems and definitions

C.1 Exponential stability

The definition of exponential stability and the connected terminology is taken from [26, Chapter 5] and is stated in

Definition C.1.1 (Exponential Stability). A C_0-semigroup $\mathcal{T}(t)$ on a Hilbert space H is *exponentially stable* if there exist positive constants M and μ such that

$$\|\mathcal{T}(t)\| \leq M\mathrm{e}^{-\mu t}, \quad t \geq 0. \tag{C.1}$$

Whereas μ is the *decay rate*, the supremum over all possible μ is the *stability margin* α of $\mathcal{T}(t)$. ◀

In (C.1), the norm of the C_0-semigroup is defined by [26, Definition A.3.9]

$$\|\mathcal{T}\| = \sup_{0 \neq h \in D(\mathcal{T})} \frac{\|\mathcal{T}h\|}{\|h\|}. \tag{C.2}$$

Note that in the case of coupled parabolic systems, where

$$\|x(t)\| \leq M\mathrm{e}^{(-\mu+c)(t-t_0)}\|x(t_0)\|, \quad c > 0 \tag{C.3}$$

is a common result, the stability margin is μ and the decay rate is always smaller by an infinitely small amount c.

C.2 Convergence properties

The convergence of the fixed-point iteration in Section 2.5.6 is one of the key aspects of the present work. Thus, some basic convergence properties shall be recalled here. The following contents are taken from [77].

Definition C.2.1 (Absolute convergence). A series $\sum a_n$ is said to converge *absolutely* if the series $\sum |a_n|$ converges. ◀

The absolute convergence is a sufficient but not necessary condition for the convergence of a series. That means that there can be functions that converge, but are not absolutely convergent, and thus are called *non-absolutely* convergent or *conditionally convergent*.

An important property considering the convergence of function series is the *uniform convergence*.

Definition C.2.2 (Uniform convergence). A sequence of functions f_n defined on X converges *uniformly* if and only if for every $\varepsilon > 0$ there exist $N \in \mathbb{N}$ and $M \in \mathbb{N}$ such that $n \geq N$ and $m \geq M$ implies

$$|f_n(x) - f_m(x)| \leq \varepsilon \tag{C.4}$$

for all $x \in X$. ◀

Moreover, the definition of uniform convergence of a function sequence to a limit function can be introduced as

Definition C.2.3 (Uniform convergence to limit function). A sequence of functions f_n defined on X converges uniformly *to a function* f if for every $\varepsilon > 0$ there is an $N \in \mathbb{N}$ such that $n \geq N$ implies

$$|f_n(x) - f(x)| \leq \varepsilon \tag{C.5}$$

for all $x \in X$. ◀

The main proposition of the uniform convergence property is the fact that for each $\varepsilon > 0$ it is possible to find *one* $N \in \mathbb{N}$ such that (C.5) holds for *all* $x \in X$. This is the difference to point-wise convergence, where for every x, an N can be found, or in other words, N is different for each x. The uniform convergence consequently implies that the function has the same convergence property at each point x, which explains the name. Due to this fact, continuity of the sequence functions f_n is inherited by the limit function f.

C.3 Calculus

The derivative of the product of two functions can be calculated according to the following rule, typically called *General Leibniz rule* and can be proved by induction.

Lemma C.3.1 (General Leibniz rule)**.** *Suppose f and g are p-times differentiable functions over x. Then, the product fg is a p-times differentiable function with*

$$\mathrm{d}_x^p(fg) = \sum_{k=0}^{p} \binom{p}{k} \mathrm{d}_x^{p-k} f \mathrm{d}_x^k g. \tag{C.6}$$

The following properties are taken from [72] and can be proved by induction.

Lemma C.3.2. *For all* $p, l \in \mathbb{N}$,

$$\sum_{q=0}^{p} \binom{p}{q} (p-q+l)!q! = \frac{(p+l+1)!}{l+1} \tag{C.7a}$$

and

$$\frac{(p+l)!}{l!} \leq \frac{(p+l+1)!}{(l+1)!} \tag{C.7b}$$

hold.

Proof of (C.7b). Knowing that from the definition of the factorial, $(n+1)! = n!(n+1)$ holds, it is easy to show that (C.7b) implies

$$\frac{(p+l)!(p+l+1)}{l!(l+1)} \geq \frac{(p+l)!}{l!}, \tag{C.8}$$

where the right-hand side is cancelled to

$$\frac{p+l+1}{l+1} \geq 1 \tag{C.9a}$$

$$p+l+1 \geq l+1 \tag{C.9b}$$

which is valid for $p \geq 0$. ■

Proof of (C.7a). For the proof, the auxiliary result

$$\sum_{q=0}^{p} \binom{p}{q} (p-q)!(q+l)! = \sum_{q=0}^{p} \binom{p}{q} (p-q+l)!q! \tag{C.10a}$$

$$= \frac{(p+l+1)!}{l+1} \tag{C.10b}$$

is required, where (C.10b) is (C.7a). Both parts of this equation are proved by induction.

For the base case of the induction proof, insert $p = 0$ to check that

$$\sum_{q=0}^{0} \binom{0}{q} (-q)!(q+l)! = \sum_{q=0}^{0} \binom{0}{q} (-q+l)!q! = \frac{(l+1)!}{l+1} \tag{C.11a}$$

$$l! = l! \qquad = \frac{l!(l+1)}{l+1}. \tag{C.11b}$$

In the next step, (C.10) is assumed valid for p and it is shown that the validity for $p+1$ results. Set $p \to p+1$ in (C.10a) and replace the binomial coefficient by

$$\binom{p+1}{q} = \frac{(p+1)!}{q!(p+1-q)!}\frac{(p-q)!}{(p-q)!} \tag{C.12a}$$

to obtain

$$\begin{aligned}
&\sum_{q=0}^{p+1} \frac{p!(p+1)}{q!(p+1-q)!(p-q)!}(p-q)!(p+1-q)!(q+l)! \\
&\quad = (p+1)\sum_{q=0}^{p} \frac{p!}{q!(p-q)!}(p-q)!(q+l)! + (p+1+l)! \\
&\quad \overset{(C.10a)}{=} (p+1)\sum_{q=0}^{p} \frac{p!}{q!(p-q)!}(p-q+l)!q! + (p+1+l)! \\
&\quad = (p+1)\sum_{q=1}^{p+1} \frac{p!}{(q-1)!(p+1-q)!}(p+1-q+l)!(q-1)! + (p+1+l)!.
\end{aligned} \tag{C.13}$$

Note that

$$(p+1+l)! = \sum_{q=0}^{0} \frac{(p+1)!}{(p+1-q)!}(p+1-q+l)! \tag{C.14}$$

to get

$$(C.13) = \sum_{q=0}^{p+1} \frac{(p+1)!}{q!(p+1-q)!}(p+1-q+l)!q! = \sum_{q=0}^{p+1} \binom{p+1}{q}(p+1-q+l)!q!, \tag{C.15}$$

proving (C.10a) by induction.

Now, set $p \to p+1$ in (C.10b) to obtain

$$\begin{aligned}
&\sum_{q=0}^{p+1} \frac{(p+1)!}{q!(p+1-q)!}(p+1-q)!(q+l)! \\
&\quad = \sum_{q=0}^{p} \frac{p!(p+1)}{q!(p-q)!}(p-q)!(q+l)! + (p+1+l)! \\
&\quad \overset{(C.10)}{=} (p+1)\frac{(p+l+1)!}{l+1} + (p+1+l)! = \frac{(p+1+l+1)(p+l+1)!}{l+1} \\
&\quad = \frac{(p+l+2)(p+l+1)!}{l+1} = \frac{(p+l+2)!}{l+1},
\end{aligned} \tag{C.16}$$

which proves (C.7a) and the lemma. ■

C.4 Important inequalities

In stability analysis, it is often possible to determine differential inequalities for functionals related to the norm of the solution. The *comparison principle* says that the solution of the differential inequality is bounded by the solution of the corresponding differential equation. It is derived from Gronwall's lemma [45] and can be found e. g. in [60, Lem. 3.4].

Lemma C.4.1 (Comparison principle)**.** *Given the differential inequality*

$$\dot{x}(t) \leq f(t,x), \quad x(t_0) \leq x_0, \quad t > t_0, \tag{C.17}$$

where x is differentiable and the function f is continuous and locally Lipschitz in x, then the solution $x(t)$ is bounded by the solution of the corresponding differential equation

$$\dot{v}(t) = f(t,v), \quad v(t_0) = x_0, \quad t > t_0 \tag{C.18}$$

i. e.

$$x(t) \leq v(t), \quad \forall t \in [t_0, \infty). \tag{C.19}$$

In the case of a linear differential inequality

$$\dot{V}(t) \leq cV(t), \quad V(t_0) \leq V_0, \tag{C.20}$$

Lemma C.4.1 directly yields

$$V(t) \leq \mathrm{e}^{c(t-t_0)}V_0. \tag{C.21}$$

D Adjoint target systems

In the time-invariant case, the duality between the target systems of state feedback controller (2.23) and observer (3.10) can be utilized to prove the stability of (3.10). The proof was presented in [114] for Robin BCs.

In the time dependent case, the procedure can formally be performed the very same way. That is, an adjoint operator to the system operator of (3.10) can be calculated at each time step t, which is regarded as a parameter of the operators. However, the stability argumentation is only valid in the time-invariant case. For the time-varying case, a deeper analysis of the resulting system operators in the framework of evolution operators (see e. g. [38, 75]) is required.

To show the duality, (3.10) is formulated as *abstract initial value problem (IVP)*

$$\dot{\tilde{e}}(t) = \mathcal{A}(t)\tilde{e}(t) \tag{D.1a}$$

$$\tilde{e}(t_0) = \tilde{e}_0 \tag{D.1b}$$

with $\tilde{e}(t) \in L_2(0,1)$ and

$$\mathcal{A}(t)h = \Lambda h_{zz} - \widetilde{A}_o(\cdot,t)h \tag{D.1c}$$

$$D(\mathcal{A}(t)) = \left\{ h \in ((0,1))^n \,\middle|\, (\tilde{\theta}_0 h)(0) = 0, (\tilde{\theta}_1 h)(1) = -\int_0^1 \widetilde{A}_1(z,t)h(z)\mathrm{d}z \right\}. \tag{D.1d}$$

Now the adjoint operator $\mathcal{A}^*$ of $\mathcal{A}$ is calculated by evaluating the equation

$$\langle \mathcal{A}x, y\rangle = \langle x, \mathcal{A}^* y\rangle \tag{D.2}$$

with $x \in D(\mathcal{A})$, $y \in D(\mathcal{A}^*)$. The utilized inner product reads

$$\langle \mathcal{A}x, y\rangle = \sum_{i=1}^{n} \int_0^1 \frac{1}{\lambda_i(z)} e_i^\top (\mathcal{A}x)(z) y_i(z)\mathrm{d}z \tag{D.3}$$

for real-valued functions $x(z), y(z) \in \mathbb{R}^n$. Inserting $\mathcal{A}$ according to (D.1c) yields

$$\int_0^1 \frac{1}{\lambda_i(z)} e_i^\top (\mathcal{A}x)(z) y_i(z) \mathrm{d}z = \int_0^1 \frac{1}{\lambda_i(z)} \underbrace{e_i^\top \Lambda(z) x''(z)}_{\lambda_i(z) x_i''(z)} y_i(z) \mathrm{d}z - \int_0^1 \frac{1}{\lambda_i(z)} e_i^\top \widetilde{A}_o(z,t) x(z) y_i(z) \mathrm{d}z, \tag{D.4}$$

where the first integral on the right-hand side can be reformulated as

$$\int_0^1 x_i''(z) y_i(z) \mathrm{d}z = x_i'(1) y_i(1) - \underbrace{x_i'(0) y_i(0)}_{0} - x_i(1) y_i'(1) + \underbrace{x_i(0) y_i'(0)}_{0} + \int_0^1 x_i(z) y_i''(z) \mathrm{d}z \tag{D.5}$$

by applying integration by parts. Therein, the term $x_i'(0) y_i(0)$ vanishes if $y_i(0) = 0$ for $i \leq m$, because $x_i'(0) = 0$ for $i > m$. Analogously, $x_i(0) y_i'(0)$ vanishes if $y_i'(0) = 0$ for $i > m$, because $x_i(0) = 0$ for $i \leq m$. Together those two conditions are the left BC for y, namely

$$E_1 E_1^\top y(0) + E_2 E_2^\top y'(0) = (\tilde{\theta}_0 y)(0) = 0. \tag{D.6}$$

Now a case distinction is needed to analyse states with Dirichlet, respectively Robin BCs at the right boundary separately. To this end, the right BC

$$S_d S_d^\top x(1) + S_r S_r^\top x'(1) = -\int_0^1 \widetilde{A}_1(z,t) x(z) \mathrm{d}z \tag{D.7}$$

is premultiplied by $e_i^\top$ to get

$$e_i^\top S_d S_d^\top x(1) + e_i^\top S_r S_r^\top x'(1) = -\int_0^1 e_i^\top \widetilde{A}_1(z,t) x(z) \mathrm{d}z \tag{D.8}$$

Now note that $e_i^\top S_d S_d^\top = e_i^\top$ if x_i has a Dirichlet BC on the right side and otherwise $e_i^\top S_d S_d^\top = 0^\top$. Similarly, $e_i^\top S_r S_r^\top = e_i^\top$ if x_i has a Robin BC at that side and $e_i^\top S_r S_r^\top = 0^\top$ else. Consequently, in the first case, (D.8) reads

$$x_i(1) = -\int_0^1 e_i^\top \widetilde{A}_1(z,t) x(z) \mathrm{d}z \tag{D.9}$$

and in the second case, (D.8) is

$$x_i'(1) = -\int_0^1 e_i^\top \widetilde{A}_1(z,t)x(z)\mathrm{d}z. \tag{D.10}$$

With (D.9), (D.5) is

$$\int_0^1 x_i''(z)y_i(z)\mathrm{d}z = x_i'(1)\underbrace{y_i(1)}_{0} + e_i^\top \int_0^1 \widetilde{A}_1(z,t)x(z)\mathrm{d}z y_i'(1) + \int_0^1 x_i(z)y_i''(z)\mathrm{d}z, \tag{D.11}$$

for $e_i^\top S_r S_r^\top = 0^\top$.

In the case $e_i^\top S_r S_r^\top = e_i^\top$, i. e. the right BC of x_i is of Robin type, (D.10) renders (D.5) to

$$\int_0^1 x_i''(z)y_i(z)\mathrm{d}z = e_i^\top \int_0^1 \widetilde{A}_1(z,t)x(z)\mathrm{d}z y_i(1) + x_i(1)\underbrace{y_i'(1)}_{0} + \int_0^1 x_i(z)y_i''(z)\mathrm{d}z, \tag{D.12}$$

for $e_i^\top S_d S_d^\top = 0^\top$.

Now note that $y_i = e_i^\top S_d S_d^\top y + e_i^\top S_r S_r^\top y$. Inserting this into (D.11) and (D.12) and adding both equations yields

$$\begin{aligned}\int_0^1 x_i''(z)y_i(z)\mathrm{d}z = e_i^\top \int_0^1 \widetilde{A}_1(z,t)x(z)\mathrm{d}z\Big(e_i^\top S_d S_d^\top y'(1) + e_i^\top S_r S_r^\top y(1)\Big) \\ + \int_0^1 x_i(z)y_i''(z)\mathrm{d}z \qquad (D.13)\\ = \int_0^1 \frac{\lambda_i(z)}{\lambda_i(z)} e_i^\top \widetilde{A}_1(z,t)x(z)\mathrm{d}z\Big(e_i^\top S_d S_d^\top y'(1) + e_i^\top S_r S_r^\top y(1)\Big) \\ + \int_0^1 \frac{\lambda_i(z)}{\lambda_i(z)} x_i(z)y_i''(z)\mathrm{d}z, \qquad (D.14)\end{aligned}$$

which can be substituted in (D.4) and (D.3) to obtain

$$\langle \mathcal{A}x, y\rangle = \sum_{i=1}^{n} \int_0^1 \frac{1}{\lambda_i(z)} \lambda_i(z) e_i^\top \widetilde{A}_1(z,t) x(z) \mathrm{d}z \Big(e_i^\top S_d S_d^\top y'(1) + e_i^\top S_r S_r^\top y(1) \Big)$$
$$+ \int_0^1 \frac{1}{\lambda_i(z)} x_i(z) \lambda_i(z) y_i''(z) \mathrm{d}z - \int_0^1 \frac{1}{\lambda_i(z)} e_i^\top \widetilde{A}_o(z,t) x(z) y_i(z) \mathrm{d}z. \quad \text{(D.15)}$$

Reformulating the sum with the help of

$$\sum_{i=1}^{n} e_i^\top A x y_i = y^\top A x = \sum_{i=1}^{n} \sum_{k=1}^{n} A_{ik} x_k y_i$$
$$= \sum_{k=1}^{n} x_k \underbrace{\sum_{i=1}^{n} A_{ki}^\top y_i}_{e_k^\top A^\top y} = \sum_{i=1}^{n} x_i e_i^\top A^\top y = x^\top A^\top y \quad \text{(D.16)}$$

for $x, y \in \mathbb{R}^n$ and $A \in \mathbb{R}^{n\times n}$, yields

$$\langle \mathcal{A}x, y\rangle = \sum_{i=1}^{n} \int_0^1 \frac{x_i(z)}{\lambda_i(z)} e_i^\top \Lambda(z) \widetilde{A}_1^\top(z,t) \mathrm{d}z \Big(S_d S_d^\top y'(1) + S_r S_r^\top y(1) \Big)$$
$$+ \int_0^1 \frac{x_i(z)}{\lambda_i(z)} e_i^\top \Lambda(z) y''(z) \mathrm{d}z - \int_0^1 \frac{x_i(z)}{\lambda_i(z)} e_i^\top \widetilde{A}_o^\top(z,t) y(z) \mathrm{d}z \quad \text{(D.17)}$$
$$= \sum_{i=1}^{n} \int_0^1 \frac{x_i(z)}{\lambda_i(z)} e_i^\top \Big(\Lambda(z) \widetilde{A}_1^\top(z,t) \big(S_d S_d^\top y'(1) + S_r S_r^\top y(1) \big)$$
$$+ \Lambda(z) y''(z) - \widetilde{A}_o^\top(z,t) y(z) \Big) \mathrm{d}z = \langle x, \mathcal{A}^* y\rangle, \quad \text{(D.18)}$$

with

$$\mathcal{A}^*(t) h = \Lambda h'' - \widetilde{A}_o^\top(\cdot,t) h + \Lambda \widetilde{A}_1^\top(\cdot,t) \Big(S_d S_d^\top h'(1) + S_r S_r^\top h(1) \Big). \quad \text{(D.19a)}$$

Including the BCs found in (D.11) and (D.12), i. e. $y_i(1) = 0$ for $e_i^\top S_r = 0$ respectively $S_d^\top y(1) = 0$ and $y_i'(1) = 0$ for $e_i^\top S_d = 0$ respectively $S_r^\top y'(1) = 0$ to the domain of $\mathcal{A}^*$, it reads

$$D(\mathcal{A}^*(t)) = \Big\{ h \in (H^2(0,1))^n \,\Big|\, (\tilde{\theta}_0 h)(0) = 0, (\tilde{\theta}_1 h)(1) = 0 \Big\} \quad \text{(D.19b)}$$

with $\tilde{\theta}_0$ and $\tilde{\theta}_1$ defined in (2.25).

Consequently, the adjoint system can be written in form of the initial boundary value problem

$$\begin{aligned}\tilde{e}_t^*(z,t) &= \Lambda\tilde{e}_{zz}^*(z,t) - \widetilde{A}_o^\top(z,t)\tilde{e}^*(z,t)\\ &\quad + \Lambda\widetilde{A}_1^\top(z,t)\Big(S_dS_d^\top\tilde{e}_z^*(1,t) + S_rS_r^\top\tilde{e}^*(1,t)\Big) \qquad \text{(D.20a)}\\ (\tilde{\theta}_0\tilde{e}^*(t))(0) &= 0 \qquad \text{(D.20b)}\\ (\tilde{\theta}_1\tilde{e}^*(t))(1) &= 0 \qquad \text{(D.20c)}\end{aligned}$$

with some initial value $\tilde{e}^*(z,0) = \tilde{e}_0^*(z) \in \mathbb{R}^n$. This is exactly the form of (2.23) with the replacements $\widetilde{A} \to \widetilde{A}_o^\top$, $\widetilde{A}_0 \to \Lambda\widetilde{A}_1^\top$, $E_1 \to S_d$ and $E_2 \to S_r$. Note that by the transposition of $\widetilde{A}_o$ and $\widetilde{A}_1$, they have the same structure as $\widetilde{A}$ and $\widetilde{A}_0$ in (2.23). In the time-invariant case, i. e. $\widetilde{A}_o(z,t) = \widetilde{A}_o(z)$, $\widetilde{A}_1(z,t) = \widetilde{A}_1(z)$, $t_0 = 0$, it is possible to show that this system is the generator of an exponentially stable C_0-semigroup, implying

$$\|\tilde{e}^*(t)\| \leq \widetilde{M}\mathrm{e}^{(\mu_{\max}-\mu_o+c)t}\|\tilde{e}^*(0)\|, \quad t \geq 0 \qquad \text{(D.21)}$$

for all $\tilde{e}^*(0) \in (H^2(0,1))^n$ satisfying the BCs (D.20b), (D.20c), an $\widetilde{M} \geq 1$ and any $c > 0$, leading to the stability margin $\mu_o - \mu_{\max}$.

In the time dependent case, statements about the solution of the original system based on the properties of the adjoint system are hardly possible. Therefore, a different stability proof is given in Section 3.6. In the time-invariant case, however, the following conclusion is possible.

According to [26, Lemma A.3.60], the norms of the C_0-semigroups of original and adjoint system are equal, i. e.

$$\|\mathcal{T}(t)\| = \|\mathcal{T}^*(t)\|, \qquad \text{(D.22)}$$

where $\mathcal{T}$ and $\mathcal{T}^*$ are the semigroups generated by $\mathcal{A}$ and, respectively. Consequently, the uniform exponential stability of (3.10) directly follows with the stability margin given in (D.21).

Bibliography

[1] O. M. Aamo, A. Smyshlyaev and M. Krstic. „Boundary control of the linearized Ginzburg–Landau model of vortex shedding“. In: *SIAM Journal on Control and Optimization* 43 (2005), pp. 1953–1971 (cit. on p. 5).

[2] I. Aksikas, A. M. Fuxman and J. F. Forbes. „Control of time-varying distributed parameter plug flow reactor by LQR“. In: *IFAC Proceedings Volumes* 41 (2008). 17th IFAC World Congress, pp. 11955–11960 (cit. on p. 5).

[3] H. Anfinsen and O. M. Aamo. „Disturbance rejection in general heterodirectional 1-D linear hyperbolic systems using collocated sensing and control“. In: *Automatica* 76 (2017), pp. 230–242 (cit. on p. 5).

[4] J. Auriol and F. D. Meglio. „Trajectory tracking for a system of two linear hyperbolic PDEs with uncertainties“. In: *IFAC-PapersOnLine* 50 (2017). 20th IFAC World Congress, pp. 7089–7095 (cit. on p. 5).

[5] A. Baccoli, Y. Orlov and A. Pisano. „On the boundary control of coupled reaction-diffusion equations having the same diffusivity parameters“. In: *53rd IEEE Conference on Decision and Control (CDC)*. 2014, pp. 5222–5228 (cit. on p. 5).

[6] A. Baccoli and A. Pisano. „Anticollocated backstepping observer design for a class of coupled reaction-diffusion PDEs“. In: *Journal of Control Science and Engineering* (2015), pp. 1–10 (cit. on pp. 5, 94).

[7] A. Baccoli, A. Pisano and Y. Orlov. „Boundary control of coupled reaction–diffusion processes with constant parameters“. In: *Automatica* 54 (2015), pp. 80–90 (cit. on p. 5).

[8] M. J. Balas. „Toward A More Practical Control Theory for Distributed Parameter Systems“. In: *Advances in Theory and Applications*. Ed. by C. LEONDES. Vol. 18. Control and Dynamic Systems. Academic Press, 1982, pp. 361–421 (cit. on p. 1).

[9] A. Balogh and M. Krstic. „Infinite dimensional backstepping-style feedback transformations for a heat equation with an arbitrary level of instability“. In: *European Journal of Control* 8 (2002), pp. 165–175 (cit. on p. 3).

[10] A. Balogh and M. Krstic. „Stability of partial difference equations governing control gains in infinite-dimensional backstepping“. In: *Systems & Control Letters* 51 (2004), pp. 151–164 (cit. on p. 3).

[11] N. Bekiaris-Liberis and R. Vazquez. „Nonlinear bilateral output-feedback control for a class of viscous Hamilton–Jacobi PDEs“. In: *Automatica* 101 (2019), pp. 223–231 (cit. on p. 131).

[12] D. M. Boskovic, M. Krstic and Weijiu Liu. „Boundary control of an unstable heat equation via measurement of domain-averaged temperature“. In: *IEEE Transactions on Automatic Control* 46 (2001), pp. 2022–2028 (cit. on p. 3).

[13] D. M. Boskovic and M. Krstic. „Nonlinear stabilization of a thermal convection loop by state feedback“. In: *Automatica* 37 (2001), pp. 2033–2040 (cit. on p. 3).

[14] D. M. Boskovic and M. Krstic. „Boundary control of chemical tubular reactors“. In: *IFAC Proceedings Volumes* 35 (2002). 15th IFAC World Congress, pp. 483–488 (cit. on p. 3).

[15] D. M. Boskovic and M. Krstic. „Stabilization of a solid propellant rocket instability by state feedback“. In: *International Journal of Robust and Nonlinear Control* 13 (2003), pp. 483–495 (cit. on p. 3).

[16] A. Bradshaw and B. Porter. „Modal control of a class of distributed-parameter systems: multi-eigenvalue assignment“. In: *International Journal of Control* 16 (1971), pp. 277–285 (cit. on p. 1).

[17] L. Camacho-Solorio, R. Vazquez and M. Krstic. „Boundary observer design for coupled reaction-diffusion systems with spatially-varying reaction“. In: *American Control Conference (ACC)*. 2017, pp. 3159–3164 (cit. on p. 6).

[18] L. Camacho-Solorio, R. Vazquez and M. Krstic. „Boundary observers for coupled diffusion-reaction systems with prescribed convergence rate“. In: *Systems & Control Letters* 135 (2020), p. 104586 (cit. on p. 6).

[19] S. Chen, R. Vazquez and M. Krstic. „Folding backstepping approach to parabolic PDE bilateral boundary control“. In: *IFAC-PapersOnLine* 52 (2019), pp. 76–81 (cit. on pp. 7, 132, 134).

[20] S. Chen, R. Vazquez and M. Krstic. „Folding bilateral backstepping output-feedback control design for an unstable parabolic PDE“. In: *IEEE Transactions on Automatic Control, submitted, available at arXiv:1906.05434v2 [math.OC]* (2019) (cit. on pp. 7, 8, 132, 134, 159, 173, 176, 177).

[21] P. Christofides. *Model-based Control of Particulate Processes*. Kluwer Academic Publishers, 2002 (cit. on p. 13).

[22] D. Colton. „Integral operators and reflection principles for parabolic equations in one space variable“. In: *Journal of Differential Equations* 15 (1973), pp. 551–559 (cit. on pp. 4, 35, 40).

[23] D. Colton. „The solution of initial-boundary value problems for parabolic equations by the method of integral operators“. In: *Journal of Differential Equations* 26 (1977), pp. 181–190 (cit. on pp. 4, 35).

[24] J.-M. Coron, L. Hu and G. Olive. „Finite-time boundary stabilization of general linear hyperbolic balance laws via Fredholm backstepping transformation“. In: *Automatica* 84 (2017), pp. 95–100 (cit. on p. 5).

[25] J.-M. Coron, R. Vazquez, M. Krstic and G. Bastin. „Local exponential H^2 stabilization of a 2×2 quasilinear hyperbolic system using backstepping“. In: *SIAM Journal on Control and Optimization* 51 (2013), pp. 2005–2035 (cit. on p. 5).

[26] R. F. Curtain and H. J. Zwart. *An Introduction to Infinite-Dimensional Linear Systems Theory*. Springer-Verlag New York, 1995 (cit. on pp. 1, 2, 10, 28, 30, 105, 109, 123, 187, 191, 209, 219).

[27] C. Delattre, D. Dochain and J. Winkin. „Sturm-Liouville systems are Riesz-spectral systems“. In: *International Journal of Applied Mathematics and Computer Science* 13 (2003), pp. 481–484 (cit. on p. 27).

[28] J. Deutscher. „Backstepping design of robust output feedback regulators for boundary controlled parabolic PDEs“. In: *IEEE Transactions on Automatic Control* 61 (2016), pp. 2288–2294 (cit. on p. 5).

[29] J. Deutscher. „Backstepping design of robust state feedback regulators for linear 2×2 hyperbolic systems“. In: *IEEE Transactions on Automatic Control* 62 (2017), pp. 5240–5247 (cit. on p. 5).

[30] J. Deutscher and J. Gabriel. „Robust state feedback regulator design for general linear heterodirectional hyperbolic systems“. In: *IEEE Transactions on Automatic Control* 63 (2018), pp. 2620–2627 (cit. on p. 5).

[31] J. Deutscher and J. Gabriel. „Fredholm backstepping control of coupled linear parabolic PDEs with input and output delays“. In: *IEEE Transactions on Automatic Control* 65 (2020), pp. 3128–3135 (cit. on pp. 5, 185).

[32] J. Deutscher and C. Harkort. „Parametric state feedback design of linear distributed-parameter systems“. In: *International Journal of Control* 82 (2009), pp. 1060–1069 (cit. on p. 1).

[33] J. Deutscher. „A backstepping approach to the output regulation of boundary controlled parabolic PDEs“. In: *Automatica* 47 (2015), pp. 2468–2473 (cit. on pp. 5, 30).

[34] J. Deutscher. „Output regulation for general linear heterodirectional hyperbolic systems with spatially-varying coefficients“. In: *Automatica* 85 (2017), pp. 34–42 (cit. on p. 5).

[35] J. Deutscher. „Remarks on the notion of backstepping for parabolic systems“. In: *Methoden und Anwendungen der Regelungstechnik*. Ed. by G. Roppenecker and B. Lohmann. Shaker Verlag, 2017, pp. 1–9 (cit. on p. 2).

[36] F. Di Meglio, R. Vazquez and M. Krstic. „Stabilization of a system of $n+1$ coupled first-order hyperbolic linear PDEs with a single boundary input“. In: *IEEE Transactions on Automatic Control* 58 (2013), pp. 3097–3111 (cit. on p. 5).

[37] F. Di Meglio, R. Vazquez, M. Krstic and N. Petit. „Backstepping stabilization of an underactuated 3×3 linear hyperbolic system of fluid flow equations“. In: *American Control Conference (ACC)*. 2012, pp. 3365–3370 (cit. on p. 5).

[38] K.-J. Engel and R. Nagel. *One-parameter semigroups for linear evolution equations*. Springer-Verlag New York, 2000 (cit. on pp. 109, 215).

[39] H. Feng and B.-Z. Guo. „Output feedback stabilization of an unstable wave equation with general corrupted boundary observation“. In: *Automatica* 50 (2014), pp. 3164–3172 (cit. on p. 5).

[40] G. F. Franklin, D. J. Powell and A. Emami-Naeini. *Feedback Control of Dynamic Systems*. 4th ed. Prentice Hall PTR, 2001 (cit. on p. 116).

[41] G. Freudenthaler, F. Göttsch and T. Meurer. „Backstepping-based extended Luenberger observer design for a Burgers-type PDE for multi-agent deployment“. In: *IFAC-PapersOnLine* 50 (2017). 20th IFAC World Congress, pp. 6780–6785 (cit. on p. 131).

[42] J. Gabriel and J. Deutscher. „State feedback regulator design for coupled linear wave equations“. In: *European Control Conference (ECC)*. 2018, pp. 3013–3018 (cit. on p. 5).

[43] F. Ge, T. Meurer and Y. Chen. „Mittag-Leffler convergent backstepping observers for coupled semilinear subdiffusion systems with spatially varying parameters“. In: *Systems & Control Letters* 122 (2018), pp. 86–92 (cit. on p. 5).

[44] N. Ghaderi and M. Keyanpour. „Backstepping design for a class of coupled parabolic PDEs with spatially varying coefficient“. In: *Asian Journal of Control* (2019), pp. 1–12 (cit. on p. 20).

[45] T. H. Gronwall. „Note on the derivatives with respect to a parameter of the solution of a system of differential equations“. In: *Annals of Mathematics* 20 (1919), pp. 292–296 (cit. on p. 213).

[46] J.-J. Gu and J.-M. Wang. „Sliding mode control for N-coupled reaction-diffusion PDEs with boundary input disturbances“. In: *International Journal of Robust and Nonlinear Control* 29 (2019), pp. 1437–1461 (cit. on p. 5).

[47] K. M. Hangos and I. T. Cameron. *Process Modelling and Model Analysis*. Process Systems Engineering. Academic Press, 2001 (cit. on p. 12).

[48] C. Harkort. *Early-Lumping Based Controller Synthesis for Linear Infinite-Dimensional Systems*. FAU University Press, 2014 (cit. on pp. 28, 29).

[49] E. Hopf. „The partial differential equation $u_t + uu_x = \mu_{xx}$“. In: *Communications on Pure and Applied Mathematics* 3 (1950), pp. 201–230 (cit. on p. 17).

[50] L. Hu, F. Di Meglio, R. Vazquez and M. Krstic. „Control of homodirectional and general heterodirectional linear coupled hyperbolic PDEs“. In: *IEEE Transactions on Automatic Control* 61 (2016), pp. 3301–3314 (cit. on pp. 5, 6).

[51] L. Hu, R. Vazquez, F. Meglio and M. Krstic. „Boundary exponential stabilization of 1-dimensional inhomogeneous quasi-linear hyperbolic systems“. In: *SIAM Journal on Control and Optimization* 57 (2019), pp. 963–998 (cit. on pp. 5, 6, 67).

[52] A. Isidori. *Nonlinear Control Systems*. 3rd ed. Springer-Verlag Berlin Heidelberg, 1995 (cit. on p. 2).

[53] A. Isidori. *Nonlinear Control Systems II*. Springer-Verlag Berlin Heidelberg, 2000 (cit. on p. 2).

[54] M. Izadi, J. Abdollahi and S. S. Dubljevic. „PDE backstepping control of one-dimensional heat equation with time-varying domain“. In: *Automatica* 54 (2015), pp. 41–48 (cit. on p. 5).

[55] L. Jadachowski, T. Meurer and A. Kugi. „Backstepping observers for linear PDEs on higher-dimensional spatial domains“. In: *Automatica* 51 (2015), pp. 85–97 (cit. on pp. 5, 93).

[56] R. al Jamal and K. Morris. „Linearized stability of partial differential equations with application to stabilization of the Kuramoto–Sivashinsky equation“. In: *SIAM Journal on Control and Optimization* 56 (2018), pp. 120–147 (cit. on p. 15).

[57] T. Kailath. *Linear Systems*. Prentice Hall, 1980 (cit. on p. 116).

[58] I. Kanellakopoulos, P. Kokotovic and A. Morse. „A toolkit for nonlinear feedback design“. In: *Systems & Control Letters* 18 (1992), pp. 83–92 (cit. on p. 2).

[59] T. Kato. *Perturbation Theory for Linear Operators*. Springer-Verlag Berlin, 1995 (cit. on pp. 188–190).

[60] H. K. Khalil. *Nonlinear Systems*. 3rd ed. Prentice-Hall, 2002 (cit. on p. 213).

[61] H. K. Khalil. *Nonlinear Control*. Pearson Education, 2015 (cit. on p. 2).

[62] S. Koga, R. Vazquez and M. Krstic. „Backstepping control of the Stefan problem with flowing liquid“. In: *American Control Conference (ACC)*. 2017, pp. 1151–1156 (cit. on p. 5).

[63] M. Krstic and A. Smyshlyaev. *Boundary Control of PDEs — A Course on Backstepping Designs*. Advances in Design and Control. SIAM, 2008 (cit. on pp. 2–4, 9, 32, 45, 141).

[64] M. Krstic, I. Kanellakopoulos and P. Kokotovic. *Nonlinear and Adaptive Control Design*. John Wiley & Sons, 1995 (cit. on pp. 2, 3).

[65] P. Lamare, N. Bekiaris-Liberis and A. M. Bayen. „Control of 2×2 linear hyperbolic systems: Backstepping-based trajectory generation and PI-based tracking“. In: *European Control Conference (ECC)*. 2015, pp. 497–502 (cit. on p. 5).

[66] B. Laroche, P. Martin and P. Rouchon. „Motion planning for the heat equation“. In: *International Journal of Robust and Nonlinear Control* 10 (2000), pp. 629–643 (cit. on pp. 80, 86).

[67] I. Lasiecka and R. Triggiani. *Control Theory for Partial Differential Equations: Continuous and Approximation Theories*. Encyclopedia of Mathematics and its Applications. Cambridge University Press, 2000 (cit. on p. 1).

[68] B. Liu, D. Boutat and D. Liu. „Backstepping observer-based output feedback control for a class of coupled parabolic PDEs with different diffusions“. In: *Systems & Control Letters* 97 (2016), pp. 61–69 (cit. on pp. 5, 94).

[69] W. Liu. „Boundary feedback stabilization of an unstable heat equation“. In: *SIAM Journal on Control and Optimization* 42 (2003), pp. 1033–1042 (cit. on pp. 3, 4, 35).

[70] D. Luenberger. „An introduction to observers“. In: *IEEE Transactions on Automatic Control* 16 (1971), pp. 596–602 (cit. on p. 96).

[71] Z.-H. Luo, B.-Z. Guo and Ö. Morgül. *Stability and Stabilization of Infinite Dimensional Systems with Applications*. Springer-Verlag London, 1999 (cit. on p. 2).

[72] T. Meurer. *Control of Higher-Dimensional PDEs*. Communications and Control Engineering. Springer Berlin Heidelberg, 2013 (cit. on pp. 5, 14, 15, 36, 60, 67–69, 185, 211).

[73] T. Meurer and A. Kugi. „Tracking control for boundary controlled parabolic PDEs with varying parameters: Combining backstepping and differential flatness“. In: *Automatica* 45 (2009), pp. 1182–1194 (cit. on pp. 5, 15, 16, 185).

[74] Y. Orlov, A. Pisano, A. Pilloni and E. Usai. „Output feedback stabilization of coupled reaction-diffusion processes with constant parameters“. In: *SIAM Journal on Control and Optimization* 55 (2017), pp. 4112–4155 (cit. on p. 5).

[75] A. Pazy. *Semigroups of Linear Operators and Applications to Partial Differential Equations*. Applied Mathematical Sciences 44. Springer-Verlag New York, 1983 (cit. on p. 215).

[76] C. D. Rahn. *Mechatronic Control of Distributed Noise and Vibration. A Lyapunov Approach*. Springer-Verlag Berlin Heidelberg, 2001 (cit. on p. 2).

[77] W. Rudin. *Principles of Mathematical Analysis*. 3rd ed. Inernational series in pure and applied mathematics. McGraw-Hill, 1976 (cit. on pp. 66, 68, 209).

[78] T. I. Seidman. „Two results on exact boundary control of parabolic equations“. In: *Applied Mathematics and Optimization* 11 (1984), pp. 145–152 (cit. on p. 4).

[79] A. Smyshlyaev and M. Krstic. „Closed-form boundary state feedbacks for a class of 1-D partial integro-differential equations“. In: *IEEE Transactions on Automatic Control* 49 (2004), pp. 2185–2202 (cit. on pp. 4, 6, 35, 40, 45, 66, 75).

[80] A. Smyshlyaev and M. Krstic. „Backstepping observers for a class of parabolic PDEs“. In: *Systems & Control Letters* 54 (2005), pp. 613–625 (cit. on pp. 5, 93).

[81] A. Smyshlyaev and M. Krstic. „On control design for PDEs with space-dependent diffusivity or time-dependent reactivity“. In: *Automatica* 41 (2005), pp. 1601–1608 (cit. on pp. 4, 5, 36, 40, 59).

[82] A. Smyshlyaev and M. Krstic. *Adaptive Control of Parabolic PDEs*. Princeton University Press, 2010 (cit. on pp. 12, 185).

[83] D. Steeves, M. Krstic and R. Vazquez. „Prescribed-time H^1-stabilization of reaction-diffusion equations by means of output feedback“. In: *European Control Conference (ECC)*. 2019, pp. 1932–1937 (cit. on p. 5).

[84] S. Tang and M. Krstic. „Sliding mode control to the stabilization of a linear 2×2 hyperbolic system with boundary input disturbance“. In: *American Control Conference (ACC)*. 2014, pp. 1027–1032 (cit. on p. 5).

[85] S.-X. Tang, L. Camacho-Solorio, Y. Wang and M. Krstic. „State-of-charge estimation from a thermal–electrochemical model of Lithium-ion batteries“. In: *Automatica* 83 (2017), pp. 206–219 (cit. on p. 5).

[86] R. Triggiani. „Boundary feedback stabilizability of parabolic equations“. In: *Applied Mathematics and Optimization* 6 (1980), pp. 201–220 (cit. on p. 13).

[87] D. Tsubakino, M. Krstic and S. Hara. „Backstepping control for parabolic PDEs with in-domain actuation“. In: *American Control Conference (ACC)*. 2012, pp. 2226–2231 (cit. on p. 93).

[88] D. Tsubakino, M. Krstic and Y. Yamashita. „Boundary control of a cascade of two parabolic PDEs with different diffusion coefficients“. In: *52nd IEEE Conference on Decision and Control (CDC)*. 2013, pp. 3720–3725 (cit. on pp. 16, 132, 185).

[89] M. Tucsnak and G. Weiss. *Observation and Control for Operator Semigroups*. Birkhäuser Basel, 2009 (cit. on p. 2).

[90] M. Valasek and N. Olgac. „Efficient pole placement technique for linear time-variant SISO systems“. In: *IEE Proceedings - Control Theory and Applications* 142 (1995), pp. 451–458 (cit. on pp. 2, 6).

[91] M. Valasek and N. Olgac. „Efficient eigenvalue assignments for general linear MIMO systems“. In: *Automatica* 31 (1995), pp. 1605–1617 (cit. on p. 6).

[92] A. Vande Wouwer, P. Saucez and C. V. Fernández. *Simulation of ODE/PDE Models with MATLAB®, OCTAVE and SCILAB*. Springer International Publishing, 2014 (cit. on pp. 84, 85).

[93] R. Vazquez and M. Krstic. „Taking a step back: a brief history of PDE backstepping“. In: *Proceedings of the 20th IFAC World Congress, Toulouse, France*. 2017, pp. 4258–4262 (cit. on pp. 4, 5).

[94] R. Vazquez and M. Krstic. „Control of 1-D parabolic PDEs with Volterra nonlinearities, Part I: Design“. In: *Automatica* 44 (2008), pp. 2778–2790 (cit. on p. 5).

[95] R. Vazquez and M. Krstic. „Control of 1-D parabolic PDEs with Volterra nonlinearities, Part II: Analysis“. In: *Automatica* 44 (2008), pp. 2791–2803 (cit. on p. 5).

[96] R. Vazquez and M. Krstic. „Bilateral boundary control of one-dimensional first- and second-order PDEs using infinite-dimensional backstepping“. In: *55th IEEE Conference on Decision and Control (CDC)*. 2016, pp. 537–542 (cit. on pp. 7, 131, 132, 134, 139).

[97] R. Vazquez and M. Krstic. „Explicit output-feedback boundary control of reaction-diffusion PDEs on arbitrary-dimensional balls“. In: *ESAIM: Control, Optimisation and Calculus of Variations* 22 (2016), pp. 1078–1096 (cit. on pp. 7, 131).

[98] R. Vazquez and M. Krstic. „Boundary control of coupled reaction-advection-diffusion systems with spatially-varying coefficients“. In: *IEEE Transactions on Automatic Control* 62 (2017), pp. 2026–2033 (cit. on pp. 6, 7, 13, 18, 20, 36).

[99] R. Vazquez, E. Schuster and M. Krstic. „A closed-form full-state feedback controller for stabilization of 3D magnetohydrodynamic channel flow“. In: *Journal of Dynamic Systems, Measurement and Control* 131 (2009). 041001 (cit. on p. 5).

[100] R. Vazquez, E. Trélat and J.-M. Coron. „Control for fast and stable laminar-to-high-Reynolds-numbers transfer in a 2D Navier-Stokes channel flow“. In: *Discrete and Continuous Dynamical Systems – B* 10 (2008), pp. 925–956 (cit. on pp. 5, 36, 67, 170).

[101] M. O. Wagner and T. Meurer. „Flatness-based feedforward control design and two-degrees-of-freedom tracking control for semilinear plug flow reactors“. In: *Journal of Process Control* 64 (2018), pp. 132–140 (cit. on p. 15).

[102] P. Wang. „Modal feedback stabilization of a linear distributed system“. In: *IEEE Transactions on Automatic Control* 17 (1972), pp. 552–553 (cit. on p. 1).

[103] S. Wang and F. Woittennek. „Backstepping-method for parabolic systems with in-domain actuation“. In: *IFAC Proceedings Volumes* 46 (2013). 1st IFAC Workshop on Control of Systems Governed by Partial Differential Equations, pp. 43–48 (cit. on pp. 132, 173, 182).

[104] S. Wang, F. Woittennek and T. Knüppel. „Feedback control for parabolic systems with in-domain actuation“. In: *PAMM* 14 (2014), pp. 901–902 (cit. on pp. 132, 173).

[105] G. Weiss. „The representation of regular linear systems on Hilbert spaces“. In: *Control and Estimation of Distributed Parameter Systems*. Ed. by F. Kappel, K. Kunisch and W. Schappacher. Birkhäuser Basel, 1989, pp. 401–416 (cit. on p. 2).

[106] G. Weiss. „Regular linear systems with feedback“. In: *Mathematics of Control, Signals and Systems* 7 (1994), pp. 23–57 (cit. on p. 2).

[107] N. C. A. Wilhelmsen, H. Anfinsen and O. M. Aamo. „Minimum time bilateral observer design for 2×2 linear hyperbolic systems“. In: *European Control Conference (ECC)*. 2019, pp. 2325–2331 (cit. on p. 132).

[108] F. Woittennek, S. Wang and T. Knüppel. „Backstepping design for parabolic systems with in-domain actuation and Robin boundary conditions“. In: *IFAC Proceedings Volumes* 47 (2014). 19th IFAC World Congress, pp. 5175–5180 (cit. on pp. 93, 132, 173, 182).

[109] H.-C. Zhou and G. Weiss. „Solving the regulator problem for a 1-D Schrödinger equation via backstepping“. In: *IFAC-PapersOnLine* 50 (2017). 20th IFAC World Congress, pp. 4516–4521 (cit. on p. 5).

Publications of the author

[110] J. Deutscher and S. Kerschbaum. „Backstepping design of robust state feedback regulators for second order hyperbolic PIDEs“. In: *IFAC-PapersOnLine* 49 (2016). 2nd IFAC Workshop on Control of Systems Governed by Partial Differential Equations CPDE 2016, pp. 80–85.

[111] J. Deutscher and S. Kerschbaum. „Backstepping control of coupled diffusion-reaction systems with spatially-varying reaction and Neumann boundary conditions“. In: *56th IEEE Conference on Decision and Control (CDC)*. 2017, pp. 2504–2510.

[112] J. Deutscher and S. Kerschbaum. „Backstepping for coupled parabolic systems with spatially-varying coefficients (in German)“. In: *at - Automatisierungstechnik* 66 (2018), pp. 558–572.

[113] J. Deutscher and S. Kerschbaum. „Backstepping control of coupled linear parabolic PIDEs with spatially varying coefficients“. In: *IEEE Transactions on Automatic Control* 63 (2018), pp. 4218–4233.

[114] J. Deutscher and S. Kerschbaum. „Output regulation for coupled linear parabolic PIDEs“. In: *Automatica* 100 (2019), pp. 360–370.

[115] J. Deutscher and S. Kerschbaum. „Robust output regulation by state feedback control for coupled linear parabolic PIDEs“. In: *IEEE Transactions on Automatic Control* 65 (2020), pp. 2207–2214.

[116] S. Kerschbaum and J. Deutscher. „Backstepping-based output regulation for systems with infinite-dimensional actuator and sensor dynamics“. In: *PAMM* 16 (2016), pp. 43–46.

[117] S. Kerschbaum and J. Deutscher. „Bilateral backstepping control of coupled linear parabolic PDEs with spatially varying coefficients“. In: *Automatica, submitted* (2019).

[118] S. Kerschbaum and J. Deutscher. „Backstepping control of coupled linear parabolic PDEs with space and time dependent coefficients“. In: *IEEE Transactions on Automatic Control* 65 (2020), pp. 3060–3067.

Related software

[119] S. Kerschbaum. *Backstepping Control of Coupled Parabolic Systems with Varying Parameters: A Matlab Library*. https://doi.org/10.5281/zenodo.4274740. Zenodo, 2020.

Advised student works

[120] C. Braun. *Führungs- und Störgrößenaufschaltung für zweidimensionale hyperbolische Systeme*. MA thesis. Lehrstuhl für Regelungstechnik, FAU Erlangen-Nürnberg, 2016.

[121] J. Fischer. *Modellierung und Regelung von Raumheizungen*. BA thesis. Lehrstuhl für Regelungstechnik, FAU Erlangen-Nürnberg, 2016.

[122] X. Li. *Simulation eines Drei-Wege-Katalysators*. Research internship. Lehrstuhl für Regelungstechnik, FAU Erlangen-Nürnberg, 2018.

[123] Y. Prummer. *Praxisnahe Regelung von Raumzeihung, -Lüftung und Verschattung*. Research internship. Lehrstuhl für Regelungstechnik, FAU Erlangen-Nürnberg, 2018.

[124] A. Regensky. *Implementierung und Vergleich verschiedener Simulationsmethoden für hyperbolische PDEs in MATLAB*. BA thesis. Lehrstuhl für Regelungstechnik, FAU Erlangen-Nürnberg, 2016.

[125] Y. Tang. *Modelling and Backstepping-Based Control of a Tubular Reactor*. MA thesis. Lehrstuhl für Regelungstechnik, FAU Erlangen-Nürnberg, 2018.

[126] S. Treis. *Optimierung von Raumheizung, -lüftung und Verschattung mittels MPC*. Research internship. Lehrstuhl für Regelungstechnik, FAU Erlangen-Nürnberg, 2017.

Index

Special symbols

Many technical processes are described by coupled parabolic partial differential equations. Time dependent characteristics, time-varying spatial domains or the linearization of a system around a desired trajectory result in systems with space and time dependent coefficients. The back-stepping control design method is developed for this system class on one-dimensional spatial domains and actuation at one or both boundaries of the domain. State feedback controller, observer and the resulting output feedback controller are determined by a constructive design method allowing to achieve uniform exponential stability with an assignable stability margin. The theoretic results are substantiated by numerous simulations.

As supplementary material, the source code for the simulations in this work is available under https://doi.org/10.5281/zenodo.4274739.

ISBN 978-3-96147-390-8

FAU UNIVERSITY PRESS 2021